



Publicly Accessible Penn Dissertations

---

2019

# Expanding Peptide Stapling With S-Tetrazine

Matthew Henry Bunner

University of Pennsylvania, [mhbunner@gmail.com](mailto:mhbunner@gmail.com)

Follow this and additional works at: <https://repository.upenn.edu/edissertations>

 Part of the [Organic Chemistry Commons](#)

---

## Recommended Citation

Bunner, Matthew Henry, "Expanding Peptide Stapling With S-Tetrazine" (2019). *Publicly Accessible Penn Dissertations*. 3374.  
<https://repository.upenn.edu/edissertations/3374>

This paper is posted at ScholarlyCommons. <https://repository.upenn.edu/edissertations/3374>  
For more information, please contact [repository@pobox.upenn.edu](mailto:repository@pobox.upenn.edu).

---

# Expanding Peptide Stapling With S-Tetrazine

## **Abstract**

ABSTRACT

EXPANDING PEPTIDE STAPLING WITH s-TETRAZINE

Matthew H. Bunner

Professor Amos B. Smith, III

This dissertation presents efforts toward the extension of synthetic methods for the creation of peptide macrocycles via the addition of dichloro-s-tetrazine to peptide sequences containing lysine, serine, threonine, and tyrosine. Chapter one reviews the work and interest of the Smith group in the s-tetrazine chromophore and the history of stapled peptides in the chemical literature. Chapter two describes (A) the development of a synthetic protocol for the creation of peptide macrocycles from peptide sequences containing a single cysteine and a single lysine residue using dichloro-s-tetrazine including discussion on amino acid tolerance and seven successful examples, (B) efforts toward the development of a synthetic protocol for the creation of peptide macrocycles from peptide sequences containing a single cysteine residue and a single serine / threonine / tyrosine residue, and (C) efforts toward the investigation of the photochemical dissociation of the created cysteine / lysine peptide macrocycles. Chapter three describes our efforts to improve the synthesis of dichloro-s-tetrazine in a large-scale procedure.

## **Degree Type**

Dissertation

## **Degree Name**

Doctor of Philosophy (PhD)

## **Graduate Group**

Chemistry

## **First Advisor**

Amos B. Smith, III

## **Subject Categories**

Organic Chemistry

EXPANDING PEPTIDE STAPLING WITH *s*-TETRAZINE

Matthew H. Bunner

A DISSERTATION

in

Chemistry

Presented to the Faculties of the University of Pennsylvania

In Partial Fulfillment of the Requirements for the

Degree of Doctor of Philosophy

2019

Supervisor of Dissertation

---

Amos B. Smith, III  
Rhodes-Thompson Professor of Chemistry

Graduate Group Chairperson

---

David W. Christianson  
Roy and Diana Vagelos Professor in Chemistry and Chemical Biology

Dissertation Committee:

Jeffrey D. Winkler, Merriam Professor of Chemistry

David M. Chenoweth, Associate Professor of Chemistry

Feng Gai, Edmund J. and Louise W. Kahn Endowed Term Professor of Chemistry

This thesis is dedicated to my family.

Every new height I've reached was thanks to the environment and foundation you  
provided.

## ACKNOWLEDGMENTS

First and foremost I would like to thank Professor Amos B. Smith, III. Your support and encouragement over the last 5 years has been incredibly valuable. There were many times that I felt lost in the woods and wanted to give up and scrap this project, then you would remind me that “nothing worth doing is easy” and I’d decide to try one more experiment. Your work ethic and your commitment to your students have displayed values I will be trying to emulate for the rest of my life.

Next, I owe an enormous thanks to the members of my committee: Professor Jeffery D. Winkler, Professor David M. Chenoweth, and Professor Feng Gai. Your helpful suggestions and constructive criticism really helped me shape this project and showed me options I had overlooked.

To the late Dr. George Furst and Dr. Jun Gu, this project would not have come as far as it did without your help, both in instructing me as to which NMR experiments would be most beneficial to my work and in making the necessary instruments available to me. The trust you placed in me to run the Cryoprobe with no supervision, and to acquire data for other research groups during off hours, opened a lot of doors when I went looking for employment.

The past and current members of the Smith Group have all come together to provide a wonderful environment for science. No one will every say what we do is easy, but it is much easier with good comrades.

Finally, I would like to thank my parents. Even from 600 miles away, you were still my cheerleaders when I needed it most.

# ABSTRACT

## EXPANDING PEPTIDE STAPLING WITH *s*-TETRAZINE

Matthew H. Bunner

Professor Amos B. Smith, III

This dissertation presents efforts toward the extension of synthetic methods for the creation of peptide macrocycles *via* the addition of dichloro-*s*-tetrazine to peptide sequences containing lysine, serine, threonine, and tyrosine. Chapter one reviews the work and interest of the Smith group in the *s*-tetrazine chromophore and the history of stapled peptides in the chemical literature. Chapter two describes (A) the development of a synthetic protocol for the creation of peptide macrocycles from peptide sequences containing a single cysteine and a single lysine residue using dichloro-*s*-tetrazine including discussion on amino acid tolerance and *seven successful examples*, (B) efforts toward the development of a synthetic protocol for the creation of peptide macrocycles from peptide sequences containing a single cysteine residue and a single serine / threonine / tyrosine residue, and (C) efforts toward the investigation of the photochemical dissociation of the created cysteine / lysine peptide macrocycles. Chapter three describes our efforts to improve the synthesis of dichloro-*s*-tetrazine in a large-scale procedure.

## TABLE OF CONTENTS

<b>ABSTRACT .....</b>	<b>iv</b>
<b>LIST OF TABLES.....</b>	<b>vii</b>
<b>LIST OF FIGURES .....</b>	<b>vii</b>
<b>CHAPTER 1. EVALUATION OF S-TETRAZINE IN BIOPHYSICS: EARLY WORK .....</b>	<b>1</b>
<b>Importance of Peptides as Therapeutics.....</b>	<b>11</b>
<b>Challenges of Peptides as Therapeutics .....</b>	<b>11</b>
<b>Early Peptide Macrocycles.....</b>	<b>12</b>
<b>Synthetic Peptide Macrocycles .....</b>	<b>14</b>
<b>Modern Stapled Peptides .....</b>	<b>16</b>
<b>References – Chapter 1.....</b>	<b>18</b>
<b>CHAPTER 2. EXPANDING PEPTIDE STAPLING WITH DICHLORO-S-TETRAZINE .....</b>	<b>24</b>
<b>Modification of Cysteine/Lysine Peptides with Dichloro-s-tetrazine.....</b>	<b>25</b>
<b>Macrocyclization of Modified Peptides (3) Possessing a Lysine Side Chain .....</b>	<b>34</b>
<b>Scope and Tolerance of Cysteine/Lysine Stapling .....</b>	<b>38</b>
<b>Cys-Tet-Lys Macrocycles as Photochemical Substrates – Unexpected Difficulties! .....</b>	<b>49</b>
<b>Summary.....</b>	<b>55</b>
<b>References – Chapter 2.....</b>	<b>57</b>
<b>CHAPTER 3 – SCALE UP PREPARATION OF DICHLORO- S-TETRAZINE (1) .....</b>	<b>61</b>

<b>References – Chapter 3.....</b>	<b>66</b>
<b>EXPERIMENTAL .....</b>	<b>69</b>
<b>APPENDIX .....</b>	<b>108</b>



## LIST OF TABLES

<b>Table 1.1.</b> Photochemical dissociation of substituted tetrazines.....	4
<b>Table 1.2.</b> Evaluation of spacer length on photocleavage of <i>s</i> -tetrazine.....	6
<b>Table 2.1.</b> Competing residue scope.....	39

## LIST OF FIGURES

<b>Figure 1.1.</b> Photodissociation of <i>s</i> -tetrazine.....	1
<b>Figure 1.2.</b> Eliminated 1,4 bonding photodissociation pathway.....	1
<b>Figure 1.3.</b> Selective photodissociation of <sup>12</sup> C <sup>15</sup> N- <i>s</i> -tetrazine.....	2
<b>Figure 1.4.</b> Synthesis of [1-Cys, 6-Cys]- <i>S,S</i> -Tet-oxytocin.....	5
<b>Figure 1.5.</b> On-resin synthesis of <i>s</i> -tetrazine trimer peptide macrocycles.....	6
<b>Figure 1.6.</b> Liquid-phase peptide coupling of tetrazine macrocycles.....	7
<b>Figure 1.7.</b> Fragment union strategy for the construction of $\alpha$ -helical peptides.....	8
<b>Figure 1.8.</b> Peptide stapling and unstapling with dichloro- <i>s</i> -tetrazine.....	9
<b>Figure 1.9.</b> Dye-conjugation by inverse electron demand Diels Alder reaction.....	10
<b>Figure 1.10.</b> Gramicidin S.....	12
<b>Figure 1.11.</b> Four possible configurations of peptide macrocycles.....	13
<b>Figure 1.12.</b> Protein secondary structure cartoon of human PCNA.....	14
<b>Figure 1.13.</b> Early all-hydrocarbon peptide stapling.....	15
<b>Figure 1.14.</b> One-component and two-component peptide stapling.....	16
<b>Figure 2.1.</b> Modification of cys-ala-lys trimer peptide with dichloro- <i>s</i> -tetrazine.....	25
<b>Figure 2.2.</b> Proposed degradation pathway of hydroxy-tetrazine.....	27
<b>Figure 2.3.</b> Attempts at two-step, one-pot macrocyclization.....	30
<b>Figure 2.4.</b> Revised plan.....	30
<b>Figure 2.5.</b> Conditions for formation of <b>3</b> .....	32

<b>Figure 2.6.</b> “Block” and “shell” freezing of a 50 mL reaction mixture in a 100 mL vessel.....	33
<b>Figure 2.7.</b> Mass spectrum of crude isolate of compound <b>3</b> .....	34
<b>Figure 2.8.</b> Investigating macrocyclization conditions.....	34
<b>Figure 2.9.</b> HPLC purification of macrocycle <b>4</b> synthesis on small scale using sodium phosphate and sodium bicarbonate.....	35
<b>Figure 2.10.</b> HPLC purification of scaled up synthesis of <b>4</b> using sodium phosphate....	36
<b>Figure 2.11.</b> Successful conditions for the synthesis of macrocycle <b>4</b> .....	37
<b>Figure 2.12.</b> LC chromatogram data for macrocycle <b>12a</b> .....	39
<b>Figure 2.13.</b> More cys-tet-lys macrocycles.....	40
<b>Figure 2.14.</b> Differences in proton exchangeability between <b>2</b> and <b>4</b> .....	42
<b>Figure 2.15.</b> Solubility problems with macrocycles.....	42
<b>Figure 2.16.</b> Attempts at making cys-ser/thr macrocycles with <i>s</i> -tetrazine.....	44
<b>Figure 2.17.</b> Attempts at forming cys-tyr macrocycles with <i>s</i> -tetrazine.....	45
<b>Figure 2.18.</b> Synthesis of <b>36</b> – reaction mixture at 60 minutes.....	45
<b>Figure 2.19.</b> HPLC and LC/MS data from the first purification of <b>36</b> .....	46
<b>Figure 2.20.</b> Second HPLC purification of macrocycle <b>36</b> and <sup>1</sup> H NMR spectrum of isolated material.....	47
<b>Figure 2.21.</b> Third HPLC purification of <b>36</b> and LC/MS analysis of isolated material...	48
<b>Figure 2.22.</b> Synthesis of small molecule alkyl-tetrazine ethers.....	49
<b>Figure 2.23.</b> UV-vis absorption spectra of <i>S,S</i> -tetrazine and <i>S,N</i> -tetrazine peptides.....	50
<b>Figure 2.24.</b> Investigation of <i>S,N</i> -tetrazine photochemistry, first attempt.....	52
<b>Figure 2.25.</b> Net difference in IR spectrum after 5 hours of irradiation.....	53
<b>Figure 2.26.</b> UV-Vis absorption during the photolysis of <b>4</b> .....	53
<b>Figure 2.27.</b> Degradation pathways of cyanamides.....	54
<b>Figure 2.28.</b> Attempted trapping strategies.....	55
<b>Figure 3.1.</b> Original synthesis of dichloro- <i>s</i> -tetrazine ( <b>1</b> ).....	61

<b>Figure 3.2.</b> Chavez and Hiskey's synthesis of dichloro- <i>s</i> -tetrazine ( <b>1</b> ) using Coburn and coworker's intermediate ( <b>39</b> ).....	62
<b>Figure 3.3.</b> Modified synthesis of dichloro- <i>s</i> -tetrazine ( <b>1</b> ) using trichloroisocyanuric acid ( <b>41</b> ).....	62
<b>Figure 3.4.</b> Use of sodium nitrite for the synthesis of 3,6-bis(3,5-dimethyl-1H-pyrazol-1-yl)- <i>s</i> -tetrazine ( <b>39</b> ).....	63
<b>Figure 3.5.</b> Full route for the synthesis of dichloro- <i>s</i> -tetrazine ( <b>1</b> ).....	64
<b>Figure A.1.</b> 500 MHz <sup>1</sup> H-NMR Spectrum of <b>Peptide 2</b> in <i>d</i> <sub>6</sub> -DMSO.....	109
<b>Figure A.2.</b> 126 MHz <sup>13</sup> C-NMR Spectrum of <b>Peptide 2</b> in <i>d</i> <sub>6</sub> -DMSO.....	110
<b>Figure A.3.</b> LC/MS Chromatogram of <b>Peptide 2</b> .....	111
<b>Figure A.4.</b> 500 MHz <sup>1</sup> H-NMR Spectrum of <b>Peptide 10a</b> in <i>d</i> <sub>6</sub> -DMSO.....	112
<b>Figure A.5.</b> 126 MHz <sup>13</sup> C-NMR Spectrum of <b>Peptide 10a</b> in <i>d</i> <sub>6</sub> -DMSO.....	113
<b>Figure A.6.</b> 126 MHz DEPT-135 Spectrum <b>Peptide 2</b> in <i>d</i> <sub>6</sub> -DMSO.....	114
<b>Figure A.7.</b> HMBC Spectrum of <b>Peptide 10a</b> in <i>d</i> <sub>6</sub> -DMSO.....	115
<b>Figure A.8.</b> LC/MS Chromatogram of <b>Peptide 10a</b> .....	116
<b>Figure A.9.</b> 500 MHz <sup>1</sup> H-NMR Spectrum of <b>Peptide 10b</b> in <i>d</i> <sub>6</sub> -DMSO.....	117
<b>Figure A.10.</b> 126 MHz <sup>13</sup> C-NMR Spectrum of <b>Peptide 10b</b> in <i>d</i> <sub>6</sub> -DMSO.....	118
<b>Figure A.11.</b> 126 MHz DEPT-135 Spectrum <b>Peptide 10b</b> in <i>d</i> <sub>6</sub> -DMSO.....	119
<b>Figure A.12.</b> HMBC Spectrum of <b>Peptide 10b</b> in <i>d</i> <sub>6</sub> -DMSO.....	120
<b>Figure A.13.</b> 500 MHz <sup>1</sup> H-NMR Spectrum of <b>Peptide 10c</b> in <i>d</i> <sub>6</sub> -DMSO.....	121
<b>Figure A.14.</b> 126 MHz <sup>13</sup> C-NMR Spectrum of <b>Peptide 10c</b> in <i>d</i> <sub>6</sub> -DMSO.....	122
<b>Figure A.15.</b> 126 MHz DEPT-135 Spectrum <b>Peptide 10c</b> in <i>d</i> <sub>6</sub> -DMSO.....	123
<b>Figure A.16.</b> COSY Spectrum of <b>Peptide 10c</b> in <i>d</i> <sub>6</sub> -DMSO.....	124
<b>Figure A.17.</b> HSQC Spectrum of <b>Peptide 10c</b> in <i>d</i> <sub>6</sub> -DMSO.....	125
<b>Figure A.18.</b> HMBC Spectrum of <b>Peptide 10c</b> in <i>d</i> <sub>6</sub> -DMSO.....	126
<b>Figure A.19.</b> 500 MHz <sup>1</sup> H-NMR Spectrum of <b>Peptide 10d</b> in <i>d</i> <sub>6</sub> -DMSO.....	127
<b>Figure A.20.</b> 126 MHz <sup>13</sup> C-NMR Spectrum of <b>Peptide 10d</b> in <i>d</i> <sub>6</sub> -DMSO.....	128

<b>Figure A.21.</b> 126 MHz DEPT-135 Spectrum <b>Peptide 10d</b> in $d_6$ -DMSO.....	129
<b>Figure A.22.</b> COSY Spectrum of <b>Peptide 10d</b> in $d_6$ -DMSO.....	130
<b>Figure A.23.</b> HSQC Spectrum of <b>Peptide 10d</b> in $d_6$ -DMSO.....	131
<b>Figure A.24.</b> HMBC Spectrum of <b>Peptide 10d</b> in $d_6$ -DMSO.....	132
<b>Figure A.25.</b> LC/MS Chromatogram of <b>Peptide 10d</b> .....	133
<b>Figure A.26.</b> 500 MHz $^1\text{H}$ -NMR Spectrum of <b>Peptide 19</b> in $d_6$ -DMSO.....	134
<b>Figure A.27.</b> 126 MHz $^{13}\text{C}$ -NMR Spectrum of <b>Peptide 19</b> in $d_6$ -DMSO.....	135
<b>Figure A.28.</b> 126 MHz DEPT-135 Spectrum <b>Peptide 19</b> in $d_6$ -DMSO.....	136
<b>Figure A.29.</b> HMBC Spectrum of <b>Peptide 19</b> in $d_6$ -DMSO.....	137
<b>Figure A.30.</b> 500 MHz $^1\text{H}$ -NMR Spectrum of <b>Peptide 32</b> in $d_6$ -DMSO.....	138
<b>Figure A.31.</b> 126 MHz $^{13}\text{C}$ -NMR Spectrum of <b>Peptide 32</b> in $d_6$ -DMSO.....	139
<b>Figure A.32.</b> 500 MHz $^1\text{H}$ -NMR Spectrum of <b>Peptide SI-1</b> in $d_6$ -DMSO.....	140
<b>Figure A.33.</b> 126 MHz $^{13}\text{C}$ -NMR Spectrum of <b>Peptide SI-1</b> in $d_6$ -DMSO.....	141
<b>Figure A.34.</b> 126 MHz DEPT-135 Spectrum of <b>Peptide SI-1</b> in $d_6$ -DMSO.....	142
<b>Figure A.35.</b> COSY Spectrum of <b>Peptide SI-1</b> in $d_6$ -DMSO.....	143
<b>Figure A.36.</b> HSQC Spectrum of <b>Peptide SI-1</b> in $d_6$ -DMSO.....	144
<b>Figure A.37.</b> HMBC Spectrum of <b>Peptide SI-1</b> in $d_6$ -DMSO.....	145
<b>Figure A.38.</b> LC/MS Chromatogram of <b>Peptide SI-1</b> .....	146
<b>Figure A.39.</b> 500 MHz $^1\text{H}$ -NMR Spectrum of <b>Peptide SI-2</b> in $d_6$ -DMSO.....	147
<b>Figure A.40.</b> 126 MHz $^{13}\text{C}$ -NMR Spectrum of <b>Peptide SI-2</b> in $d_6$ -DMSO.....	148
<b>Figure A.41.</b> 126 MHz DEPT-135 Spectrum of <b>Peptide SI-2</b> in $d_6$ -DMSO.....	149
<b>Figure A.42.</b> COSY Spectrum of <b>Peptide SI-2</b> in $d_6$ -DMSO.....	150
<b>Figure A.43.</b> HSQC Spectrum of <b>Peptide SI-2</b> in $d_6$ -DMSO.....	151
<b>Figure A.44.</b> HMBC Spectrum of <b>Peptide SI-2</b> in $d_6$ -DMSO.....	152
<b>Figure A.45.</b> LC/MS Chromatogram of <b>Peptide SI-2</b> .....	153
<b>Figure A.46.</b> 500 MHz $^1\text{H}$ -NMR Spectrum of <b>Peptide SI-3</b> in $d_6$ -DMSO.....	154

<b>Figure A.47.</b> 126 MHz $^{13}\text{C}$ -NMR Spectrum of <b>Peptide SI-3</b> in $d_6$ -DMSO.....	155
<b>Figure A.48.</b> 126 MHz DEPT-135 Spectrum of <b>Peptide SI-3</b> in $d_6$ -DMSO.....	156
<b>Figure A.49.</b> LC/MS Chromatogram of <b>Peptide SI-3</b> .....	157
<b>Figure A.50.</b> 500 MHz $^1\text{H}$ -NMR Spectrum of <b>Peptide SI-4</b> in $d_6$ -DMSO.....	158
<b>Figure A.51.</b> 126 MHz $^{13}\text{C}$ -NMR Spectrum of <b>Peptide SI-4</b> in $d_6$ -DMSO.....	159
<b>Figure A.52.</b> 126 MHz DEPT-135 Spectrum of <b>Peptide SI-4</b> in $d_6$ -DMSO.....	160
<b>Figure A.53.</b> COSY Spectrum of <b>Peptide SI-4</b> in $d_6$ -DMSO.....	161
<b>Figure A.54.</b> HSQC Spectrum of <b>Peptide SI-4</b> in $d_6$ -DMSO.....	162
<b>Figure A.55.</b> HMBC Spectrum of <b>Peptide SI-4</b> in $d_6$ -DMSO.....	163
<b>Figure A.56.</b> LC/MS Chromatogram of <b>Peptide SI-4</b> .....	164
<b>Figure A.57.</b> 500 MHz $^1\text{H}$ -NMR Spectrum of <b>Peptide SI-5</b> in $d_6$ -DMSO.....	165
<b>Figure A.58.</b> 126 MHz $^{13}\text{C}$ -NMR Spectrum of <b>Peptide SI-5</b> in $d_6$ -DMSO.....	166
<b>Figure A.59.</b> LC/MS Chromatogram of <b>Peptide SI-5</b> .....	167
<b>Figure A.60.</b> 500 MHz $^1\text{H}$ -NMR Spectrum of <b>Peptide SI-6</b> in $d_6$ -DMSO.....	168
<b>Figure A.61.</b> 126 MHz $^{13}\text{C}$ -NMR Spectrum of <b>Peptide SI-6</b> in $d_6$ -DMSO.....	169
<b>Figure A.62.</b> 126 MHz DEPT-135 Spectrum of <b>Peptide SI-6</b> in $d_6$ -DMSO.....	170
<b>Figure A.63.</b> 500 MHz $^1\text{H}$ -NMR Spectrum of <b>Peptide SI-7</b> in $d_6$ -DMSO.....	171
<b>Figure A.64.</b> 126 MHz $^{13}\text{C}$ -NMR Spectrum of <b>Peptide SI-7</b> in $d_6$ -DMSO.....	172
<b>Figure A.65.</b> 126 MHz DEPT-135 Spectrum of <b>Peptide SI-7</b> in $d_6$ -DMSO.....	173
<b>Figure A.66.</b> HMBC Spectrum of <b>Peptide SI-7</b> in $d_6$ -DMSO.....	174
<b>Figure A.67.</b> LC/MS Chromatogram of <b>Peptide SI-7</b> .....	175
<b>Figure A.68.</b> 500 MHz $^1\text{H}$ -NMR Spectrum of <b>Peptide SI-8</b> in $d_6$ -DMSO.....	176
<b>Figure A.69.</b> 126 MHz $^{13}\text{C}$ -NMR Spectrum of <b>Peptide SI-8</b> in $d_6$ -DMSO.....	177
<b>Figure A.70.</b> 126 MHz DEPT-135 Spectrum of <b>Peptide SI-8</b> in $d_6$ -DMSO.....	178
<b>Figure A.71.</b> LC/MS Chromatogram of <b>Peptide SI-8</b> .....	179
<b>Figure A.72.</b> 500 MHz $^1\text{H}$ -NMR Spectrum of <b>Peptide SI-9</b> in $d_6$ -DMSO.....	180

<b>Figure A.73.</b> 126 MHz $^{13}\text{C}$ -NMR Spectrum of <b>Peptide SI-9</b> in $d_6$ -DMSO.....	181
<b>Figure A.74.</b> LC/MS Chromatogram of <b>Peptide SI-9</b> .....	182
<b>Figure A.75.</b> 500 MHz $^1\text{H}$ -NMR Spectrum of <b>Macrocycle 4</b> in $d_6$ -DMSO.....	183
<b>Figure A.76.</b> 126 MHz $^{13}\text{C}$ -NMR Spectrum of <b>Macrocycle 4</b> in $d_6$ -DMSO.....	184
<b>Figure A.77.</b> 126 MHz DEPT-135 Spectrum of <b>Macrocycle 4</b> in $d_6$ -DMSO.....	185
<b>Figure A.78.</b> HMBC Spectrum of <b>Macrocycle 4</b> in $d_6$ -DMSO.....	186
<b>Figure A.79.</b> 500 MHz $^1\text{H}$ -NMR Spectrum of <b>Macrocycle 12c</b> in $d_6$ -DMSO.....	187
<b>Figure A.80.</b> 126 MHz $^{13}\text{C}$ -NMR Spectrum of <b>Macrocycle 12c</b> in $d_6$ -DMSO.....	188
<b>Figure A.81.</b> 126 MHz DEPT-135 Spectrum of <b>Macrocycle 12c</b> in $d_6$ -DMSO.....	189
<b>Figure A.82.</b> TOCSY Spectrum of <b>Macrocycle 12c</b> in $d_6$ -DMSO.....	190
<b>Figure A.83.</b> HSQC Spectrum of <b>Macrocycle 12c</b> in $d_6$ -DMSO.....	191
<b>Figure A.84.</b> HMBC Spectrum of <b>Macrocycle 12c</b> in $d_6$ -DMSO.....	192
<b>Figure A.85.</b> 500 MHz $^1\text{H}$ -NMR Spectrum of <b>Macrocycle 12d</b> in $d_6$ -DMSO.....	193
<b>Figure A.86.</b> 126 MHz $^{13}\text{C}$ -NMR Spectrum of <b>Macrocycle 12d</b> in $d_6$ -DMSO.....	194
<b>Figure A.87.</b> 126 MHz DEPT-135 Spectrum of <b>Macrocycle 12d</b> in $d_6$ -DMSO.....	195
<b>Figure A.88.</b> COSY Spectrum of <b>Macrocycle 12d</b> in $d_6$ -DMSO.....	196
<b>Figure A.89.</b> HSQC Spectrum of <b>Macrocycle 12d</b> in $d_6$ -DMSO.....	197
<b>Figure A.90.</b> HMBC Spectrum of <b>Macrocycle 12d</b> in $d_6$ -DMSO.....	198
<b>Figure A.91.</b> 500 MHz $^1\text{H}$ -NMR Spectrum of <b>Macrocycle 13</b> in $d_6$ -DMSO.....	199
<b>Figure A.92.</b> 126 MHz $^{13}\text{C}$ -NMR Spectrum of <b>Macrocycle 13</b> in $d_6$ -DMSO.....	200
<b>Figure A.93.</b> 126 MHz DEPT-135 Spectrum of <b>Macrocycle 13</b> in $d_6$ -DMSO.....	201
<b>Figure A.94.</b> COSY Spectrum of <b>Macrocycle 13</b> in $d_6$ -DMSO.....	202
<b>Figure A.95.</b> HSQC Spectrum of <b>Macrocycle 13</b> in $d_6$ -DMSO.....	203
<b>Figure A.96.</b> HMBC Spectrum of <b>Macrocycle 13</b> in $d_6$ -DMSO.....	204
<b>Figure A.97.</b> 500 MHz $^1\text{H}$ -NMR Spectrum of <b>Macrocycle 14</b> in $d_6$ -DMSO.....	205
<b>Figure A.98.</b> 126 MHz $^{13}\text{C}$ -NMR Spectrum of <b>Macrocycle 14</b> in $d_6$ -DMSO.....	206

<b>Figure A.99.</b> 126 MHz DEPT-135 Spectrum of <b>Macrocycle 14</b> in $d_6$ -DMSO.....	207
<b>Figure A.100.</b> COSY Spectrum of <b>Macrocycle 14</b> in $d_6$ -DMSO.....	208
<b>Figure A.101.</b> HSQC Spectrum of <b>Macrocycle 14</b> in $d_6$ -DMSO.....	209
<b>Figure A.102.</b> HMBC Spectrum of <b>Macrocycle 14</b> in $d_6$ -DMSO.....	210
<b>Figure A.103.</b> 500 MHz $^1\text{H}$ -NMR Spectrum of <b>Macrocycle 15</b> in $d_6$ -DMSO.....	211
<b>Figure A.104.</b> 126 MHz $^{13}\text{C}$ -NMR Spectrum of <b>Macrocycle 15</b> in $d_6$ -DMSO.....	212
<b>Figure A.105.</b> 126 MHz DEPT-135 Spectrum of <b>Macrocycle 15</b> in $d_6$ -DMSO.....	213
<b>Figure A.106.</b> COSY Spectrum of <b>Macrocycle 15</b> in $d_6$ -DMSO.....	214
<b>Figure A.107.</b> HSQC Spectrum of <b>Macrocycle 15</b> in $d_6$ -DMSO.....	215
<b>Figure A.108.</b> HMBC Spectrum of <b>Macrocycle 15</b> in $d_6$ -DMSO.....	216
<b>Figure A.109.</b> 500 MHz $^1\text{H}$ -NMR Spectrum of <b>Macrocycle 16</b> in $d_6$ -DMSO.....	217
<b>Figure A.110.</b> 126 MHz $^{13}\text{C}$ -NMR Spectrum of <b>Macrocycle 16</b> in $d_6$ -DMSO.....	218
<b>Figure A.111.</b> 126 MHz DEPT-135 Spectrum of <b>Macrocycle 16</b> in $d_6$ -DMSO.....	219
<b>Figure A.112.</b> COSY Spectrum of <b>Macrocycle 16</b> in $d_6$ -DMSO.....	220
<b>Figure A.113.</b> HSQC Spectrum of <b>Macrocycle 16</b> in $d_6$ -DMSO.....	221
<b>Figure A.114.</b> 126 MHz $^{13}\text{C}$ -NMR Spectrum of <b>Compound 42</b> in $\text{D}_2\text{O}$ .....	222
<b>Figure A.115.</b> 500 MHz $^1\text{H}$ -NMR Spectrum of <b>Compound 43</b> in $\text{CDCl}_3$ .....	223
<b>Figure A.116.</b> 126 MHz $^{13}\text{C}$ -NMR Spectrum of <b>Compound 43</b> in $\text{CDCl}_3$ .....	224
<b>Figure A.117.</b> 500 MHz $^1\text{H}$ -NMR Spectrum of <b>Compound 39</b> in $\text{CDCl}_3$ .....	225
<b>Figure A.118.</b> 126 MHz $^{13}\text{C}$ -NMR Spectrum of <b>Compound 39</b> in $\text{CDCl}_3$ .....	226
<b>Figure A.119.</b> 126 MHz $^{13}\text{C}$ -NMR Spectrum of <b>Compound 38</b> in $d_6$ -DMSO.....	227
<b>Figure A.120.</b> 126 MHz $^{13}\text{C}$ -NMR Spectrum of <b>Compound 1</b> in $\text{CDCl}_3$ .....	228

## CHAPTER 1. Evaluation of *s*-Tetrazine in Biophysics: Early Work

In 1975, King and Hochstrasser reported that, upon excitation at an appropriate wavelength by a tunable dye laser, *s*-tetrazine would fragment to give two equivalents of hydrogen cyanide and one equivalent of nitrogen gas (**Figure 1.1**).<sup>1</sup> This discovery

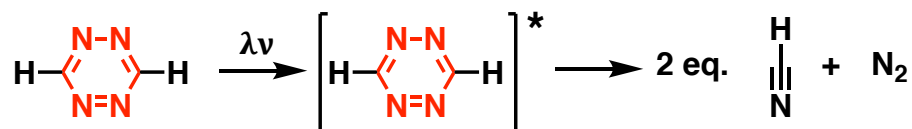


**Figure 1.1.** Photodissociation of *s*-tetrazine<sup>1</sup>

was followed by a collaborative effort between King, Hochstrasser, and Smith to investigate the reaction pathway of this photodissociation *via* the synthesis and subsequent decomposition of 1,4-*s*-tetrazine-<sup>15</sup>N<sub>2</sub>. Through mass analysis of the products of the photolysis, King *et al.* were able to show that it was highly unlikely a Dewar-benzene type intermediate was involved because the required 1,4-bonding pattern would yield nitrogen gas molecules registering *m/z* values of 28 or 30 (**Figure 1.2**). Instead, the *m/z* value observed was 29, corresponding to exclusively <sup>14</sup>N<sup>15</sup>N molecular nitrogen.<sup>2</sup>

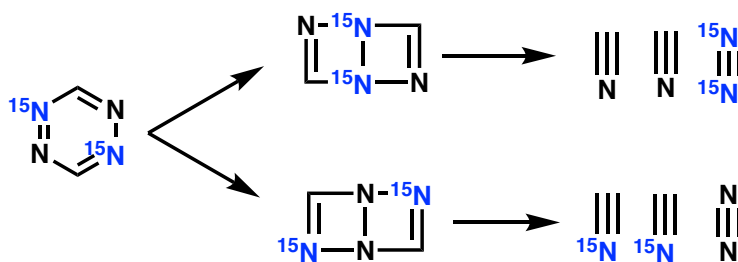


**Figure 1.2.** Eliminated 1,4 bonding photodissociation pathway<sup>2</sup>



Dellinger and other members of this collaboration also reported a method for the exclusive photodecomposition of  $^{12}\text{C}_2^{14}\text{N}_4$ -tetrazine in the presence of *s*-tetrazine molecules containing the natural abundance of  $^{13}\text{C}$  and  $^{15}\text{N}$ , thereby proving that the enrichment of a material *via* photo-ablation was possible (**Figure 1.3**).<sup>3,4</sup> This constituted laser-induced isotope separation.

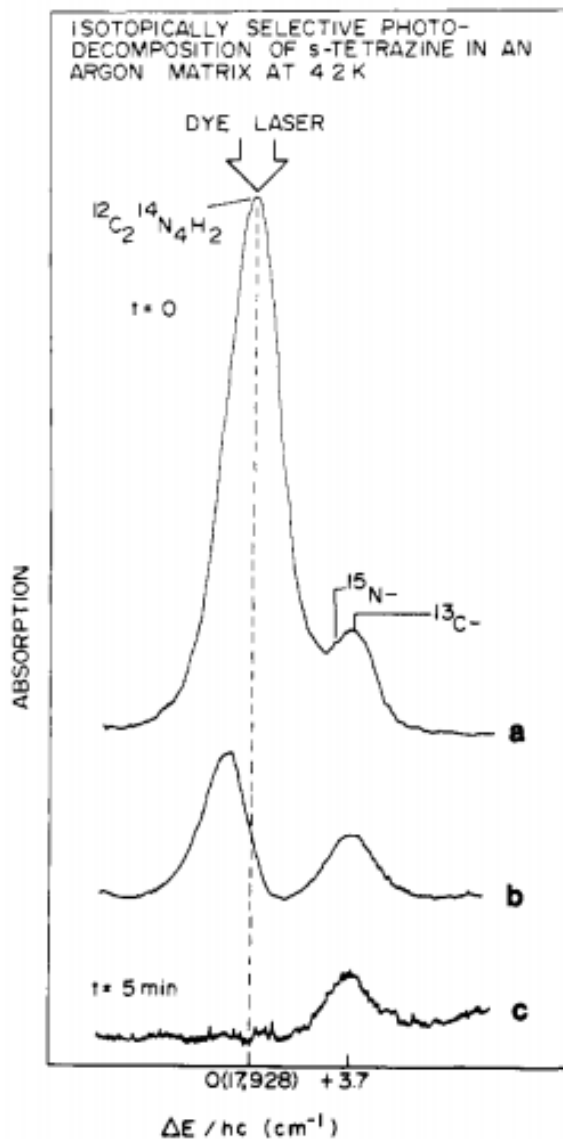


**Figure 1.3.** Selective photodissociation of  $^{12}\text{C}^{15}\text{N}$ -*s*-tetrazine. Reprinted with permission from *J. Am. Chem. Soc.* **1977**, 99(22), 7138-7142. Copyright 1997 American Chemical Society.<sup>4</sup>

A wealth of literature appeared over the next few years concerning the reaction pathways of different *s*-tetrazine derivatives and how those pathways changed based on irradiation in vapor phase, mixed crystal, or solution phase experiments.<sup>5-10</sup> The conclusions drawn from these experiments were that the photodissociation pathway of *s*-tetrazines is highly dependent on substitution, solvent, photon energy, and light source intensity.<sup>6,7</sup> One trend that held throughout these investigations was that attaching substituents to the parent ring lowered the yield of the photodissociation.<sup>7,8</sup> This trend is exemplified by 3,6-diphenyl-*s*-tetrazine,<sup>8</sup> in that  $\pi$ -bond delocalization outside of the tetrazine core permits the phenyl substituents to serve as “heat fins” for the dissipation of vibrational energy (**Table 1.1, Entry 1-3**). However, Tucker and coworkers were able to demonstrate that including sulfur disrupts the vibrational connection to the substituents, thereby increasing the efficiency of the photochemical process. Two possible explanations exist as to why the change to sulfur increases the yield of the photochemical reaction. One is that the sulfur atoms are sufficiently massive to serve as a barrier to energy transfer *via* vibration.<sup>11</sup> This effect is referred to as “the heavy atom-effect.”<sup>12</sup> The other possible explanation is that the switch to sulfur has opened up new photochemical pathways that did not exist in the carbon and hydrogen substituted *s*-tetrazines. There was some experimental evidence presented for this, but further work was never carried out.<sup>11</sup> Other work also highlight the huge difference in photochemical properties between *s*-tetrazines substituted with heteroatoms.<sup>13-15</sup> Not only could 3,6-*bis*(benzylthio)-*s*-tetrazine undergo photolysis at an acceptable yield under irradiation by 355 nm light, but the compound would also undergo photolysis upon irradiation with a 410 nm light source (**Table 1.1, Entry 4**). This made the *bis*(benzylthio)-tetrazine derivative amenable to

biological investigation because peptides and proteins do not generally absorb at this wavelength. This beneficial effect carried over to an *s*-tetrazine derivative substituted with two cysteine residues (**Table 1, Entry 5**). Upon irradiation, fragmentation of the tetrazine chromophore occurred within a few hundred picoseconds, making this a possible molecule for studying folding interactions in proteins.

Table 1.1. Photochemical dissociation of substituted tetrazines. <sup>11</sup>		
Entry	R	Yield (Light Source)
1		~90% (532 nm)
2		~17% (532 nm)
3		~1% (532 nm)
4		24% (355 nm)
		12% (410 nm)
5		11% (410 nm)

To verify the compatibility of the *s*-tetrazine chromophore with biological systems and peptide synthesis, Tucker and coworkers developed a method to bridge two proximal cysteine residues of a growing peptide chain during solid phase peptide synthesis *via* dichloro-*s*-tetrazine (**1**) and an orthogonal protection strategy using highly acid-labile monomethoxytrityl (Mmt) in place of the trityl groups standard to Fmoc solid phase peptide synthesis (**Figure 1.4**).<sup>11</sup> This resulted in the creation of an oxytocin

analogue with *s*-tetrazine bridging the disulfide bond, proving that the tetrazine chromophore was compatible with both Fmoc solid phase peptide synthesis and with cyclic peptides.<sup>11</sup> Photolysis rate and yield of this cyclic tetrazine construct was similar to the acyclic versions (Table 1.1, Entry 4-5).<sup>11</sup>

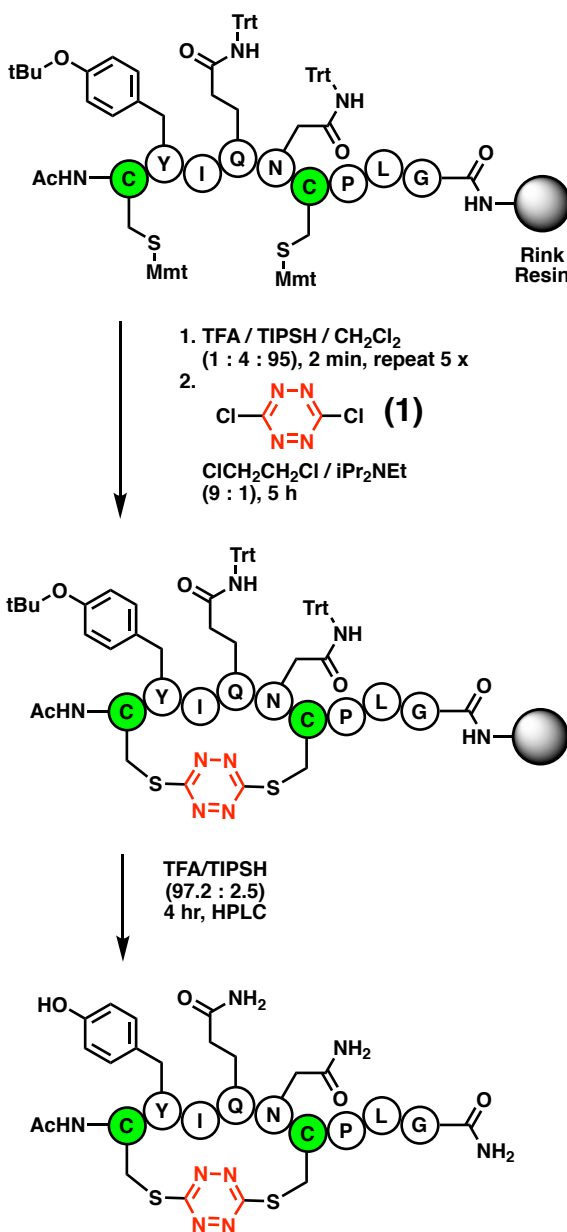
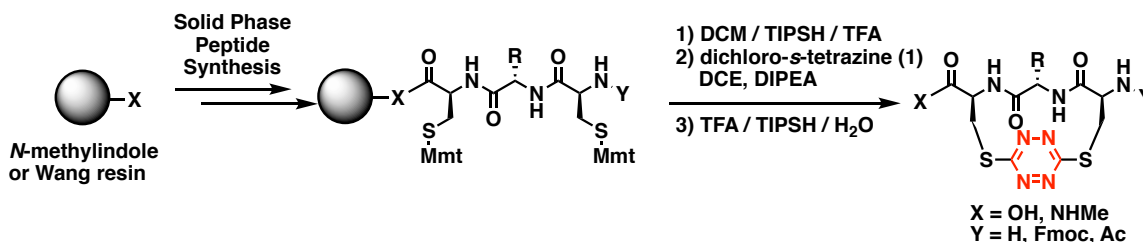


Figure 1.4. Synthesis of [1-Cys, 6-Cys]-*S,S*-Tet-oxytocin<sup>11</sup>

This method for the creation of *s*-tetrazine cyclic peptides *via* incorporation of dichloro-*s*-tetrazine during solid phase synthesis was then further investigated by Abdo and coworkers.<sup>16</sup> To test the amino acid compatibility of the synthetic protocol, Abdo *et al.* synthesized a series of peptide trimers featuring two cysteine residues in an *i, i+2* arrangement with a variable central amino acid (**Figure 1.5**).<sup>16</sup> A variety of reactive or



**Figure 1.5.** On-resin synthesis of *s*-tetrazine trimer peptide macrocycles<sup>16</sup>

sterically bulky amino acids were included at the variable position (R), with all tested residues except arginine being well tolerated.<sup>16</sup> Next, using this method, the effect of amino acid spacer length (*i, i+x*) on the photochemical reaction of *s*-tetrazine was evaluated (**Table 1.2**).<sup>16</sup> The original *i, i+2* configuration, corresponding to a half turn of

Table 1.2. Evaluation of spacer length on photocleavage of <i>s</i> -tetrazine <sup>16</sup>		
<p> <math>h\nu</math> (355 nm)  R = Ala, Lys  X = OH, NHMe  Y = H, Fmoc, Ac  n = 1 - 3 </p>		
Entry	Cys Relationship	Photochemical Yield
1	( <i>i, i + 2</i> )	> 25 %
2	( <i>i, i + 3</i> )	> 15 %
3	( <i>i, i + 4</i> )	~ 10 %

an  $\alpha$ -helix, was found to give the best yield (**Table 1.2, Entry 1**). Finally, Abdo and coworkers demonstrated that, while this on-resin macrocyclization method was not amendable to long peptide sequences, these trimer peptide macrocycles could undergo further liquid phase peptide couplings, so other peptide fragments could be added to build up larger peptide structures of interest (**Figure 1.6**).<sup>16</sup>

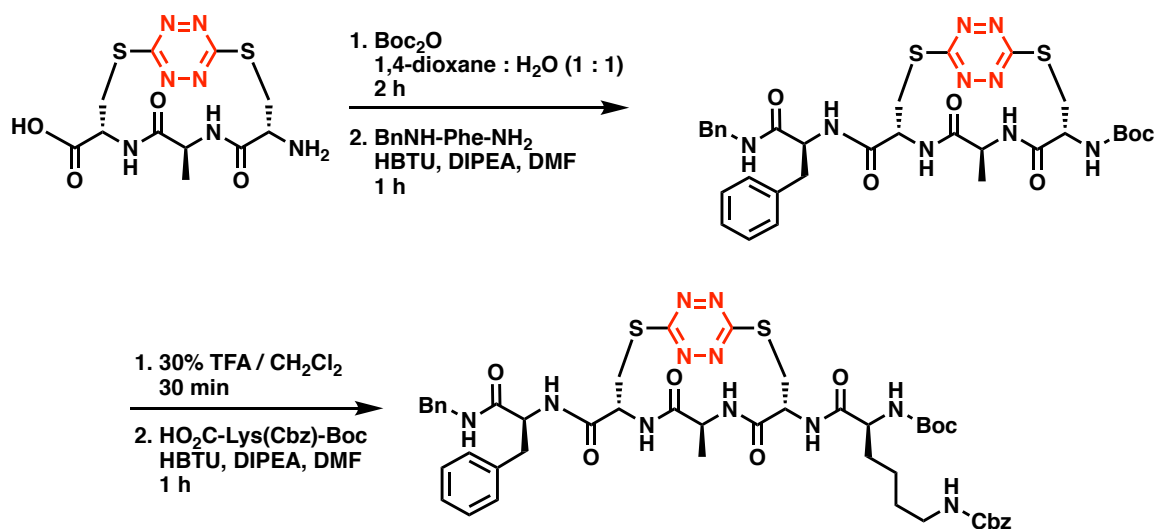


**Figure 1.6.** Liquid-phase peptide coupling of tetrazine macrocycles<sup>16</sup>

These trimer peptide tetrazine macrocycles were then used as the cores of a tri-component union strategy to make alanine-rich  $\alpha$ -helical peptides with a constrained photo-cleavable kink built into the center (**Figure 1.7**).<sup>17</sup> By strategically placing  $^{13}\text{C}$ - $^{18}\text{O}$  labeled carbonyl pairs at different points within the peptide, it was possible to measure rotational changes in the peptide backbone using ultrafast 2D-IR spectroscopy.<sup>18</sup> Upon photochemical cleavage of the tetrazine chromophore, the kinked helix at the center of the peptide was released, and progress of the formation of a single new helical turn could be followed *via* the unique IR signal of the enriched carbonyl pair. These measurements established that the kink does not propagate through the helix upon release. Rather, a

simple rotation about the previously restricted backbone to reestablish a full turn of the helix.<sup>18</sup> According to Hochstrasser (private communication to Smith) there is currently no theory to explain this folding process.

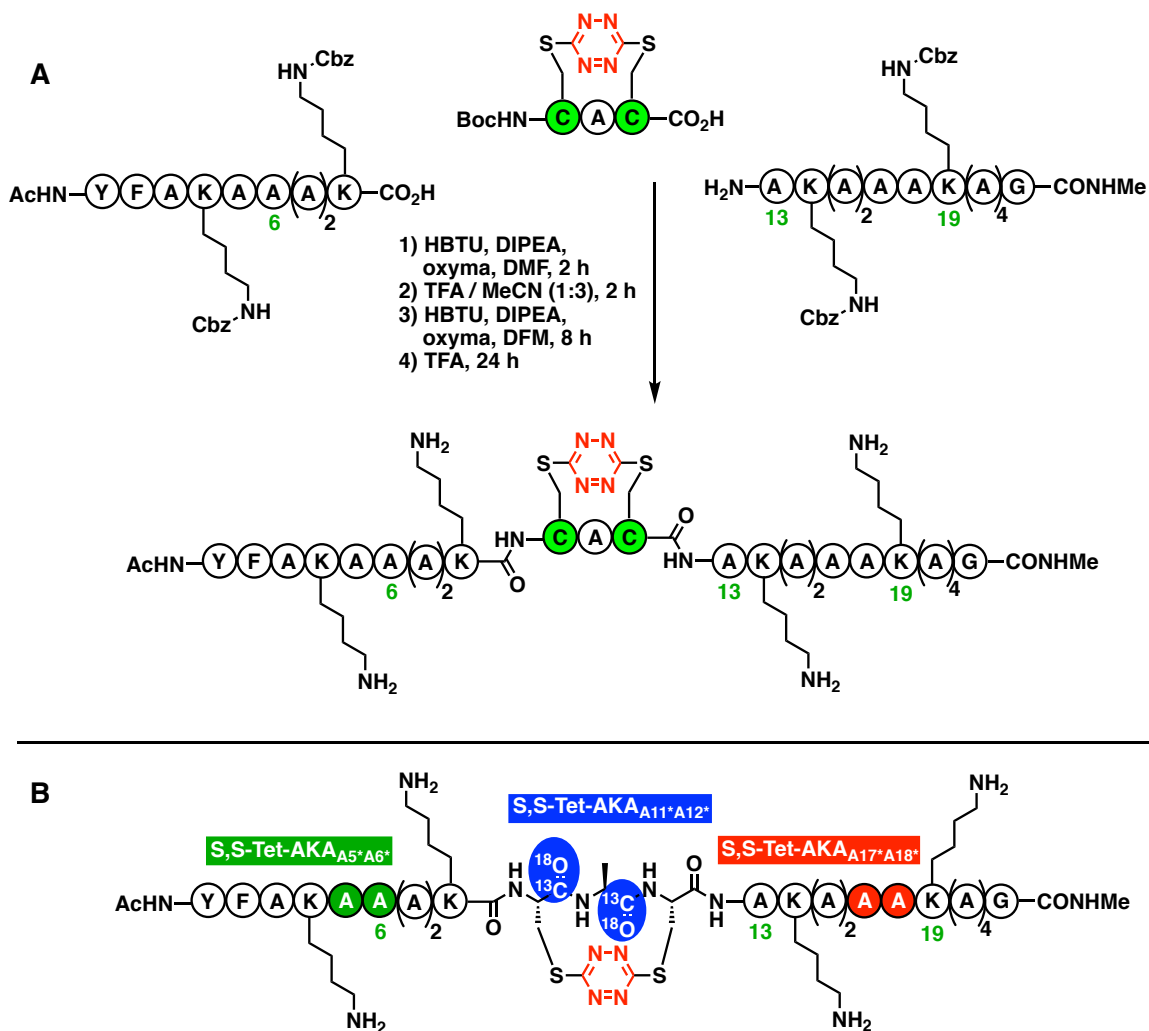


**Figure 1.7.** A) Fragment union strategy for the construction of  $\alpha$ -helical peptides<sup>17</sup> B) Placement of  $^{13}\text{C}$ - $^{18}\text{O}$  labeled carbonyls for 2D-IR experiments<sup>18</sup>

With this background, Brown and Smith devised and reported a method to get away from on-resin synthesis and instead to incorporate the *s*-tetrazine linker into fully deprotected peptides in solution. That is, they developed a method for the creation of stapled peptides, *via* the incorporation of dichloro-*s*-tetrazine between the thiol side-

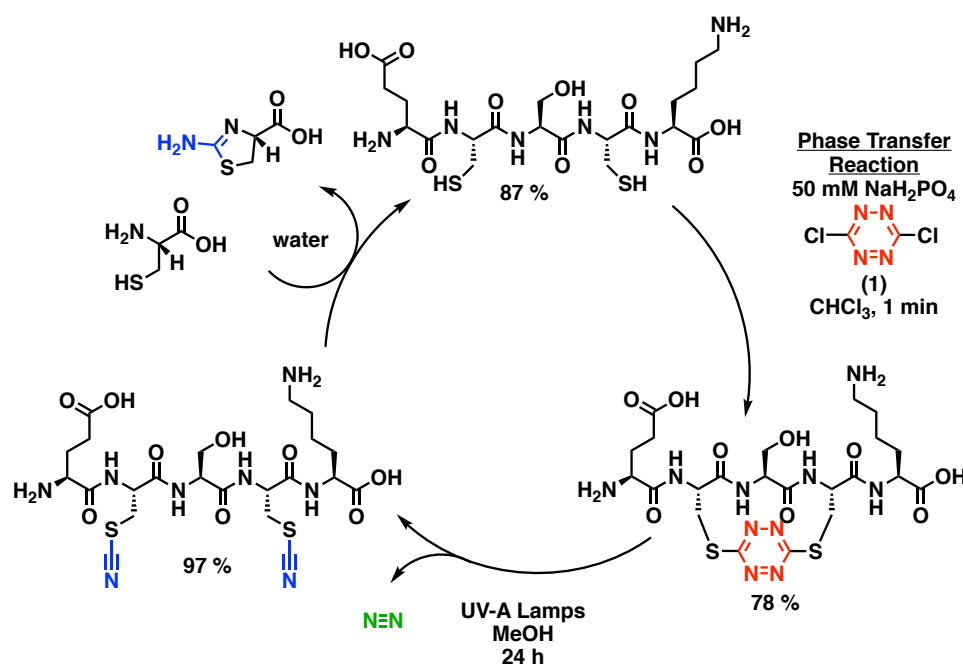


**Figure 1.8.** Peptide stapling and unstapling with dichloro-*s*-tetrazine (1)<sup>19</sup>

chains of two proximal cysteine residues in unprotected peptides prepared by standard Fmoc solid-phase peptide synthesis (SPPS).<sup>19</sup> Following purification, these stapled peptides could be subjected to steady-state irradiation under UV-A lamps, cleaving the tetrazine chromophore and releasing the peptide macrocycle as the dithiocyanate. Unlike the early introduction of staples like Grubbs and Verdine (*vide infra*),<sup>20,21</sup> this was the first example of a synthetic organic staple that could be successfully removed with little perturbation to the parent peptide. These masked thiols could then be freed by exposing



the dithiocyanate peptide to a solution of cysteine, removing the nitriles in a fashion similar to native-chemical ligation (**Figure 1.8**).<sup>22</sup> Brown was also able to perform an inverse electron-demand Diels-Alder reaction between the tetrazine chromophore and a fluorescein dye conjugated to bicyclononyl (**Figure 1.9**).<sup>19</sup> This reaction, commonly called “tetrazine ligation,” is a bioorthogonal click reaction and the most common use of tetrazine in the literature today.<sup>23,24</sup>

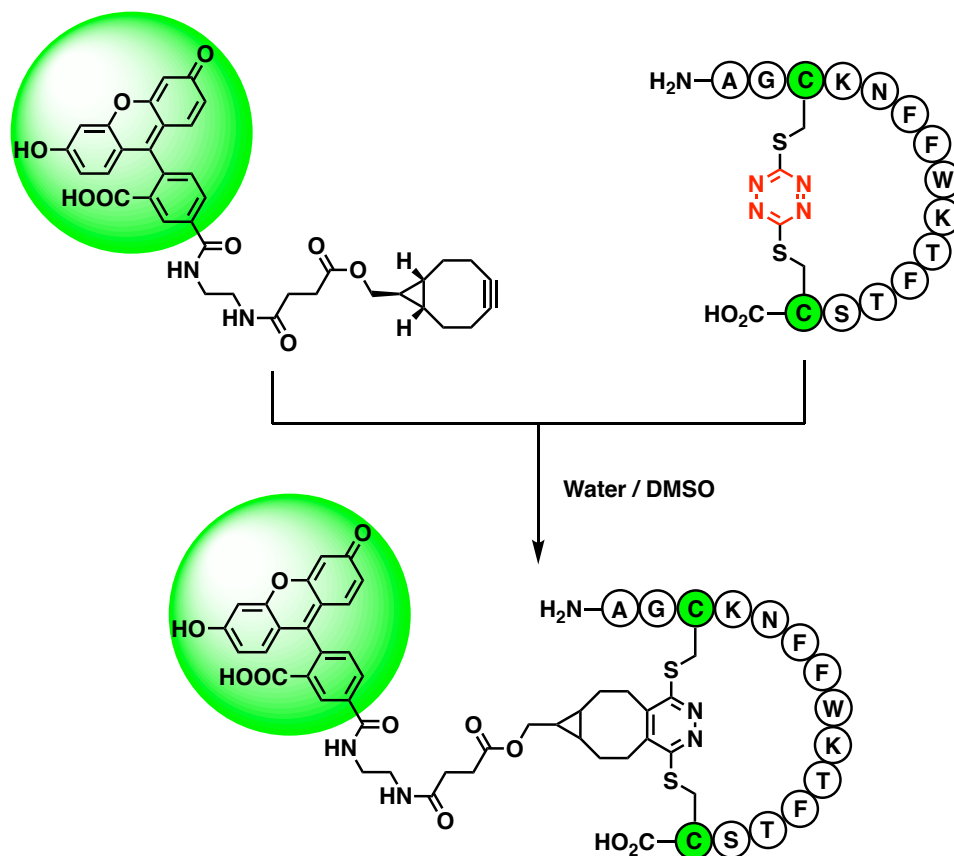


**Figure 1.9.** Dye-conjugation by inverse electron demand Diels Alder reaction<sup>19</sup>

The question that remained at this point in the Hochstrasser-Smith collaboration was: *Are there other nucleophile side chains that might participate in cysteine cyclic ligations to expand the utility of this cyclic peptide construct tactic?* Before we discuss our investigative effort to probe this question, we should provide some discussion on (a)

the history of peptide macrocycles, (b) their importance to the chemical community, (c) prominent methods for their creation, and (d) where *s*-tetrazine fits within that history.

### **Importance of Peptides as Therapeutics**

Peptides and proteins have long been thought to hold great therapeutic potential by the medicinal chemistry community.<sup>25</sup> Through the manipulation of their primary structure and secondary conformations, it might be possible to unlock new peptide tools to probe biological mysteries or treat illnesses. That is, peptides nicely bridge the chemical space in between small molecules and large biologics,<sup>26</sup> offering the potential therapeutics to modulate targets previously considered “undruggable.”<sup>25</sup> For example, small molecules are typically considered ill-suited to target the shallow activation site and large surface area of protein-protein interactions (PPIs).<sup>27</sup> Small molecules are also more likely to produce side effects because of the accumulation of metabolites in sensitive tissues.<sup>28</sup> When compared to larger biologics, peptides are often better suited to modulating intracellular targets as their smaller size increases their relative ability to diffuse across cell membranes.<sup>28</sup> From a more practical standpoint, peptides also have a much lower manufacturing cost, and much better room-temperature stability, than large biological therapeutics.<sup>28</sup>

### **Challenges of Peptides as Therapeutics**

This is not to say that peptides are free of challenges as therapeutic molecules. Being made of amino acids, peptides are typically considered poor targets because of their pharmacokinetic profile.<sup>28</sup> Because many proteolytic enzymes recognize common structural motifs in unmodified peptides, they typically have poor *in vivo* stability against

proteases.<sup>28</sup> Additionally, the liver and kidneys both rapidly remove circulating peptides from the blood, often resulting in biological half-lives in the range of minutes.<sup>28</sup> The oral availability of peptides is also rather poor due to low absorption by the impermeable gastrointestinal epithelium, the activity of peptidases, and the acidic environment of the stomach.<sup>29</sup> Lastly, peptides tend not to be as conformationally rigid as small molecules.<sup>26</sup> The time peptides spend sampling different local energy minima across conformational space is time not spent providing a therapeutic benefit, lowering binding efficiency and overall efficacy.

### Early Peptide Macrocycles

Nature provided inspiration for a solution to these problems with the discovery of antibacterial peptide gramicidin S (**Figure 1.10**) by Gause and Brazhnikova in 1944.<sup>30</sup> Syngé later identified that gramicidin S is a cyclic peptide.<sup>31</sup> Used to treat septic gunshot wounds in World War II, this therapeutically useful cyclic peptide paved the way for the thousands of cyclic peptides known today.<sup>28</sup> Many of these peptide macrocycles have

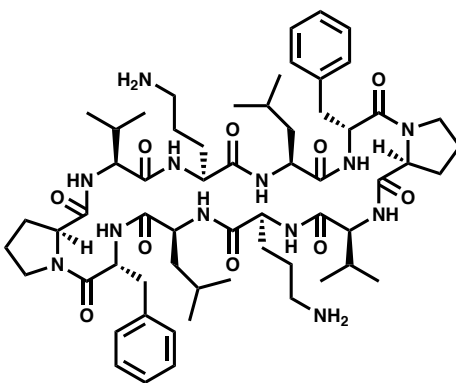


**Figure 1.10.** Gramicidin S

therapeutic properties, like oxytocin, cyclosporine a, colistin, and somatostatin.<sup>32</sup> The conformational constraint created by the cyclic configuration of these molecules imparts many beneficial properties that are not found in their linear counterpart.<sup>33</sup> Cyclic peptides are often more potent, resistant to proteolytic degradation, and are better able to penetrate cell membranes.<sup>32</sup>

Depending on the functional groups present within a peptide, macrocyclization can occur in four ways: head-to-tail, head-to-side chain, side chain-to-tail, or side chain-to-side chain (Figure 1.11).<sup>32</sup> The most common peptide macrocycle found in nature involves a head-to-tail cyclization, forming a large lactam ring between the N- and C-terminus.<sup>34</sup> The second most common cyclic peptides are side chain-to-side chain macrocycles formed via disulfide bridge between the thiols of two cysteine residues.<sup>33,34</sup> Because both of these structural motifs are common in nature, proteins have evolved to specifically target these bonds for degradation. So while these early macrocycles did

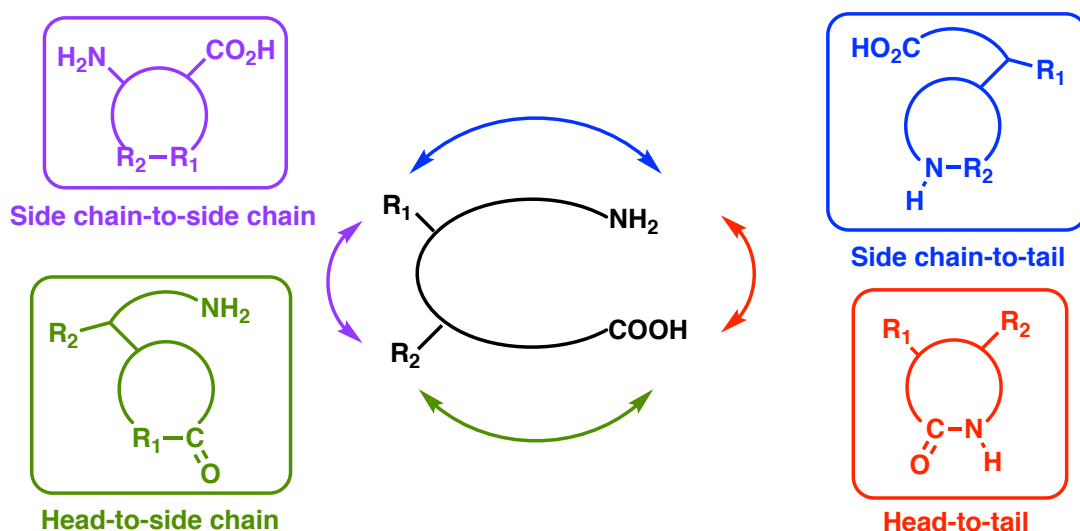


**Figure 1.11.** Four possible configurations of peptide macrocycles<sup>32</sup>

exhibit a conformational rigidity that caused them to spend more time in an active form, they were still susceptible to the same degradative weaknesses discussed above for their linear counterparts. To overcome this, scientists began developing methods of creating peptide macrocycles using non-naturally observed bond linkages.

### Synthetic Peptide Macrocycles

The rational design of bioactive peptide macrocycles ultimately seeks to replicate the naturally occurring three-dimensional secondary structures of proteins, such as turns,  $\alpha$ -helices, and  $\beta$ -sheets (**Figure 1.12**). The largest class of protein secondary structure, and therefore the most commonly featured structural motif in protein-protein interactions (PPIs), is the  $\alpha$ -helix.<sup>35</sup> The most common way of creating stable  $\alpha$ -helical peptides is through the creation of side chain-to-side chain macrocycles, early on referred to as

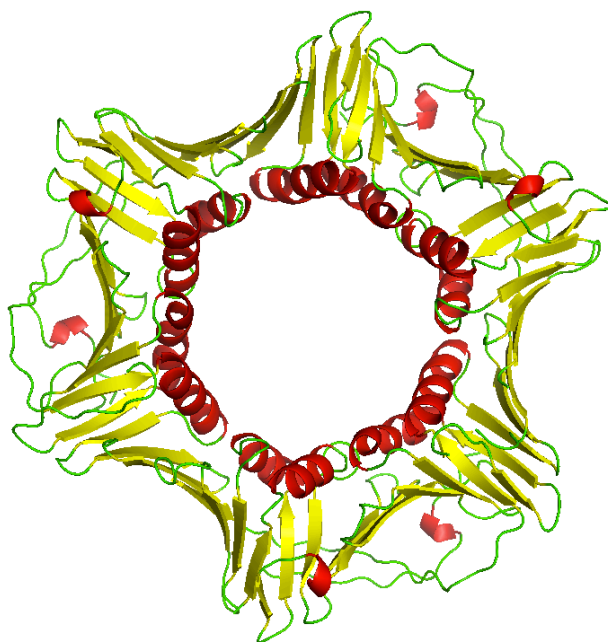


**Figure 1.12.** Protein secondary structure cartoon of Human PCNA (PDB - 1AXC) (turns are green, helices are red, sheets are yellow)

“stapled” peptides, although the term has now come to include all side chain-to-side chain peptide macrocycles.<sup>36</sup> The first major breakthrough in the creation of stapled peptides using non-native bonds was achieved by Blackwell and Grubbs via ring closing metathesis using two allylic ether serine residues spaced in an *I, i+4* fashion (**Figure 1.13**).<sup>20</sup> This work was later expanded upon by Verdine and coworkers when they introduced an all hydrocarbon staple, investigating stereochemical configuration,  $\alpha$ -substitution, linker length, and residue spacing for the optimal increase in overall helicity and eventual biological activity.<sup>21</sup> The current state of all-hydrocarbon peptide stapling

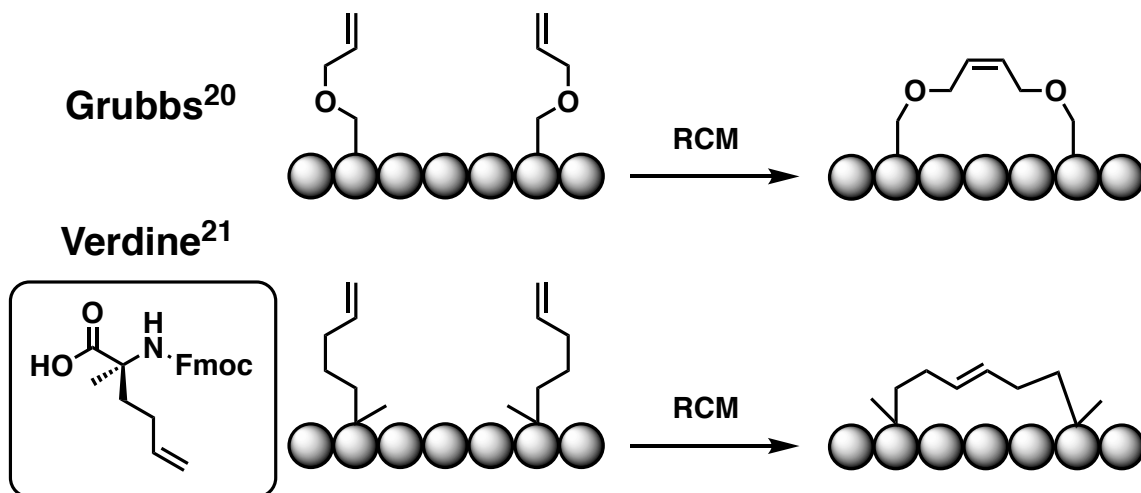


**Figure 1.12.** Early all-hydrocarbon peptide stapling

has been nicely reviewed by Walensky and Bird.<sup>38</sup> The successful implementation of a synthetic staple resulting in improved biological activity by Verdine and coworkers ignited a veritable arms race to develop new methods for the creation of peptide macrocycles.

## Modern Stapled Peptides

From this beginning, the field of peptide stapling has exploded in the last 20 years as more and more techniques emerge. These methods can be divided into two categories: one-component and two-component stapling (**Figure 1.14**).<sup>37</sup> One-component stapling is an intramolecular strategy that uses side-chain functionality present within the peptide to form the macrocycles. Prominent examples from this category include (a) lactam stapling

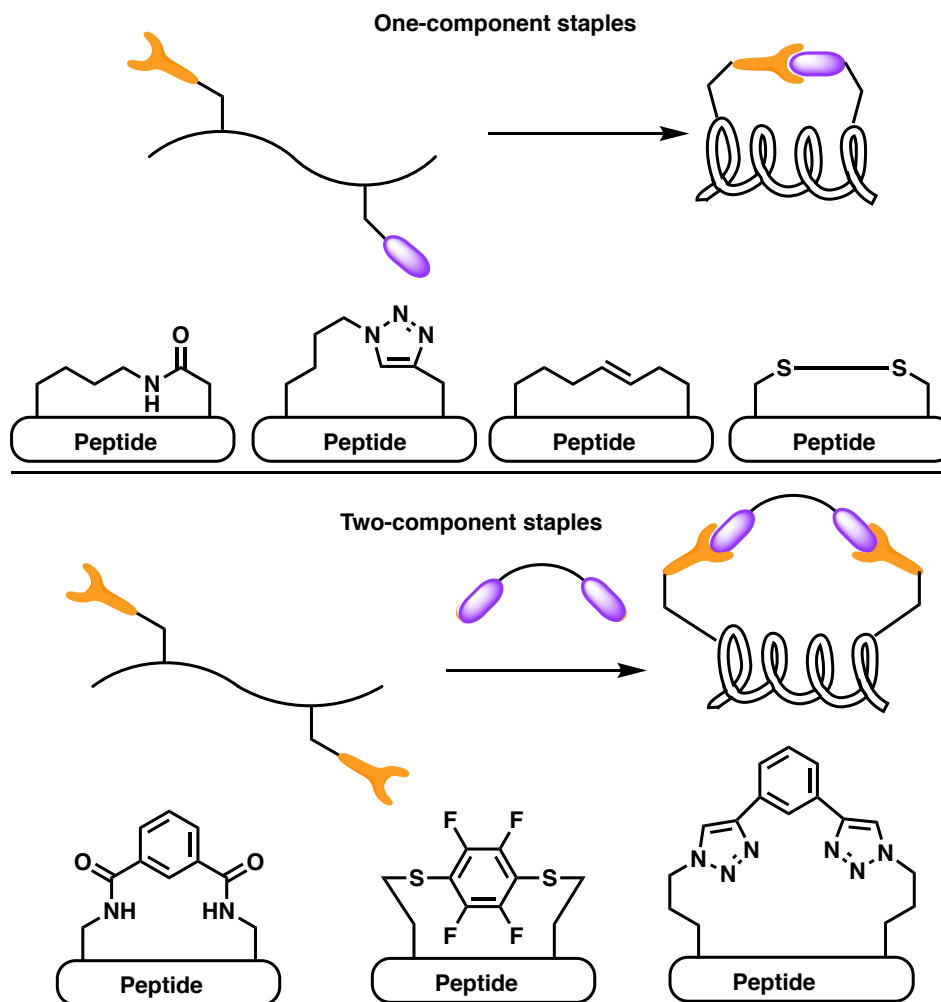


**Figure 1.13.** One-component and two component peptide stapling<sup>37</sup>

using native lysine and aspartic acid residues originally pioneered by Rosenblatt<sup>39</sup> and extensively studied by Fairlie,<sup>40</sup> (b) the all-hydrocarbon work already discussed by Grubbs<sup>20</sup> and Verdine,<sup>21</sup> (c) thiol-ene click photochemistry as pioneered by Anseth,<sup>41</sup> and (d) the copper catalyzed azide-alkyne cycloaddition, brought to solid phase peptide synthesis by Meldal.<sup>42</sup> Two-component stapling on the other hand, comprises an intermolecular, bicomponent strategy that joins the side-chains of two amino acids with a second component to form a macrocycle by bridging the two residues.<sup>43</sup> The chemical space of two component staples is incredibly diverse, with great strides made by the following series of colleagues: Pentelute,<sup>44-49</sup> Pentelute and Buchwald,<sup>50-51</sup> Woolley,<sup>52-54</sup> DeGrado and Greenbaum,<sup>55</sup> Caddick and Chudasama,<sup>56</sup> Wilson,<sup>57</sup> Inouye,<sup>58</sup> Baran,<sup>59</sup> Derda,<sup>60</sup> Rivera,<sup>61</sup> and Spring.<sup>62-63</sup> These strategies taken together come with unique benefits and drawbacks. Many involve the use of poisonous metals, which can be hard to remove to a satisfactory level for eventual biological medical application. Others involve the use of non-natural amino acids, which increase the cost of production. These stapling strategies also do not allow for the cleavage of the peptide macrocycle (i.e., unstapling) without significantly damaging the peptide.



## References – Chapter 1

1. Hochstrasser, R.M.; King, D.S. *J. Am. Chem. Soc.* **1975**, *97(16)*, 4760-4762.
2. King, D.S.; Denny, C.T.; Hochstrasser, R.M.; Smith, A.B., III. *J. Am. Chem. Soc.* **1977**, *99(1)*, 271-273.
3. Dellinger, B.; King, D.S.; Hochstrasser, R.M.; Smith, A.B., III. *J. Am. Chem. Soc.* **1977**, *99(9)*, 3197-3198.
4. Dellinger, B.; King, D.S.; Hochstrasser, R.M.; Smith, A.B., III. *J. Am. Chem. Soc.* **1977**, *99(22)*, 7138-7142.
5. Hochstrasser, R.M.; King, D.S.; Smith, A.B., III. *J. Am. Chem. Soc.* **1977**, *99(12)*, 3923-3933.
6. Paczkowski, M.; Pierce, R.; Smith, A.B., III; Hochstrasser, R.M. *Chem. Phys. Lett.* **1980**, *72(1)*, 5-9.
7. Haynam, C.A.; Young, L.; Morter, C.; Levy, D.H. *J. Chem. Phys.* **1984**, *81(11)*, 5216-5217.
8. Windisch, V.L.; Smith, A.B., III; Hochstrasser, R.M. *J. Chem. Phys.* **1988**, *92*, 5366-5370.
9. Scheiner, A.C.; Schaefer, H.F., III. *J. Chem. Phys.* **1987**, *87(6)*, 3539-3556.
10. Zhao, X.; Miller, W.B.; Hintsä, E.J.; Lee, Y.T. *J. Chem. Phys.* **1989**, *90(10)*, 5527-5535.
11. Tucker, M.J.; Courter, J.R.; Chen, J.; Atasoylu, O.; Smith, A.B., III; Hochstrasser, R.M. *Angew. Chem. Int. Ed.* **2010**, *49*, 3612-3616.
12. Lopez, V.; Marcus, R.A. *Chem. Phys. Lett.* **1982**, *93(3)*, 232-234.

13. Gong, Y.-H.; Miomandre, F.; Méallet-Renault, R.; Badré, S.; Galmiche, L.; Tang, J.; Audebert, P.; Clavier, G. *Eur. J. Org. Chem.* **2009**, 6121-6128.
14. McGrane, S.D.; Bolme, C.A.; Greenfield, M.T.; Chavez, D.E.; Hanson, S.K.; Scharff, R.J.; *J. Phys. Chem. A* **2016**, *120*, 895-902.
15. Allain, C.; Piard, J.; Brosseau, A.; Han, M.; Paquier, J.; Marchandier, T.; Lequeux, M.; Boissière, C.; Audebert, P. *ACS Appl. Mater. Interfaces*. **2016**, *8*, 19843-19846.
16. Abdo, M.; Brown, S.P.; Courter, J.R.; Tucker, M.J.; Hochstrasser, R.M.; Smith, A.B., III. *Org. Lett.* **2012**, *14(13)*, 3518-3521.
17. Courter, J.R.; Abdo, M.; Brown, S.P.; Tucker, M.J.; Hochstrasser, R.M.; Smith, A.B., III. *J. Org. Chem.* **2014**, *79*, 759-768.
18. Tucker, M.J.; Abdo, M.; Courter, J.R.; Chen, J.; Brown, S.P.; Smith, A.B., III; Hochstrasser, R.M. *Proc. Natl. Acad. Sci.* **2013**, *110(43)*, 17314-17319.
19. Brown, S.P.; Smith, A.B., III. *J. Am. Chem. Soc.* **2015**, *137*, 4034-4037.
20. Blackwell, H.E.; Grubbs, R.H. *Angew. Chem. Int. Ed.* **1998**, *37(23)*, 3281-3284.
21. Schafmeister, C.E.; Po, J.; Verdine, G.L. *J. Am. Chem. Soc.* **2000**, *122*, 5891-5892.
22. Dawson, P.E.; Muir, T.W.; Clark-Lewis, I.; Kent, S.B.H. *Science*. **1994**, *266*, 776-779.
23. Blackman, M.L.; Royzen, M.; Fox, J.M.; *J. Am. Chem. Soc.* **2008**, *130*, 13518-13519.
24. Devaraj, N.K.; Weissleder, R.; Hilderbrand, S.A. *Bioconjugate Chem.* **2008**, *19*, 2297-2299.

25. Klein, M. *Expert Opin. Drug Discov.* **2017**, *12(11)*, 1117-1125.
26. Morrison, C. *Nat. Rev. Drug Discov.* **2018**, *17*, 531-533.
27. Craik, D.J.; Fairlie, D.P.; Liras, S.; Price, D. *Chem. Biol. Drug Des.* **2013**, *81*, 136-147.
28. Tsomaia, N. *Eur. J. Med. Chem.* **2015**, *94*, 459-470.
29. Renukuntla, J.; Vadlapudi, A.D.; Patel, A.; Boddu, S.H.S.; Mitra, A.K. *Int. J. Pharm.* **2013**, *447*, 75-93.
30. Gause, G.F.; Brazhnikova, M.G. *Nature.* **1944**, *3918*, 703.
31. Synge, R.L.M. *Biochem. J.* **1945**, *39*, 363-367.
32. White, C.J.; Yudin, A.K. *Nat. Chem.* **2011**, *3*, 509-524.
33. Fairlie, D.P.; Dantas de Araujo, A. *Biopolymers (Peptide Science)*. **2016**, *106(6)*, 843-852.
34. Lawson, K.V.; Rose, T.E.; Harran, P.G. *Proc. Natl. Acad. Sci.* **2013**, E3753-E3760.
35. Pelay-Gimeno, M.; Glas, A.; Kock, O.; Grossmann, T.N. *Angew. Chem. Int. Ed.* **2015**, *54*, 8896-8927.
36. Azzarito, V.; Long, K.; Murphy, N.S.; Wilson, A.J. *Nat. Chem.* **2013**, *5*, 161-173.
37. Lau, Y.H.; de Andrade, P.; Wu, Y.; Spring, D.R. *Chem. Soc. Rev.* **2015**, *44*, 91-102.
38. Walensky, L.D.; Bird, G.H. *J. Med. Chem.* **2014**, *57*, 6275-6288.
39. Chorev, M.; Roubini, E.; McKee, R.L.; Gibbons, S.W.; Goldman, M.E.; Caulfield, M.P.; Rosenblatt, M. *Biochem.* **1991**, *30*, 5968-5974.

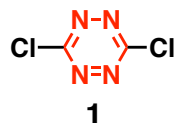
40. Shepherd, N.E.; Hoang, H.N.; Abbenante, G.; Fairlie, D.P. *J. Am. Chem. Soc.* **2005**, *127*, 2974-2983.
41. Aimetti, A.A.; Shoemaker, R.K.; Lin, C.-C.; Anseth, K.S. *Chem. Commun.* **2010**, *46*, 4061-4063.
42. Tornøe, C.W.; Christensen, C.; Meldal, M. *J. Org. Chem.* **2002**, *67*, 3057-3064.
43. Iegre, J.; Gaynord, J.S.; Robertson, N.S.; Sore, H.F.; Hyvönen, M.; Spring, D.R. *Adv. Therap.* **2018**, *1*, 1800052.
44. Spokoyny, A.M.; Zou, Y.; Ling, J.J.; Yu, H.; Lin, Y.-S.; Pentelute, B.L. *J. Am. Chem. Soc.* **2013**, *135*, 5936-5949.
45. Zhang, C.; Dai, P.; Spokoyny, A.M.; Pentelute, B.L. *Org. Lett.* **2014**, *16*, 3652-3655.
46. Zou, Y.; Spokoyny, A.M.; Zhang, C.; Simon, M.D.; Yu, H.; Lin, Y.-S.; Pentelute, B.L. *Org. Biomol. Chem.* **2014**, *12*, 566-573.
47. Vinogradov, A.A.; Choo, Z.-N.; totaro, K.A.; Pentelute, B.L.; *Org. Lett.* **2016**, *18*, 1226-1229.
48. Lautrtte, G.; Touti, F.; Lee, H.G.; Dai, P.; Pentelute, B.L. *J. Am. Chem. Soc.* **2016**, *138*, 8340-8343.
49. Wolfe, J.M.; Fadzen, C.M.; Holden, R.L.; Yao, M.; Hanson, G.J.; Pentelute, B.L. *Angew. Chem. Int. Ed.* **2018**, *57*, 4756-4759.
50. Rojas, A.J.; Zhang, C.; Vinogradova, E.V.; Buchwald, N.H.; Reilly, J.; Pentelute, B.L.; Buchwald, S.L. *Chem. Sci.* **2017**, *8*, 4257-4263.
51. Rojas, A.; Pentelute, B.L.; Buchwald, S.L. *Org. Lett.* **2017**, *19*, 4263-4266.

52. Kumita, J.R.; Smart, O.S.; Woolley, G.A. *Proc. Natl. Acad. Sci.* **2000**, *97*(8), 3803-3808.
53. Flint, D.G.; Kumita, J.r.; Smart, O.S.; Woolley, G.A. *Chem. Biol.* **2002**, *9*, 391-397.
54. Woolley, G.A. *Acc. Chem. Res.* **2005**, *38*, 486-493.
55. Jo, H.; Meinhardt, N.; Wu, Y.; Kulkarni, S.; Hu, X.; Low, K.E.; Pavies, P.L.; DeGrado, W.F.; Greenbaum, D.C. *J. Am. Chem. Soc.* **2012**, *134*, 17704-17713.
56. Lee, M.T.W.; Maruani, A.; Baker, J.R.; Caddick, S.; Chudasama, V. *Chem. Sci.* **2016**, *7*, 799-802.
57. Grison, C.M.; Burslem, G.M.; Miles, J.A.; Pilsl, L.K.A.; Yeo, D.J.; Imani, Z.; Warriner, S.L.; Webb, M.E.; Wilson, A.J. *Chem. Sci.* **2017**, *8*, 5166-5171.
58. Fujimoto, K.; Majino, M.; Inouye, M. *Chem. Eur. J.* **2008**, *14*, 857-863.
59. Malins, L.R.; deGruyter, J.N.; Robbins, K.J.; Scola, P.M.; Eastgate, M.D.; Ghadiri, M.R.; Baran, P.S. *J. Am. Chem. Soc.* **2017**, *139*, 5233-5241.
60. Kalhor-Monfared, S.; Jafari, M.R.; Patterson, J.T.; Kitov, P.I.; Dwyer, J.J.; Nuss, J.M.; Derda, R. *Chem. Sci.* **2016**, *7*, 3785-3790.
61. Vasco, A.V.; Pérez, C.S.; Moralex, F.E.; Garay, H.E.; Vasilev, D.; Gavin, J.A.; Wessjohann, L.A.; Rivera, D.G.; *J. Org. Chem.* **2015**, *80*, 6697-6707.
62. Lau, Y.H.; Wu, Y.; Rossmann, M.; Tan, B.X.; de Andrade, P.; Tan, Y.S.; Verma, C.; McKenzie, G.J.; Venkitaramn, A.R.; Hyvönen, M.; Spring, D.R. *Angew. Chem. Int. Ed.* **2016**, *54*, 15410-15413.
63. Lau, Y.H.; de Andrade, P.; Quah, S.-T.; Rossmann, M.; Laraia, L.; Sköld, N.; Sum, T.J.; Rowling, P.J.E.; Joseph, T.L.; Verma, C.; Hyvönen, M.; Itzhaki, L.S.;

Venkitaraman, A.R.; Brown, C.J.; Lane, D.P.; Spring, D.R. *Chem. Sci.* **2014**, *5*, 1804-1809.

## CHAPTER 2. Expanding Peptide Stapling with Dichloro-*s*-Tetrazine

While the work of Brown and Smith<sup>1</sup> nicely validated the use of dichloro-*s*-tetrazine (**1**) as a peptide stapling and unstapling reagent in peptide sequences containing



two free cysteine residues and in turn highlighted the utility of this tactic, the use of two cysteine residues can be problematic. Cysteine is one of the least commonly encoded proteogenic amino acids.<sup>2-3</sup> Hence, every inclusion of a cysteine in a natural amino acid sequence is purposeful, but the inclusion of cysteine residues in sequences solely for use of the stapling tactic can add unnecessary difficulty. For example, cysteine makes an excellent nucleophilic scavenger,<sup>2</sup> and in particular it tends to pick up cationic fragments cleaved from other residues in the global deprotection and resin cleavage protocols common to Fmoc-SPPS.<sup>4</sup> The inclusion of other thiol scavengers in the cleavage cocktail can of course help minimize this byproduct formation, but as the intramolecular cation transfer from another residue to cysteine proceeds faster than an intermolecular one, some amount of undesired adduct is usually isolated. Cysteine is also sensitive to oxidation.<sup>2-4</sup> Therefore peptides containing free cysteine need to be handled in dilute, acidic environments to suppress the formation of disulfides. The free thiol side-chains of cysteine are also quite hydrophobic, making it necessary to include ion-forming residues like arginine or lysine in the sequence to aid solubility. Finally, the presence of cysteine

is accompanied by a characteristic odor that many find unpleasant. Although workable, more than a few scientists may avoid handling these compounds for that reason. *For all these reasons, the feasibility of utilizing other nucleophilic side chain-containing amino acids, lysine in particular, to form stapled peptides from dichloro-s-tetrazine was explored as the subject of this thesis.*

### Modification of Cysteine/Lysine Peptides with Dichloro-*s*-tetrazine

This research program was thus initiated by investigating the modification of a cys-ala-lys trimer peptide, isolated as the trifluoroacetic acid (TFA) salt (**2**), with dichloro-

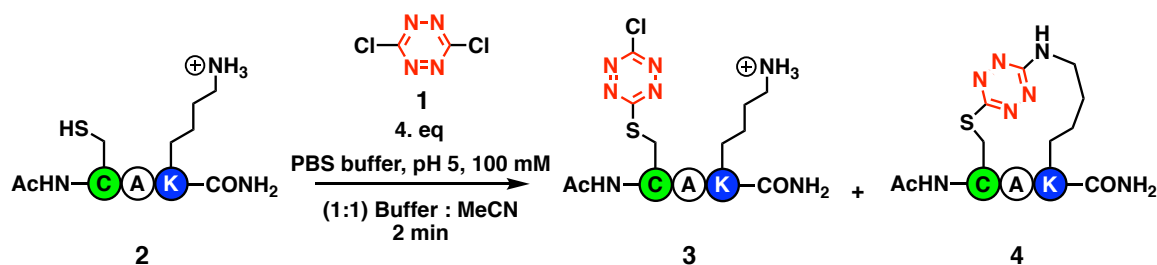
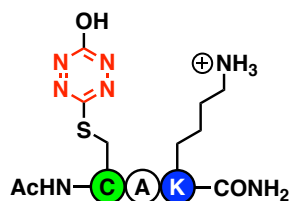


**Figure 2.1.** Modification of cys-ala-lys trimer peptide with dichloro-*s*-tetrazine

*s*-tetrazine (**1**), expecting to arrive at the acyclic product **3** or the closed macrocycle **4** (**Figure 2.1**). Not wanting to repeat history, the first conditions explored involved the exact protocol previously developed by Brown and Smith for the creation of tetrazine-bridged disulfide macrocycles from peptides containing two proximal cysteine residues.<sup>1</sup> Isolation and purification by HPLC and analysis by LCMS showed the isolated material to be an approximate 2:1 mixture of the desired *para*-chloro product **3** to undesired *para*-hydroxy product **5**.





5

Attempts at further purification of the isolated mixture resulted in the almost complete loss of **3**, with a small amount of closed macrocycle **4** detectable in the chromatogram along with the major product **5**. One might think that this still provides a path forward, as alcohols can be converted to any number of electron-withdrawing leaving groups that are useful in the  $S_NAr$  reaction manifold, but this fails to take into account the extremely electron deficient character of tetrazines and their potential to undergo cyclo-elimination. If one were to draw the resonance contributor of **5** wherein one of the lone pairs of the phenolic alcohol is delocalized into the *s*-tetrazine ring, the subsequent movement of electrons would result in the dissociation of the *s*-tetrazine moiety, yielding an equivalent of nitrogen gas, isocyanic acid (**6**), and thiocyanate peptide **7** (**Figure 2.2**). This proposed degradation pathway of **3** to **5** to **7** is supported by mass spectrometry evidence. After five minutes, the major component of the reaction mixture is still product **3** with little sign of degradation (**Figure 2.2C**). However, after stirring 24 hours, new mass spectrometry analysis (**Figure 2.2D**) clearly shows that, while some compound **3** still remains, the major components of the sample are now compounds **5** and **7**. The results of this experiment made it abundantly clear that the competing reactivity of water while handling any compounds such as **3** would be a complicating factor not observed in previous studies by Brown.<sup>1</sup> Because of this

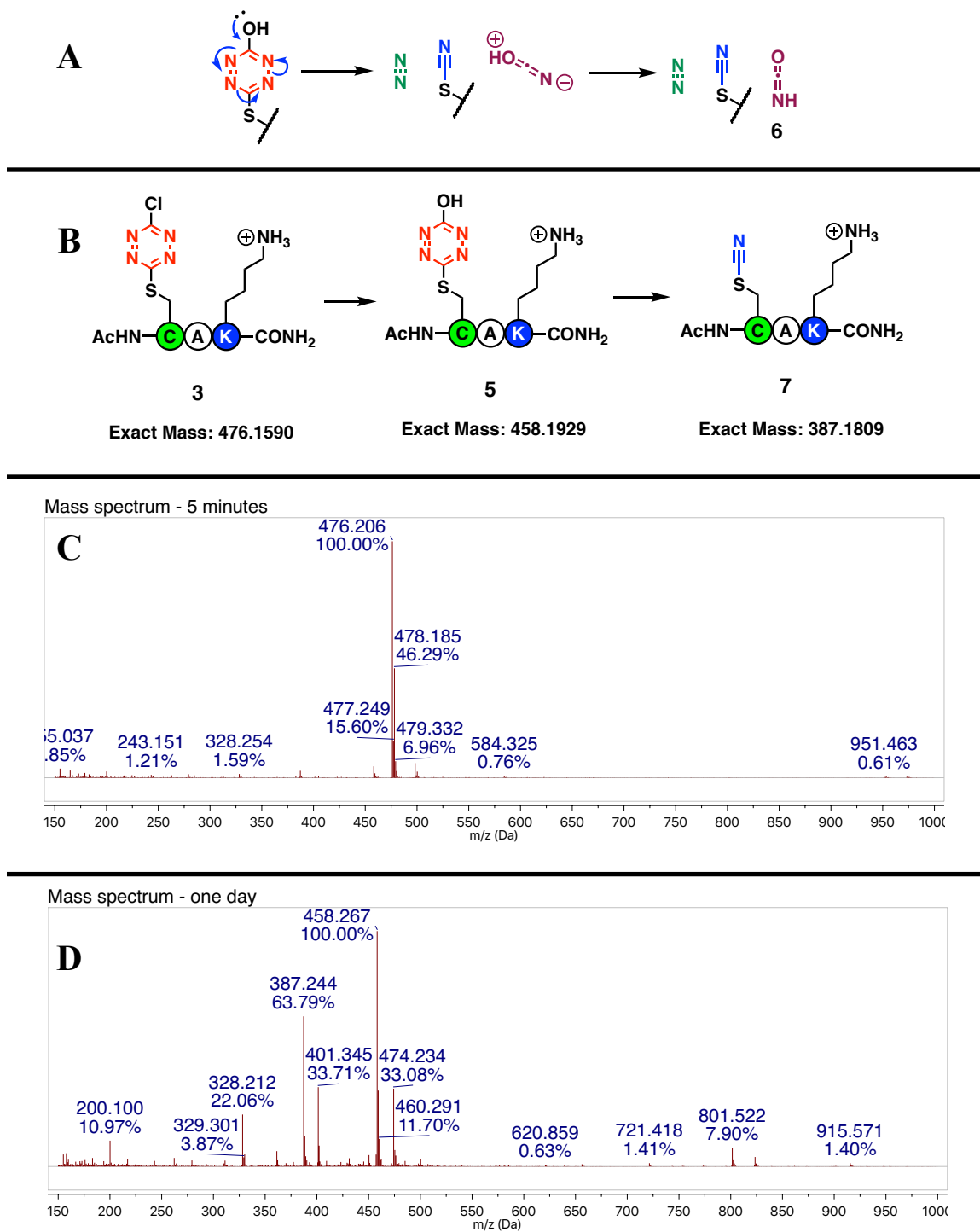


**Figure 2.2.** A) Proposed degradation pathway of hydroxy-tetrazine; B) Degradation of **3** to **5** to **7** with molecular weights; C) Formation of compound **3** – mass spectrum of the reaction mixture after 5 minutes; D) Formation of compound **3** – mass spectrum of the reaction mixture after one day

particular difficulty, consideration would have to be paid not just to which reagents and conditions were used, but also to how the material was handled throughout the overall reaction process in order to minimize time spent in contact with water.

The non-innocence of water posed an interesting/difficult problem. In classic organic chemistry, the solution would entail replacement of water with a different solvent. Highly polar organic solvents that exhibit no nucleophilic character certainly exist, with acetonitrile (MeCN), dimethylsulfoxide (DMSO), and *N,N*-dimethylformamide (DMF) often playing a role in reactions requiring these properties. However, acetonitrile does not adequately dissolve many of the peptide sequences when isolated as salts. As a solid/liquid biphasic reaction mixture would lead to an artificially high concentration of the peptide substrate, leading to complications with dimerization, acetonitrile was ruled out as a possible solvent. DMF and DMSO would be better solvent choices for peptides, but they are difficult to remove once the reaction is complete due to their high boiling point. Again, in classic organic synthesis the product of the reaction can often be extracted into a more volatile organic solvent after the reaction mixture has been appropriately diluted with water, but the peptide products remain in the aqueous fraction, especially if the lysine residue is still present as an ammonium salt. Vacuum distillation can also be employed, but removal of the last residual solvent still usually requires diluting the mixture with a more volatile co-solvent such as water or methanol and then concentrating again several times. Exposing compounds such as **3** to the required temperature to achieve vacuum distillation of DMF/DMSO for the length of time required for such dilute reactions would also be ill advised from a stability standpoint. These solvents can be evaporated by blowing stream of air over the surface of the

solution, but the extremely dilute conditions usually used in macrocyclization reactions (~1-5 mM) mean that this method of drying would again take a prohibitively long time.<sup>5-6</sup> While DMF and DMSO are regularly employed in peptide modification chemistry, workup and purification of protocols utilizing these solvents involves HPLC purification to isolate the compound from the solvent.<sup>7-9</sup> As discussed above, HPLC purification is not an option at this stage.

Without a viable alternative, water would have to remain in our reaction protocol. Therefore, the first part of reaction optimization for the transformation from **2** to **3** required a careful evaluation of when water was introduced and what can be done to mitigate the degradation undergone by product **3**. One way to cut exposure to water would be to eliminate HPLC purification and carry the crude material directly forward instead of trying to isolate **3** as a pure compound. The first attempt at this strategy entailed a two-step protocol skipping any isolation or workup of **3**. Instead, dibasic sodium phosphate salt would be immediately added after the two-minute stirring period to afford an appropriate pH in an attempt to arrive at macrocycle **4** in a one-pot process (**Figure 2.3**). However, instead of desired product **4**, LC/MS analysis revealed the major product was compound **8**. Attempts to ameliorate this issue by using a 1:1 ratio of peptide **2** to dichloro-*s*-tetrazine (**1**) resulted in increased formation of dimer **9** (**Figure 2.3**).

Given we were trying to avoid purification, formation of dimer **9** cannot be allowed to occur because of the potential to divert other equivalents of **3** away from macrocycle formation upon pH change in a polymeric fashion. Therefore, it was important to keep the equivalents of dichloro-*s*-tetrazine (**1**) sufficiently high to achieve

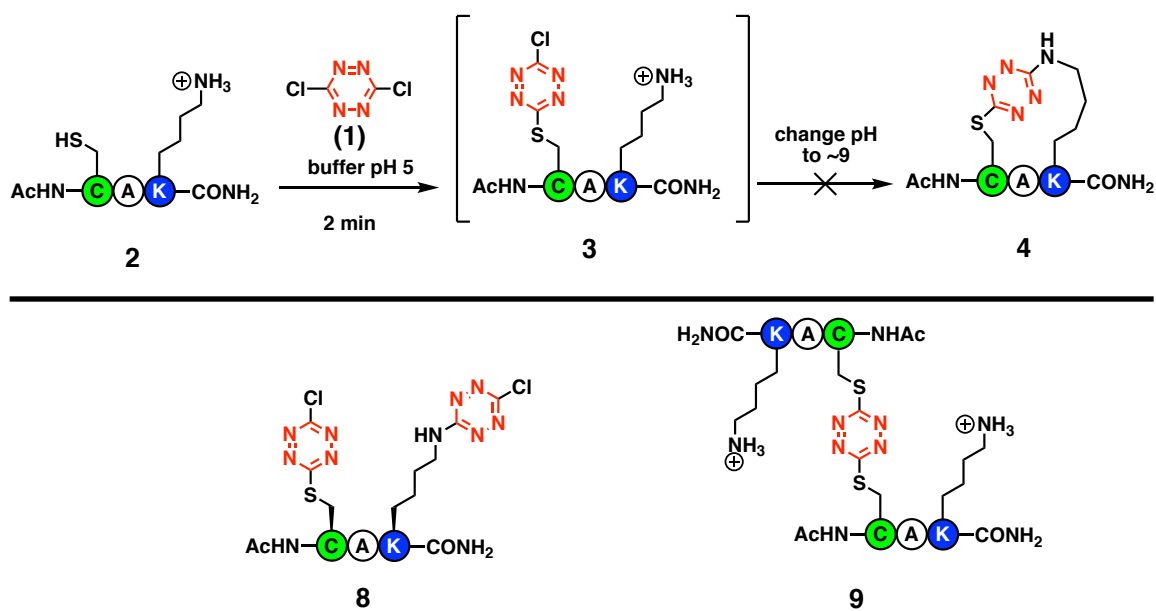


**Figure 2.3.** Attempts at two-step, one-pot macrocyclization

full consumption of **2** and not to permit any formation of dimer **9**. Because changing pH to achieve a two-step one-pot macrocyclization under these conditions resulted in significant formation of compound **8**, as discussed above, this indicates that the isolation of compound **3** by lyophilization before performing the macrocyclization step would be required (**Figure 2.4**). Pleasingly, removal of excess dichloro-*s*-tetrazine (**1**) was not a problem in this reaction sequence given that it is sufficiently volatile to be removed by sublimation with the solvent during lyophilization.

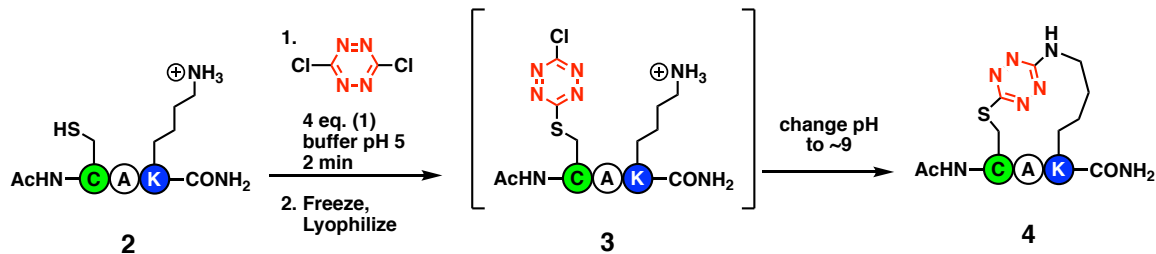


**Figure 2.4.** Revised plan

The next factor that required improvement was the stability of the crude isolate containing intermediate **3**. The large excess of sodium phosphate (100 mM buffer vs. 1 mM peptide) in solution appeared to be leading to inconsistency in lyophilization process. That is, the concentration of salt within the flask increases as the water and acetonitrile sublimate. This would sometimes result in the ice to thawing, destroying the isolated material. Even in reactions that had been successfully dried, there was some doubt as to how much water the salt would retain. For example, the crude isolate of compound **3** could only be stored in a freezer for a few days before converting to compound **5**. To ameliorate this issue, various other buffer species were evaluated to see if one would give better performance than the phosphate buffer (PBS) currently being employed. Criteria for success was a high conversion of **2** to **3**, with minimal formation of **5**, both before and after lyophilization when analyzed by LC/MS. Using the conditions described above, a number of buffers including ammonium phosphate, sodium acetate, and sodium citrate at 100 mM were evaluated. The reaction was also performed in Milli-Q water as a control. All buffers performed similarly, showing complete consumption of **2** and ~95% **3** by LC/MS analysis after stirring for 2 minutes, except for sodium acetate, which gave a 2:1:2 mix of compounds **3**, **4**, and **5**. Surprisingly, the reaction run with Milli-Q water performed just as well as the successful buffer trials. This observation turned out to be a pivotal discovery because, after lyophilization, the only compounds present in the flask were **3** and **5**. Importantly, this crude isolate of compound **3** could now be stored for roughly two weeks without exhibiting significant degradation.

As a result of these experiments, suitable conditions were now available for the isolation of compound **3** in acceptable purity to carry forward without the need for HPLC

purification (**Figure 2.5**). However, initially there were some difficulties in consistently producing these results. Applying even greater levels of scrutiny to our attempt at

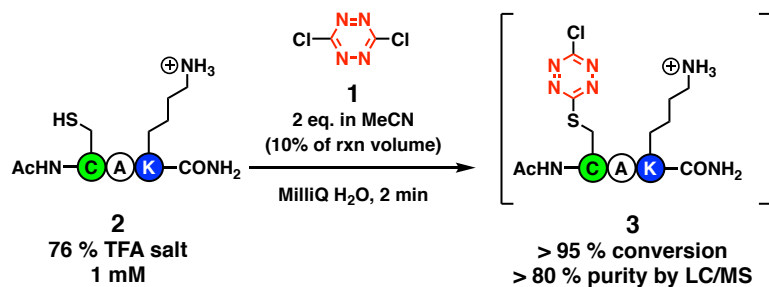


**Figure 2.5.** Conditions for formation of **3**

achieving reproducibility, we found that the inconsistency in the results reflected different lengths of time required to completely lyophilize the reaction mixture. That is, the longer it took to lyophilize the reaction mixture, the more of the unwanted compound **5** was produced. To curtail this issue, particular care had to be taken as to how the reaction vessel was frozen. There are two ways to freeze a sample to prepare for lyophilization, referred to here as “block freezing” and “shell freezing” (**Figure 2.6**). The water/acetonitrile mixture that makes up the solvent for these reactions is readily frozen in preparation for lyophilization by submerging the reaction vessel in a dry ice / acetone bath. To block freeze a compound, the flask could be placed in a cooling bath and allowed to stand until the contents had fully solidified. As shown in **Figure 2.6**, this results in a mass of ice that is not evenly distributed around the edge of the flask. Because the rate of evaporation depends on available surface area, this manner of sample preparation would often require multiple days to yield dry isolate. If the reaction vessel were instead constantly rotated sitting in the bath, the frozen reaction mixture would be evenly distributed around the flask with a much greater surface area, providing access to



**"Block Freezing"**  
Days to sublimate



**"Shell Freezing"**  
12 hours to sublimate

**Figure 2.6.** "Block" and "shell" freezing of a 50 mL reaction mixture in a 100 mL vessel

dry material in roughly 12 hours. This also set an upper limit on the scale of this reaction. As long as the reaction volume was kept under 50% of the total volume of the vessel, (e.g., 50 mL of a 100 mL round bottom flask), the crude material could be recovered in 12 – 24 hours depending on the current workload on the lyophilizer. If the reaction volume was closer to 80% of the total volume or higher, the reaction mixture would not have the favorable shell surface area to volume ratio regardless of freezing method and would take many days to yield dry material. To this end, a rotary evaporator could be employed to rotate the reaction vessel in order to achieve a uniform thickness of frozen material without requiring the experimenter to manually turn each flask. This last critical observation as to the influence drying time had upon the reaction finally yielded consistently reproducible results (>95% conversion of **2** to **3**, >80% purity by mass spectrometry [**Figure 2.7**]) that would now permit closure of the macrocycle to be investigated.



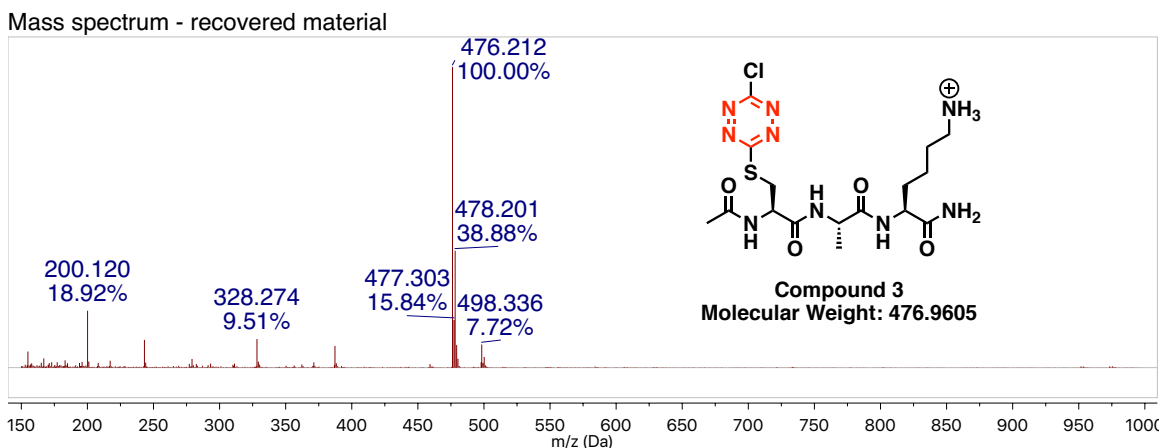


**Figure 2.7.** Mass spectrum of crude isolate of compound 3

### Macrocyclization of Modified Peptides (3) Possessing a Lysine Side Chain

The investigation into conditions to reliably furnish macrocycle **4** was begun by testing phosphate and carbonate buffer systems at 0.1 M strength between pH 8 – 11 (**Figure 2.8**). Earlier investigations, *vide supra*, exploring the feasibility of a two-step, one-pot procedure for the synthesis of **4**, resulting in the synthesis of *bis*-tetrazine adduct

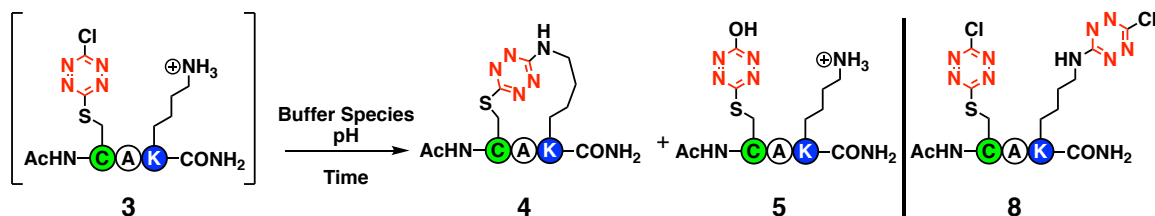


**Figure 2.8.** Investigating macrocyclization conditions

**8** (**Figure 2.8**), had already indicated that the *N*<sup>ε</sup>-amino group of lysine could indeed participate as a nucleophile in the PBS buffer system at pH ~ 9. The observance that the two-step, one-pot attempt largely resulted in the synthesis of compound **8** also served to illustrate that **1** is a more reactive electrophile than **3**, as is to be expected from

observance of electronegativity. This result begs the question of whether or not it will be possible to effectively cyclize **3**. Once again, the major competing reaction pathway would entail solvolysis by water at the *para* position to form compound **5**. It was observed during the reaction condition screen that raising the pH of the buffer resulted in an increase in the amount of compound **5** present in the mixture. Pleasingly, PBS buffer and sodium bicarbonate both gave access to macrocycle **4** at pH ~8.5 after stirring at room temperature for two hours. The true difference in usability between the two buffer systems became apparent when scaling beyond test reactions and attempting to purify *via* HPLC. As with the reaction to form compound **2**, the macrocyclization reaction was run under dilute conditions (1 mM of **3**, based on the original amount of **2**) to impede the formation of dimers. Under these conditions 100 equivalents of the buffer species in the reaction mixture needed to be removed. On small scale (~5 mg starting peptide), this did not create a major problem as the lyophilized crude material could easily be dissolved in 1 mL of water and the total solute would not overload the capacity of the HPLC column, resulting in a clean separation of components (**Figure 2.9**). However, as the reaction

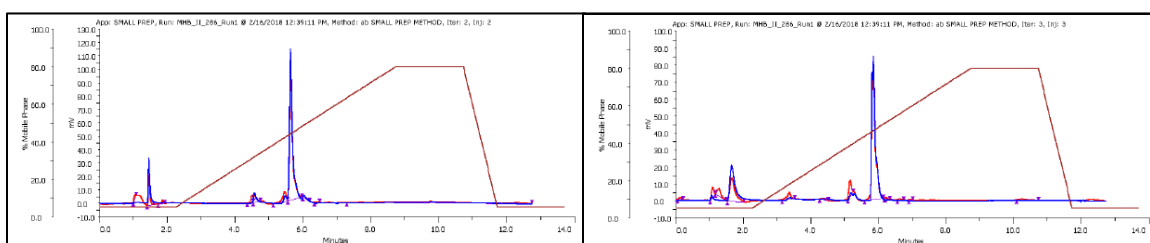


**Figure 2.9.** HPLC purification of macrocycle **4** synthesis on small scale using sodium phosphate (left) and sodium bicarbonate (right)

was scaled up, it became increasingly difficult to purify the reaction run with the sodium phosphate buffer system (**Figure 2.10**). The crude isolate had to be diluted far beyond what was necessary for the peptide material alone before purification to avoid saturating

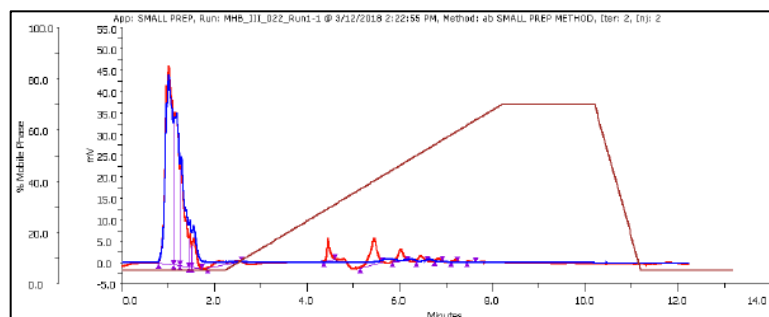
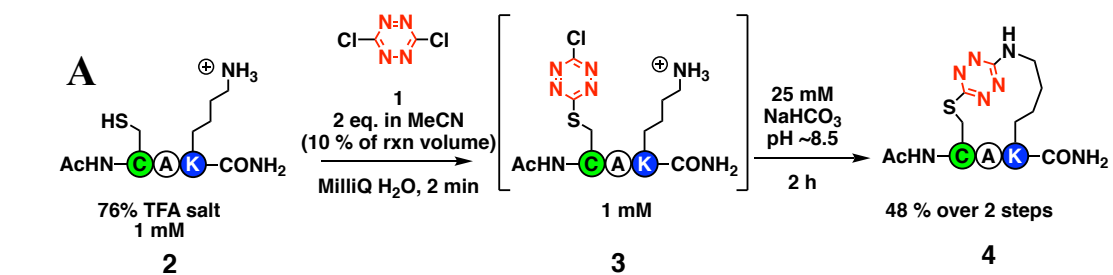
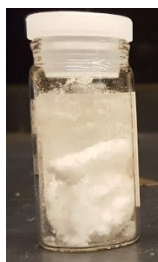


**Figure 2.10.** HPLC purification of scaled up synthesis of **4** using sodium phosphate. Too much salt saturates the column, preventing any retention / purification of material.

the HPLC column with all the salt remaining after lyophilization. Attempts were made to ameliorate this issue utilizing dialysis and reverse phase “flash” column chromatography as tactics of removing salt prior to HPLC purification, but these procedures added extra days of processing time for, at best, modest benefit. Ultimately, neither of these measures ameliorated the need for multiple HPLC purifications to arrive at clean material. Working with residual carbonate buffer proved much more facile. Samples containing residual sodium bicarbonate buffer could be prepared for HPLC purification by dissolving the crude isolate in a 1:1 mixture of water and trifluoroacetic acid, allowing much of the salt to evolve from solution as carbon dioxide. This tactic avoided the excessive HPLC purification that was needed when using 100 mM sodium phosphate buffer, especially as the carbonate buffer strength could be lowered to 25 mM with no loss of function. This final change permitted the successful synthesis and isolation of pure macrocycle **4** after stirring for 2 hours at room temperature in 48% yield over the two steps discussed above (**Figure 2.11**).



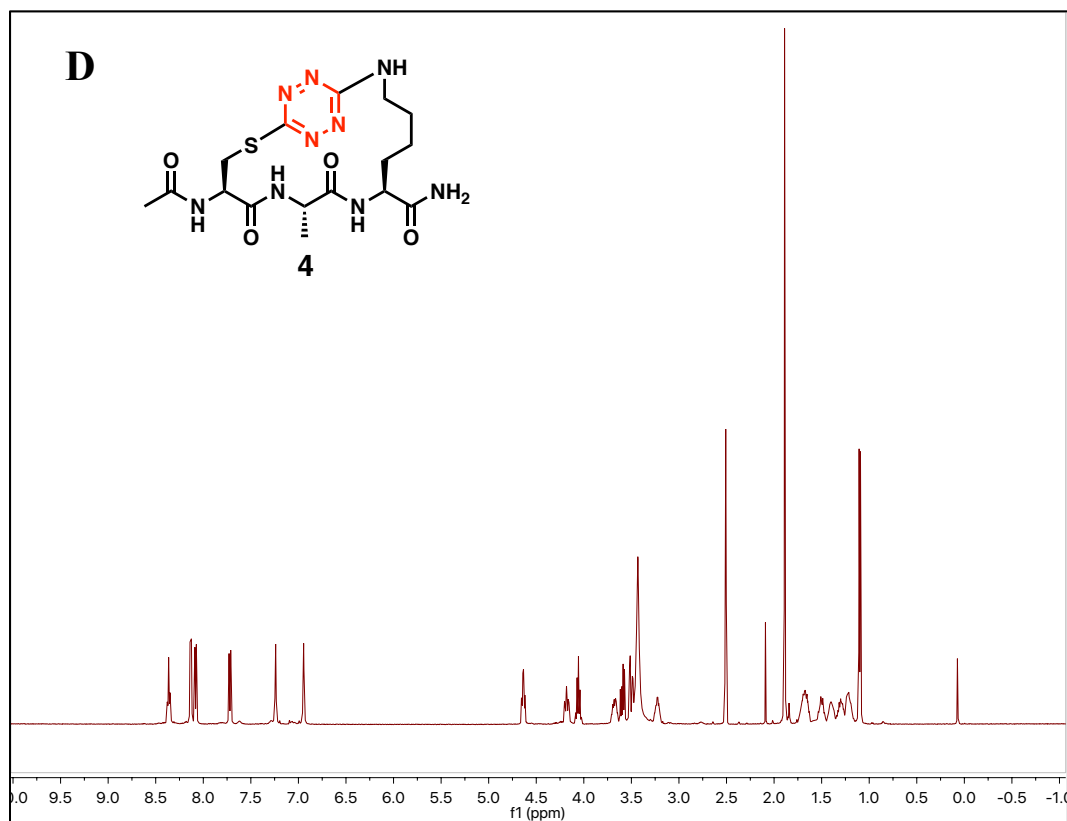
**B**



**C**



**D**

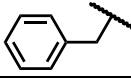
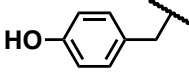
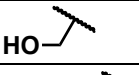
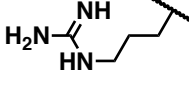


**Figure 2.11.** **A)** Successful conditions for the synthesis of macrocycle **4**; **B)** isolated starting peptide **2** as amorphous white powder; **C)** isolated pure macrocycle **4** as amorphous orange powder; **D)**  $^1\text{H}$  NMR spectrum of macrocycle **4** in  $d_6$ -DMSO

## Scope and Tolerance of Cysteine/Lysine Stapling

The aim of the next series of experiments was application of this newly developed synthetic protocol to other peptide sequences containing a single cysteine and a single lysine. The first question was whether the presence of other nucleophilic side chains would interfere with *S,N*-macrocycle formation. To this end, a series of heptamer peptides with the cysteine and lysine residues in an *i, i+4* relationship, with a variable residue in an *i+1* relationship relative to cysteine was synthesized (**Table 2.1**). Using phenylalanine (**10a**) as a control, tyrosine (**10b**), serine (**10c**), and arginine (**10d**) residues were interrogated. In every case, conversion of starting peptide **10a-d** to acyclic intermediate **11a-d** could be readily observed *via* LCMS. However, when attempting to form macrocycles **12a-d**, unexpected results were encountered! Macrocycle **12a** was proposed as a control example, but none of the desired product was isolated after purification. LC/MS testing at 60 and 120 minutes revealed that desired product **12a** formed cleanly with little else in the chromatogram, but the HPLC trace and post-lyophilization LC/MS analysis revealed degradation during the purification process (**Figure 2.12**). Compound **12b** exhibited the same behavior. Pleasingly, peptides **10c** and **10d** did provide the desired stapled peptides **12c** and **12d** in 37% yield and 61% yield respectively. Looking at the results displayed in **Table 2.1**, the determining factor of this compound series would appear to be steric bulk rather than chemical reactivity. That is, there must be some amount of steric clash in the cys-phe-leu or cys-tyr-leu sequence of **12a** or **12b** respectively that causes **12a-b** to be less stable than **12c-d**.

**Table 2.1.** Competing residue scope

Entry	X residue	Side chain	11x LCMS Conversion	12x isolated yield (2 steps)
a	Phe		95%	0%
b	Tyr		80%	0%
c	Ser		92%	37%
d	Arg		92%	61%

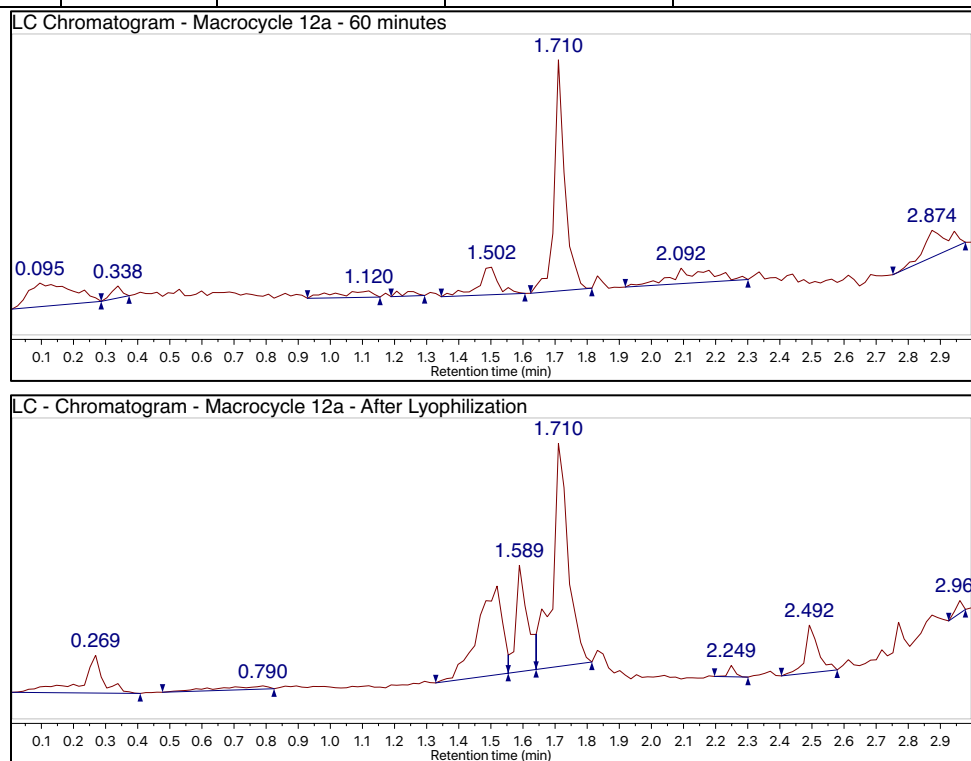


**Figure 2.12.** LC chromatogram data for macrocycle **12a**; Top - reaction at 60 minutes; Bottom - sample post lyophilization

To test this theory, the synthesis of macrocycles **13-16** (Figure 2.13) was explored. Pleasingly, all attempts proved successful, providing access to macrocycles **13-16** in modest to fair yield (20 – 63%) over the two steps! Attempts to construct two larger peptide macrocycles (**17-18**) containing cysteine and lysine residues on opposite ends of the peptide chain showed successful construction of the macrocycle by LC/MS, but these constructs did not survive attempts at purification. Given the length of these peptide chains, steric clashing no longer seems a viable answer as to why these sequences do not

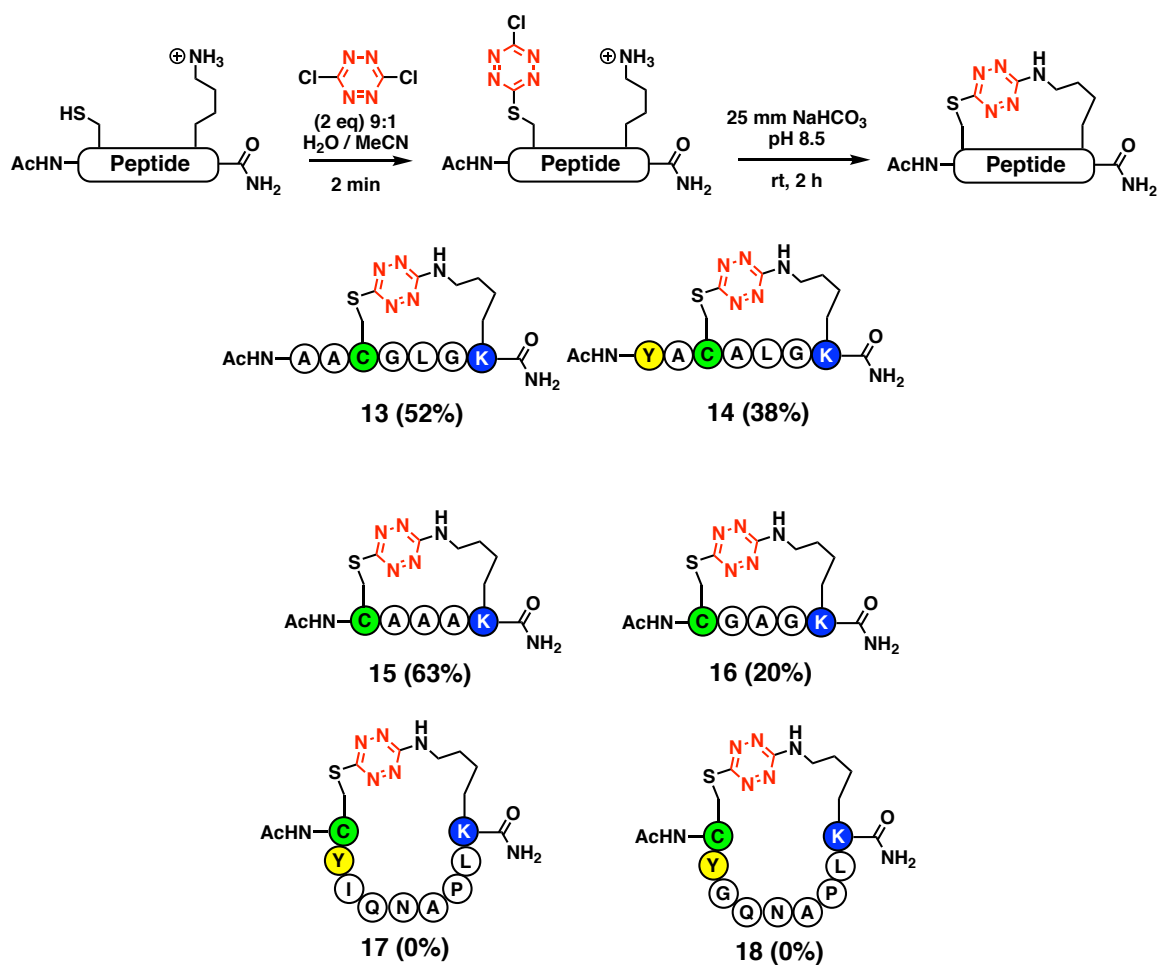


**Figure 2.13.** More cys-tet-lys macrocycles survive purification. We propose that the adjacent tyrosine residue must exhibit another undesirable property other than the steric encumbrance discussed above, such as

competing as a nucleophile or somehow rendering the macrocycles more susceptible to hydrolysis. The role of tyrosine will be discussed further below.

The results presented above identify some of the problems that have been encountered with this stapling tactic. The *S,N*-tetrazine linkage appears to have issues with instability, with steric encumbrance possibly contributing somewhat to the problem. Additionally, these macrocycles are much less soluble than the parent peptides. Not only are macrocycles less soluble than their linear peptide counterparts as a general rule, but upon cyclization the initially present ammonium group on the lysine side chain is replaced with a group that is much less soluble, given how much more difficult it is to ionize the nitrogen now attached to the tetrazine ring after macrocyclization. This idea is born out by NMR integration evidence, wherein the linear parent chain ammonium hydrogen signal integrates for an obvious 3 protons, but the exocyclic nitrogen proton of the macrocycle only integrates for 1. Moreover, the NMR signal of this proton exhibits distinct splitting pattern showing that it does not readily exchange, exchangeability being a characteristic of acidic protons as exhibited by the ammonium protons in **2** (**Figure 2.14**). The good news is that this effect can be mollified by the inclusion of arginine residues, which were shown to be tolerated as indicated in **Table 2.1** (see example **12d**). In fact, this proved to be the best performing example of that screen! Alternatively, peptide **19** and acyclic intermediate **20** were completely water soluble, but macrocycle **21** could only be dissolved in 2:1 trifluoroacetic acid and tetrafluoroethanol. The loss of aqueous solubility in macrocycle **21** was so great that it crashed out inside the steel tubing in the HPLC instrument *and* further on the column during HPLC purification and thus could



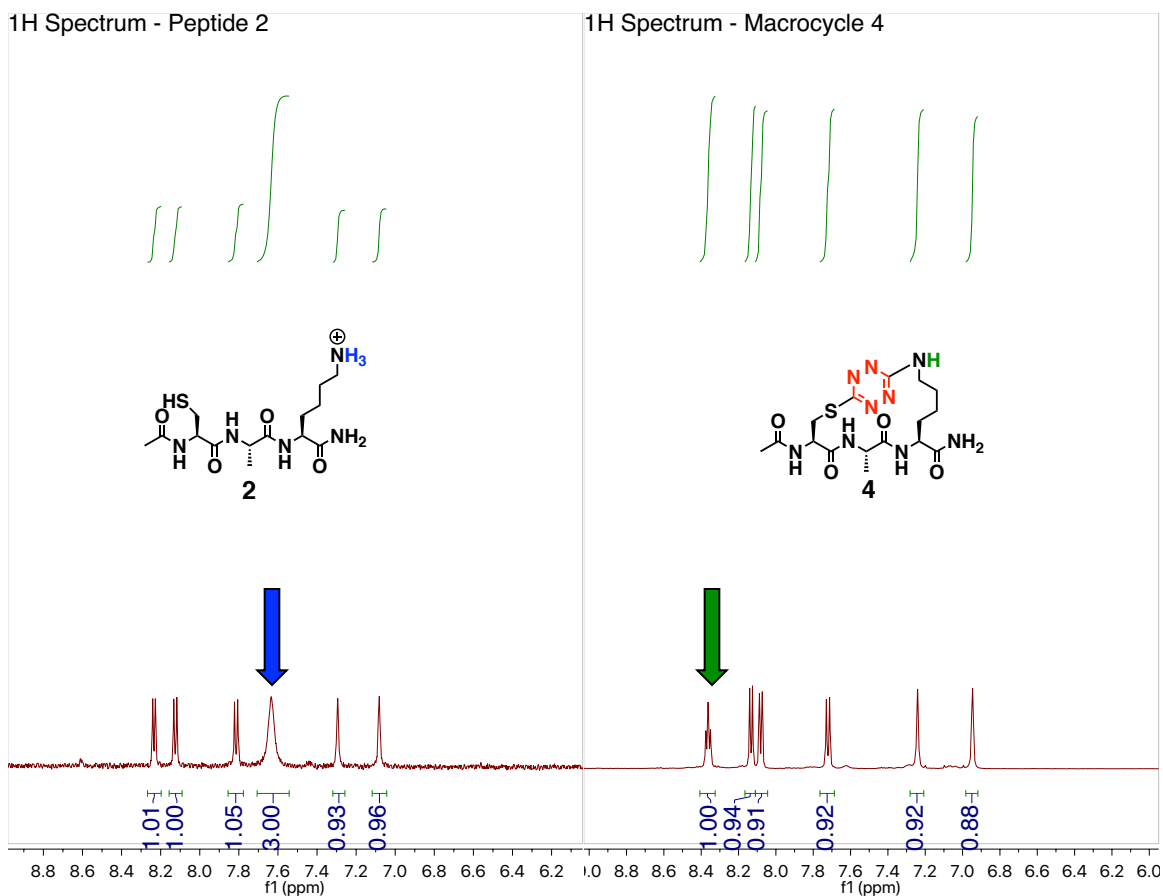


**Figure 2.14.** Differences in proton exchangeability between **2** and **4** in lysine  $\epsilon$ -amino group

not be purified (**Figure 2.15**). The stark contrast in solubility and performance between **12d** and **21** serves to highlight how dependent this method is on the peptide substrate.

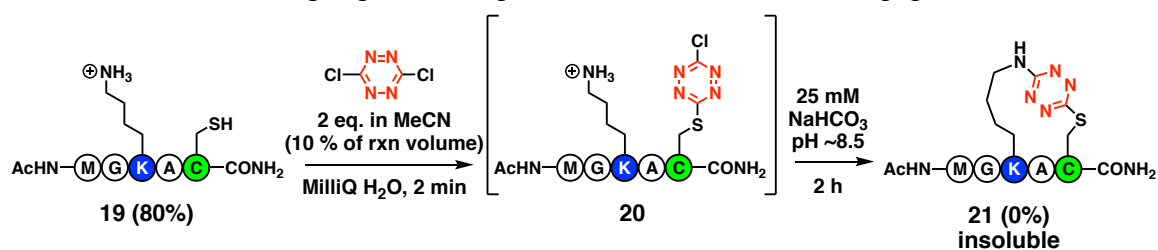


**Figure 2.15.** Solubility problems with macrocycles

In summary, we set out to translate the previously developed method of creating *s*-tetrazine peptide macrocycles using peptide sequences containing two cysteine residues

to peptide sequences containing a single cysteine and a single lysine. While this investigation ultimately resulted in the successful synthesis and purification of *seven S,N*-tetrazine macrocycles in yields of 20-63%, it was also made clear during this work that the method displayed much less general applicability than that previously developed by Brown and Smith.<sup>1</sup> In the course of this investigation we encountered problems stemming from competing reactivity from solvent, stability of material, and substrate restrictions based on steric encumbrance. Our efforts toward circumventing these problems have been enumerated and, where possible, solutions have been implemented and tested.

The existence of alkyl tetrazine ethers in the literature and the evidence that the presence of tyrosine also plays a negative role in the formation of cys-tet-lys macrocycles encouraged us to investigate if this method could be employed to create peptide macrocycles using cysteine and serine, threonine, or tyrosine as nucleophilic side chains.<sup>10-19</sup> We therefore explored three peptide sequences (**22-24**) as initial trial candidates for serine and threonine (**Figure 2.16**). Unfortunately these sequences exhibited slightly worse aqueous solubility than the cysteine / lysine counterparts, so we had to include PBS buffer (10 mM, pH~5) and change the acetonitrile/buffer ratio from 1:9 to 1:1. We also raised the equivalents of dichloro-*s*-tetrazine employed back to 4. Intermediates **25-27** could be observed by LC/MS using these conditions. We next attempted to close intermediates **25-27** to macrocycles **28-30** using PBS buffer at pH 6-9, periodically testing the reaction mixture using LC/MS out to one hour. While a mass hit for the desired compounds could occasionally be seen in the MS chromatogram, nothing survived in the crude isolate post-lyophilization. We also tried heating the reactions to

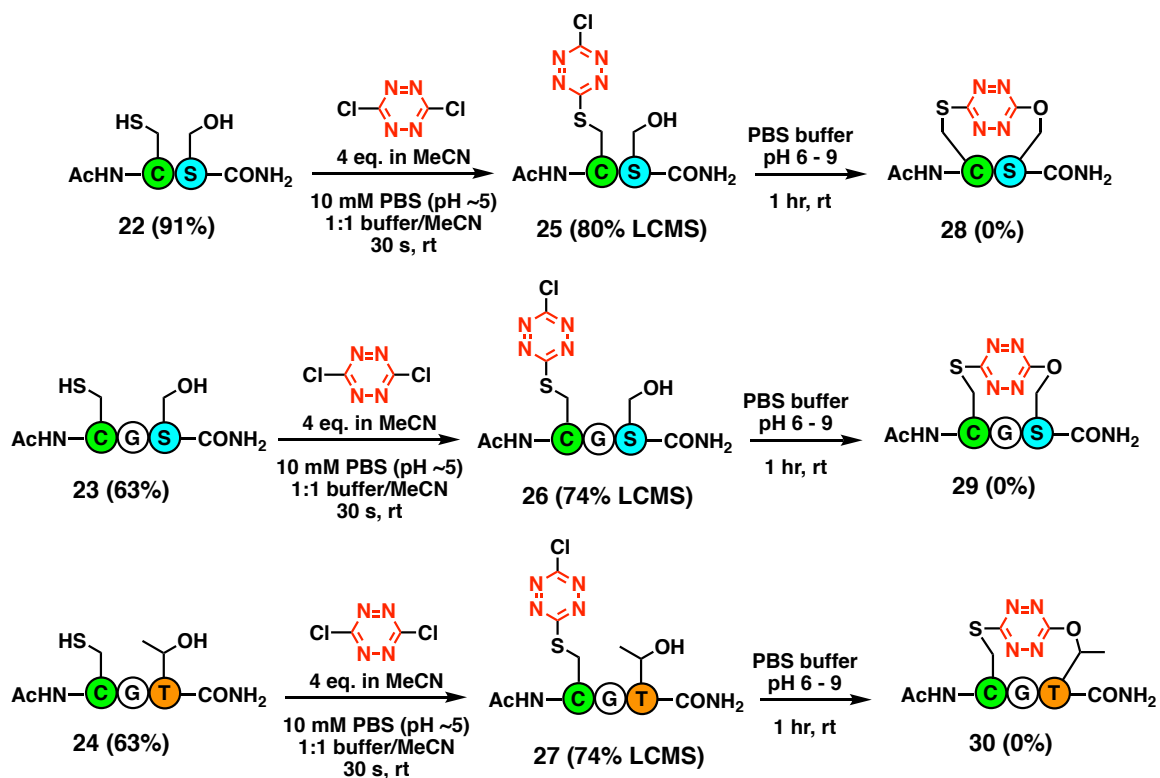


**Figure 2.16.** Attempts at making cys-ser/thr macrocycles with *s*-tetrazine<sup>19</sup>

35°C and saw a small uptick in the amount of macrocycle being formed, but it again did not survive purification.

We also explored the use of two sequences (31-32) shown in **Figure 2.17** to investigate the creation of macrocycles with cysteine and tyrosine.<sup>19</sup> To synthesize the acyclic intermediates 33-34, we could use either the previously discussed method (**Figure 2.16**) for peptides containing serine and threonine, or the method previously developed for the cysteine/lysine macrocycles. Both gave acceptable results for the cysteine/tyrosine peptide substrates. Again we investigated a number of buffers in different pH ranges to find conditions to form macrocycles 35-36. Optimal conditions for the formation of 35 (as observed by LC/MS) were found employing PBS (pH 7.5) over one hour at room temperature, while 36 was most reliably formed with ammonium phosphate (pH 6)

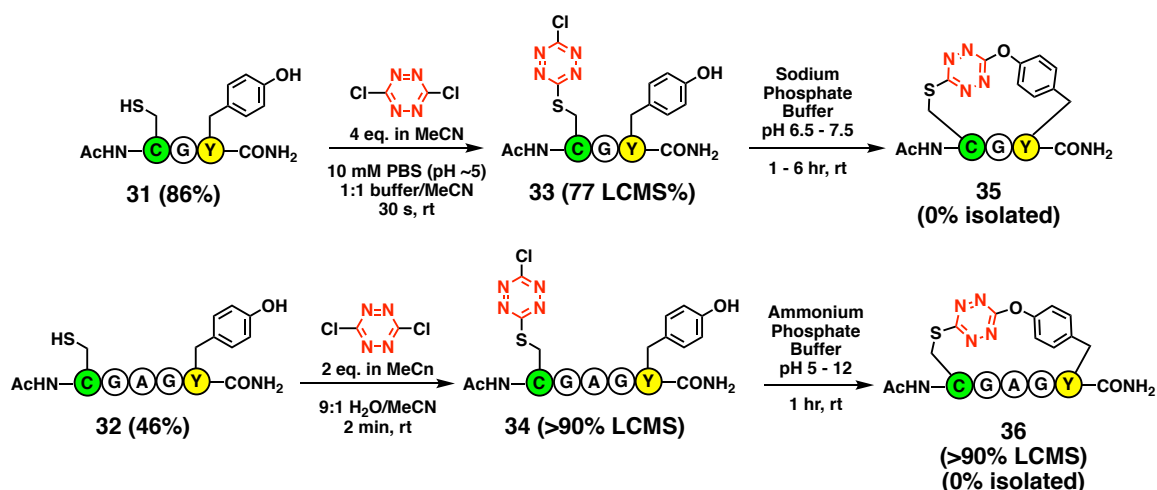


**Figure 2.17.** Attempts at forming cys - tyr macrocycles with *s*-tetrazine<sup>19</sup>

(**Figure 2.18**), also over an hour at room temperature. Unlike the serine/threonine cycles discussed above, the correct mass signals were in fact present by LC/MS analysis of the material recovered from HPLC purification of **35-36** after lyophilization (**Figure 2.19**).

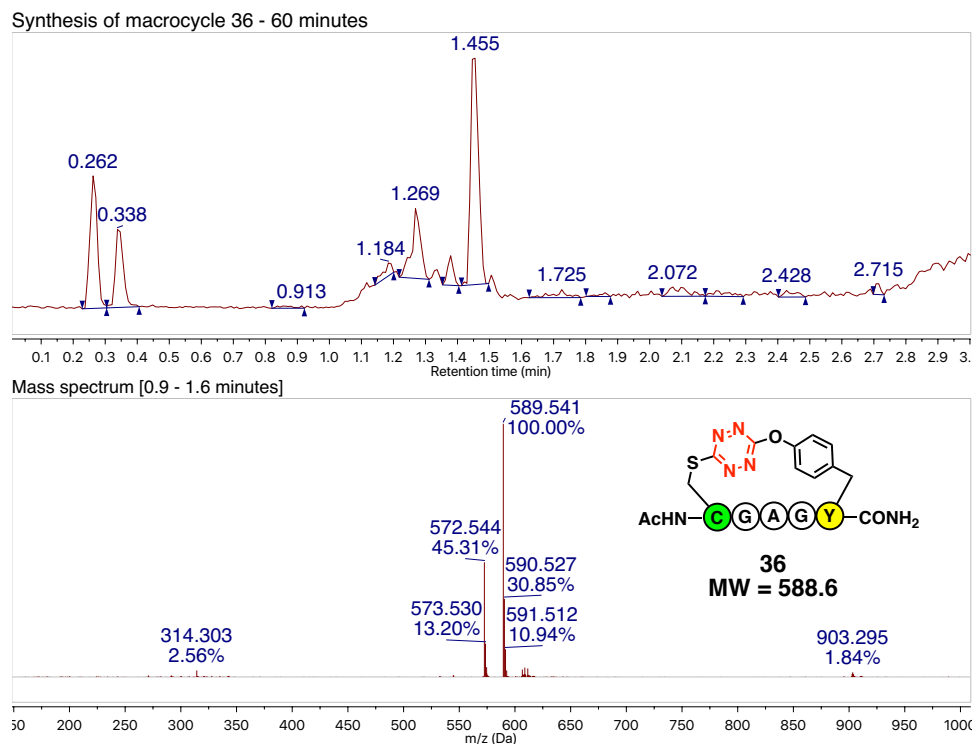
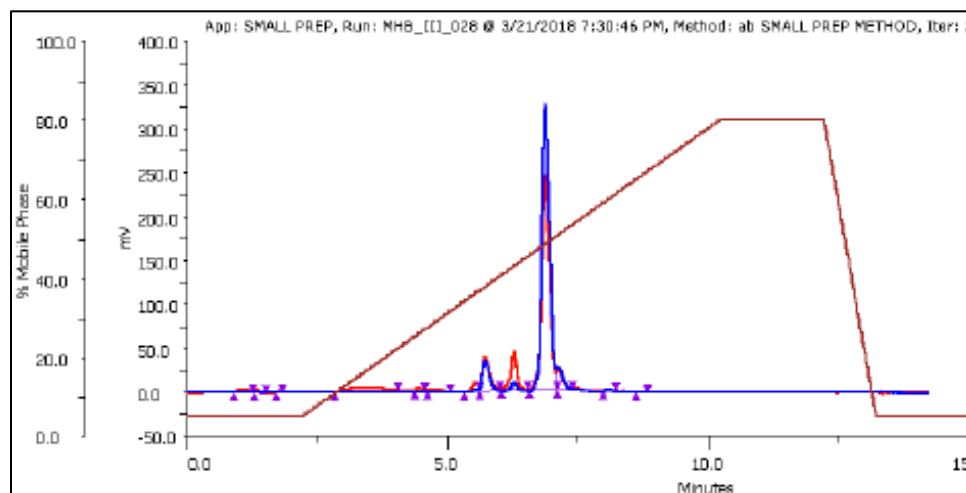
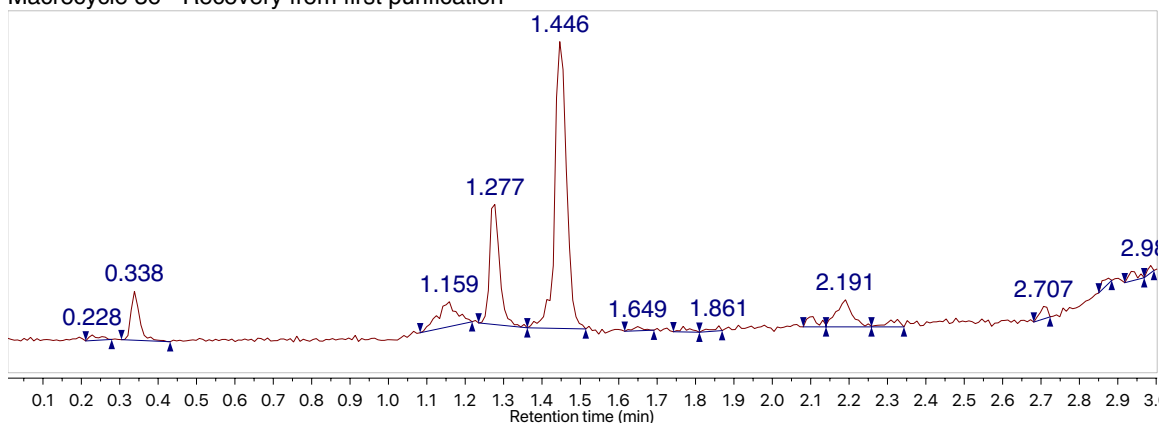


**Figure 2.18.** Synthesis of **36** - reaction mixture at 60 minutes



Macrocycle **36** - Recovery from first purification



Mass spectrum [1.0 - 1.55 minutes]

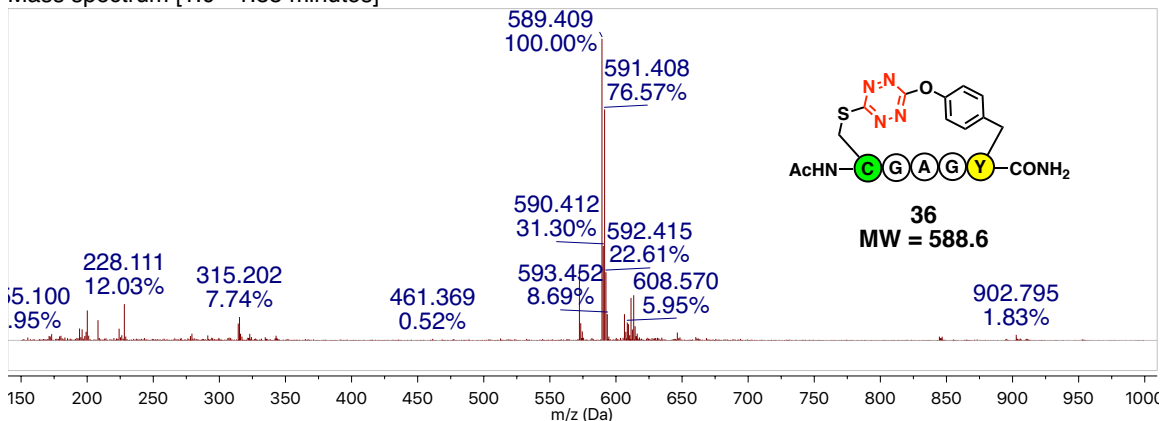


**Figure 2.19.** HPLC (top) and LC/MS (bottom) data from the first purification of **36**

However, we found the isolate also retained a small amount of hydrolyzed product. Not discouraged by this, the products were again purified by HPLC (**Figure 2.20**, top). The purification chromatogram clearly revealed separation of the minor hydrolysis

contaminant, but  $^1\text{H}$  NMR analysis of the isolated material indicated the isolated material was not a single pure compound (**Figure 2.20**, bottom). Of particular importance was the

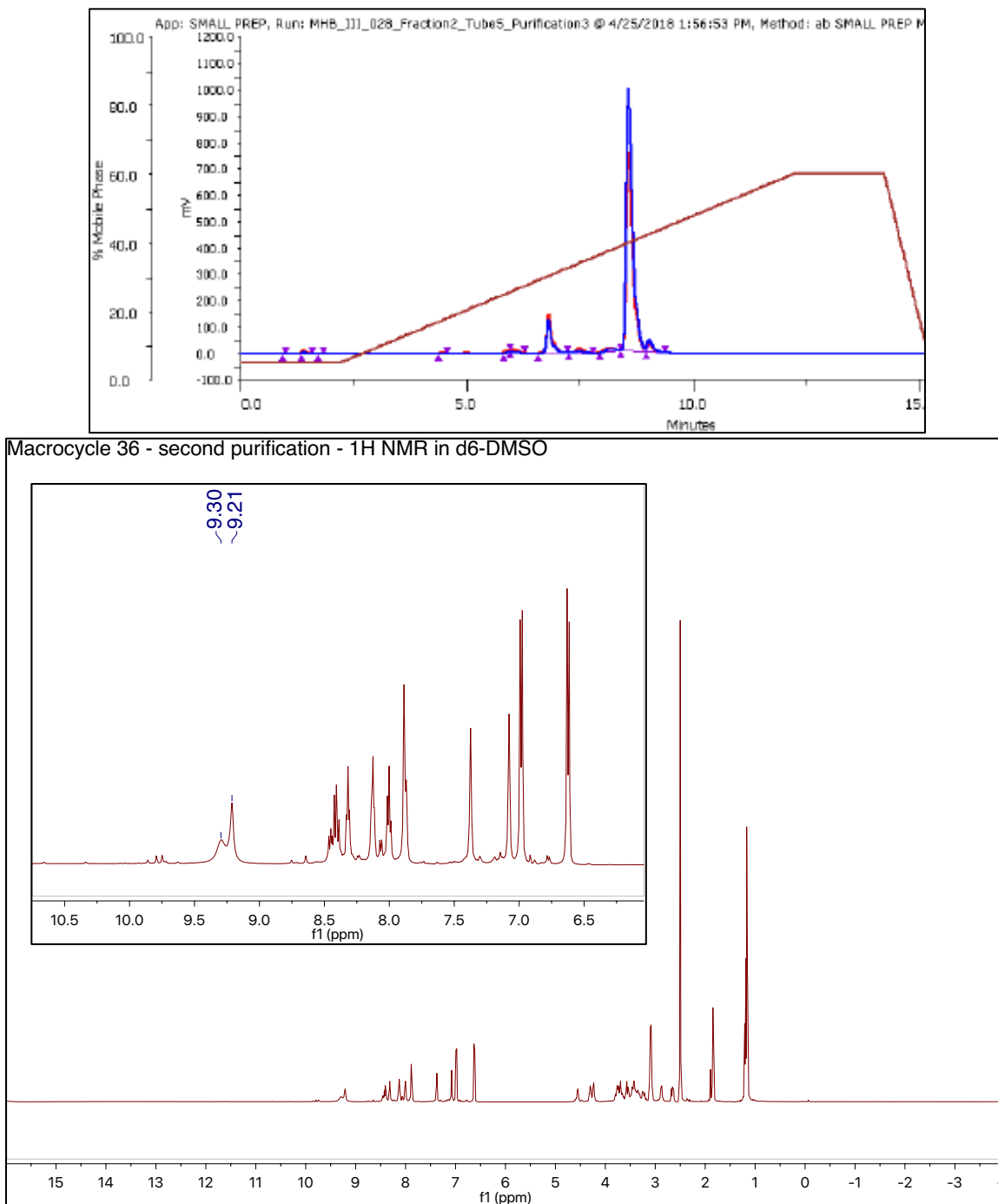


**Figure 2.20.** Second HPLC purification of macrocycle **36** (top) and  $^1\text{H}$  NMR spectrum of isolated material (bottom) (~70% pure)

small peak at  $\sigma = 9.30-9.21$ , corresponding to the phenolic proton of the tyrosine side chain, showing that this sample once again contained acyclic material. A third HPLC purification clearly showed removal of the same impurity with the same retention time, while LCMS analysis of the recovered material again showed that the impurity had reappeared (**Figure 2.21**). To verify that the compounds were hydrolyzing in the presence of water, macrocycle **36** was stirred in Milli-Q water and the progress of solvolysis was monitored by LC/MS. After a 5 days, only 40% of the macrocycle remained.

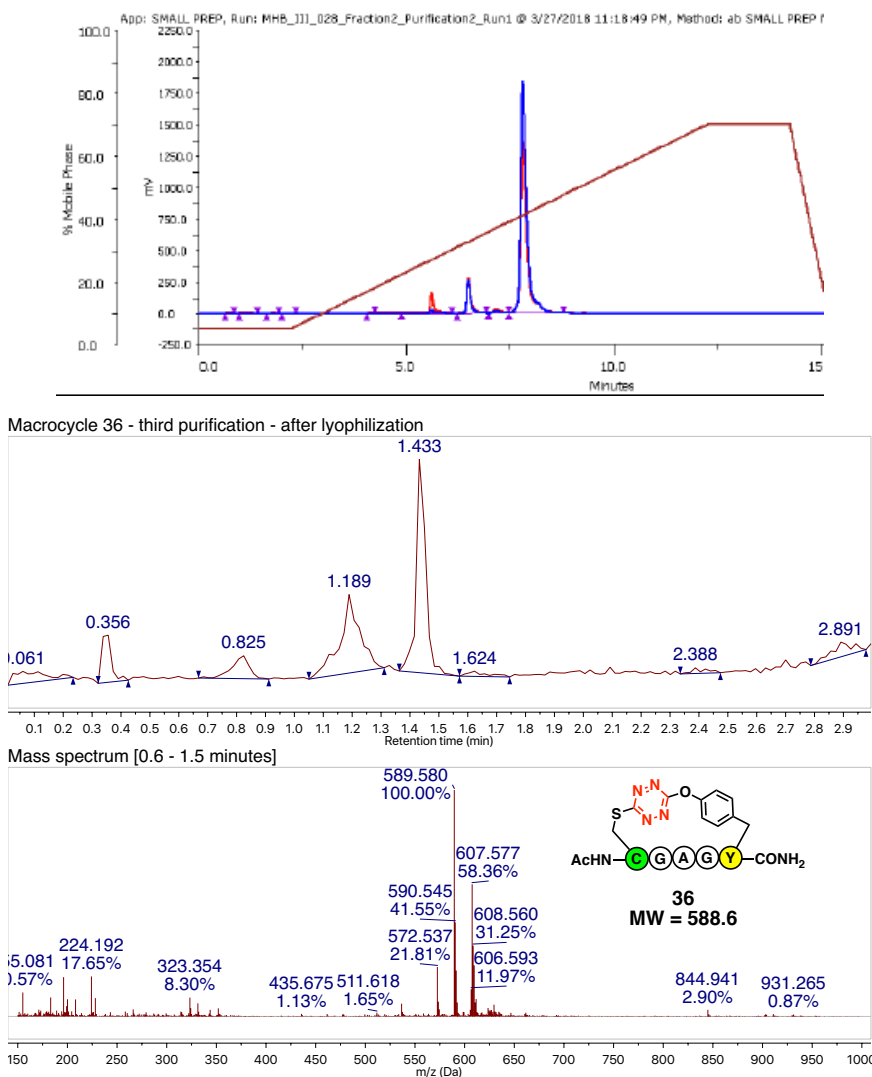


**Figure 2.21.** Third HPLC purification of **36** and LC/MS analysis of isolated material

The results of these investigations reveal that it is simply not feasible to use dichloro-*s*-tetrazine as a reagent for the creation of peptide macrocycles using cysteine and serine, threonine, or tyrosine. While alkyl-tetrazine ethers exist in the literature, they are largely produced with modest success at best (25% average) and even successful examples make use of quite harsh conditions (**Figure 2.22**).<sup>10-11,13</sup> Despite the initial pro-

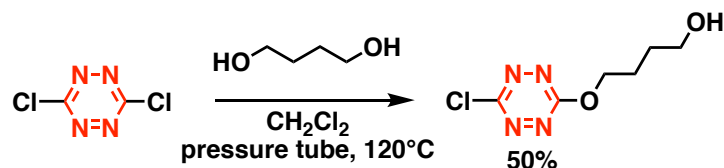


**Figure 2.22.** Synthesis of small molecule alkyl-tetrazine ethers<sup>11</sup>

-mise given by the successful formation of these macrocycles *in situ*, the aqueous sensitivity we observed also seems to be born out by many procedures calling for the use of rigorously dry solvent or molecular sieves.<sup>10-11</sup> Perhaps this problem could be ameliorated if the inverse electron demand Diels-Alder reaction were performed on the macrocycle before purification. The staple should then be less susceptible to hydrolysis once its electron deficiency is improved, although there would be no way to photochemically remove the staple after this modification. Nonetheless, its possible that employing this method could result in a stable stapled peptide.

### **Cys-Tet-Lys Macrocycles as Photochemical Substrates – Unexpected Difficulties!**

As the foray into the chemistry of *s*-tetrazines within the Smith group began by studying photochemistry,<sup>20-23</sup> it would be remiss of us to not conduct some investigation into the photochemistry of the *S,N*-tetrazine macrocycles, although this was an endeavor where the collaboration of the late Robin Hochstrasser would be sorely missed! First, an



assessment of the changes in physical properties moving from *S,S*- to *S,N*-tetrazine substituted macrocycles had to be undertaken with particular regard to how such changes might effect the photochemistry. As discussed in **Chapter 1**, it has been put forth in the literature that *bis* sulfur substitution of *s*-tetrazines allowed for photochemical decompositions to occur because the sulfur atoms acted as barriers to the dissipation of

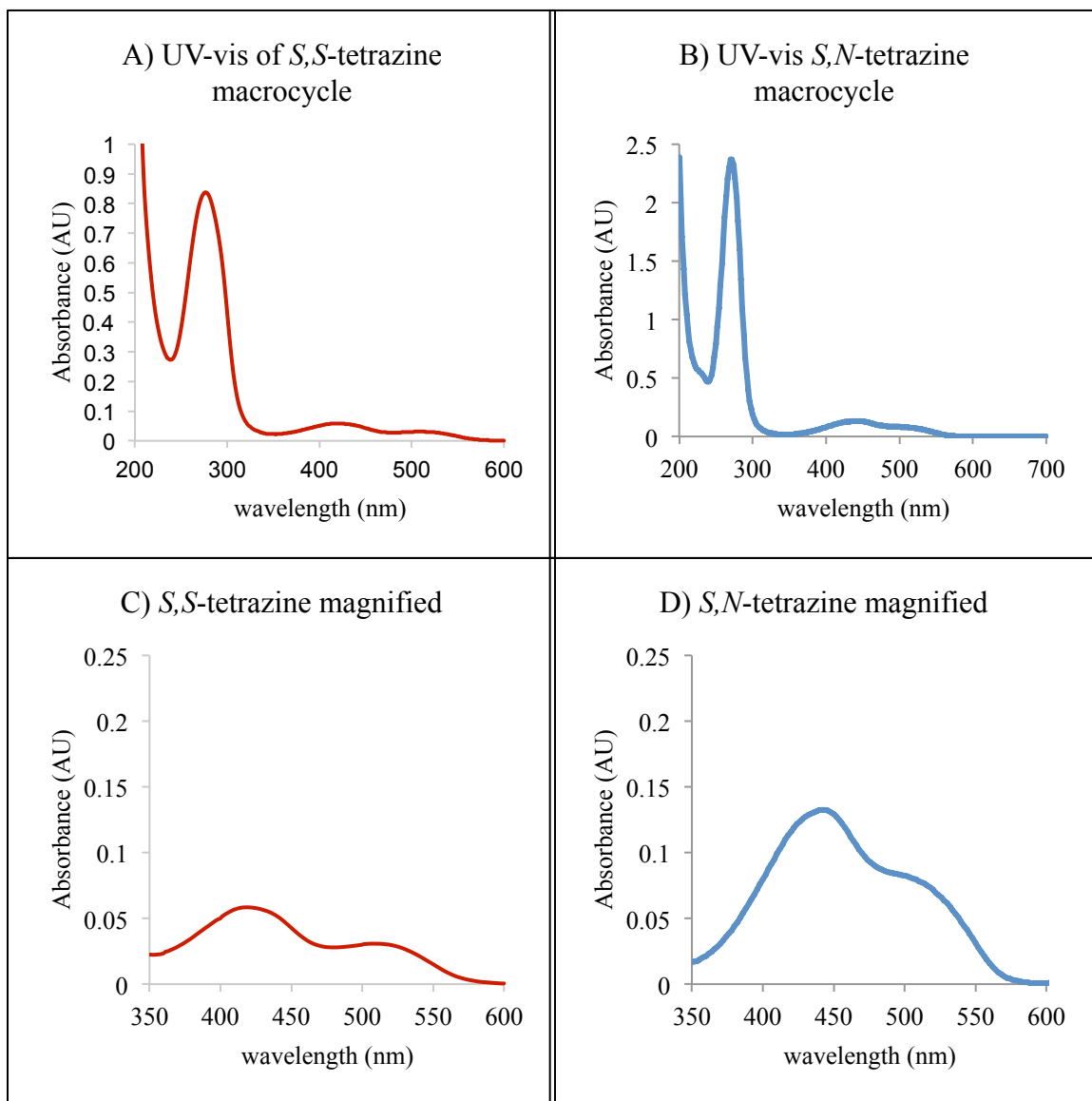


**Figure 2.23.** UV-vis absorption spectra of a *S,S*-tetrazine (**A**) and *S,N*-tetrazine peptide macrocycle (**B**). The 350-600 nm region has been expanded in graphs **C** and **D**. The two absorption peaks are much closer together for *S,N*-tetrazine and for *S,S*-tetrazine.<sup>1</sup>

absorbed energy *via* vibrational relaxation.<sup>24-25</sup> It was apparent that trading one of the sulfur atoms for nitrogen may increase the photochemical stability of the *S,N*-tetrazines by increasing avenues for the vibrational dissipation of energy. UV-vis spectroscopy (**Figure 2.23**) also shows that the  $n - \pi^*$  and  $\pi - \pi^*$  transitions are much closer in energy in the *S,N*-tetrazine system than in *S,S*-tetrazines. These two transitions typically correspond to the two absorption bands in the 350 – 600 nm region.<sup>10-11</sup> While there have been several reports of amino-substituted tetrazines, including discussions on their fluorescent properties, none have mentioned pursuing photodissociation of these compounds.<sup>10-11,26-29</sup>

Our first investigation into the photochemistry of stapled macrocycle **4** began with the conditions employed by Brown and Smith to achieve unstapling of the *S,S*-tetrazine macrocycles.<sup>1</sup> That is, a 3 mg sample of pure macrocycle **4** was dissolved in ~10 mL of methanol and sparged with O<sub>2</sub> gas before being irradiated with UV-B lamps ( $\lambda_{\text{max}} = 312$  nm) over 17 hours, testing the progress of the reaction by LC/MS taking periodic aliquots every 60 minutes (**Figure 2.24**). There have been conflicting reports in the literature about the ability of tetrazine to undergo intersystem crossing and inhabit a triplet-excited state.<sup>10-11,29-31</sup> Molecular oxygen is included as a sparging gas to quench this pathway.<sup>32</sup> Even after 17 hours, we did not witness complete reaction of the starting macrocycle **4** (ca. 10 % remaining). LC/MS analysis revealed a broad range of components, most of which seemed to result from indiscriminate degradation of either **4** or the expected photocleavage product **37**. The mixture was concentrated by passing a

stream of air over the surface of the solution until dry, and then the residue was dissolved in water to be purified *via* HPLC. Unfortunately, no single compound could be isolated in

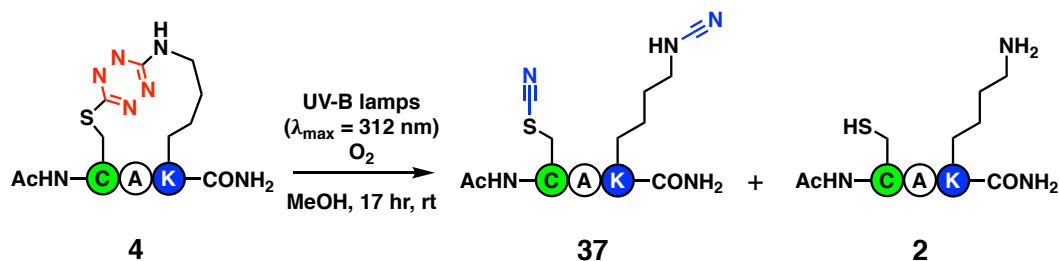


**Figure 2.24.** Investigation of *S,N*-tetrazine photochemistry, first attempt sufficient quantity for further evaluation after the attempted purification. The experiment was repeated with a 1.5 mg sample of **4** that gave similar results. Again, the main components of the mixture after irradiation were compounds **2** and **37**, but nothing could be isolated.

It was somewhat disheartening that we were unable to isolate a clean product from these trials. In order to gain more evidence that the photochemical degradation of macrocycle **3** was preceding in a similar fashion to the *bis* sulfur analogues, we next performed the photolysis *via* irradiation with 254 nm light in a mixture of n-propyl alcohol and water using an IR cell with CaF lenses (insoluble in water) to verify the products by IR signal. Pleasingly, the net difference in IR absorption before and after 5 hours of irradiation clearly revealed two new signals at 2223  $\text{cm}^{-1}$  and 2156  $\text{cm}^{-1}$ , characteristic of the cyanamide and thiocyanate functionalities, respectively (**Figure 2.25**). We also tracked the decrease in UV absorbance @ 265 nm during the course of the photolysis experiment by irradiating 350  $\mu\text{g}$  of **4** in 3 mL of 2:1 acetonitrile and water with UV-C bulbs ( $\lambda_{\text{max}} = 254 \text{ nm}$ ) in a quartz cuvette (**Figure 2.26**). With this spectral

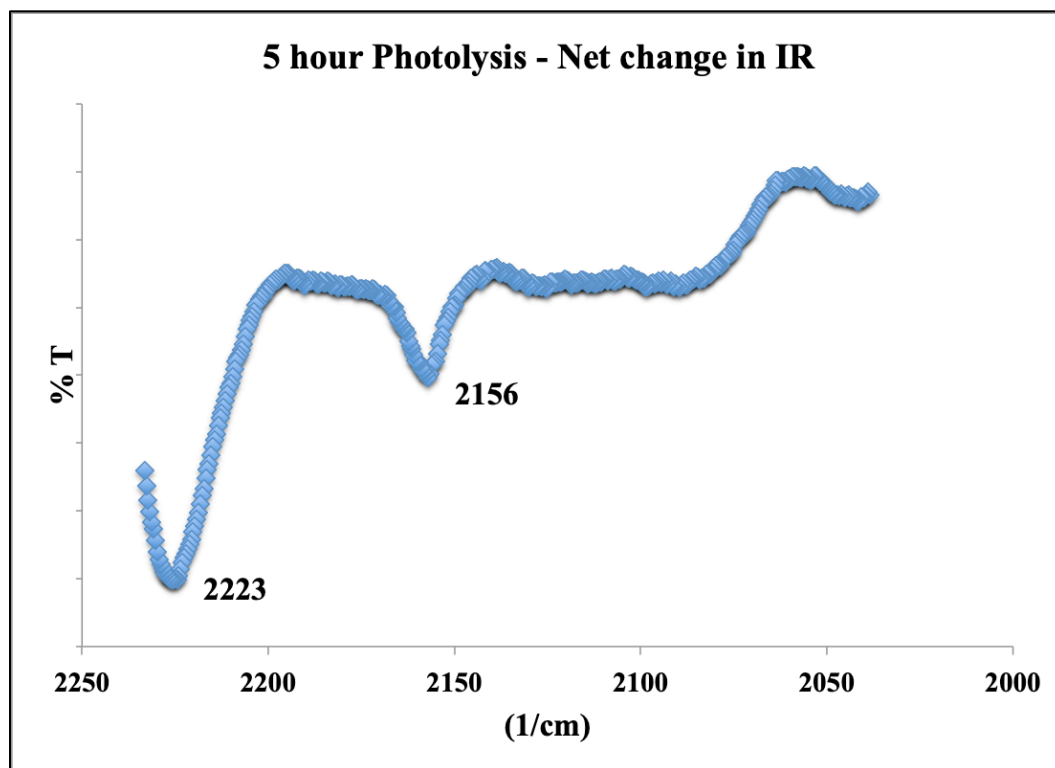


Figure 2.25. Net difference in IR spectrum after 5 hours of irradiation

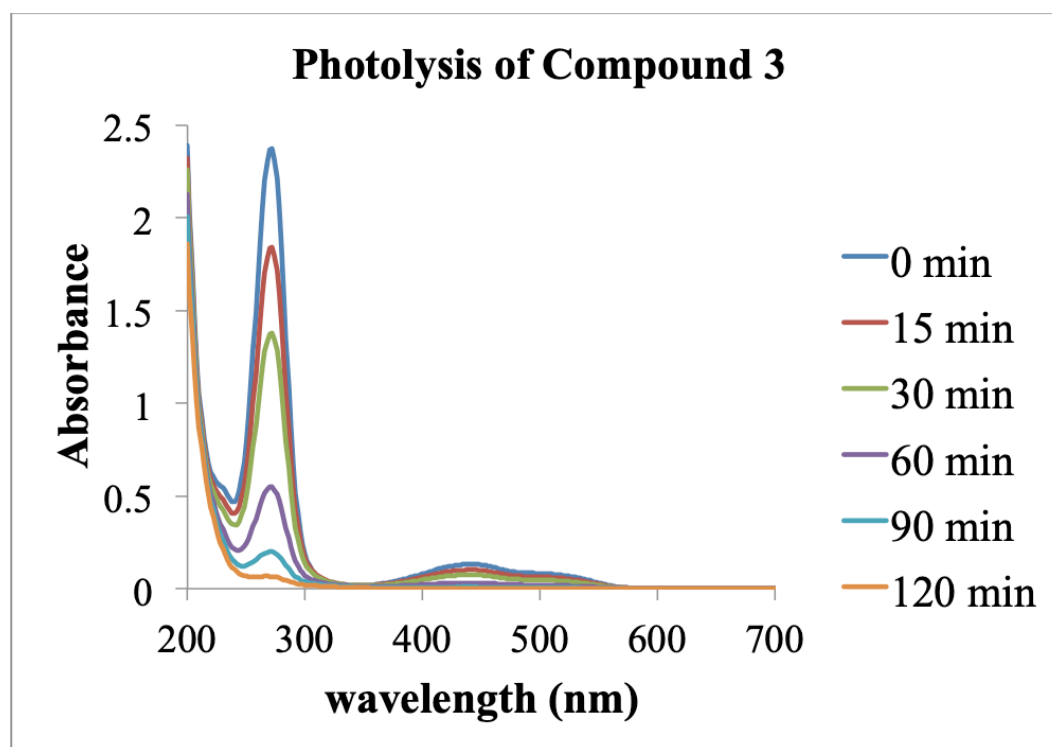
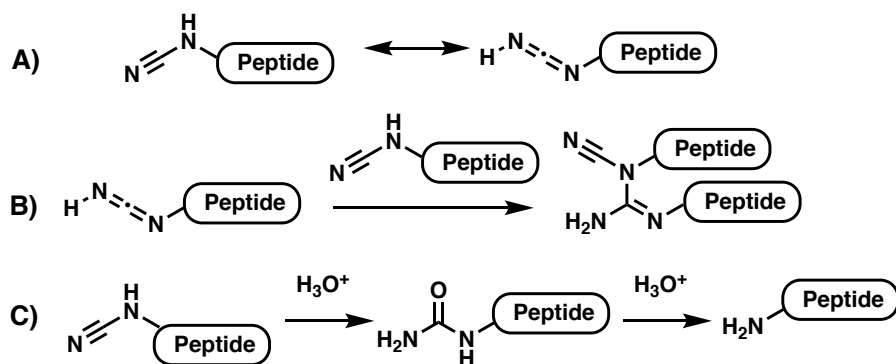


Figure 2.26. UV-Vis absorption during the photolysis of 4



**Figure 2.27.** Degradation pathways of cyanamides;<sup>33</sup> A) isomerization to carbodiimides;<sup>34</sup> B) dimerization and oligomerization to form melamines;<sup>35</sup> C) hydrolysis to give free amines<sup>36</sup>

evidence bolstering our confidence that the photochemical fragmentation of the *S,N*-tetrazine moiety was proceeding as we originally proposed, we turned our thoughts to proposed product **37** (Figure 2.24). The only difference between this structure and the structures resulting from photolysis of the *bis* sulfur substituted tetrazines was the presence of the cyanamide moiety. A search of the literature revealed three different degradation pathways this functional group could be susceptible to under these conditions (Figure 2.27).<sup>33</sup>

The remainder of our efforts concerning the photolysis reaction of macrocycle **4** were focused on attempting to develop a strategy to trap compound **37** and isolate a stable product. Some of the structures we hoped to be able to produce are shown in Figure 2.28. Along with these trapping strategies, we tried irradiating macrocycle **3** at different wavelengths and using different solvent mixtures during the reaction. Unfortunately, none of these strategies bore fruit. Clearly, the photochemistry of the *S,N*-tetrazine staples was more complicated than that of the *S,S*-tetrazine staples previously

developed in the Smith group and, as time was running short, further studies were considered outside the scope of this thesis.<sup>1,,24,37-39</sup>

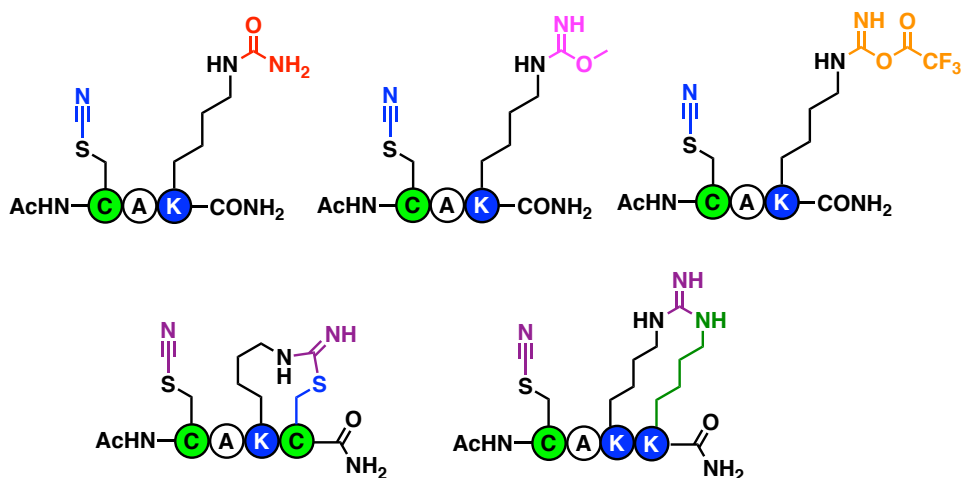


**Figure 2.28.** Attempted trapping strategies

## Summary

The goal of this Thesis work was to take methods previously developed by Brown and Smith<sup>1</sup> for the use of dichloro-*s*-tetrazine in the creation of stapled peptides and to investigate how far that method could be extended to include residues other than cysteine. In the course of this investigation, we developed a method for the successful creation of stapled peptides using a single cysteine and single lysine residue (*seven example explored*, 20 – 54% yield over the two steps). Although this method lacked the general tolerance and applicability of the method previously developed for two cysteine residues we were pleased that some stapling with a cysteine / lysine peptide is possible. Unfortunately we found that this method could not be successfully extended to include serine, threonine, or tyrosine.<sup>19</sup> Regarding the photochemistry of the newly created *S,N*-tetrazine macrocycles, we demonstrated by IR analysis that macrocycle **4** does in fact

undergo photochemical dissociation in a similar fashion to the previous work of Brown and Smith,<sup>1</sup> although isolation of definable products proved unsuccessful. Although this answer was not as positive as we might have hoped, these results clearly demonstrate the limited breath this chemistry can be extended with respect to peptide systems, thus answering the question we originally set out to investigate.

## References – Chapter 2

1. Brown, S.P.; Smith, A.B., III. *J. Am. Chem. Soc.* **2015**, *137*, 4034-4037.
2. Spice, C.D.; Davis, B.G. *Nat. Commun.* **2014**, *5*, 4740.
3. Canovas, C.; Moreau, M.; Bernhard, C.; Oudot, A.; Guillemin, M.; Denat, F.; Goncalves, V. *Angew. Chem. Int. Ed.* **2018**, *57*, 10646-10650.
4. Solé, N.A.; Barany, G. *J. Org. Chem.* **1992**, *57*, 5399-5403.
5. Yudin, A.K. *Chem. Sci.* **2015**, *6*, 30-49.
6. White, C.J.; Yudin, A.K. *Nat. Chem.* **2011**, *3*, 509-524.
7. Aimetti, A.A.; Shoemaker, R.K.; Lin, C.-C.; Anseth, K.S.; *Chem. Commun.* **2010**, *46*, 4061-4063.
8. Lautrette, G.; Touti, F.; Lee, H.G.; Dai, P.; Pentelute, B.L.; *J. Am. Chem. Soc.* **2016**, *138*, 8340-8343.
9. Wolfe, J.M.; Fadzen, C.M.; Holden, R.L.; Yao, M.; Hanson, G.J.; Pentelute, B.L. *Angew. Chem. Int. Ed.* **2018**, *57*, 4756-4759.
10. Gong, Y.-H.; Miomandre, F.; Méallet-Renault, R.; Badré, S.; Galmiche, L.; Tang, J.; Audebert, P.; Clavier, G. *Eur. J. Org. Chem.* **2009**, 6121-6128.
11. Clavier, G.; Audebert, P. *Chem. Rev.* **2010**, *110*, 3299-3314.
12. Novák, Z.; Bostai, B.; Csékei, M.; Lőrinez, K.; Kotschy, A. *Heterocycl.* **2003**, *60* (12), 2653-2668.
13. Saracoglu, N. *Tetrahedron.* **2007**, *63*, 4199-4236.
14. McGrane, S.D.; Bolme, C.A.; Greenfield, M.T.; Chavez, D.E.; Hanson, S.K.; Scharff, R.J. *J. Phys. Chem. A.* **2016**, *120*, 895-902.



15. Allain, C.; Piard, J.; Brosseau, A.; Han, M.; Paquier, J.; Marchandier, T.; Lequeux, M.; Boissière, C.; Audebert, P. *ACS Appl. Mater. Interfaces*. **2016**, *8*, 19843-19846.
16. Chavez, D.E.; Parrish, D.A.; Mitchell, L. *Angew. Chem. Int. Ed.* **2016**, *55*, 8666-8669.
17. Audebert, P.; Miomandre, F.; Clavier, G.; Vernières, M.-C.; Badré, S.; Méallet-Renault, R. *Chem. Eur. J.* **2005**, *11*, 5667-5673.
18. Malinge, J.; Allain, C.; Brosseau, A.; Audebert, P. *Angew. Chem. Int. Ed.* **2012**, *51*, 8534-8537.
19. Mardjuki, R. *Expanding the Utility of the Dichloro-S-Tetrazine Peptide Staple*. Master's Thesis. University of Pennsylvania. 2017.
- Spectral data for compounds **14a-c** and **17a** can be found in the SI.
20. King, D.S.; Denny, C.T.; Hochstrasser, R.M.; Smith, A.B., III. *J. Am. Chem. Soc.* **1977**, *99* (1), 271-273.
21. Dellinger, B.; King, D.S.; Hochstrasser, R.M.; Smith, A.B., III. *J. Am. Chem. Soc.* **1977**, *99* (9), 3197-3198.
22. Hochstrasser, R.M.; King, D.S.; Smith, A.B., III. *J. Am. Chem. Soc.* **1977**, *99* (12), 3923-3933.
23. Dellinger, B.; King, D.S.; Hochstrasser, R.M.; Smith, A.B., III. *J. Am. Chem. Soc.* **1977**, *99* (22), 7138-7142.
24. Tucker, M.J.; Courter, J.R.; Chen, J.; Atasoylu, O.; Smith, A.B., III; Hochstrasser, R.M. *Angew. Chem. Int. Ed.* **2010**, *49*, 3612-3616.
25. Lopez, V.; Marcus, R.A.; *Chem. Phys. Lett.* **1982**, *93* (3), 232-234.

26. Alfanco, J.C.; Matinez, S.J., III; Levy, D.H. *J. Chem. Phys.* **1991**, *94*(4), 2475-2481.
27. Chavez, D.E.; Hiskey, M.A.; *J. Energ. Mater.* **1999**, *17*, 3577-377.
28. Coburn, M.D.; Ott, D.G. *J. Heterocycl. Chem.* **1990**, *27* (7), 1941-1945.
29. Coburn, M.D.; Buntain, G.A.; Harris, B.W.; Hiskey, M.A.; Lee, K.-Y.; Ott, D.G. *J. Heterocycl. Chem.* **1991**, *28* (8), 2049-2050.
30. Scheiner, A.C.; Schnaefel, H.F., III. *J. Chem. Phys.* **1987**, *87* (6), 3539-3556.
31. Gückel, F.; Maki, A.H.; Neugebauer, F.A.; Schweitzer, D.; Vogler, H. *Chem. Phys.* **1992**, *164*, 217-227.
32. Ågren, H.; Vahtras, O. *Chem. Phys.* **1994**, *181*, 291-304.
33. Nau, W.M.; Scaiano, J.C. *J. Phys. Chem.* **1996**, *100*, 11360-11367.
34. GÜthner, T.; Mertschenk, B. (2006). Cyanamides. In *Ullmann's Encyclopedia of Industrial Chemistry*, (Ed.). doi:10.1002/14356007.a08\_139.pub2 (Accessed Dec 26, 2018)
35. Duvernay, F.; Chiavassa, T.; Borget, F.; Aycard, J.-P. *J. Phys. Chem. A.* **2005**, *109*, 603-608.
36. Jürgens, B.; Irran, E.; Senker, J.; Kroll, P.; Müller, H.; Schnick, W. *J. Am. Chem. Soc.* **2003**, *125*, 10288-10300.
37. Kiyoi, T.; Seko, N.; Yoshino, K.; Ito, Y. *J. Org. Chem.* **1993**, *58*, 5118-5120.
38. Abdo, M.; Brown, S.P.; Couter, J.R.; Tucker, M.J.; Hochstrasser, R.M.; Smith, A.B., III. *Org. Lett.* **2012**, *14* (13), 3518-3521.
39. Courter, J.R.; Abdo, M.; Brown, S.P.; Tucker, M.J.; Hochstrasser, R.M.; Smith, A.B., III. *J. Org. Chem.* **2014**, *79*, 759-768.

40. Tucker, M.J.; Abdo, M.; Couter, J.R.; Chen, J.; Brown, S.P.; Smith, A.B., III; Hochstrasser, R.M. *Proc. Natl. Acad. Sci.* **2013**, *110* (43), 17314-17319.

## CHAPTER 3 – SCALE UP PREPARATION OF DICHLORO-*S*-TETRAZINE (1)

The synthesis of dichloro-*s*-tetrazine (**1**) was first reported by Schirmer and coworkers in 1986 as part of a search for new herbicides.<sup>1</sup> This synthesis was achieved by reacting dimethylthio-*s*-tetrazine (**38**)<sup>2</sup> with chlorine gas **Figure 3.1**. Compound **1**

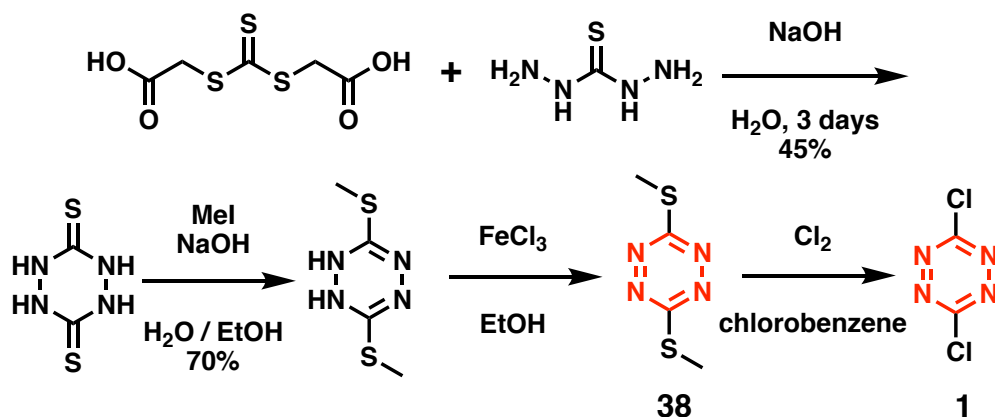


**Figure 3.1.** Original synthesis of dichloro-*s*-tetrazine (**1**)<sup>1</sup> from dimethylthio-*s*-tetrazine (**38**)<sup>2</sup>

reappeared in the literature in 1998 when Sparey and Harrison first reported examples of using **1** as a substrate in the inverse electron demand Diels Alder reaction between tetrazines and unsaturated compounds, originally communicated by Carboni and Lindsey.<sup>3-4</sup> The synthesis of **1** was reported again in 1999 as part of Chavez and Hiskey's ongoing search for high nitrogen content energetic materials.<sup>5</sup> While Chavez and Hiskey's report made good use of the advances made by Coburn and coworkers in the synthesis of 3,6-diamino-*s*-tetrazine by using 3,6-*bis*(3,5-dimethyl-1H-pyrazol-1-yl)-*s*-tetrazine (**39**, **Figure 3.2**)<sup>6-7</sup> as a replacement for the difficult to access **38**, the final

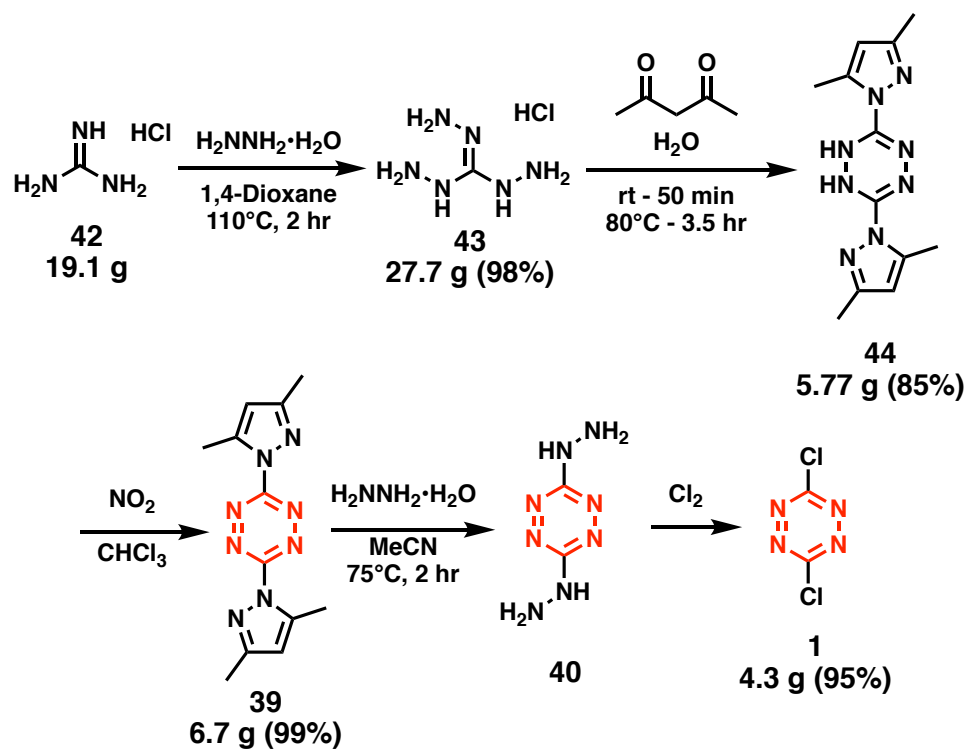


**Figure 3.2.** Chavez and Hiskey's synthesis of dichloro-*s*-tetrazine (**1**)<sup>5</sup> using Coburn and coworker's intermediate (**39**)<sup>7</sup>

conversion from 3,6-dihydrazineyl-*s*-tetrazine (**40**) to dichloro-*s*-tetrazine (**1**) again made use of chlorine gas.<sup>5</sup> In 2006, Helm and coworkers communicated a useful modification to that procedure by replacing chlorine gas with the much more mild trichloroisocyanuric acid (**41**) (**Figure 3.3**).<sup>8</sup> The switch to this much safer and more efficient oxidant (as it can be weighed and transferred as a dry solid and be stored on a shelf at room temperature) made the synthesis of dichloro-*s*-tetrazine much more accessible.<sup>9</sup> Another important modification came from Gong and coworkers when they communicated the replacement of  $\text{NO}_2$  gas with sodium nitrite in the formation of 3,6-*bis*(3,5-dimethyl-1H-pyrazol-1-yl)-*s*-tetrazine (**39**) in 2006 (**Figure 3.4**).<sup>10</sup>

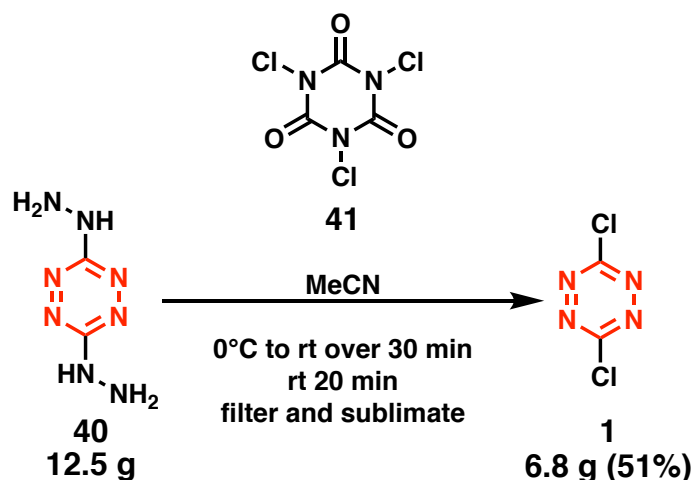


**Figure 3.3.** Modified synthesis of dichloro-*s*-tetrazine (**1**) using trichloroisocyanuric acid (**41**); It is worth noting that the authors purified **1** by sublimation rather than filtration through celite. As **1** is thermally unstable, the low yield can be attributed to the method of purification.<sup>8</sup>

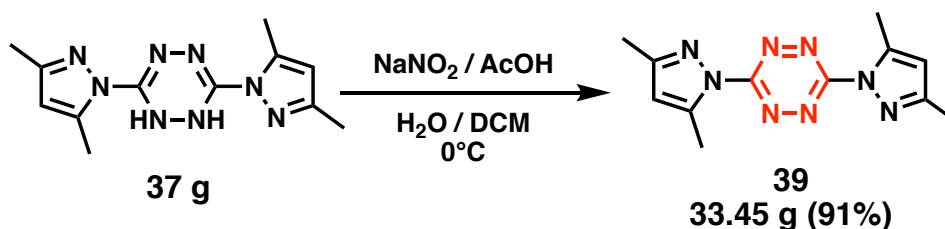


**Figure 3.4.** Use of sodium nitrite for the synthesis of 3,6-bis(3,5-dimethyl-1H-pyrazol-1-yl)-*s*-tetrazine (**41**)<sup>10</sup>

Both **1** and **39** are often featured in the literature as versatile synthons for the synthesis of tetrazines *via* S<sub>N</sub>Ar displacement.<sup>11-13</sup> The *s*-tetrazine chromophore continues to provide new avenues of research on photoactive high explosives from the Los Alamos National Laboratory in the constant search for new high - energy materials.<sup>14-19</sup> In the biological realm, dichloro-*s*-tetrazine (**1**) has been used as a starting point for the synthesis of stapled peptides and proteins,<sup>20-24</sup> site-specific dual-labeling of peptides and proteins,<sup>25</sup> and the templated synthesis of ternary biological constructs.<sup>26</sup> In drug delivery, in inverse electron demand Diels Alder reaction has been used in to

develop a “click to release” strategy pairing antibody-guided delivery of a drug molecule, the release of which is triggered by tetrazine ligation.<sup>27-31</sup> In small molecule organic chemistry, **1** continues to be a source of new fluorophores,<sup>10-11,13,32-33</sup> a partner in cross-coupling reactions,<sup>34-35</sup> and a building block for materials chemistry.<sup>36-37</sup>

Despite this frequent and widely varied usage, no one has communicated a verified scalable procedure for the synthesis of 3,6-dichloro-*s*-tetrazine (**1**). Having scaled up the procedure communicated by Gong and coworkers, we sought to fill this need by submitting a safe, scalable synthetic protocol to *Organic Synthesis*, as we believe this represents the most reliable route to the production of dichloro-*s*-tetrazine available today (Figure 3.5). The steps from guanidine hydrochloride (**42**) through the formation of **44**

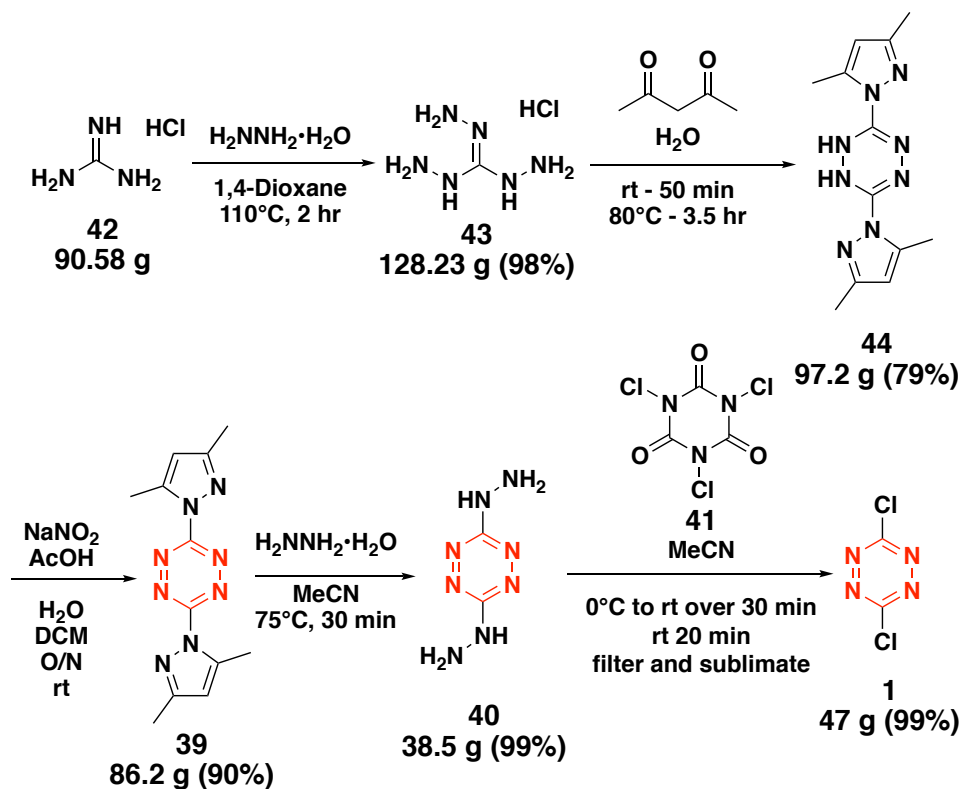


Figure 3.5. Full route for the synthesis of dichloro-*s*-tetrazine (**1**)

were first reported by Coburn and coworkers.<sup>7</sup> The only modification made to these steps was the addition of an aqueous workup for the isolation of **44** rather than the original method of filtration followed by drying *in vacuo*. While this added separation necessitates additional solvent usage, raising the environmental impact of the process, it dramatically accelerates access to pure, dry **44**. The transformation from **44** to **39** was first communicated by Gong and coworkers using chemistry that had been previously applied to tetrazine syntheses following the Pinner route.<sup>10,38</sup> While the gaseous nitric oxide oxidation communicated by Coburn and coworkers works faster, gaseous nitric oxide and Dreschel's Bottle reaction vessels are not as common in synthetic laboratories as they once were. The *in situ* generation of nitrous acid *via* sodium nitrite and acetic acid communicated by Gong uses much more common reagents to achieve the same transformation in comparable yield (>90%) and is therefore much more generally accessible.<sup>10</sup> The transformation from **39** to **40** was communicated by Chavez and Hiskey, who also made several different salts of **40** and determined that the material could be handled relatively safely under 120°C through differential thermal analysis.<sup>5</sup> The method for final transformation to dichloro-*s*-tetrazine (**1**) was originally communicated by Helm and coworkers.<sup>8</sup> The use of trichloroisocyanuric acid (**41**) as chlorine source and oxidant is preferable because **41** is a bench stable, free flowing powder and therefore much more safe and accessible than chlorine gas cylinders. Pleasingly, this final step is the only one that involves detailed purification. We found that multiple passes of the reaction mixture through a celite plug provides adequately pure material (only 1 carbon detectable by <sup>13</sup>C NMR). However, **1** can be purified further by vacuum sublimation if rigorously pure material should be required.



### References – Chapter 3

1. Shirmer, U.; Wuerzer, B.; Meyer, N.; Neugebauer, F.A.; Fischer, H. *Ger. Offen.* DE 3508214. **1986**.
2. Sandström, J. *Acta. Chem. Scand.* **1961**, *15* (7), 1575-1582.
3. Sparey, T.J.; Harrison, T. *Tet. Lett.* **1998**, *39*, 5973-5874.
4. Carboni, R.A.; Lindsey, R.V., JR. *Am. Chem. Soc.* **1959**, *81* (16), 4342-4346.
5. Chavez, D.E.; Hiskey, M.A. *J. Energ. Mater.* **1999**, *17*, 357-377.
6. Coburn, M.D.; Ott, D.G. *J. Heterocycl. Chem.* **1990**, *27* (7), 1941-1945.
7. Coburn, M.D.; Buntain, G.A.; Harris, B.W.; Hiskey, M.A.; Lee, K.-Y.; Ott, D.G. *J. Heterocycl. Chem.* **1991**, *28*, 2049-2050.
8. Helm, M.D.; Plant, A.; Harrity, J.P.A. *Org. Biomol. Chem.* **2006**, *4*, 4278-4280.
9. Tilstam, U.; Weinmann, H. *Org. Process Res. Dev.* **2002**, *6* (4), 384-393.
10. Gong, Y.-H.; Miomandre, F.; Méallet-Renault, R.; Badré, S.; Galmiche, L.; Tang, J.; Audebert, P.; Clavier, G. *Eur. J. Org. Chem.* **2009**, 6121-6128.
11. Novák, Z.; Bostai, B.; Csékei, M.; Lörinez, K.; Kotschy, A. *Heterocycles.* **2003**, *60* (12), 2653-2668.
12. Saracoglu, N. *Tetrahedron.* **2007**, *63*, 4199-4236.
13. Clavier, G.; Audebert, P. *Chem. Rev.* **2010**, *110*, 3299-3314.
14. McGrane, S.D.; Bolme, C.A.; Greenfield, M.T.; Chavez, D.A.; Hanson, S.K.; Scharff, R.J. *J. Phys. Chem. A.* **2016**, *120*, 895-902.
15. Chavez, D.A.; Hiskey, M.A.; Naud, D.L.; *Propellants Explos. Pyrotech.* **2004**, *29* (4), 209-215.

16. Greenfield, M.T.; McGrane, S.D.; Bolme, C.A.; Bjorgaard, J.A.; Nelson, T.R.; Tretiak, S.; Scharff, R.J. *J. Phys. Chem. A* **2015**, *119*, 4846-4855.
17. Chavez, D.A.; Parrish, D.A.; Mitchell, L. *Angew. Chem. Int. Ed.* **2016**, *55*, 8666-8669.
18. Chavez, D.A.; Myers, T.W.; Veauthier, J.M.; Greenfield, M.T.; Scharff, R.J.; Parrish, D.A. *Synlett* **2015**, *26*, 2029-2032.
19. Chavez, D.A.; Hanson, S.K.; Veauthier, J.M.; Parrish, D.A. *Angew. Chem. Int. Ed.* **2013**, *52*, 6876-6879.
20. Tucker, M.J.; Courter, J.R.; Chen, J.; Atasoylu, O.; Smith, A.B., III; Hochstrasser, R.M. *Angew. Chem. Int. Ed.* **2010**, *49*, 3612-3616.
21. Abdo, M.; Brown, S.P.; Courter, J.R.; Tucker, M.J.; Hochstrasser, R.M.; Smith, A.B., III. *Org. Lett.* **2012**, *14* (13), 3518-3521.
22. Courter, J.R.; Abdo, M.; Brown, S.P.; Tucker, M.J.; Hochstrasser, R.M.; Smith, A.B., III. *J. Org. Chem.* **2014**, *79*, 759-768.
23. Tucker, M.J.; Abdo, M.; Courter, J.R.; Chen, J.; Brown, S.P.; Smith, A.B., III; Hochstrasser, R.M. *Proc. Natl. Acad. Sci.* **2013**, *110* (43), 17314-17319.
24. Brown, S.P.; Smith, A.B., III. *J. Am. Chem. Soc.* **2015**, *137*, 4034-4037.
25. Canovas, C.; Moreau, M.; Bernhard, C.; Oudot, A.; Guillemin, M.; Denat, F.; Goncalves, V. *Angew. Chem. Int. Ed.* **2018**, *57*, 10646-10650.
26. Rao, B.V.; Dhokale, S.; Rajamohanan, P.R.; Hotha, S. *Chem. Commun.* **2013**, *49*, 10808-10810.
27. Versteegen, R.M.; Rossin, R.; Hoeve, W.t.; Janssen, H.M.; Robillard, M.S. *Angew. Chem. Int. Ed.* **2013**, *52*, 14112-14116.

28. Fan, X.; Ge, Y.; Lin, F.; Yang, Y.; Zhang, G.; Ngai, W.S.C.; Lin, Z.; Zheng, S.; Wang, J.; Zhao, J.; Li, J.; Chen, P.R. *Angew. Chem. Int. Ed.* **2016**, *55*, 14046-14050.
29. Rossin, R.; Duijnhoven, S.M.J.v.; Hoeve, W.t.; Janssen, H.M.; Kleijn, L.H.J.; Hoeben, F.J.M.; Versteegen, R.M.; Robillard, M.S. *Bioconjugate Chem.* **2016**, *27*, 1697-1706.
30. Carlson, J.C.T.; Mikula, H.; Weissleder, R. *J. Am. Chem. Soc.* **2018**, *140*, 3603-3612.
31. Okai, P.N.A.; Agustin, E.; Miller, M.R.; Sheng, J.; Royzen, M. *J. Biomol. Struct. Dyn.* **2015**, *33*, 56-57.
32. Audebert, P.; Miomandre, F.; Clavier, G.; Vernières, M.-C.; Badré, S.; Méallet-Renault, R. *Chem. Eur. J.* **2005**, *11*, 5667-5673.
33. Maline, J.; Allain, C.; Brosseau, A.; Audebert, P. *Angew. Chem. Int. Ed.* **2012**, *51*, 8534-8537.
34. Bender, A.M.; Chopko, T.C.; Bridges, T.M.; Lindsley, C.W. *Org. Lett.* **2017**, *19*, 5693-5696.
35. Novák, Z.; Kotschy, A. *Org. Lett.* **2003**, *5* (19), 3495-3497.
36. Liu, H.-B.; Zhang, Q.; W, M.-X. *Angew. Chem. Int. Ed.* **2018**, *57*, 6536-6540.
37. Zhu, J.; Hiltz, J.; Lennox, R.B.; Schirmacher, R. *Chem. Commun.* **2013**, *49*, 10275-10277.
38. Pinner, A. *Ber. Dtsch. Chem. Ges.* **1897**, *30*, 1871.

## EXPERIMENTAL

**Reaction Equipment.** Peptides were synthesized on a Liberty Blue<sup>TM</sup> Automated Microwave Peptide Synthesizer (CEM Corporation). N-terminus capping reactions and cleavage from resin were performed in peptide synthesis vessels (20 – 30 mL) fit with coarse fritted glass support and Teflon stopcocks. Peptide synthesis vessels were agitated on a Lab Line Mistral Multi-Mixer (Model 4600). Photochemical Experiments were performed in a Rayonet<sup>TM</sup> Srinivasan-Griffin Photoreactor (The Southern New England Ultraviolet Company) using light sources at 420 nm (LuzChwem [LZC-420]), 350-385 nm (Southern New England Ultraviolet Company [RPR-3500A]), 315 nm (Sankyo Denki [G8TSE]), or 254 nm (Southern New England Ultraviolet Company [RPR-2537A]).

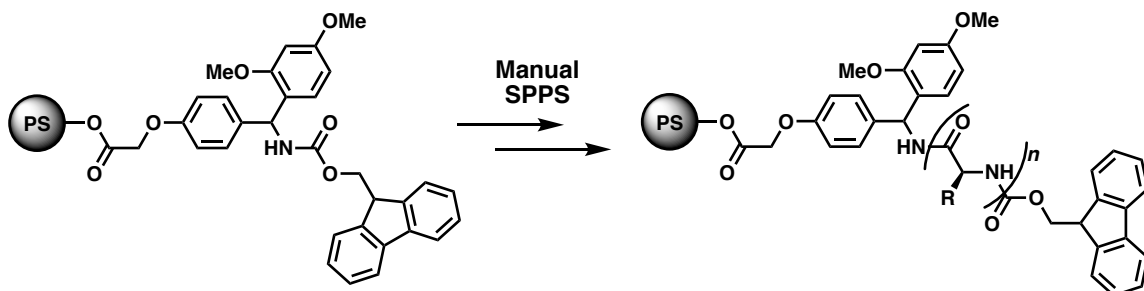
**Chromatography.** Preparatory-scale reverse-phase chromatography was performed with a Gilson 215 liquid handler/injector fitted with a Gilson binary HPLC pump system (model 333/334) and a Gilson UV/Vis dual wavelength detector (model 156). Gilson Trilution<sup>TM</sup> LC software was used as the control interface for the described instrument configuration. Chromatographies were carried out on a Waters Sunfire<sup>TM</sup> Prep C<sub>18</sub> 5  $\mu$ m OBD<sup>TM</sup>, 19mm ID x 100 mm column (Part No. 186002567), or a Vydac Preperative C<sub>18</sub> 10  $\mu$ m, 300 Å, 22 mm ID x 100 mm column (Cat. No. 218TP1022). The eluent was acetonitrile (HPLC grade, Fisher Chemical) and Milli-Q water, purified from facility DI water with a Millipore Simplicity<sup>TM</sup> water purification system (Cat. No. SIMS00000) equipped with a SimpliPak<sup>TM</sup> 1 filter (Millipore, Cat. No. SIPK0SIA1), with a 0.1% trifluoroacetic acid buffer unless otherwise noted. Gradients and flow rate were

compound-specific. Peptides were isolated using a Labconco Freezone 12 Plus lyophilizer modified to run off an Edwards 28 2-stage vacuum pump.

**Instruments Used for Obtaining Spectral Data.** 1D and 2D NMR spectra were recorded on a Bruker Avance III equipped with a 5 mm DCH CyroProbe platform. The low-resolution LC-MS analyses were conducted using a Waters Acquity<sup>TM</sup> UPLC system equipped with an SQ detector for mass analysis and a TUV detector for optical analysis. The LC-MS samples were analyzed as solutions in water or acetonitrile, prepared at 0.15 – 0.20 mg/mL concentration. The LC-MS chromatography was carried out on a Water Acquity<sup>TM</sup> HSS-C<sub>18</sub> column (2.1 x 50 mm; 1.8 μm; Part No. 188003532) with linear gradients of 0.10% formic acid in acetonitrile and 0.10% formic acid water. Accurate mass measurement was obtained on Waters LC-TOF mass spectrometer (model LCT-XE Premier) using electrospray ionization in positive or negative mode, depending upon the analyte. Waters software calibrates and reports by use of neutral atomic masses. The mass of the electron is not included. All FTIR spectra were taken on a Nicolet 6700 FTIR spectrometer or PerkinElmer FTIR (model Spectrum BX).

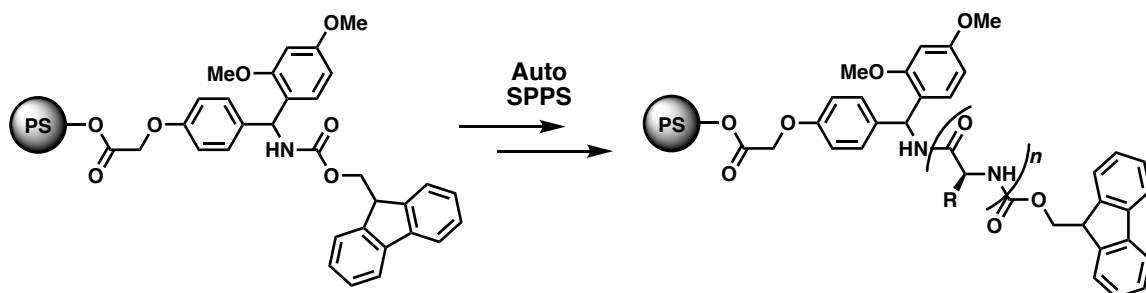
**General Resin Washing Procedure.** Resin washing was conducted with the indicated volume of named solvent and repeated as described. Each wash was allowed to contact resin beads for ~30 seconds. At the end of each washing cycle, the solvent was pushed through the frit of the peptide synthesis vessel using a barbed inlet air adapter with a 14/20 male ground glass joint. In peptide synthesis vessels without a ground glass joint, a neoprene rubber filter adapter was added to facilitate a tight seal.

## General Procedure for Manual Solid – Phase Peptide Synthesis



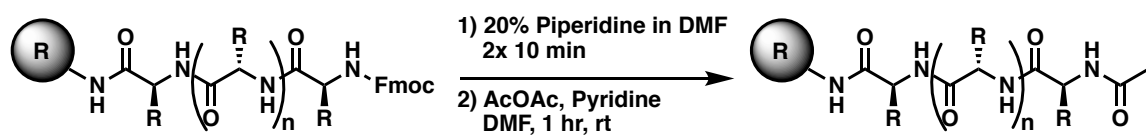
**Manual Solid Phase Peptide Synthesis.** Designated resin was weighed out and placed in a clean, dry peptide synthesis vessel. Resin was swollen with ~4mL of DCM for 30 minutes. Resin was washed with DMF (2 x 2mL), a solution of 20% piperidine in DMF (2 x 5mL, allowing each wash to contact resin for 10 minutes before being drained), and DMF (5 x ~4mL). A premixed solution (coupling cocktail) of fmoc-protected amino acid, Oxyma, HBTU, and DIPEA in 5mL of semi-dry (stored over 4Å sieves) DMF was added to the resin and the vessel was gently rocked for 1 hour. The coupling cocktail was drained; resin was washed with DMF (2 x 3mL), 20% piperidine in DMF solution (2 x 5mL, allowing each wash to contact resin for 10 minutes before draining), and DMF (5 x ~4 mL). The next coupling cocktail was then added. The cycle of coupling cocktail mixing and addition, 1 hour of gentle rocking, and subsequent washes was repeated for each amino acid in the peptide. After the last DMF was sequence, the resin was washed with DCM (2 x 5 mL) and stored under vacuum.

## General Procedure for Automated Solid Phase Peptide Synthesis.



**Solid Phase Peptide Synthesis (SPPS).** Peptides were synthesized on a CEM Liberty Blue microwave assisted automated peptide synthesizer. All couplings were done with the “standard coupling procedure” included in the liberty blue software. Deprotection solution was 10 g of piperidine in 10 mL of ethanol and 90 mL of *N*-methyl-pyrrolidone. Coupling reagents were *N,N'*-diisopropylcarbodiimide and 1-hydroxybenzotriazole monohydrate. *N*-terminus was left fully protected at the end of the synthesis. The resin-bound peptide was transferred to a peptide synthesis vessel, washed with DMF (2 x 5 mL) and DCM (2 x 5 mL), and stored under vacuum.

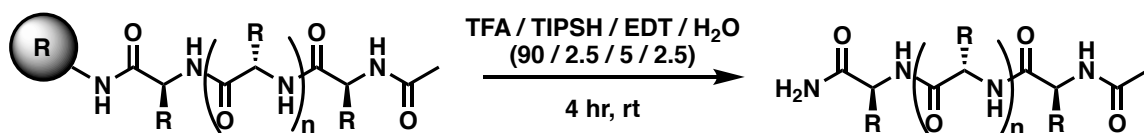
## General Procedure for *N*-terminus Peptide Capping



***N*-terminus Peptide Capping.** The peptide synthesis vessel containing the resin-bound peptide was removed from the vacuum line and the resin was swelled in DCM (~7 mL) for 1 hour. The solvent was drained and the resin was washed with DMF (2 x 5 mL). The premixed Fmoc deprotection solution consisting of 20% piperidine in DMF (5 mL) was

added to the synthesis vessel and allowed to maintain contact with the resin for 10 minutes before being drained from the vessel. This deprotection cycle was repeated twice, after which the resin was washed with DMF (5 x 5 mL). A premixed capping solution consisting of acetic anhydride (20 equivalents) and pyridine (20 equivalents) in DMF (6 mL) was added to the peptide synthesis vessel and was allowed to maintain contact with the resin for 1 hour with gentle oscillation on a Mistral Multi-Mixer (Lab Line Instruments). After 1 hour, the capping solution was drained and the resin was washed with DMF (2 x 5 mL) and DCM (2 x 5 mL) and stored under vacuum.

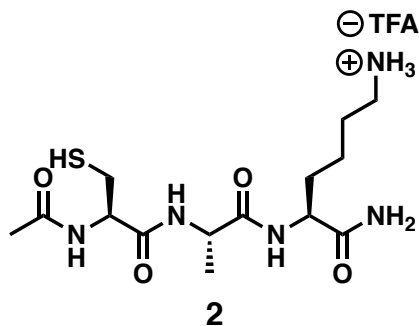
### General Procedure for Peptide Cleavage and Global Deprotection



**Peptide Cleavage and Global Deprotection.** The peptide synthesis vessel containing the resin bound peptide was removed from the vacuum line. DCM (~7 mL) was added to the vessel and the resin was swelled for 1 hour. The DCM was drained and 7 mL of a premixed peptide cleavage cocktail (9 mL TFA, 0.5 mL EDT, 0.25 mL H<sub>2</sub>O, and 0.25 mL TIPSH) was added to the vessel. The cleavage cocktail was allowed to make contact with the resin beads for 4 hours while the vessel was subjected to gentle rocking. The solution was drained into a 50 mL round bottom flask and the remaining cleavage cocktail (~3 mL) was used to wash the beads before also being drained into the round bottom flask. The combined cleavage cocktail was concentrated under reduced pressure and the crude peptide was precipitated from solution by the addition of diethyl ether. The

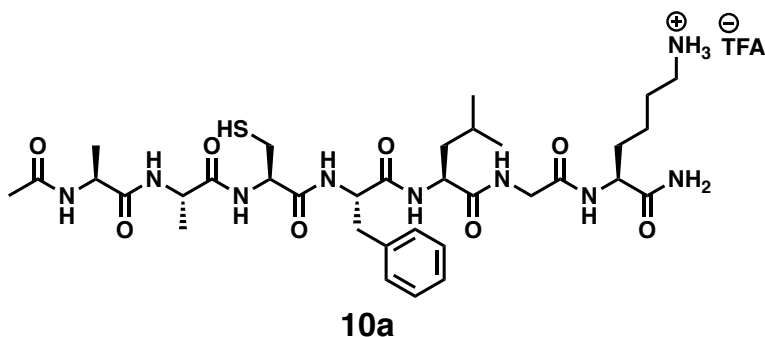


crude peptide was isolated by vacuum filtration in a cinkered glass funnel and dried *in vacuo*. Each peptide was then purified by HPLC as indicated.



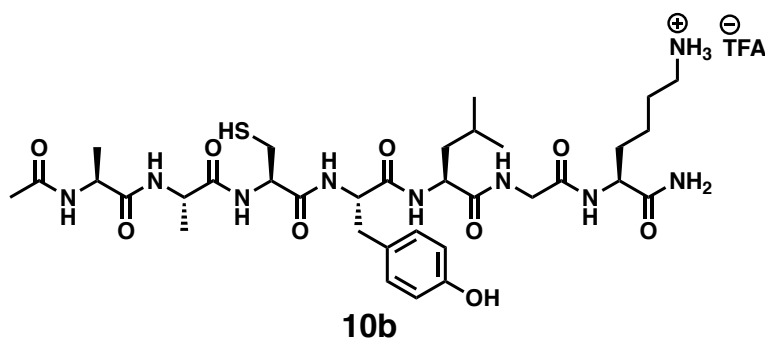
**Peptide 2.** Prepared by automated SPPS from Rink Amide AM resin (0.49 mmol, 1.05 g) according to the procedures given above. Isolated residue was dissolved in 4 mL of Milli-Q water and purified by reverse-phase chromatography (gradient 5 – 50% organic over 5 minutes at a 20 mL/minute flow rate) on the Gilson HPLC setup with the Sunfire column discussed above. Fractions were collected with 210 nm detection with a 20 mV threshold. After lyophilization, compound was isolated as 167.1 mg (78%) of amorphous white powder as the TFA salt: AMM (ESI) Found  $m/z$  362.1866 [(M+H)<sup>+</sup>; calcd for C<sub>14</sub>H<sub>28</sub>N<sub>5</sub>O<sub>4</sub>S: 362.1862]; <sup>1</sup>H NMR (500 MHz, DMSO-*d*<sub>6</sub>) δ 8.23 (d,  $J$  = 6.9 Hz, 1H), 8.12 (d,  $J$  = 7.8 Hz, 1H), 7.81 (d,  $J$  = 8.2 Hz, 1H), 7.64 (s, 3H), 7.29 (d,  $J$  = 2.1 Hz, 1H), 7.07 (d,  $J$  = 2.1 Hz, 1H), 4.37 (td,  $J$  = 7.6, 5.4 Hz, 1H), 4.23 (p,  $J$  = 7.1 Hz, 1H), 4.14 (td,  $J$  = 8.6, 5.0 Hz, 1H), 2.76 (ddd,  $J$  = 12.0, 8.9, 5.7 Hz, 3H), 2.69 – 2.60 (m, 1H), 2.41 (t,  $J$  = 8.5 Hz, 1H), 2.36 (p,  $J$  = 1.9 Hz, 1H), 1.87 (s, 3H), 1.66 (ddd,  $J$  = 13.8, 10.8, 6.0 Hz, 1H), 1.49 (p,  $J$  = 7.9, 6.7 Hz, 3H), 1.34 – 1.26 (m, 1H), 1.22 (d,  $J$  = 7.1 Hz, 3H). <sup>13</sup>C NMR (126 MHz, DMSO) δ 173.44, 171.97, 171.06, 169.95, 169.68, 158.19, 115.97,

55.08, 52.09, 48.69, 40.02, 39.85, 39.69, 39.52, 39.35, 39.19, 39.02, 38.73, 31.46, 26.68, 26.52, 26.19, 22.56, 22.24, 17.84, 17.74, 17.33; IR (KBr,  $\text{cm}^{-1}$ ) 3283 (br), 3198 (w), 3072 (w), 2934 (w), 1675 (s), 1621 (s), 1539 (s), 1424 (s), 1393 (w), 1373 (s), 1289 (w), 1200 (s), 1187 (s), 1135 (s), 838 (w), 800 (w), 722 (s), 691 (s), 625 (s), 600 (s).



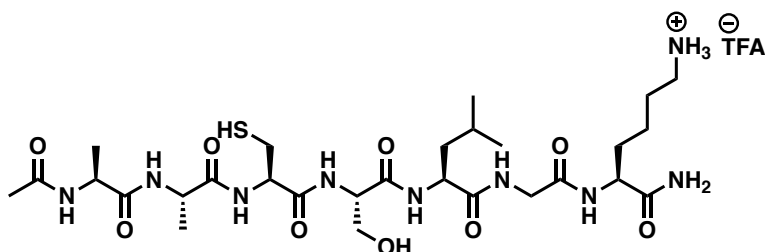
**Peptide 10a.** Prepared by automated SPPS from Rink Amide AM resin (0.513 mmol, 1.09 g) according to the procedures given above. Isolated residue was dissolved in 2 mL of Milli-Q water, 2 mL of acetonitrile, and 2 mL of trifluoroacetic acid before being purified by reverse-phase chromatography (gradient 10 – 70% organic over 8 minutes at a 20 mL/minute flow rate) on the Gilson HPLC setup with the Sunfire column discussed above. Fractions were collected with 210 nm detection with a 20 mV threshold. After lyophilization, compound was isolated as 144 mg (33%) of amorphous white powder as the TFA salt: AMM (ESI) Found  $m/z$  750.3990  $[(M+H)^+]$ ; calcd for  $\text{C}_{34}\text{H}_{56}\text{N}_9\text{O}_8\text{S}$ : 750.3973];  $^1\text{H}$  NMR (500 MHz,  $\text{DMSO}-d_6$ )  $\delta$  8.19 – 7.99 (m, 5H), 7.88 – 7.83 (m, 2H), 7.66 (s, 4H), 7.35 (s, 1H), 7.27 – 7.15 (m, 6H), 7.08 (s, 1H), 4.52 (td,  $J = 8.8, 4.5$  Hz, 1H), 4.37 – 4.10 (m, 4H), 3.72 (d,  $J = 5.7$  Hz, 2H), 3.04 (dd,  $J = 14.1, 4.5$  Hz, 1H), 2.90 – 2.71 (m, 3H), 2.71 – 2.64 (m, 2H), 2.24 (t,  $J = 8.6$  Hz, 1H), 1.83 (s, 3H), 1.74 – 1.65 (m, 1H), 1.60 (h,  $J = 6.7$  Hz, 1H), 1.49 (ddd,  $J = 23.4, 11.5, 5.3$  Hz, 6H), 1.37 – 1.21 (m, 1H),

1.17 (d,  $J = 7.1$  Hz, 5H), 0.85 (dd,  $J = 24.5, 6.5$  Hz, 6H).  $^{13}\text{C}$  NMR (126 MHz, DMSO)  $\delta$  173.46, 172.47, 172.25, 170.85, 169.46, 169.30, 168.53, 157.91 (q,  $J = 31.2$  Hz), 137.58, 129.21, 128.09, 126.31, 117.17 (q,  $J = 299.6$  Hz), 54.83, 53.91, 52.03, 51.22, 48.29, 48.25, 42.07, 40.78, 38.73, 37.14, 31.33, 26.66, 26.21, 24.02, 23.10, 22.51, 22.49, 22.27, 21.58, 18.04, 17.70. IR (KBr,  $\text{cm}^{-1}$ ) 3269 (br), 3054 (br), 2926 (br), 1626 (s), 1522 (s), 1198 (s), 1177 (w), 1130 (w), 830 (w), 796 (w), 699 (w), 695 (w).



**Peptide 10b.** Prepared by automated SPPS from Rink Amide AM resin (0.46 mmol, 1.08 g) according to the procedures given above. Isolated residue was dissolved in 7 mL of Milli-Q water and 3 mL acetonitrile before being purified by reverse-phase chromatography (gradient 5 – 60% organic over 8 minutes at a 20 mL/minute flow rate) on the Gilson HPLC setup with the Sunfire column discussed above. Fractions were collected with 210 nm detection with a 5 mV threshold. After lyophilization, compound was isolated as 301 mg (68%) of amorphous white powder as the TFA salt: AMM (ESI) Found  $m/z$  766.3945 [(M+H) $^+$ ]; calcd for  $\text{C}_{34}\text{H}_{56}\text{N}_9\text{O}_9\text{S}$ : 766.3922];  $^1\text{H}$  NMR (500 MHz, DMSO- $d_6$ )  $\delta$  9.20 (s, 1H), 8.13 (d,  $J = 7.1$  Hz, 1H), 8.10 (d,  $J = 7.2$  Hz, 1H), 8.03 (dd,  $J = 6.9, 3.9$  Hz, 2H), 7.99 (d,  $J = 8.0$  Hz, 1H), 7.89 (d,  $J = 7.9$  Hz, 1H), 7.85 (d,  $J = 8.1$  Hz, 1H), 7.66 (s, 3H), 7.35 (s, 1H), 7.10 (s, 1H), 7.01 (d,  $J = 8.5$  Hz, 2H), 6.62 (d,  $J = 8.5$  Hz, 2H), 4.41 (td,  $J = 8.5, 4.5$  Hz, 1H), 4.32 (td,  $J = 7.4, 5.4$  Hz, 1H), 4.24 (ddt,  $J =$

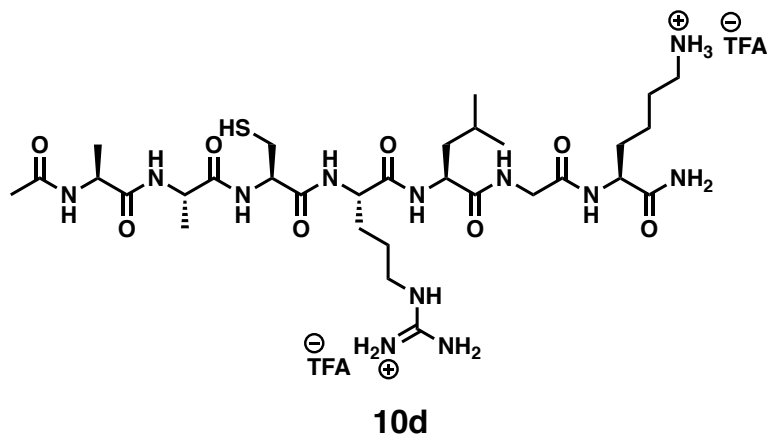
14.2, 12.5, 7.4 Hz, 3H), 4.15 (td,  $J = 8.6, 4.9$  Hz, 1H), 3.78 – 3.65 (m, 2H), 2.91 (dd,  $J = 14.1, 4.5$  Hz, 1H), 2.80 – 2.62 (m, 5H), 2.26 (t,  $J = 8.6$  Hz, 1H), 1.83 (s, 3H), 1.69 (ddt,  $J = 13.9, 9.5, 5.6$  Hz, 1H), 1.60 (hept,  $J = 6.7$  Hz, 1H), 1.49 (tdd,  $J = 14.9, 12.1, 10.8, 6.4$  Hz, 5H), 1.28 (dq,  $J = 16.5, 8.8, 8.2$  Hz, 2H), 1.18 (dd,  $J = 7.1, 4.9$  Hz, 6H), 0.87 (d,  $J = 6.6$  Hz, 3H), 0.82 (d,  $J = 6.4$  Hz, 3H);  $^{13}\text{C}$  NMR (126 MHz, DMSO)  $\delta$  173.50, 172.51, 172.29 (2C), 171.03, 169.45, 169.32, 168.55, 158.00 (q,  $J = 30.6$  Hz), 155.83, 130.15, 127.56, 117.28 (q,  $J = 300.5$  Hz), 114.89, 54.89, 54.30, 52.05, 51.21, 48.33, 48.26, 42.09, 40.75, 38.74, 36.37, 31.33, 26.67, 26.24, 24.01, 23.11, 22.53, 22.29, 21.58, 18.06, 17.71; IR (KBr,  $\text{cm}^{-1}$ ) 3274 (br), 3073 (br), 2932 (br), 1625 (s), 1529 (s), 1443 (w), 1201 (s), 1138 (br), 834 (w), 800 (w), 721 (s), 619 (w), 551 (w).



**10c**

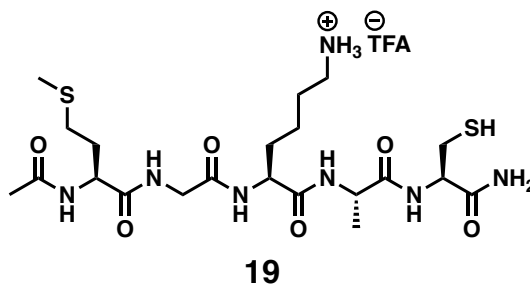
**Peptide 10c.** Prepared by automated SPPS from Rink Amide AM resin (0.513 mmol, 1.09 g) according to the procedures given above. Isolated residue was dissolved in 2 mL of Milli-Q water, 1 mL of acetonitrile, and 1 mL of trifluoroacetic acid before being purified by reverse-phase chromatography (gradient 10 – 50% organic over 7 minutes at a 20 mL/minute flow rate) on the Gilson HPLC setup with the Sunfire column discussed above. Fractions were collected with 210 nm detection with a 20 mV threshold. After lyophilization, compound was isolated as 125 mg (32%) of amorphous white powder as

the TFA salt: AMM (ESI) Found  $m/z$  712.3452 [(M+Na)<sup>+</sup>]; calcd for C<sub>28</sub>H<sub>51</sub>N<sub>9</sub>O<sub>9</sub>SNa: 712.3428]; <sup>1</sup>H NMR (500 MHz, DMSO-*d*<sub>6</sub>) δ 8.16 – 8.06 (m, 3H), 8.03 (dd,  $J = 10.7, 7.7$  Hz, 2H), 7.95 (d,  $J = 7.8$  Hz, 1H), 7.83 (d,  $J = 8.2$  Hz, 1H), 7.67 (s, 3H), 7.33 (s, 1H), 7.07 (s, 1H), 5.06 (s, 1H), 4.42 (q,  $J = 7.3$  Hz, 1H), 4.34 – 4.19 (m, 4H), 4.14 (td,  $J = 8.6, 4.9$  Hz, 1H), 3.69 (dd,  $J = 16.9, 5.9$  Hz, 2H), 3.59 (ddd,  $J = 27.0, 10.6, 5.9$  Hz, 2H), 2.74 (dp,  $J = 13.7, 7.6, 6.2$  Hz, 4H), 2.37 (t,  $J = 8.5$  Hz, 1H), 1.83 (s, 3H), 1.66 (dtq,  $J = 33.4, 12.9, 6.5$  Hz, 2H), 1.49 (dt,  $J = 14.2, 6.5$  Hz, 5H), 1.34 – 1.15 (m, 8H), 0.85 (dd,  $J = 23.1, 6.5$  Hz, 6H); <sup>13</sup>C NMR (126 MHz, DMSO) δ 173.50, 172.47, 172.40, 172.35, 170.03, 169.69, 169.29, 168.55, 158.01 (q,  $J = 31.2$  Hz), 117.21 (q,  $J = 299.9$  Hz), 61.49, 55.17, 54.77, 52.08, 51.38, 48.33, 48.20, 42.13, 40.52, 38.75, 31.29, 26.66, 26.26, 24.08, 23.12, 22.52, 22.29, 21.49, 18.06, 17.76; IR (KBr, cm<sup>-1</sup>) 3276 (br), 3055 (br), 2926 (br), 1627 (s), 1520 (s) 1419 (w), 1200 (s), 1172 (w), 1130 (w), 1062 (w), 951 (w), 807 (w), 761 (w), 718 (w), 667 (w).



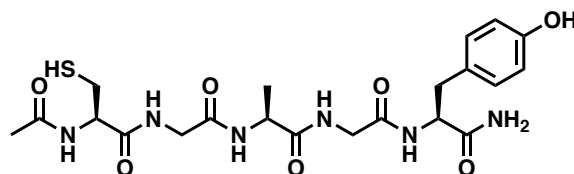
**Peptide 10d.** Prepared by automated SPPS from Rink Amide AM resin (0.506 mmol, 1.08 g) according to the procedures given above. Isolated residue was dissolved in 4 mL of Milli-Q water before being purified by reverse-phase chromatography (gradient 10 – 60% organic over 6 minutes at a 20 mL/minute flow rate) on the Gilson HPLC setup with the Sunfire column discussed above. Fractions were collected with 210 nm detection with a 20 mV threshold. After lyophilization, compound was isolated as 239 mg (54%) of amorphous white powder as the TFA salt: AMM (ESI) Found  $m/z$  781.4138 [(M+Na)<sup>+</sup>; calcd for C<sub>31</sub>H<sub>58</sub>N<sub>12</sub>O<sub>8</sub>NaS: 781.4119]; <sup>1</sup>H NMR (500 MHz, DMSO-*d*<sub>6</sub>) δ 8.20 – 8.09 (m, 3H), 8.07 (d,  $J$  = 7.6 Hz, 1H), 7.95 (d,  $J$  = 7.5 Hz, 2H), 7.89 (d,  $J$  = 8.0 Hz, 1H), 7.78 (s, 3H), 7.67 (t,  $J$  = 5.4 Hz, 1H), 7.52 – 6.91 (m, 6H), 4.37 (q,  $J$  = 7.1 Hz, 1H), 4.31 – 4.18 (m, 4H), 4.14 (td,  $J$  = 8.4, 5.1 Hz, 1H), 3.81 – 3.67 (m, 2H), 3.08 (q,  $J$  = 6.4 Hz, 2H), 2.75 (q,  $J$  = 7.6 Hz, 4H), 2.38 (t,  $J$  = 8.6 Hz, 1H), 1.83 (s, 3H), 1.76 – 1.39 (m, 11H), 1.38 – 1.09 (m, 8H), 0.96 – 0.70 (m, 6H); <sup>13</sup>C NMR (126 MHz, DMSO) δ 173.56, 172.61, 172.46, 172.35, 171.15, 169.70, 169.49, 168.63, 158.66 (q,  $J$  = 31.8 Hz), 156.83, 117.05 (q,  $J$  = 298.6 Hz), 54.98, 52.43, 52.17, 51.14, 48.42, 42.01, 40.87, 40.43, 38.72, 31.36,

28.86, 26.69, 26.11, 25.02, 24.11, 23.11, 22.53, 22.31, 21.54, 17.98, 17.70; IR (KBr,  $\text{cm}^{-1}$ ) 3270 (br), 3047 (br), 2931 (br), 1653 (s), 1521 (s), 1417 (w), 1366 (w), 1200 (s), 1175 (s), 1129 (s), 831 (w), 798 (w), 718 (w).



**Peptide 19.** Prepared by automated SPPS from Rink Amide AM resin (0.509 mmol, 1.08 g) according to the procedures given above. Isolated residue was dissolved in 10 mL of Milli-Q water before being purified by reverse-phase chromatography (gradient 5 – 75% organic over 9 minutes at a 20 mL/minute flow rate) on the Gilson HPLC setup with the Sunfire column discussed above. Fractions were collected with 210 nm detection with a 5 mV threshold. After lyophilization, compound was isolated as 133 mg (23%) of amorphous white powder as the TFA salt: AMM (ESI) Found  $m/z$  517.7574 [(M+H)<sup>+</sup>; calcd for C<sub>34</sub>H<sub>56</sub>N<sub>9</sub>O<sub>9</sub>S: 517.7586]; <sup>1</sup>H NMR (500 MHz, DMSO-*d*<sub>6</sub>)  $\delta$  8.25 (t,  $J$  = 5.8 Hz, 1H), 8.21 – 8.12 (m, 2H), 7.92 (d,  $J$  = 7.9 Hz, 1H), 7.84 (d,  $J$  = 8.0 Hz, 1H), 7.71 (s, 3H), 7.37 (s, 1H), 7.22 (s, 1H), 4.42 – 4.18 (m, 4H), 3.83 – 3.57 (m, 2H), 2.97 – 2.65 (m, 5H), 2.54 – 2.40 (m, 1H), 2.26 (dd,  $J$  = 9.0, 7.8 Hz, 1H), 2.03 (s, 3H), 1.94 – 1.86 (m, 1H), 1.85 (s, 3H), 1.76 (dt,  $J$  = 11.2, 7.6, 3.8 Hz, 1H), 1.67 (tt,  $J$  = 14.0, 5.9 Hz, 1H), 1.59 – 1.46 (m, 4H), 1.39 – 1.19 (m, 4H); <sup>13</sup>C NMR (126 MHz, DMSO)  $\delta$  172.15, 171.95, 171.49, 171.40, 169.81, 168.88, 158.11 (q,  $J$  = 31.7 Hz), 117.06 (q,  $J$  = 299.3 Hz), 54.63,

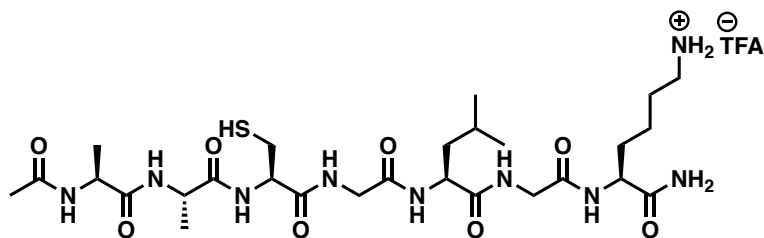
52.21, 52.19, 48.58, 42.10, 40.02, 38.75, 31.41, 31.33, 29.58, 26.69, 26.17, 22.55, 22.19, 17.59, 14.58; IR (KBr,  $\text{cm}^{-1}$ ) 3284 (br), 3072 (w), 2932 (w), 1625 (s), 1537 (s) 1436 (w), 1291 (s), 1201 (s), 1166 (s), 1134 (w), 836 (w), 800 (w), 721 (w), 618 (w).



### 32

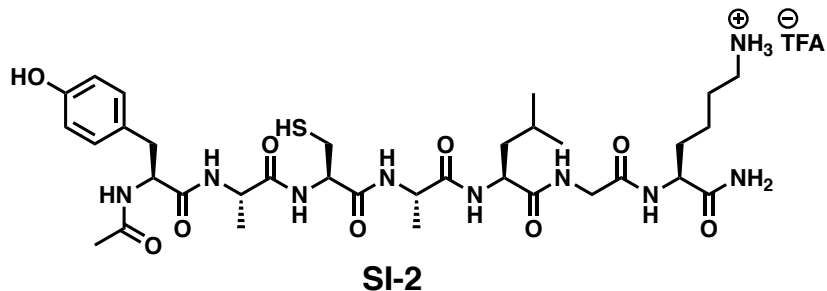
**Peptide 32.** Prepared by manual SPPS from Rink Amide resin (0.5 mmol, 1.09 g) according to the procedures given above. Isolated residue was dissolved in 10 mL of a 1:4 mix of water/acetonitrile before being purified by reverse-phase chromatography (gradient 5 – 60% organic over 6 minutes at a 20 mL/minute flow rate) on the Gilson HPLC setup with the Sunfire column discussed above. Fractions were collected with 210 nm detection with a 20 mV threshold. After lyophilization, compound was isolated as 98 mg (38%) of amorphous white powder: AMM (ES) Found  $m/z$  511.1959 [(M+H)<sup>+</sup>; calcd for C<sub>21</sub>H<sub>31</sub>N<sub>6</sub>O<sub>7</sub>S: 511.1975]; <sup>1</sup>H NMR (500 MHz, DMSO-*d*<sub>6</sub>)  $\delta$  9.17 (s, 1H), 8.29 (t,  $J$  = 5.8 Hz, 1H), 8.19 – 8.09 (m, 2H), 8.02 (d,  $J$  = 7.1 Hz, 1H), 7.87 (d,  $J$  = 8.4 Hz, 1H), 7.37 (s, 1H), 7.08 (s, 1H), 6.99 (d,  $J$  = 8.3 Hz, 2H), 6.62 (d,  $J$  = 8.2 Hz, 2H), 4.41 – 4.28 (m, 2H), 4.24 (p,  $J$  = 7.1 Hz, 1H), 3.72 (p,  $J$  = 5.9 Hz, 3H), 3.56 (dd,  $J$  = 16.6, 5.6 Hz, 1H), 2.88 (dd,  $J$  = 13.9, 4.8 Hz, 1H), 2.76 (ddd,  $J$  = 13.9, 8.7, 5.5 Hz, 1H), 2.66 (ddd,  $J$  = 13.8, 11.7, 5.3 Hz, 2H), 2.44 (t,  $J$  = 8.5 Hz, 1H), 1.87 (s, 3H), 1.20 (d,  $J$  = 7.1 Hz, 3H); <sup>13</sup>C NMR (126 MHz, DMSO)  $\delta$  173.03, 172.49, 170.36, 169.73, 168.54, 168.36, 155.76, 130.09, 128.02, 114.90, 55.30, 54.24, 48.38, 42.06, 41.95, 36.83, 26.02, 22.57, 18.10; IR (KBr,  $\text{cm}^{-1}$ ) 3287 (br), 1624 (s), 1516 (s) 1439 (w), 1234 (w), 831 (w), 603 (w).





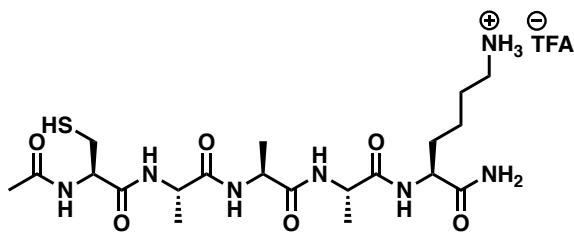
**SI - 1**

**Peptide SI-1.** Prepared by automated SPPS from Rink Amide resin (0.503 mmol, 1.09 g) according to the procedures given above. Isolated residue was dissolved in 8 mL of Milli-Q water before being purified by reverse-phase chromatography (gradient 10 – 90% organic over 10 minutes at a 15 mL/minute flow rate) on the Gilson HPLC setup with the Sunfire column discussed above. Fractions were collected with 210 nm detection with a 20 mV threshold. After lyophilization, compound was isolated as 194 mg (46%) of amorphous white powder as the TFA salt: AMM (ESI) Found  $m/z$  660.3517 [(M+H)<sup>+</sup>; calcd for C<sub>27</sub>H<sub>50</sub>N<sub>9</sub>O<sub>8</sub>S: 660.3503]; <sup>1</sup>H NMR (500 MHz, DMSO-*d*<sub>6</sub>) δ 8.25 (t,  $J$  = 5.8 Hz, 1H), 8.20 (t,  $J$  = 5.7 Hz, 1H), 8.14 (d,  $J$  = 7.1 Hz, 1H), 8.10 (d,  $J$  = 7.1 Hz, 1H), 7.99 (d,  $J$  = 7.8 Hz, 1H), 7.94 (d,  $J$  = 7.8 Hz, 1H), 7.82 (d,  $J$  = 8.2 Hz, 1H), 7.69 (s, 3H), 7.34 (s, 1H), 7.08 (s, 1H), 4.36 (td,  $J$  = 7.3, 5.3 Hz, 1H), 4.31 – 4.20 (m, 3H), 4.14 (td,  $J$  = 8.6, 4.9 Hz, 1H), 3.79 – 3.64 (m, 4H), 2.79 – 2.70 (m, 3H), 2.48 – 2.43 (m, 1H), 1.83 (s, 3H), 1.73 – 1.36 (m, 7H), 1.35 – 1.10 (m, 8H), 0.90 – 0.80 (m, 6H); <sup>13</sup>C NMR (126 MHz, DMSO) δ 173.48, 172.54, 172.40, 172.32, 169.88, 169.36, 168.68, 168.59, 158.03 (q,  $J$  = 31.3 Hz), 117.10 (q,  $J$  = 299.3 Hz), 54.95, 52.04, 51.18, 48.34, 48.27, 42.11, 42.05, 40.74, 38.73, 31.30, 26.65, 26.17, 24.08, 23.04, 22.52, 22.24, 21.61, 18.03, 17.61; IR (KBr, cm<sup>-1</sup>) 3380 (br), 3270 (br), 3043 (br), 2921 (br), 2858 (w), 1627 (s), 1521 (s), 1419 (w), 1199 (s), 1171 (s), 1127 (s), 832 (w), 798 (w), 720 (w), 668 (w).



**Peptide SI-2.** Prepared by automated SPPS from Rink Amide resin (0.503 mmol, 1.09 g) according to the procedures given above. Isolated residue was dissolved in 8 mL of Milli-Q water and 4 mL of trifluoroacetic acid before being purified by reverse-phase chromatography (gradient 10 – 90% organic over 10 minutes at a 15 mL/minute flow rate) on the Gilson HPLC setup with the Sunfire column discussed above. Fractions were collected with 210 nm detection with a 20 mV threshold. After lyophilization, compound was isolated as 268 mg (60%) of amorphous white powder as the TFA salt: AMM (ESI) Found  $m/z$  766.3912  $[(M+H)^+]$ ; calcd for  $C_{34}H_{56}N_9O_9S$ : 766.3922];  $^1H$  NMR (500 MHz, DMSO- $d_6$ )  $\delta$  9.17 (s, 1H), 8.22 (d,  $J = 7.1$  Hz, 1H), 8.15 – 8.08 (m, 2H), 8.05 – 7.94 (m, 3H), 7.83 (d,  $J = 8.1$  Hz, 1H), 7.63 (s, 3H), 7.33 (s, 1H), 7.08 (s, 1H), 7.03 (d,  $J = 8.4$  Hz, 2H), 6.63 (d,  $J = 8.0$  Hz, 2H), 4.46 – 4.34 (m, 2H), 4.34 – 4.20 (m, 3H), 4.15 (td,  $J = 8.7$ , 4.8 Hz, 1H), 3.71 (d,  $J = 5.6$  Hz, 2H), 2.87 (dd,  $J = 14.0$ , 4.2 Hz, 1H), 2.80 – 2.66 (m, 4H), 2.65 – 2.53 (m, 1H), 2.44 – 2.35 (m, 1H), 1.79 – 1.56 (m, 5H), 1.56 – 1.39 (m, 5H), 1.37 – 1.14 (m, 8H), 0.91 – 0.77 (m, 6H);  $^{13}C$  NMR (126 MHz, DMSO)  $\delta$  173.45, 172.35, 172.29, 172.12, 171.60, 169.30, 169.27, 168.56, 157.76 (d,  $J = 30.4$  Hz), 155.73, 130.07, 128.08, 117.39 (d,  $J = 301.0$  Hz), 114.83, 54.73, 54.28, 52.04, 51.24, 48.34, 42.07, 40.71, 38.75, 36.66, 31.28, 26.64, 26.26, 24.09, 23.06, 22.99, 22.49, 22.28, 21.59, 17.83, 17.81; IB (KBr,  $cm^{-1}$ ) 3280 (br), 2982 (br), 2937 (br), 2928 (br), 2870 (w), 1628

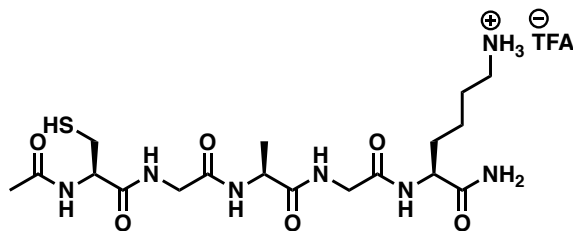
(s), 1516 (s), 1442 (s), 1365 (w), 1215 (w), 1200 (s), 1174 (s), 1133 (s), 832 (w), 798 (w), 720 (w).



**SI-3**

**Peptide SI-3.** Prepared by automated SPPS from Rink Amide resin (0.502 mmol, 1.07 g) according to the procedures given above. Isolated residue was dissolved in 4 mL Milli-Q water, 4 mL trifluoroacetic acid, and 2 mL acetonitrile before being purified by reverse-phase chromatography (gradient 10 – 60% organic over 60 minutes at a 15 mL/minute flow rate) on the Gilson HPLC setup with the Sunfire column discussed above. Fractions were collected with 210 nm detection with a 20 mV threshold. After lyophilization, compound was isolated as 100 mg (32%) of amorphous white powder as the TFA salt: AMM (ESI) Found  $m/z$  504.2617 [(M+H)<sup>+</sup>; calcd for C<sub>20</sub>H<sub>38</sub>N<sub>7</sub>O<sub>6</sub>S: 504.2604]; <sup>1</sup>H NMR (500 MHz, DMSO-*d*<sub>6</sub>)  $\delta$  8.21 (d,  $J$  = 6.9 Hz, 1H), 8.11 (d,  $J$  = 7.7 Hz, 1H), 7.98 (d,  $J$  = 7.1 Hz, 1H), 7.92 (d,  $J$  = 7.0 Hz, 1H), 7.74 (d,  $J$  = 8.1 Hz, 1H), 7.62 (s, 3H), 7.25 (s, 1H), 7.07 (s, 1H), 4.37 (q,  $J$  = 7.4 Hz, 1H), 4.26 – 4.17 (m, 3H), 4.13 (td,  $J$  = 8.4, 5.3 Hz, 1H), 2.75 (hept,  $J$  = 6.7, 6.2 Hz, 3H), 2.65 (dt,  $J$  = 13.5, 7.9 Hz, 1H), 2.40 (t,  $J$  = 8.4 Hz, 1H), 1.87 (s, 3H), 1.71 – 1.62 (m, 1H), 1.50 (h,  $J$  = 7.1, 6.3 Hz, 3H), 1.35 – 1.14 (m, 12H); <sup>13</sup>C NMR (126 MHz, DMSO)  $\delta$  173.35, 172.08, 172.03, 171.89, 169.85, 169.58, 54.99, 52.00, 48.49, 48.38, 48.31, 38.75, 31.40, 26.66, 26.15, 22.53, 22.18, 17.89, 17.84, 17.77; IR (KBr, cm<sup>-1</sup>) 3361 (br), 3275 (br), 3193 (br), 3060 (br), 2969 (br), 2928 (br), 2867 (br), 2767 (br), 2655 (br), 2546 (br), 1669 (s), 1623 (s), 1533 (s), 1443 (s), 1419 (s), 1375 (s),

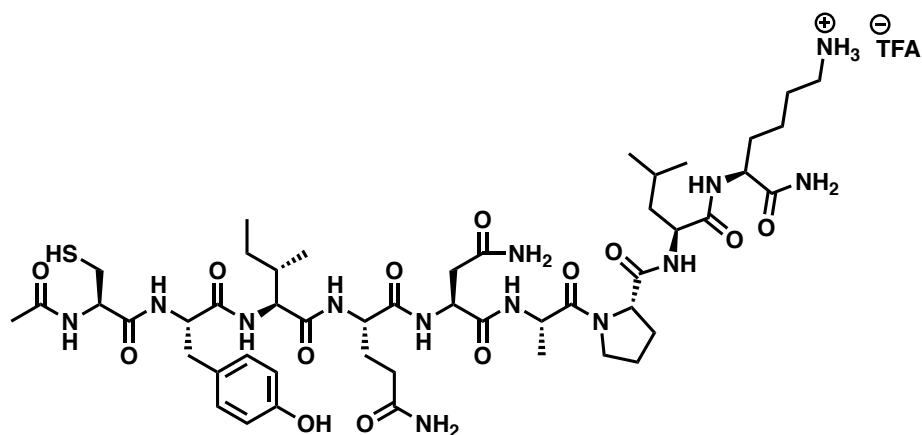
1373 (s), 1284 (w), 1200 (s), 1174 (s), 1132 (s), 1057 (w), 1036 (w), 963 (w), 916 (w), 835 (w), 798 (w), 721 (w), 599 (w).



**SI-4**

**Peptide SI-4.** Prepared by automated SPPS from Rink Amide AM resin (0.507 mmol, 994 mg) according to the procedures given above. Isolated residue was dissolved in 6 mL of Milli-Q water and 2 mL of trifluoroacetic acid before being purified by reverse-phase chromatography (gradient 1 – 30% organic over 8 minutes at a 20 mL/minute flow rate) on the Gilson HPLC setup with the Sunfire column discussed above. Fractions were collected with 210 nm detection with a 20 mV threshold. After lyophilization, compound was isolated as 119 mg (40%) of amorphous white powder as the TFA salt: AMM (ESI) Found  $m/z$  476.2289  $[(M+H)^+]$ ; calcd for  $C_{18}H_{34}N_7O_6S$ : 476.2291];  $^1H$  NMR (500 MHz, DMSO- $d_6$ )  $\delta$  8.30 (t,  $J = 5.8$  Hz, 1H), 8.22 – 8.14 (m, 2H), 8.03 (d,  $J = 7.0$  Hz, 1H), 7.80 (d,  $J = 8.2$  Hz, 1H), 7.64 (s, 3H), 7.32 (s, 1H), 7.08 (s, 1H), 4.33 (td,  $J = 7.5, 5.5$  Hz, 1H), 4.24 (p,  $J = 7.0$  Hz, 1H), 4.15 (td,  $J = 8.7, 4.8$  Hz, 1H), 3.81 – 3.65 (m, 4H), 2.81 – 2.62 (m, 4H), 2.45 (t,  $J = 8.5$  Hz, 1H), 1.88 (s, 3H), 1.74 – 1.64 (m, 1H), 1.57 – 1.44 (m, 3H), 1.35 – 1.13 (m, 5H);  $^{13}C$  NMR (126 MHz, DMSO)  $\delta$  173.48, 172.62, 170.42, 169.82, 168.66, 168.60, 157.82 (q,  $J = 30.6$  Hz), 117.33 (d,  $J = 300.9$  Hz), 55.37, 52.02, 48.46, 42.17, 42.09, 38.74, 31.23, 26.62, 25.94, 22.56, 22.23, 17.92; IR (KBr,  $cm^{-1}$ ) 3374 (br),

3279 (br), 3051 (br), 2917 (br), 1623 (s), 1522 (s), 1419 (w), 1195 (s), 1172 (s), 1127 (s), 831 (w), 797 (w), 717 (w).

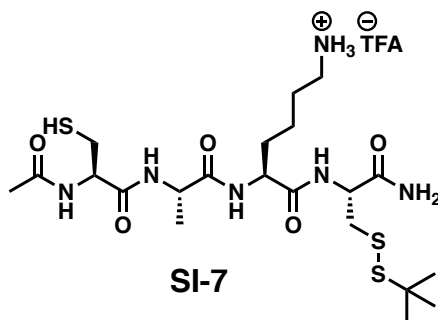


### SI-5

**Peptide SI-5.** Prepared by manual SPPS from Rink Amide resin (0.15 mmol, 255 mg) according to the procedures given above. Isolated residue was dissolved in 50/50 mix of water/acetonitrile before being purified by reverse-phase chromatography (gradient 5 – 40% organic over 10 minutes at a 20 mL/minute flow rate) on the Gilson HPLC setup with the Vydac column discussed above. Fractions were collected with 224 nm detection with a 20 mV threshold. After lyophilization, compound was isolated as 168 mg (70%) of amorphous white powder as the TFA salt: AMM (ES) Found  $m/z$  865.4714 [(M+H)<sup>+</sup>; calcd for C<sub>38</sub>H<sub>65</sub>N<sub>12</sub>O<sub>9</sub>S: 865.4718]; <sup>1</sup>H NMR (500 MHz, DMSO-*d*<sub>6</sub>) δ 9.14 (s, 1H), 8.05 (dd,  $J$  = 12.0, 7.6 Hz, 2H), 8.00 (d,  $J$  = 8.1 Hz, 2H), 7.89 – 7.86 (m, 2H), 7.83 (d,  $J$  = 8.4 Hz, 1H), 7.69 – 7.60 (m, 5H), 7.31 (s, 1H), 7.20 (s, 1H), 7.14 (s, 1H), 7.05 (s, 1H), 7.00 (d,  $J$  = 8.4 Hz, 2H), 6.87 (s, 1H), 6.75 (s, 1H), 6.61 (d,  $J$  = 8.4 Hz, 2H), 4.56 – 4.42 (m, 2H), 4.37 – 4.26 (m, 2H), 4.17 (dtd,  $J$  = 29.5, 14.0, 7.8 Hz, 4H), 3.63 – 3.49 (m, 1H), 2.91 (dd,  $J$  = 14.1, 4.2 Hz, 1H), 2.79 – 2.52 (m, 4H), 2.40 (dd,  $J$  = 15.7, 7.0 Hz, 1H), 2.20 (t,  $J$



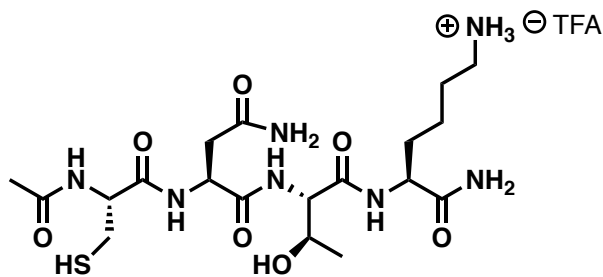
amorphous white powder as the TFA salt: AMM (ESI) Found  $m/z$  517.7574 [(M+2H)<sup>2+</sup>; calcd for C<sub>34</sub>H<sub>56</sub>N<sub>9</sub>O<sub>9</sub>S: 517.7586]; <sup>1</sup>H NMR (500 MHz, DMSO-*d*<sub>6</sub>) δ 9.20 (s, 1H), 8.27 (t,  $J$  = 5.7 Hz, 1H), 8.20 (d,  $J$  = 7.8 Hz, 1H), 8.11 – 8.02 (m, 3H), 7.91 (t,  $J$  = 7.9 Hz, 2H), 7.70 (d,  $J$  = 8.8 Hz, 4H), 7.34 (s, 1H), 7.28 (s, 1H), 7.18 (s, 1H), 7.09 (s, 1H), 7.00 (d,  $J$  = 8.5 Hz, 2H), 6.93 (s, 1H), 6.82 (s, 1H), 6.62 (d,  $J$  = 8.5 Hz, 2H), 4.58 – 4.43 (m, 2H), 4.42 – 4.31 (m, 2H), 4.30 – 4.20 (m, 2H), 4.13 (ddd,  $J$  = 16.9, 14.1, 8.1 Hz, 2H), 3.72 (qd,  $J$  = 16.6, 5.7 Hz, 2H), 3.55 (ddt,  $J$  = 25.8, 9.9, 6.7 Hz, 2H), 2.93 (dd,  $J$  = 14.0, 4.4 Hz, 1H), 2.78 – 2.65 (m, 4H), 2.62 – 2.52 (m, 2H), 2.39 (dd,  $J$  = 15.6, 7.6 Hz, 1H), 2.23 (t,  $J$  = 8.5 Hz, 1H), 2.14 – 1.97 (m, 3H), 1.91 – 1.43 (m, 13H), 1.36 – 1.20 (m, 2H), 1.16 (d,  $J$  = 6.9 Hz, 3H), 0.88 (d,  $J$  = 6.6 Hz, 3H), 0.82 (d,  $J$  = 6.4 Hz, 3H); <sup>13</sup>C NMR (126 MHz, DMSO) δ 174.02, 173.48, 171.86, 171.77, 171.50, 171.40, 171.09, 170.72, 170.45, 170.06, 169.63, 168.83, 158.51 (q,  $J$  = 32.5 Hz), 155.83, 130.16, 127.68, 117.26 (q,  $J$  = 298.0 Hz), 114.88, 59.70, 54.97, 54.53, 52.18, 52.06, 51.57, 49.54, 46.72, 46.63, 42.13, 39.78, 38.76, 36.85, 36.45, 31.37, 31.26, 28.96, 27.98, 26.60, 26.04, 24.53, 24.26, 23.11, 22.53, 22.24, 21.52, 16.78; IR (KBr, cm<sup>-1</sup>) 3288 (br), 3190 (br), 2950 (br), 1652 (s), 1441 (s), 1201 (s), 1175 (s), 1134 (s), 800 (w), 721 (w), 596 (w).



**Peptide SI-7.** Prepared by automated SPPS from Rink Amide AM resin (0.509 mmol, 1.08 g) according to the procedures given above. Isolated residue was dissolved in 3 mL of Milli-Q water and 1 mL of acetonitrile before being purified by reverse-phase chromatography (gradient 5 – 75% organic over 8 minutes at a 20 mL/minute flow rate) on the Gilson HPLC setup with the Sunfire column discussed above. Fractions were collected with 210 nm detection with a 5 mV threshold. After lyophilization, compound was isolated as 170 mg (50%) of amorphous white powder as the TFA salt: AMM (ESI) Found  $m/z$  553.2295 [(M+H)<sup>+</sup>; calcd for C<sub>21</sub>H<sub>41</sub>N<sub>6</sub>O<sub>5</sub>S<sub>3</sub>: 553.2301]; <sup>1</sup>H NMR (500 MHz, DMSO-*d*<sub>6</sub>) δ 8.25 (d, *J* = 6.8 Hz, 1H), 8.10 (d, *J* = 7.8 Hz, 1H), 8.02 (d, *J* = 7.6 Hz, 1H), 7.97 (d, *J* = 8.0 Hz, 1H), 7.63 (s, 3H), 7.38 (s, 1H), 7.25 (s, 1H), 4.38 (qd, *J* = 8.0, 5.1 Hz, 2H), 4.29 – 4.16 (m, 2H), 3.10 (dd, *J* = 12.9, 5.0 Hz, 1H), 2.97 (dd, *J* = 13.0, 8.6 Hz, 1H), 2.79 – 2.70 (m, 3H), 2.69 – 2.65 (m, 1H), 2.39 (t, *J* = 8.5 Hz, 1H), 1.88 (s, 3H), 1.72 – 1.63 (m, 1H), 1.59 – 1.44 (m, 3H), 1.39 – 1.26 (m, 11H), 1.23 (d, *J* = 7.1 Hz, 3H); <sup>13</sup>C NMR (126 MHz, DMSO) δ 172.44, 171.43, 171.32, 169.92, 169.60, 157.75 (d, *J* = 30.4 Hz), 117.34 (d, *J* = 300.8 Hz), 54.95, 52.62, 52.01, 48.62, 47.78, 42.47, 38.76, 31.11, 29.59, 26.60, 26.20, 22.57, 22.14, 17.76; IR (KBr, cm<sup>-1</sup>) 3285 (br), 3073 (br), 2963 (br),



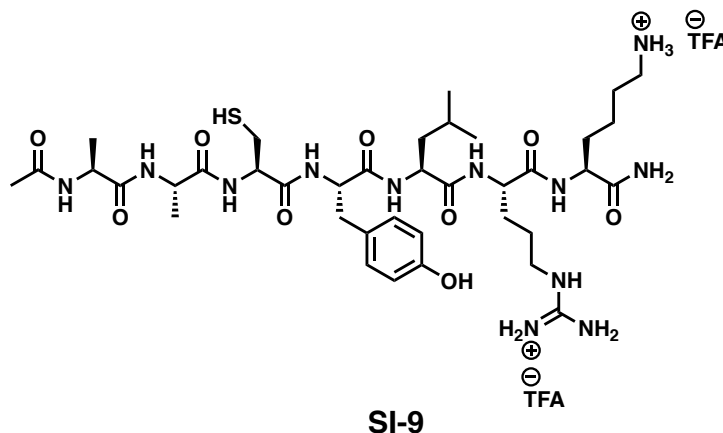
1623 (s), 1536 (s), 1427 (w), 1287 (w), 1201 (s), 1178 (s), 1135 (s), 836 (w), 799 (w), 721 (s), 618 (w), 595 (w).



**SI-8**

**Peptide SI-8.** Prepared by manual SPPS from Rink Amide resin (0.20 mmol, 465 mg) according to the procedures given above. Isolated residue was dissolved in Milli-Q water and purified by reverse-phase chromatography (gradient 5 – 75% organic over 10 minutes at a 20 mL/minute flow rate) on the Gilson HPLC setup with the Vydac column discussed above. Fractions were collected with 210 nm detection with a 20 mV threshold. After lyophilization, compound was isolated as 100.1 mg (81%) of amorphous white powder as the TFA salt: AMM (ES) Found  $m/z$  528.2222 [(M+Na)<sup>+</sup>; calcd for C<sub>19</sub>H<sub>35</sub>N<sub>7</sub>O<sub>7</sub>SNa: 528.2216]; <sup>1</sup>H NMR (500 MHz, DMSO-*d*<sub>6</sub>) δ 8.45 (d,  $J$  = 7.5 Hz, 1H), 8.21 (d,  $J$  = 7.7 Hz, 1H), 7.91 (d,  $J$  = 8.2 Hz, 1H), 7.73 (s, 3H), 7.69 (d,  $J$  = 7.9 Hz, 1H), 7.51 (s, 1H), 7.17 (s, 1H), 7.13 (s, 1H), 7.00 (s, 1H), 5.04 (s, 1H), 4.61 (q,  $J$  = 6.9 Hz, 1H), 4.37 (q,  $J$  = 7.1 Hz, 1H), 4.14 (ddd,  $J$  = 20.3, 8.5, 4.0 Hz, 2H), 4.07 (dd,  $J$  = 6.5, 4.0 Hz, 1H), 2.76 (ddq,  $J$  = 14.0, 8.7, 5.3, 4.7 Hz, 3H), 2.64 (ddd,  $J$  = 22.3, 15.5, 7.4 Hz, 2H), 2.47 (dd,  $J$  = 15.5, 6.5 Hz, 1H), 2.36 (t,  $J$  = 8.5 Hz, 1H), 1.89 (s, 3H), 1.73 (tt,  $J$  = 10.4, 5.0 Hz, 1H), 1.56 (ddd,  $J$  = 21.8, 12.3, 5.9 Hz, 2H), 1.49 (d,  $J$  = 7.0 Hz, 1H), 1.30 (dddt,  $J$

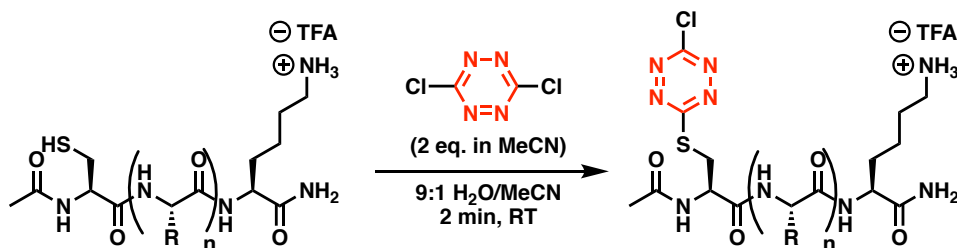
= 27.1, 22.9, 11.2, 6.8 Hz, 2H), 1.05 (d,  $J = 6.3$  Hz, 3H);  $^{13}\text{C}$  NMR (126 MHz, DMSO)  $\delta$  173.71, 171.83, 171.19, 170.08, 169.78, 169.63, 66.33, 58.34, 55.17, 52.43, 49.89, 38.73, 36.62, 30.84, 26.61, 26.15, 22.51, 22.39, 19.55; IR (KBr,  $\text{cm}^{-1}$ ) 3401 (br), 3250 (br), 3210 (br), 3075 (br), 2980 (br), 1671 (s), 1654 (s), 1540 (s), 1534 (s), 1415 (w), 1240 (w), 110 (w), 930 (w), 884 (w).



**Peptide SI-9.** Prepared by manual SPPS from Rink Amide resin (0.20 mmol, 465 mg) according to the procedures given above. Isolated residue was dissolved in 8 mL of Milli-Q water and 7 mL of acetonitrile before being purified by reverse-phase chromatography (gradient 20 – 60% organic over 15 minutes at a 20 mL/minute flow rate) on the Gilson HPLC setup with the Vydan column discussed above. Fractions were collected with 210 nm detection with a 20 mV threshold. After lyophilization, compound was isolated as 91.4 mg (73%) of amorphous white powder as the TFA salt: AMM (ES) Found  $m/z$  865.4714 [(M+H) $^+$ ]; calcd for  $\text{C}_{38}\text{H}_{65}\text{N}_{12}\text{O}_9\text{S}$ : 865.4718];  $^1\text{H}$  NMR (500 MHz, DMSO- $d_6$ )  $\delta$  9.43 – 8.99 (m, 3H), 8.10 (dd,  $J = 11.8, 7.0$  Hz, 2H), 8.02 – 7.90 (m, 3H), 7.87 (d,  $J = 7.7$  Hz, 1H), 7.79 (q,  $J = 7.3, 6.3$  Hz, 3H), 7.65 (t,  $J = 5.7$  Hz, 1H), 7.52 – 6.75 (m, 10H), 6.62 (d,  $J = 8.1$  Hz, 3H), 4.41 (td,  $J = 8.7, 4.1$  Hz, 1H), 4.35 – 4.18 (m, 4H), 4.15 (td,  $J =$

8.2, 5.0 Hz, 1H), 3.10 (q,  $J = 6.6$  Hz, 2H), 2.92 (dd,  $J = 14.3, 4.1$  Hz, 1H), 2.81 – 2.62 (m, 4H), 2.25 (t,  $J = 8.6$  Hz, 1H), 1.84 (s, 3H), 1.78 – 1.38 (m, 10H), 1.38 – 1.12 (m, 7H), 0.85 (dd,  $J = 21.5, 6.5$  Hz, 6H);  $^{13}\text{C}$  NMR (126 MHz, DMSO)  $\delta$  173.30, 172.56, 172.35, 172.01, 170.97, 170.94, 169.52, 169.41, 158.51 (q,  $J = 31.4$  Hz), 156.82, 155.82, 130.04, 127.54, 117.08 (q,  $J = 299.2$  Hz), 114.88, 55.05, 54.35, 52.21, 52.14, 51.17, 48.43, 48.40, 40.68, 40.45, 38.66, 36.29, 31.40, 28.83, 26.63, 26.03, 24.92, 24.04, 23.08, 22.47, 22.17, 21.51, 17.89, 17.55; IR (KBr,  $\text{cm}^{-1}$ ) 3422 (br), 2957 (br), 2937 (br), 2172 (w), 1640 (s), 1525 (s), 1437 (w) 1374 (w), 1209 (s), 1155 (s), 1018 (br), 823 (w), 803 (w).

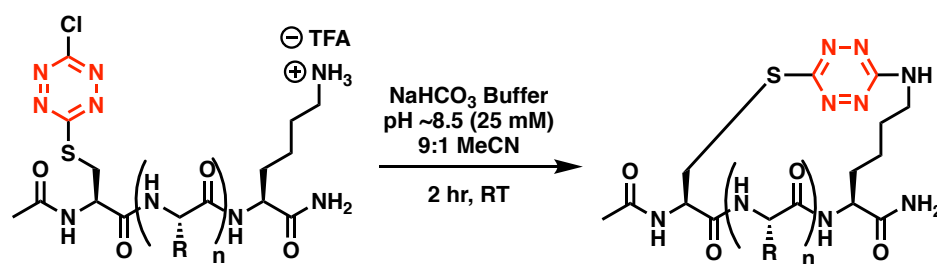
### General Procedure for Modifying Peptides with Dichloro-*s*-tetrazine



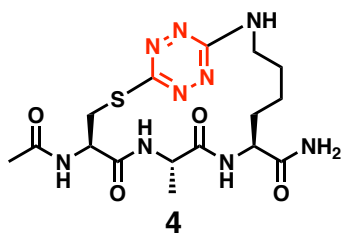
**Procedure for modifying peptides with dichloro-*s*-tetrazine.** Purified peptide (as TFA salt) was dispensed into a round bottom flask equipped with a magnetic stir bar and dissolved in Milli-Q water. Dichloro-*s*-tetrazine was weighed into a separate test tube and dissolved in acetonitrile. The ratio of the two solvents was 9 / 1 water / acetonitrile and the volume of the combined mix was enough to make a 1 mM solution of the purified peptide. The total volume of the reaction should not exceed half the volume of the round bottom flask. The solution of dichloro-*s*-tetrazine was poured into the round bottom flask and the reaction mixture was vigorously stirred for 2 minutes. The stir bar was removed

and the flask was attached to a rotary evaporator. The water bath of the rotary evaporator was replaced with a dry ice/acetone bath and the reaction mixture was frozen in a thin film about the flask. The frozen flask was placed inside a lyophilizer jar and dried *in vacuo* via lyophilization.

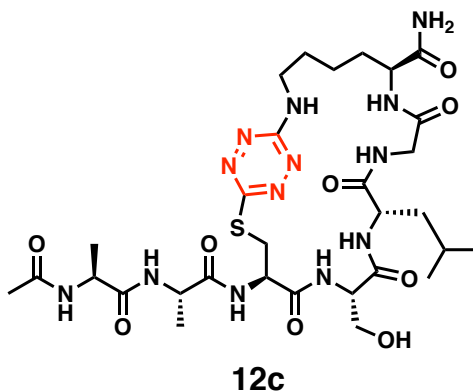
### General Procedure for Macrocyclization of Acyclic Dichloro-*s*-tetrazine Peptides



**Macrocyclization of Acyclic Dichloro-*s*-tetrazine Peptides.** Isolated material recovered from the lyophilizer was reconstituted in 9 / 1 mix of NaHCO<sub>3</sub> buffer (made with Milli-Q water, pH 8.5, 25 mM) / acetonitrile. A magnetic stir bar was added and the reaction was allowed to stir for 2 hours before the stir bar was removed and the contents of the flask were frozen as described in the **general procedure for modifying peptides with dichloro-*s*-tetrazine**. After drying the contents of the flask were reconstituted and purified as described.

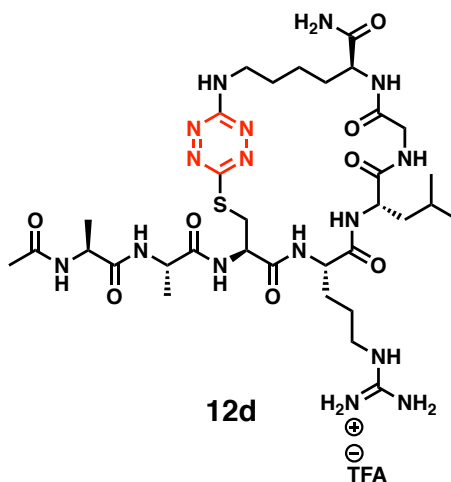


**Macrocycle 3.** Prepared from **Peptide 2** (0.099 mmol, 47.3 mg) as described above in **general procedure for modifying peptides with dichloro-s-tetrazine** and **general procedure for macrocyclization of acyclic dichloro-s-tetrazine peptides**. Isolated residue was dissolved in 7 mL of trifluoroacetic acid and 3 mL of Milli-Q water before being purified by reverse-phase chromatography (gradient 5 – 95% organic over 10 minutes at a 20 mL/minute flow rate) on the Gilson HPLC setup with the Sunfire column discussed above. Fractions were collected with 210 nm detection with a 20 mV threshold. After lyophilization, compound was isolated as 42.7 mg (48%) of amorphous orange powder: AMM (ES) Found  $m/z$  440.1828 [(M+H)<sup>+</sup>; calcd for C<sub>16</sub>H<sub>26</sub>N<sub>9</sub>O<sub>4</sub>S]; <sup>1</sup>H NMR (500 MHz, DMSO-*d*<sub>6</sub>, 1% v/v TMS) δ 8.37 (t,  $J$  = 6.3 Hz, 1H), 8.13 (d,  $J$  = 7.4 Hz, 1H), 8.08 (d,  $J$  = 7.7 Hz, 1H), 7.72 (d,  $J$  = 8.7 Hz, 1H), 7.24 (s, 1H), 6.95 (s, 1H), 4.64 (td,  $J$  = 7.3, 3.4 Hz, 1H), 4.18 (td,  $J$  = 9.9, 8.9, 3.5 Hz, 1H), 4.06 (p,  $J$  = 7.0 Hz, 1H), 3.68 (ddt,  $J$  = 13.7, 6.8, 3.5 Hz, 1H), 3.63 – 3.46 (m, 2H), 3.28 – 3.17 (m, 1H), 1.89 (s, 3H), 1.78 – 1.59 (m, 2H), 1.56 – 1.46 (m, 1H), 1.46 – 1.35 (m, 1H), 1.35 – 1.26 (m, 1H), 1.26 – 1.14 (m, 2H), 1.10 (d,  $J$  = 6.9 Hz, 3H); <sup>13</sup>C NMR (126 MHz, DMSO) δ 173.82, 170.98, 169.08, 167.92, 163.35, 160.93, 52.84, 51.21, 47.73, 31.96, 31.11, 30.76, 27.45, 22.52, 22.07, 19.62, 1.16; IR (KBr, cm<sup>-1</sup>) 3405 (br), 3292 (br), 3054 (w), 2924 (br), 2854 (br), 1653 (s), 1636 (s), 1560 (s), 1522 (s), 1437 (w), 1196 (w), 1042 (w), 938 (w).



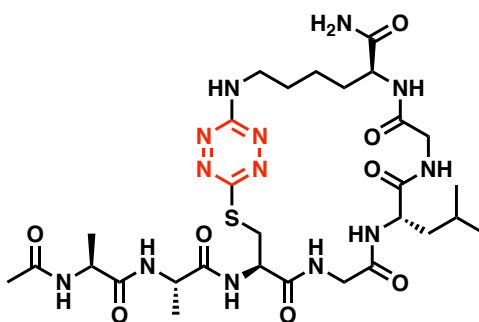
**Macrocycle 12c.** Prepared from **Peptide 10c** (0.0549 mmol, 44.1 mg) as described above in **general procedure for modifying peptides with dichloro-s-tetrazine** and **general procedure for macrocyclization of acyclic dichloro-s-tetrazine peptides**. Isolated residue was dissolved in 3 mL of Milli-Q water, 1 mL of trifluoroacetic acid, and 2 mL of acetonitrile before being purified by reverse-phase chromatography (gradient 10 – 70% organic over 8 minutes at a 15 mL/minute flow rate) on the Gilson HPLC setup with the Sunfire column discussed above. Fractions were collected with 210 nm detection with a 20 mV threshold. After lyophilization, compound was isolated as 15.7 mg (37%) of amorphous orange powder: AMM (ES) Found  $m/z$  768.3575  $[(M+H)^+]$ ; calcd for  $C_{30}H_{50}N_{13}O_9S$ ];  $^1H$  NMR (500 MHz,  $DMSO-d_6$ )  $\delta$  8.45 (t,  $J = 6.2$  Hz, 1H), 8.28 (d,  $J = 6.8$  Hz, 1H), 8.21 (d,  $J = 6.8$  Hz, 1H), 8.16 – 8.05 (m, 2H), 7.90 (t,  $J = 6.0$  Hz, 1H), 7.68 – 7.56 (m, 2H), 7.13 (s, 1H), 7.02 (s, 1H), 4.53 (td,  $J = 6.9, 5.2$  Hz, 1H), 4.25 (td,  $J = 7.1, 5.1$  Hz, 2H), 4.20 – 4.13 (m, 1H), 4.05 (td,  $J = 9.1, 8.4, 4.0$  Hz, 1H), 3.96 (dt,  $J = 7.3, 4.8$  Hz, 2H), 3.68 – 3.26 (m, 9H), 1.83 (s, 3H), 1.74 – 1.39 (m, 7H), 1.32 – 1.13 (m, 8H), 0.90 – 0.80 (m, 6H);  $^{13}C$  NMR (126 MHz,  $DMSO$ )  $\delta$  173.76, 173.06, 172.75, 172.46, 170.10, 170.00, 169.34, 168.48, 163.75, 160.76, 60.95, 56.30, 52.70, 52.23, 51.84, 48.59, 48.23, 41.99, 40.37, 39.58, 32.45, 30.99, 27.81, 24.07, 23.04, 22.61, 22.50, 21.53, 18.00, 17.47;

IR (KBr,  $\text{cm}^{-1}$ ) 3295 (br), 3052 (br), 2936 (br), 2930 (br), 2865 (s), 1653 (s), 1560 (s), 1522 (br), 1457 (s), 1374 (s), 1197 (s), 1170 (w), 1129 (w), 1041 (w), 936 (w).



**Macrocycle 12d.** Prepared from **Peptide 10d** (0.106 mmol, 104.8 mg) as described above in **general procedure for modifying peptides with dichloro-s-tetrazine** and **general procedure for macrocyclization of acyclic dichloro-s-tetrazine peptides**. Isolated residue was dissolved in 3 mL of Milli-Q water, 1 mL of trifluoroacetic acid, and 2 mL of acetonitrile before being purified by reverse-phase chromatography (gradient 5 – 70% organic over 8 minutes at a 15 mL/minute flow rate) on the Gilson HPLC setup with the Sunfire column discussed above. Fractions were collected with 210 nm detection with a 20 mV threshold. After lyophilization, compound was isolated as 61.7 mg (37%) of amorphous orange powder as the TFA salt: AMM (ES) Found  $m/z$  837.4274 [(M+H)<sup>+</sup>; calcd for C<sub>33</sub>H<sub>57</sub>N<sub>16</sub>O<sub>8</sub>S]; <sup>1</sup>H NMR (500 MHz, DMSO-*d*<sub>6</sub>)  $\delta$  8.45 (t,  $J$  = 6.2 Hz, 1H), 8.26 (d,  $J$  = 6.7 Hz, 2H), 8.16 (d,  $J$  = 6.8 Hz, 2H), 7.92 (t,  $J$  = 6.1 Hz, 1H), 7.70 (d,  $J$  = 8.2 Hz, 1H), 7.62 (d,  $J$  = 7.5 Hz, 1H), 7.47 (t,  $J$  = 5.8 Hz, 1H), 7.43 – 6.61 (m, 5H), 4.47 (q,  $J$  =

6.7 Hz, 1H), 4.29 – 4.10 (m, 3H), 4.09 – 3.91 (m, 2H), 3.72 – 3.57 (m, 4H), 3.39 – 3.32 (m, 2H), 3.16 – 3.00 (m, 2H), 1.86 (s, 3H), 1.79 – 1.39 (m, 11H), 1.23 (t,  $J = 7.0$  Hz, 9H), 0.96 – 0.72 (m, 6H);  $^{13}\text{C}$  NMR (126 MHz, DMSO)  $\delta$  173.78, 173.19, 173.09, 172.45, 171.34, 170.26, 169.74, 168.44, 163.66, 160.83, 158.06 (q,  $J = 31.7$  Hz), 156.64, 53.47, 52.80, 52.25, 51.61, 48.92, 48.72, 41.97, 40.40, 40.35, 40.20, 32.11, 30.88, 28.47, 27.84, 25.05, 24.22, 23.05, 22.56, 22.53, 21.42, 17.76, 17.38; IR (KBr,  $\text{cm}^{-1}$ ) 3318 (br), 3060 (br), 2951 (br), 2930 (br), 2867 (w), 1653 (s), 1552 (s), 1533 (s), 1448 (w), 1437 (w), 1369 (w), 1200 (s), 1174 (s), 1131 (s), 1042 (w), 940 (w), 831 (w), 798 (w), 668 (w).

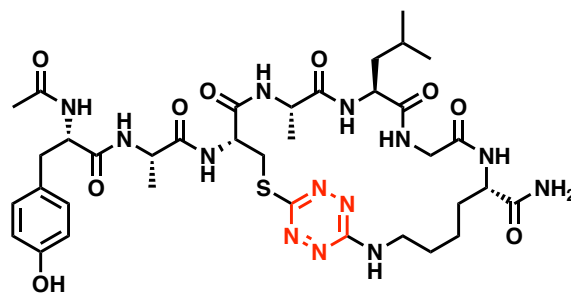


**13**

**Macrocycle 13.** Prepared from **Peptide SI-1** (0.0677 mmol, 52.4 mg) as described above in **general procedure for modifying peptides with dichloro-s-tetrazine** and **general procedure for macrocyclization of acyclic dichloro-s-tetrazine peptides**. Isolated residue was dissolved in 3 mL of Milli-Q water and 3 mL of trifluoroacetic acid before being purified by reverse-phase chromatography (gradient 10 – 65% organic over 20 minutes at a 15 mL/minute flow rate) on the Gilson HPLC setup with the Sunfire column discussed above. Fractions were collected with 210 nm detection with a 20 mV threshold. After lyophilization, compound was isolated as 26 mg (52%) of amorphous orange



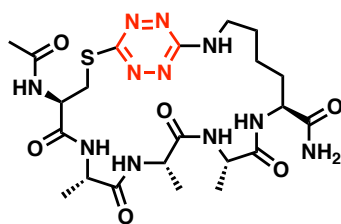
powder: AMM (ES) Found  $m/z$  760.3317 [(M+Na)<sup>+</sup>; calcd for C<sub>29</sub>H<sub>47</sub>N<sub>13</sub>O<sub>8</sub>NaS]; <sup>1</sup>H NMR (500 MHz, DMSO-*d*<sub>6</sub>) δ 8.52 (t,  $J$  = 6.1 Hz, 1H), 8.33 (t,  $J$  = 6.0 Hz, 1H), 8.19 (t,  $J$  = 6.2 Hz, 2H), 8.12 – 8.06 (m, 2H), 7.78 (d,  $J$  = 6.9 Hz, 1H), 7.57 (d,  $J$  = 8.1 Hz, 1H), 7.15 (s, 1H), 7.03 (s, 1H), 4.47 (q,  $J$  = 6.1 Hz, 1H), 4.31 – 4.21 (m, 2H), 4.15 – 4.01 (m, 2H), 3.81 – 3.69 (m, 1H), 3.63 – 3.33 (m, 7H), 1.84 (s, 3H), 1.75 – 1.40 (m, 7H), 1.38 – 1.13 (m, 8H), 0.95 – 0.76 (m, 6H); <sup>13</sup>C NMR (126 MHz, DMSO) δ 173.75, 172.82, 172.60, 172.40, 169.94, 169.34, 169.32, 168.63, 163.60, 160.61, 52.97, 52.53, 52.20, 48.45, 48.25, 42.73, 42.14, 39.77, 39.71, 32.51, 31.26, 28.34, 24.15, 22.88, 22.86, 22.52, 21.58, 18.10, 17.43; IR (KBr, cm<sup>-1</sup>) 3287 (br), 3054 (br), 2936 (s), 2930 (s), 2867 (s), 1653 (s), 1523 (s), 1437 (s), 1369 (s), 1326 (w), 1194 (s), 1167 (s), 1042 (w), 939 (w), 690 (w), 543 (w).



**14**

**Macrocycle 14.** Prepared from **Peptide SI-2** (0.0507 mmol, 44.6 mg) as described above in **general procedure for modifying peptides with dichloro-s-tetrazine** and **general procedure for macrocyclization of acyclic dichloro-s-tetrazine peptides**. Isolated residue was dissolved in 3 mL of Milli-Q water, 2 mL of trifluoroacetic acid, and 1 mL of acetonitrile before being purified by reverse-phase chromatography (gradient 10 – 70%

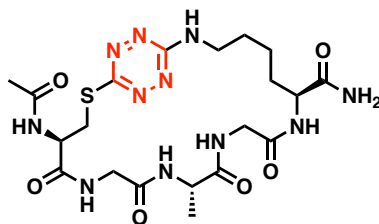
organic over 20 minutes at a 15 mL/minute flow rate) on the Gilson HPLC setup with the Sunfire column discussed above. Fractions were collected with 210 nm detection with a 20 mV threshold. After lyophilization, compound was isolated as 16.4 mg (38%) of amorphous orange powder: AMM (ES) Found  $m/z$  844.3905 [(M+H)<sup>+</sup>; calcd for C<sub>36</sub>H<sub>54</sub>N<sub>13</sub>O<sub>9</sub>S]; <sup>1</sup>H NMR (500 MHz, DMSO-*d*<sub>6</sub>) δ 9.16 (s, 1H), 8.46 (t,  $J$  = 6.2 Hz, 1H), 8.34 (dd,  $J$  = 8.7, 6.5 Hz, 2H), 8.19 (d,  $J$  = 6.9 Hz, 1H), 8.05 (d,  $J$  = 8.1 Hz, 1H), 7.90 (t,  $J$  = 5.9 Hz, 1H), 7.62 (d,  $J$  = 7.8 Hz, 2H), 7.13 – 6.96 (m, 3H), 6.64 (d,  $J$  = 8.4 Hz, 2H), 4.50 – 4.38 (m, 2H), 4.22 (p,  $J$  = 7.0 Hz, 1H), 4.11 (ddd,  $J$  = 10.0, 7.2, 4.9 Hz, 1H), 4.03 (td,  $J$  = 9.5, 8.6, 3.9 Hz, 1H), 3.90 (p,  $J$  = 7.1 Hz, 2H), 3.68 – 3.57 (m, 3H), 3.57 – 3.41 (m, 2H), 3.36 (dd,  $J$  = 13.4, 6.6 Hz, 1H), 3.02 – 2.90 (m, 1H), 2.63 (dd,  $J$  = 14.1, 10.3 Hz, 1H), 1.84 – 1.67 (m, 4H), 1.66 – 1.39 (m, 6H), 1.37 – 1.11 (m, 8H), 0.95 – 0.76 (m, 6H); <sup>13</sup>C NMR (126 MHz, DMSO) δ 173.71, 173.21, 172.61, 172.46, 172.10, 169.80, 169.41, 168.53, 163.72, 160.64, 155.73, 130.02, 128.12, 114.85, 54.22, 53.00, 52.38, 51.92, 49.36, 48.96, 42.13, 40.15, 39.92, 36.54, 32.45, 30.96, 27.87, 24.22, 22.97, 22.77, 22.49, 21.52, 17.36, 17.26; IR (KBr, cm<sup>-1</sup>) 3290 (br), 3061 (br), 2948 (s), 2930 (s), 2860 (s), 1653 (s), 1516 (s), 1447 (s), 1368 (s), 1337 (w), 1253 (s), 1232 (s), 1200 (s), 1132 (s), 1042 (w), 940 (w), 832 (w), 797 (w), 719 (w), 668 (w).



15

**Macrocycle 15.** Prepared from **Peptide SI-3** (0.0489 mmol, 30.2 mg) as described above in **general procedure for modifying peptides with dichloro-s-tetrazine** and **general procedure for macrocyclization of acyclic dichloro-s-tetrazine peptides**. Isolated residue was dissolved in 3 mL of Milli-Q water and 3 mL of trifluoroacetic acid before being purified by reverse-phase chromatography (gradient 10 – 50% organic over 8 minutes at a 15 mL/minute flow rate) on the Gilson HPLC setup with the Sunfire column discussed above. Fractions were collected with 210 nm detection with a 20 mV threshold. After lyophilization, compound was isolated as 17.8 mg (63%) of amorphous orange powder: AMM (ES) Found  $m/z$  582.2568 [(M+H)<sup>+</sup>; calcd for C<sub>22</sub>H<sub>36</sub>N<sub>11</sub>O<sub>6</sub>S]; <sup>1</sup>H NMR (500 MHz, DMSO-*d*<sub>6</sub>) δ 8.57 – 8.50 (m, 2H), 8.47 (d,  $J$  = 6.5 Hz, 1H), 7.75 (d,  $J$  = 6.4 Hz, 1H), 7.57 (d,  $J$  = 6.6 Hz, 1H), 7.43 (d,  $J$  = 8.3 Hz, 1H), 7.06 (s, 1H), 6.87 (s, 1H), 4.38 (q,  $J$  = 5.5 Hz, 1H), 4.10 – 3.96 (m, 4H), 3.73 (p,  $J$  = 7.1 Hz, 1H), 3.62 – 3.44 (m, 3H), 3.32 (dq,  $J$  = 13.2, 6.4 Hz, 1H), 1.92 (s, 3H), 1.79 – 1.68 (m, 1H), 1.64 – 1.45 (m, 3H), 1.37 – 1.11 (m, 10H); <sup>13</sup>C NMR (126 MHz, DMSO) δ 173.69, 172.76, 172.64, 171.95, 170.88, 170.44, 163.70, 160.46, 54.09, 52.70, 49.54, 49.41, 48.87, 39.97, 32.73, 31.08, 27.94, 23.02, 22.72, 17.24, 17.06, 16.60; IR (KBr, cm<sup>-1</sup>) 3286 (br), 3050 (w), 2959

(w), 2927 (br), 2857 (w), 1653 (s), 1534 (s), 1457 (s), 1373 (s), 1192 (s), 1169 (s), 1042 (w), 938 (w).



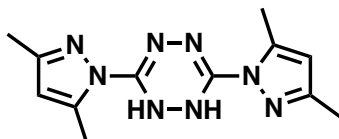
**16**

**Macrocycle 10d.** Prepared from **Peptide SI-4** (0.0555 mmol, 32.7 mg) as described above in **general procedure for modifying peptides with dichloro-s-tetrazine** and **general procedure for macrocyclization of acyclic dichloro-s-tetrazine peptides**. Isolated residue was dissolved in 3 mL of Milli-Q water and 1 mL of trifluoroacetic acid before being purified by reverse-phase chromatography (gradient 5 – 50% organic over 10 minutes at a 15 mL/minute flow rate) on the Gilson HPLC setup with the Sunfire column discussed above. Fractions were collected with 210 nm detection with a 20 mV threshold. After lyophilization, compound was isolated as 6.1 mg (20%) of amorphous orange powder: AMM (ES) Found  $m/z$  576.2088 [(M+Na)<sup>+</sup>; calcd for C<sub>20</sub>H<sub>31</sub>N<sub>11</sub>O<sub>6</sub>NaS]; <sup>1</sup>H NMR (500 MHz, DMSO-*d*<sub>6</sub>) δ 8.53 (t,  $J$  = 6.1 Hz, 1H), 8.47 – 8.39 (m, 2H), 8.01 (t,  $J$  = 6.1 Hz, 1H), 7.93 (d,  $J$  = 6.2 Hz, 1H), 7.56 (d,  $J$  = 8.2 Hz, 1H), 7.11 (s, 1H), 7.03 (s, 1H), 4.47 (q,  $J$  = 6.3 Hz, 1H), 4.13 – 3.99 (m, 2H), 3.76 – 3.67 (m, 2H), 3.60 (d,  $J$  = 5.6 Hz, 1H), 3.58 – 3.55 (m, 1H), 3.55 – 3.53 (m, 1H), 3.52 – 3.34 (m, 7H, contains water), 1.90 (s, 3H), 1.76 – 1.65 (m, 1H), 1.64 – 1.44 (m, 4H), 1.38 – 1.19 (m, 7H); <sup>13</sup>C NMR (126 MHz, DMSO) δ 173.74, 172.71, 170.31, 170.23, 169.27, 168.62, 163.64, 160.57,

53.09, 52.57, 49.38, 42.75, 42.12, 39.91, 32.78, 31.14, 28.27, 22.87, 22.59, 17.27; IR (KBr,  $\text{cm}^{-1}$ ) 3294 (br), 3053 (br), 2930 (s), 2853 (w), 1652 (s), 1543 (s), 1538 \*s(, 1435 (w), 1414 (w), 1405 (w), 1372 (w), 1353 (w), 1333 (w), 1195 (w), 1124 (w), 1042 (w), 1012 (w), 942 (w).

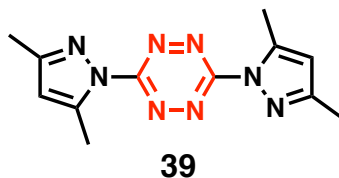


**Triaminoguanidine hydrochloride (43).** A 2 L, 2-neck round bottom flask equipped with a reflux condenser was charged with guanidine•hcl (88.8 g, 0.9292 mol) and 1,4-dioxane (400 mL). The mixture was magnetically stirred and hydrazine hydrate (3.07 mol, 152 mL) was added. After the addition, all solids had dissolved. The reaction mixture was heated to 100°C with magnetic stirring for two hours, during which time a white solid precipitated from the solution. The flask was removed from heat and stirring was halted, allowing the contents to room temperature and settle. The solid was collected by vacuum filtration and washed with 500 mL of Et<sub>2</sub>O. Filtrate was dried *in vacuo* for 3 hours, and then the solid was ground to a fine powder in a mortar and pestle. The solid was then dried overnight to yield 128.2 g (98%) of triaminoguanidine hydrochloride (**26**) as a white crystalline solid. <sup>13</sup>C NMR (126 MHz, D<sub>2</sub>O)  $\delta$  = 159.7; IR (KBr,  $\text{cm}^{-1}$ ) 3308 (s), 3179 (br), 2760 (br), 2630 (br), 2542 (br), 2444 (br), 2298 (br), 2056 (s), 1994 (w), 1817 (w), 1667 (s), 1602 (s), 1315 (s), 1118 (s), 936 (br), 731 (s), 600 (br).

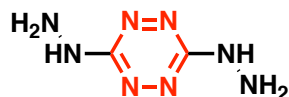


**44**

**3,6-Bis(3,5-dimethyl-1H-pyrazol-1-yl)-1,4-dihydro-1,2,4,5-tetrazine (44).** A 3-neck, 3 L round bottom flask was equipped with a mechanical stirrer and placed in an oil bath. The flask was charged with triaminoguanidium hydrochloride (0.91 mol, 128 g) and DI-water (1 L). The stirrer was turned on and the solid dissolved. 2,4-Pentanedione (1.82 mol, 190 mL) was slowly added over a 1-hour period. After the addition was complete, the mixture was stirred at room temperature for 30 minutes. During the addition and the room temperature stirring period, the solution turned from colorless to bright yellow. The temperature of the oil bath was raised to 80°C and the reaction was allowed to continue with mechanical stirring for another 4 hours. The product precipitates from solution during this time. Stirring was halted and the flask was removed from the oil bath. After cooling to room temperature, the precipitate was isolated from the reaction mixture by vacuum filtration. The precipitate was then washed with cold DI-water. The precipitate was then dissolved in dichloromethane (1 L) and washed with water (2 x 500 mL). The organic layer was dried over sodium sulfate, filtered, and concentrated *in vacuo*. Product **27** was isolated as 97.2 g (79%) as a yellow powder:  $^1\text{H}$  NMR (500 MHz, Chloroform-*d*)  $\delta$  8.06 (s, 2H), 5.96 (s, 2H), 2.49 (s, 6H), 2.22 (s, 6H);  $^{13}\text{C}$  NMR (126 MHz,  $\text{CDCl}_3$ )  $\delta$  150.09, 145.92, 142.44, 110.01, 13.94, 13.61.



**3,6-Bis(3,5-dimethyl-1H-pyrazol-1-yl)-1,2,4,5-tetrazine (39).** A single-neck 4 L round bottom flask was equipped with a stir bar and charged with sodium nitrite (1 mol, 69 g) dissolved in 1.5 L DI water. Compound **44** (0.356 mol, 97 g) was dissolved in 1 L dichloromethane and added to the flask. Acetic acid (0.854 mol, 49 mL) was added to a drop funnel, which was attached to the reaction vessel. The acetic acid was slowly added over the course of 10 minutes. The reaction was stirred magnetically for 14 hours, after which no further bubbling was witnessed. The reaction mixture was transferred to a separatory funnel and ~300 mL of 5% (w/w) NaCO<sub>3</sub> solution was added. The mixture was shaken, venting to allow escape of generated CO<sub>2</sub>. The aqueous and organic layers were separated. The organic layer was dried over sodium sulfate, which was subsequently removed by vacuum filtration. The organic layer was then concentrated *in vacuo*. The isolated solid was triturated with diethyl ether (~300 mL). Compound **39** was isolated as 86.2 g (90%) of amorphous red powder: <sup>1</sup>H NMR (500 MHz, Chloroform-*d*) δ 6.17 (s, 1H), 2.69 (s, 3H), 2.37 (s, 3H); <sup>13</sup>C NMR (126 MHz, CDCl<sub>3</sub>) δ 159.40, 154.56, 143.87, 111.99, 14.77, 13.96.

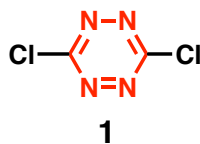


40

**CAUTION:** The dihydrazinyltetrazine product was found to undergo exothermic de-composition above 120 °C when analyzed by DSC-TGA under air and ramping the temperature at 50/minute. No decomposition was observed when dihydrazinyltetrazine was held at 80°C under air for 60 minutes. As a precaution an inert atmosphere is highly recommended to prevent any oxidation during the course of the reaction.

**3,6-Dihydrazineyl-1,2,4,5-tetrazine (40).** In a 1 L round bottom flask, *bis*-dimethylpyrazolyl-1,2,4,5-tetrazine (0.318 mol, 86 g) was suspended in acetonitrile (500 mL). Hydrazine hydrate (0.670, 33 mL) was then added neat via drop funnel over 15 minutes with magnetic stirring. The reaction vessel was equipped with a reflux condenser and the mixture was heated to 85°C of 30 minutes. The reaction vessel was removed from heat and allowed to cool to room temperature. The vessel is placed in an ice bath and, after the contents have cooled to 0°C, the product is isolated by vacuum filtration and dried *in vacuo*. Dihydrazinyltetrazine was isolated as 38.5 g (99%) of free-flowing dark-red amorphous powder: <sup>13</sup>C NMR (126 MHz, DMSO) δ 163.36. This compound was carried immediately to the next step.



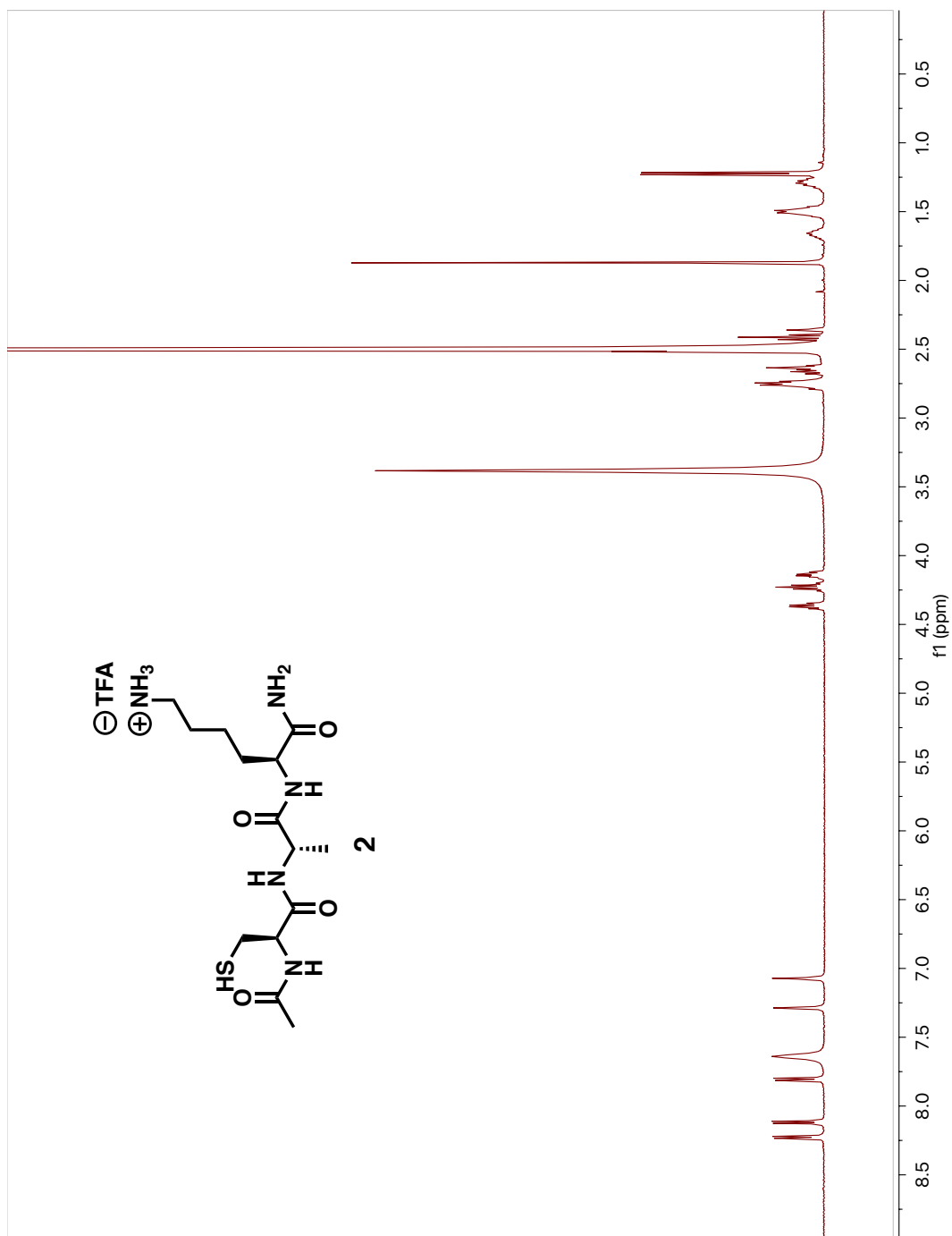


**3,6-Dichloro-1,2,4,5-tetrazine (1).** In a single-neck, 4 L round bottom flask, dihydrazinyltetrazine (**40**) (0.318 mol, 38.5 g) was suspended in acetonitrile (500 mL). The flask was equipped with a stir bar and placed in an ice bath on a magnetic stirring plate. In a separate beaker, of trichloroisocyanuric acid (0.6517 mol, 151.3 g) is transferred to an addition funnel and slowly added to the suspension of dihydrazinyltetrazine, being careful to keep the internal temperature of the reaction mixture below room temperature. After the addition is complete and the temperature of the reaction mixture has stabilized, the flask is removed from the ice bath and the mixture is allowed to stir at room temperature for 30 minutes. The reaction mixture was vacuum filtered and the white solid precipitate was washed with acetonitrile. The solvent was stripped from the filtrate via rotovap (22°C, 70 torr). Dichlorotetrazine can sublime and decomposes under high heat, so careful attention should be paid to keep temperature low and watch for the distinctive orange color of the product to collect in the cold trap. Removal of the acetonitrile results in the isolation of the crude product as a red-orange solid with a strong smell of chlorine. This solid was then dissolved in dichloromethane and passed through a celite plug. The resulting filtrate was concentrated *in vacuo*, again being cautious to prevent loss of volatile dichlorotetrazine. This filtration procedure was repeated 2 times until only 1 <sup>13</sup>C carbon signal showed in the NMR spectrum and all

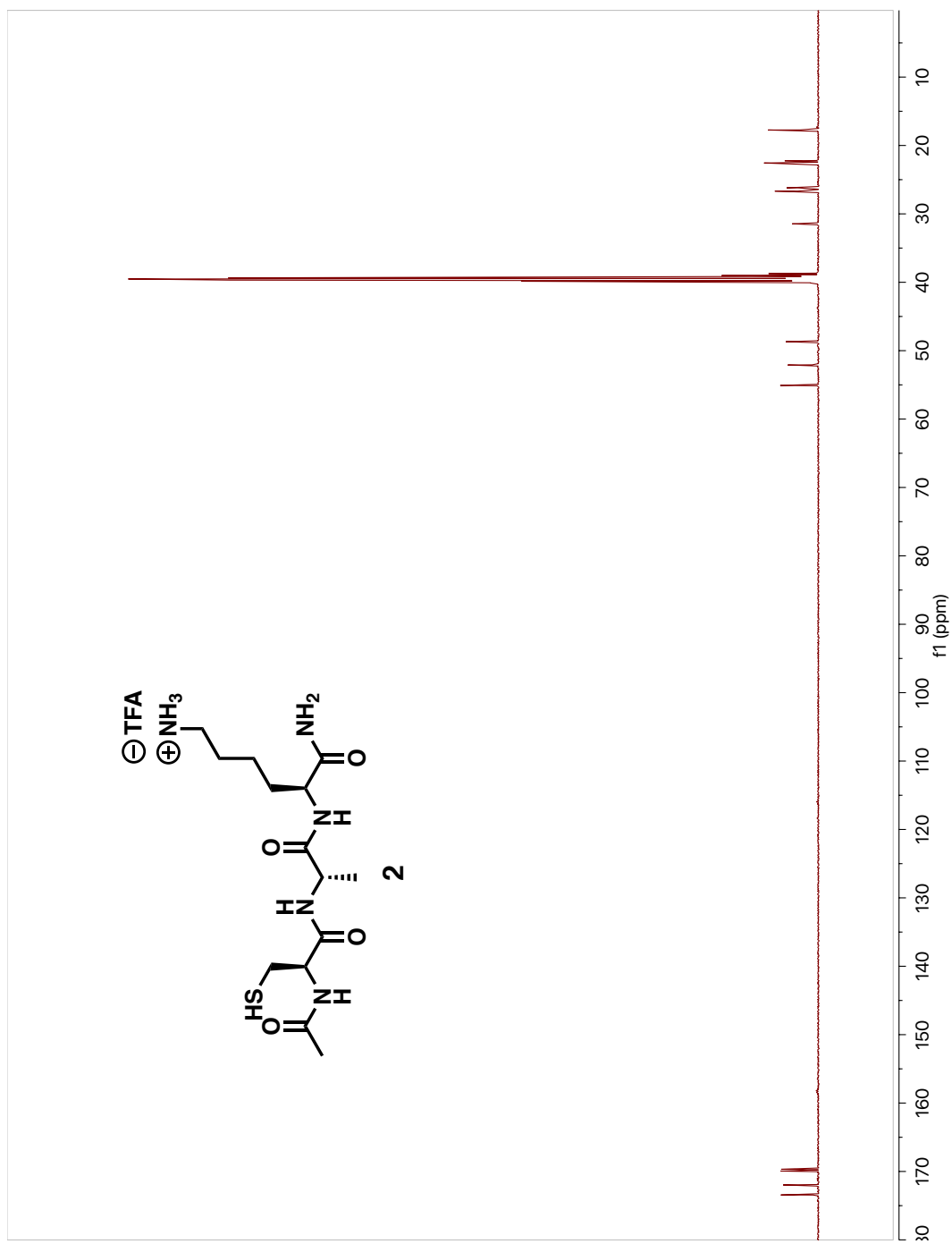
smell of chlorine was gone. Pure dichlorotetrazine was isolated as 47 g (99%) of orange crystalline solid:  $^{13}\text{C}$  NMR (126 MHz,  $\text{CDCl}_3$ )  $\delta$  168.25.

# **APPENDIX**

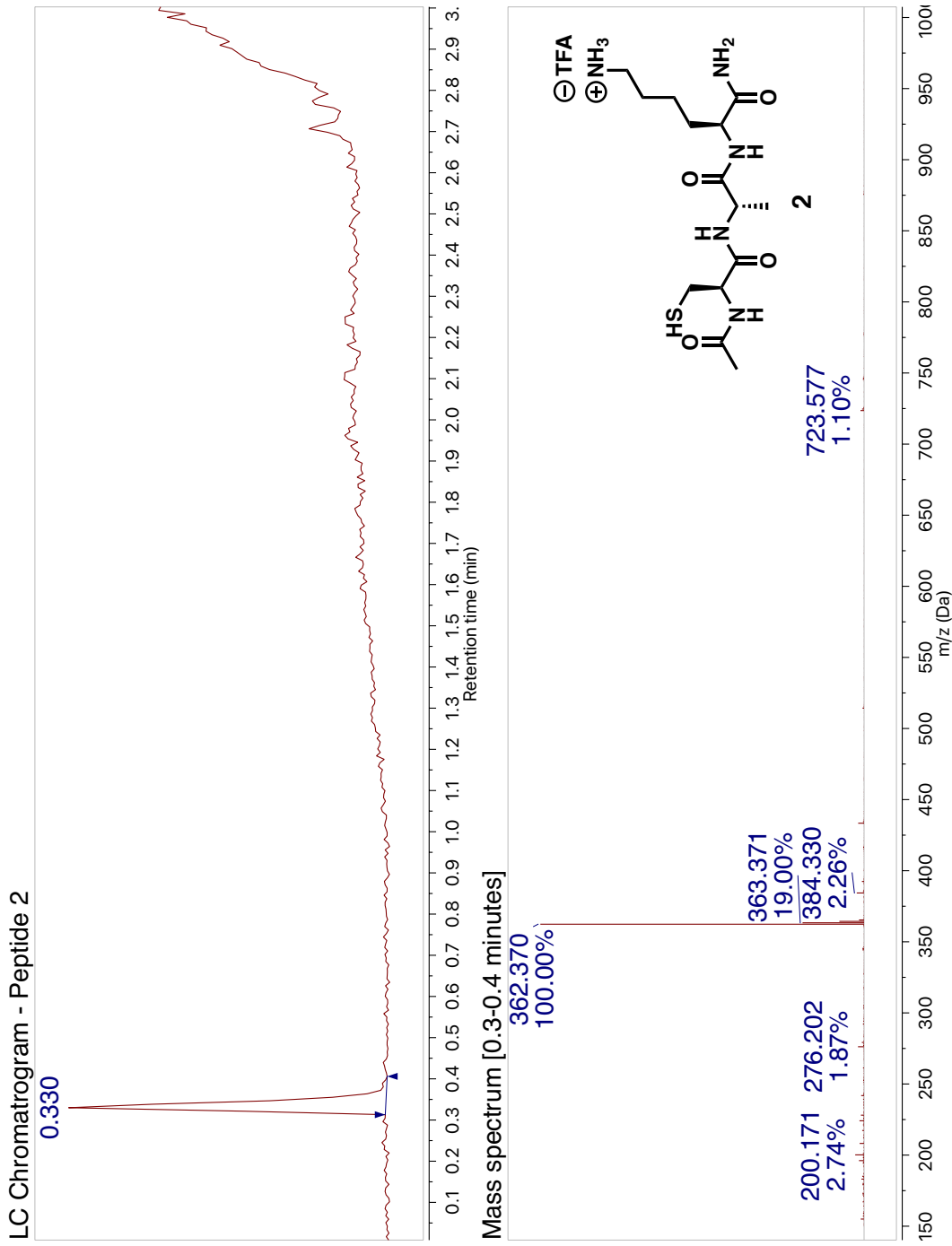
Relevant Spectra



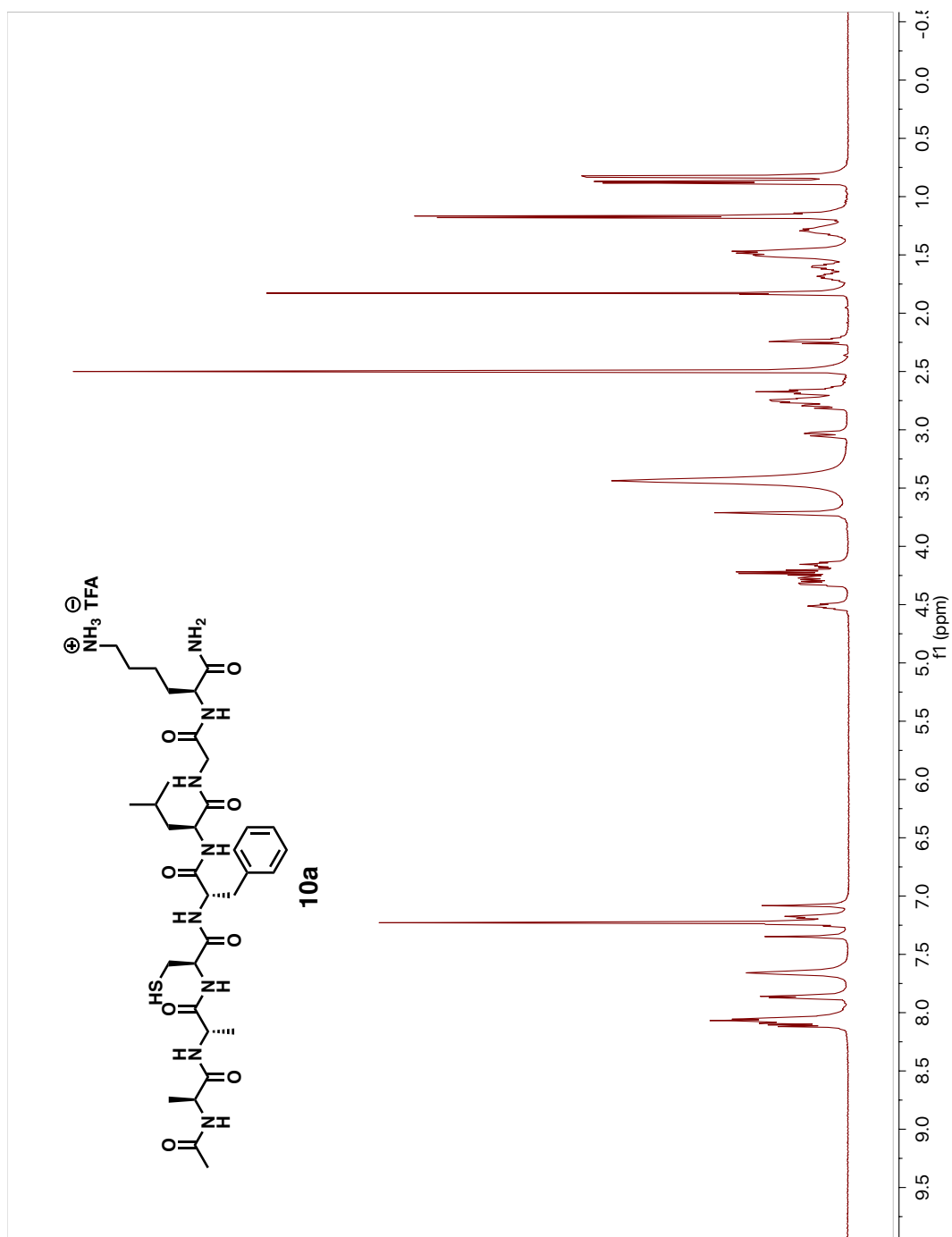
**Figure A.1.** 500 MHz <sup>1</sup>H-NMR Spectrum of Peptide 2 in *d*<sub>6</sub>-DMSO



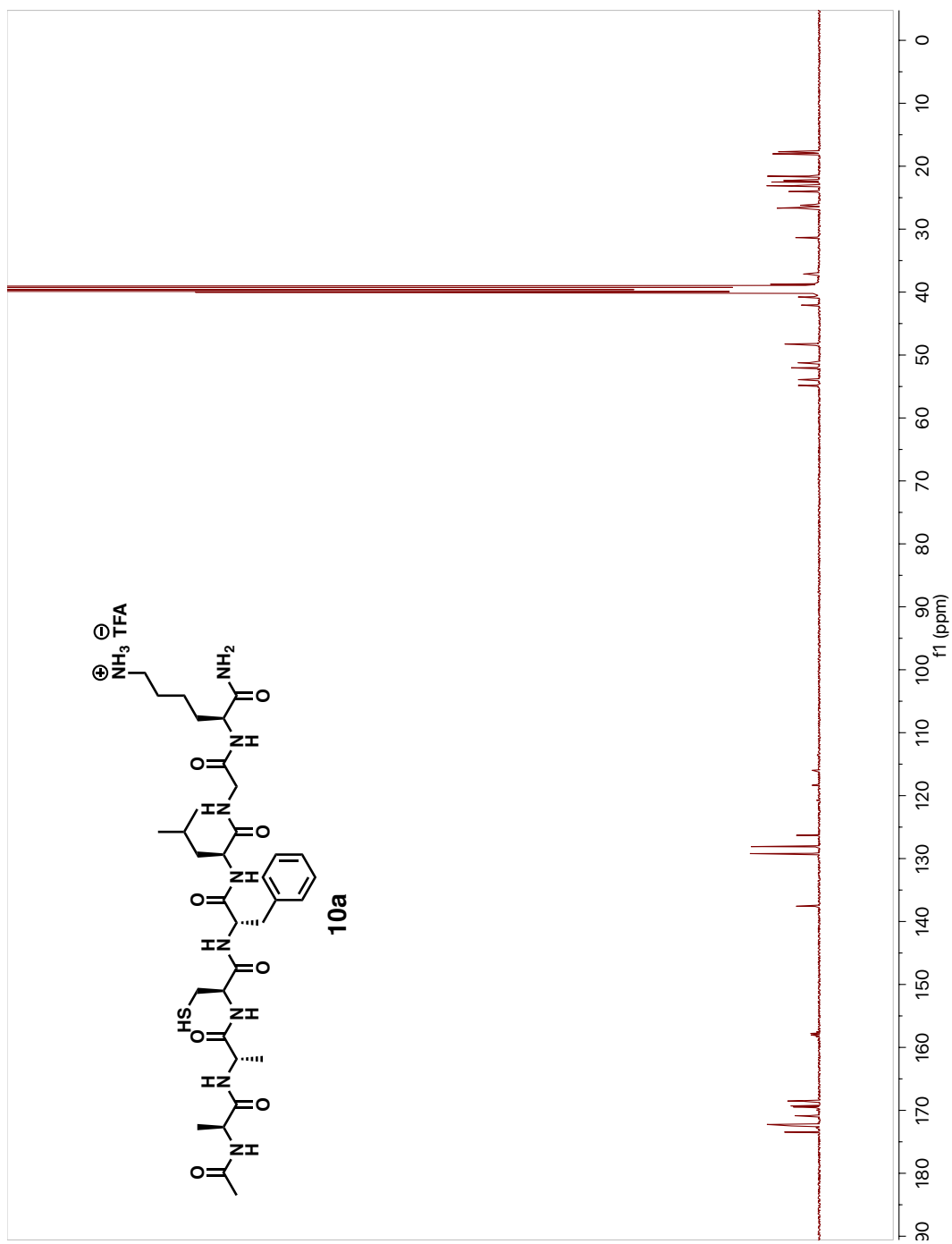
**Figure A.2.** 126 MHz  $^{13}\text{C}$ -NMR Spectrum of Peptide 2 in  $d_6$ -DMSO



**Figure A.3.** LC/MS Chromatogram of Peptide 2

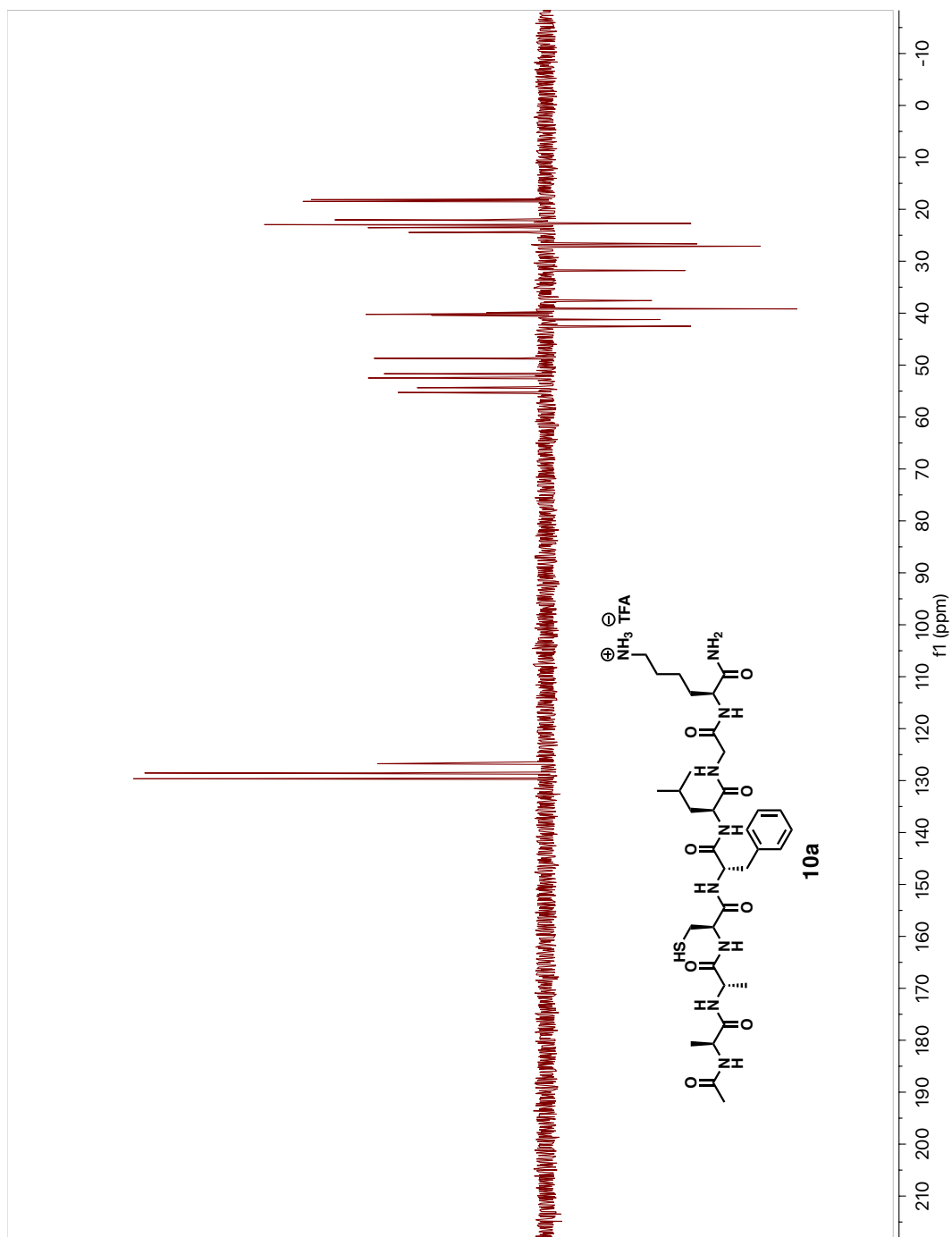


**Figure A.4.** 500 MHz <sup>1</sup>H-NMR Spectrum of Peptide 10a in *d*<sub>6</sub>-DMSO

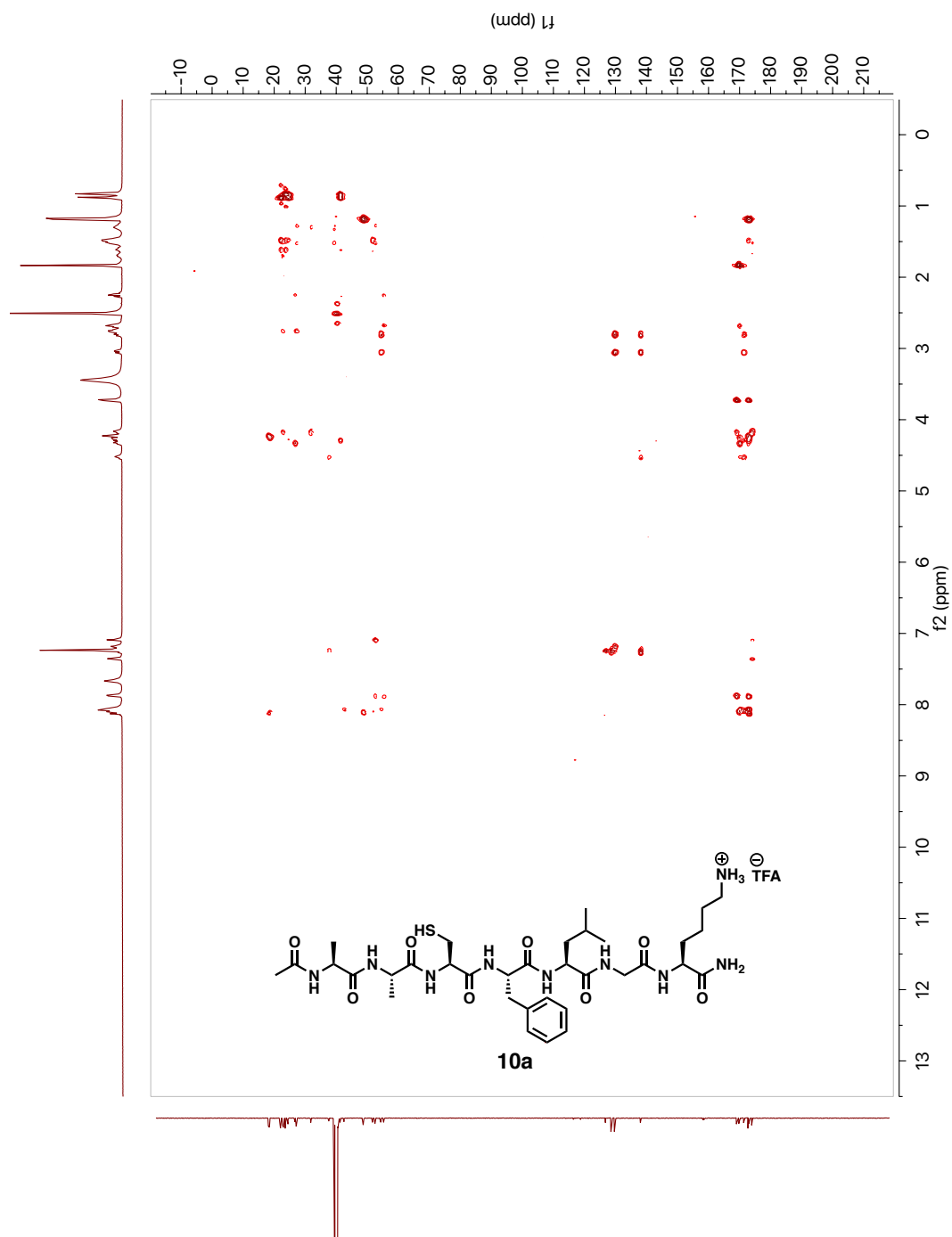


**Figure A.5.** 126 MHz  $^{13}\text{C}$ -NMR Spectrum of Peptide **10a** in  $d_6$ -DMSO





**Figure A.6.** 126 MHz DEPT-135 Spectrum of Peptide 10a in  $d_6$ -DMSO



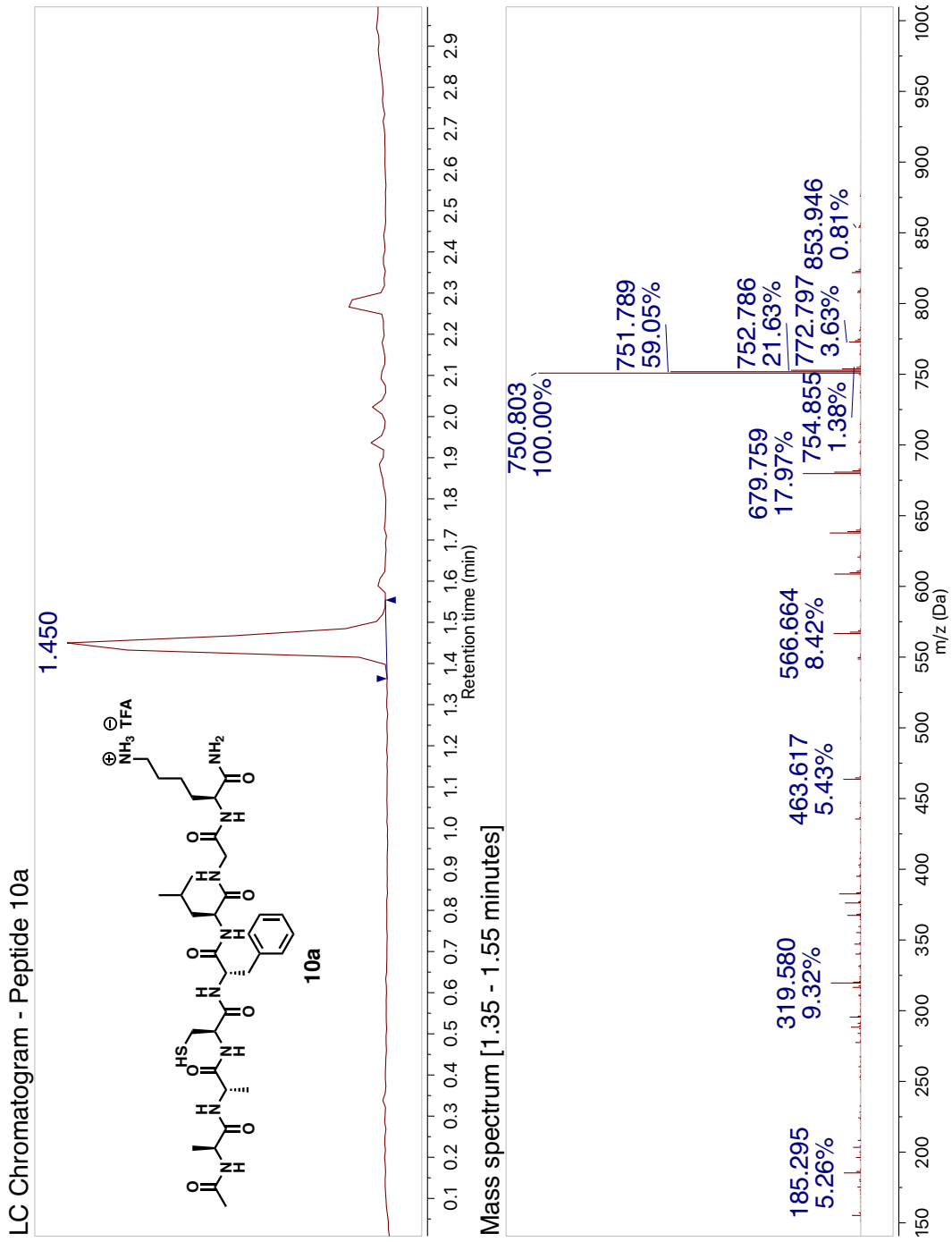


**Figure A.8.** LC/MS Chromatogram of Peptide 10a

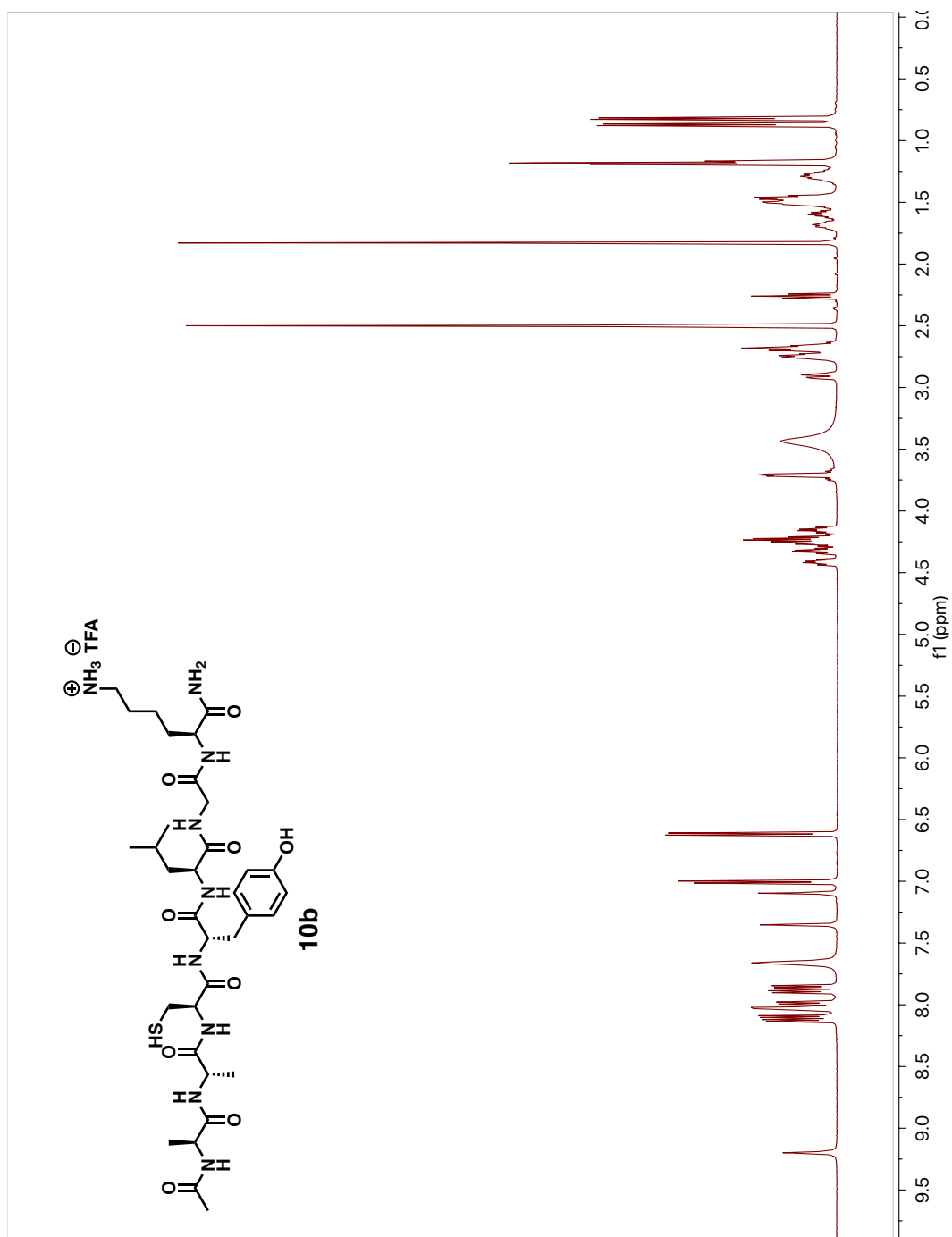


**Figure A.9.** 500 MHz <sup>1</sup>H-NMR Spectrum of Peptide 10b in *d*<sub>6</sub>-DMSO

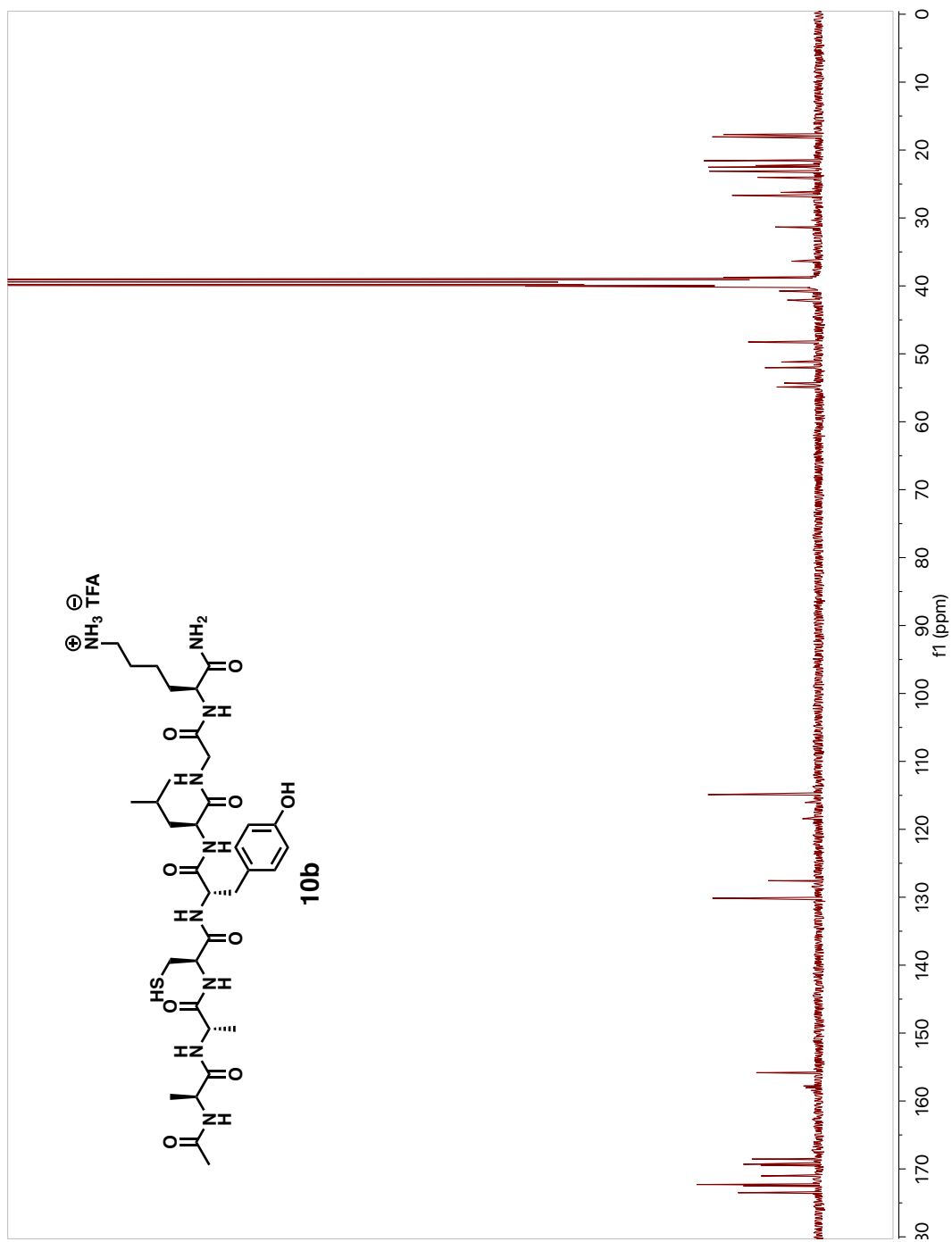


**Figure A.10.** 126 MHz  $^{13}\text{C}$ -NMR Spectrum of Peptide **10b** in  $d_6$ -DMSO

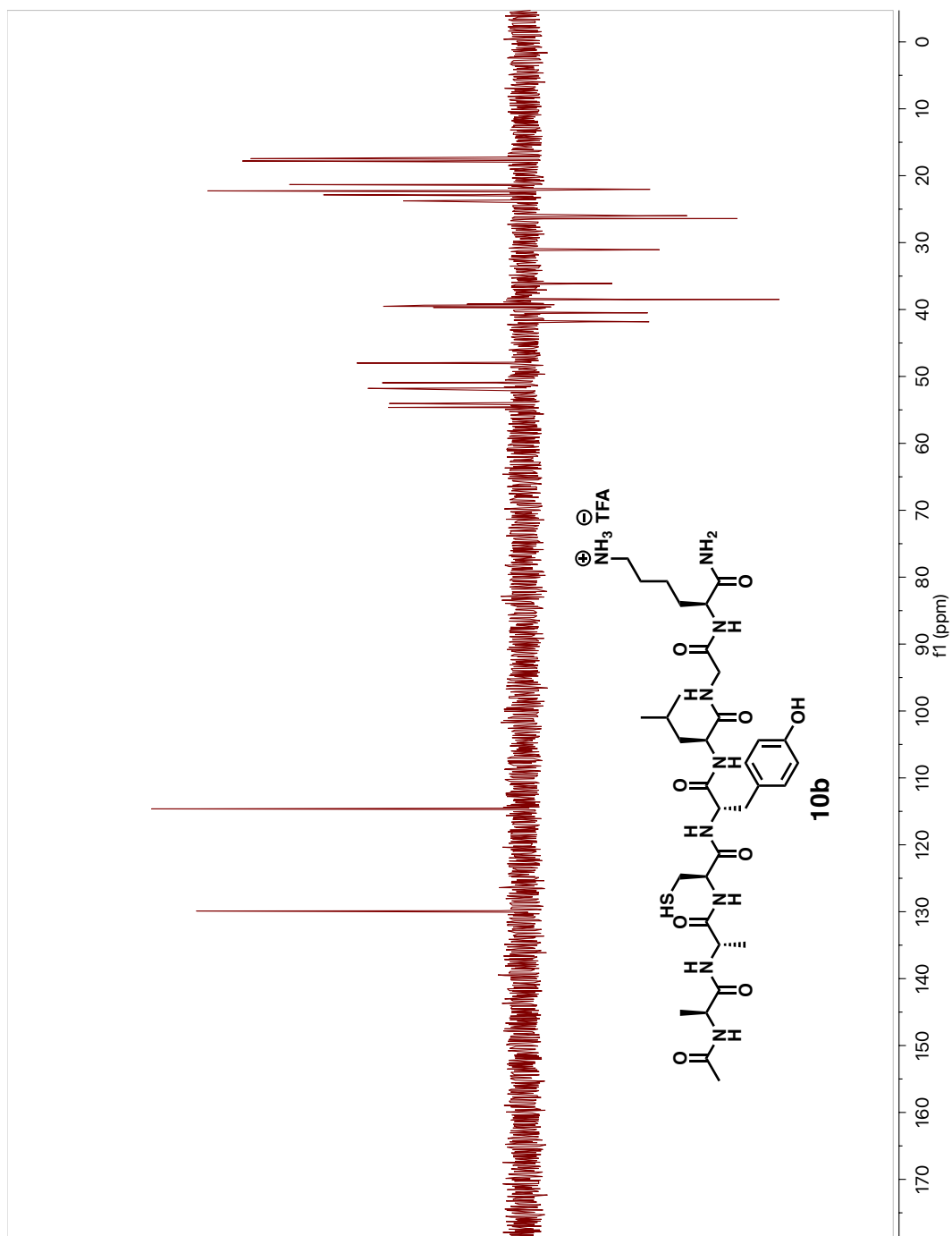


**Figure A.11.** 126 MHz DEPT-135 Spectrum of Peptide **10b** in *d*<sub>6</sub>-DMSO

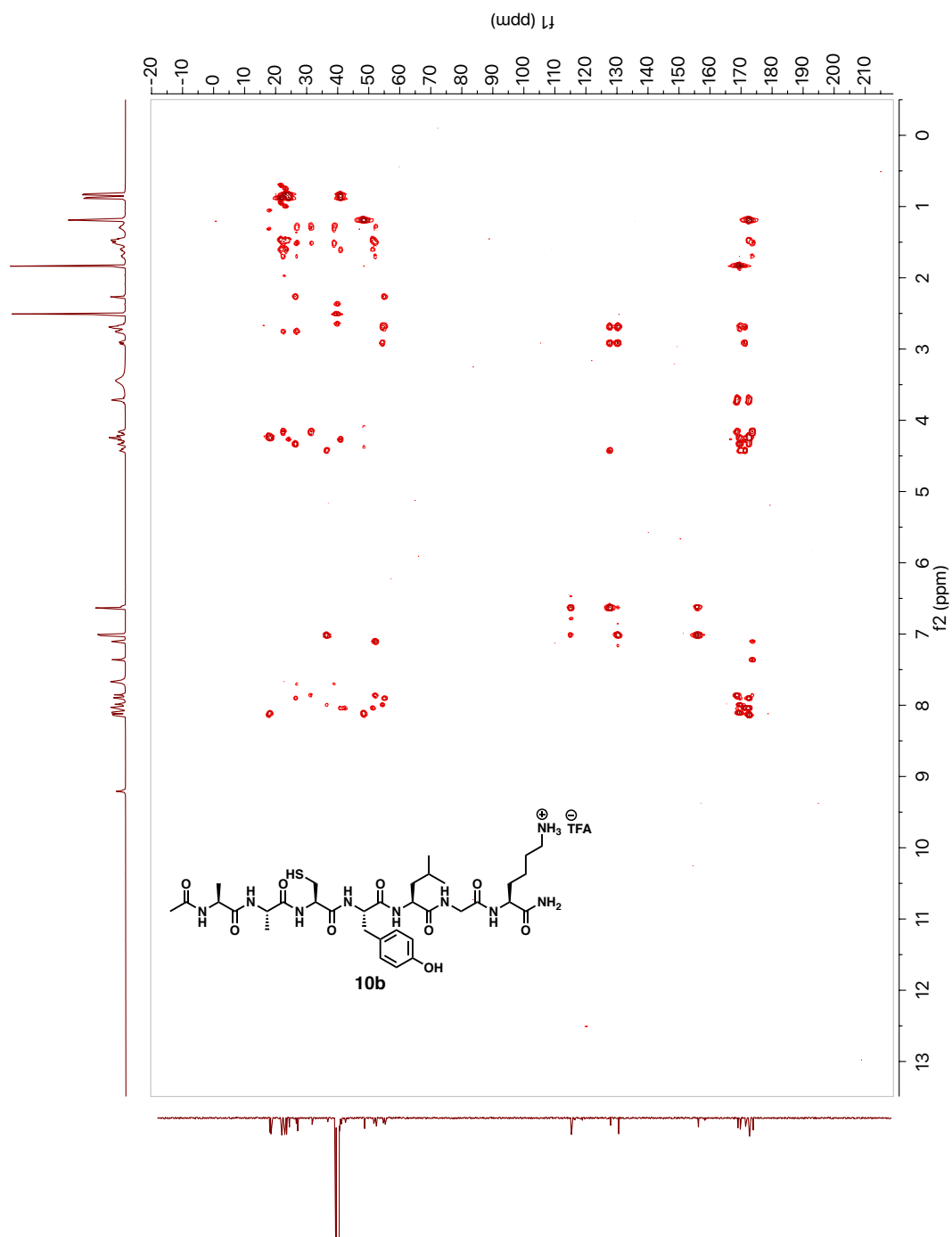
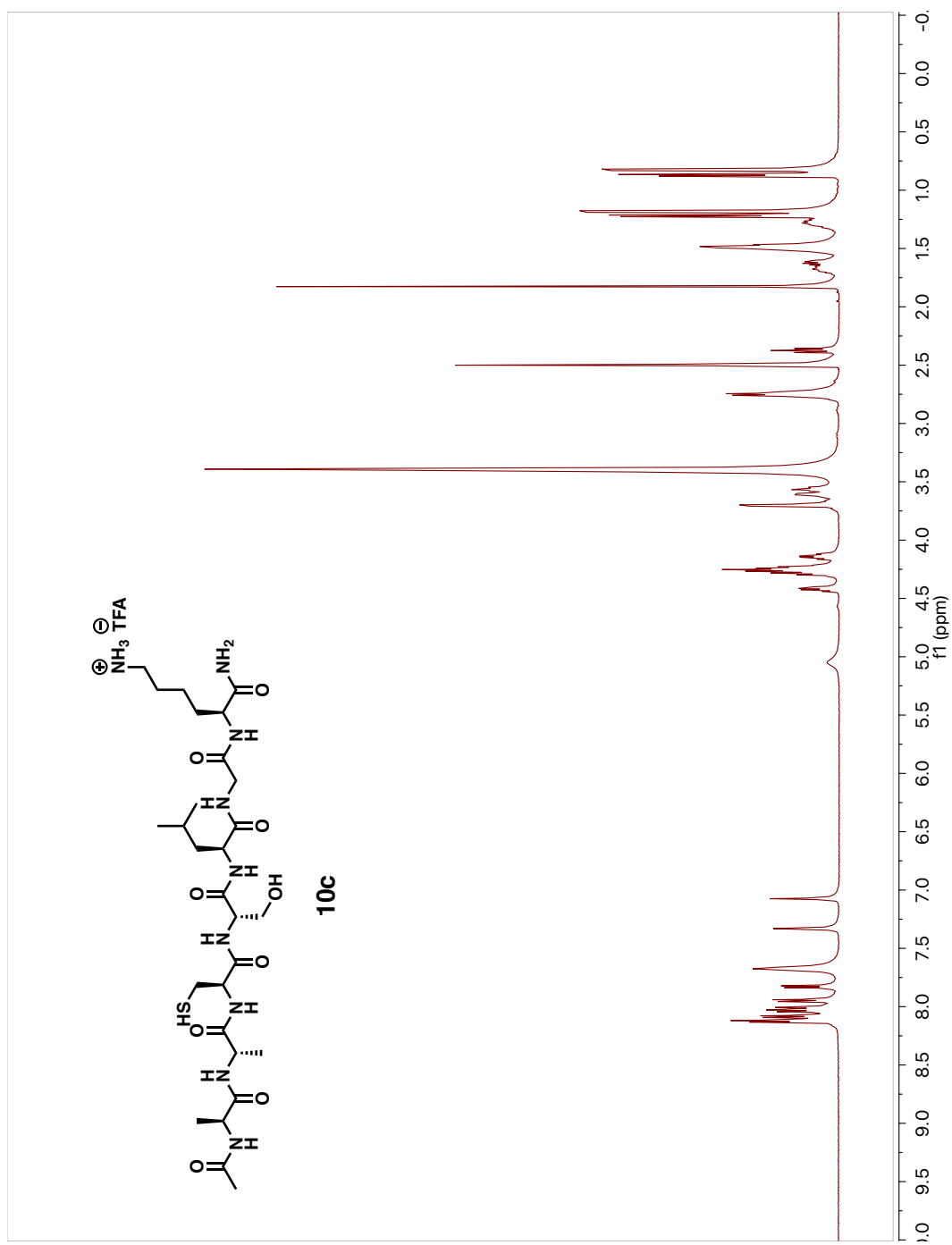
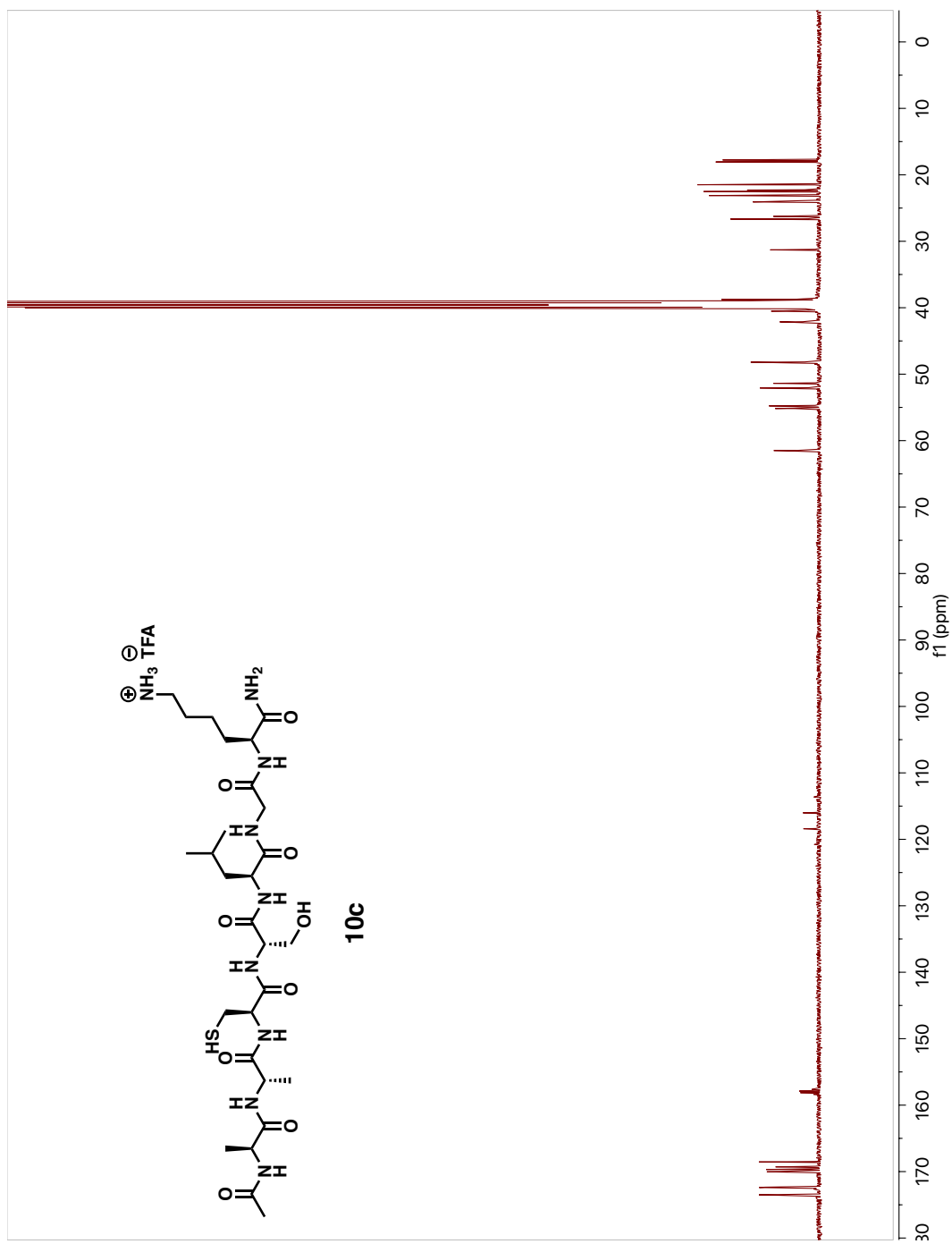


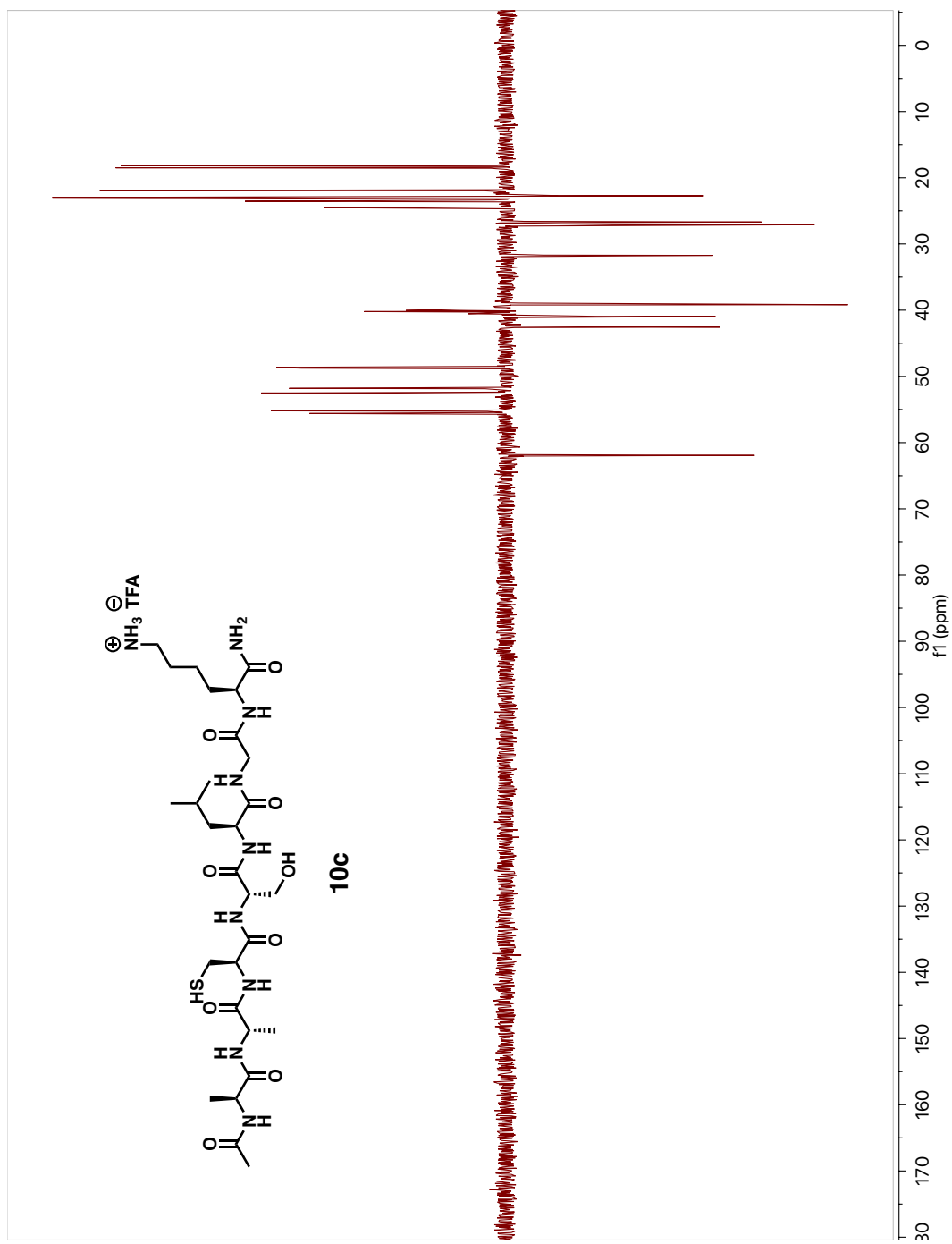
Figure A.12. HMBC Spectrum of Peptide 10b in  $d_6$ -DMSO



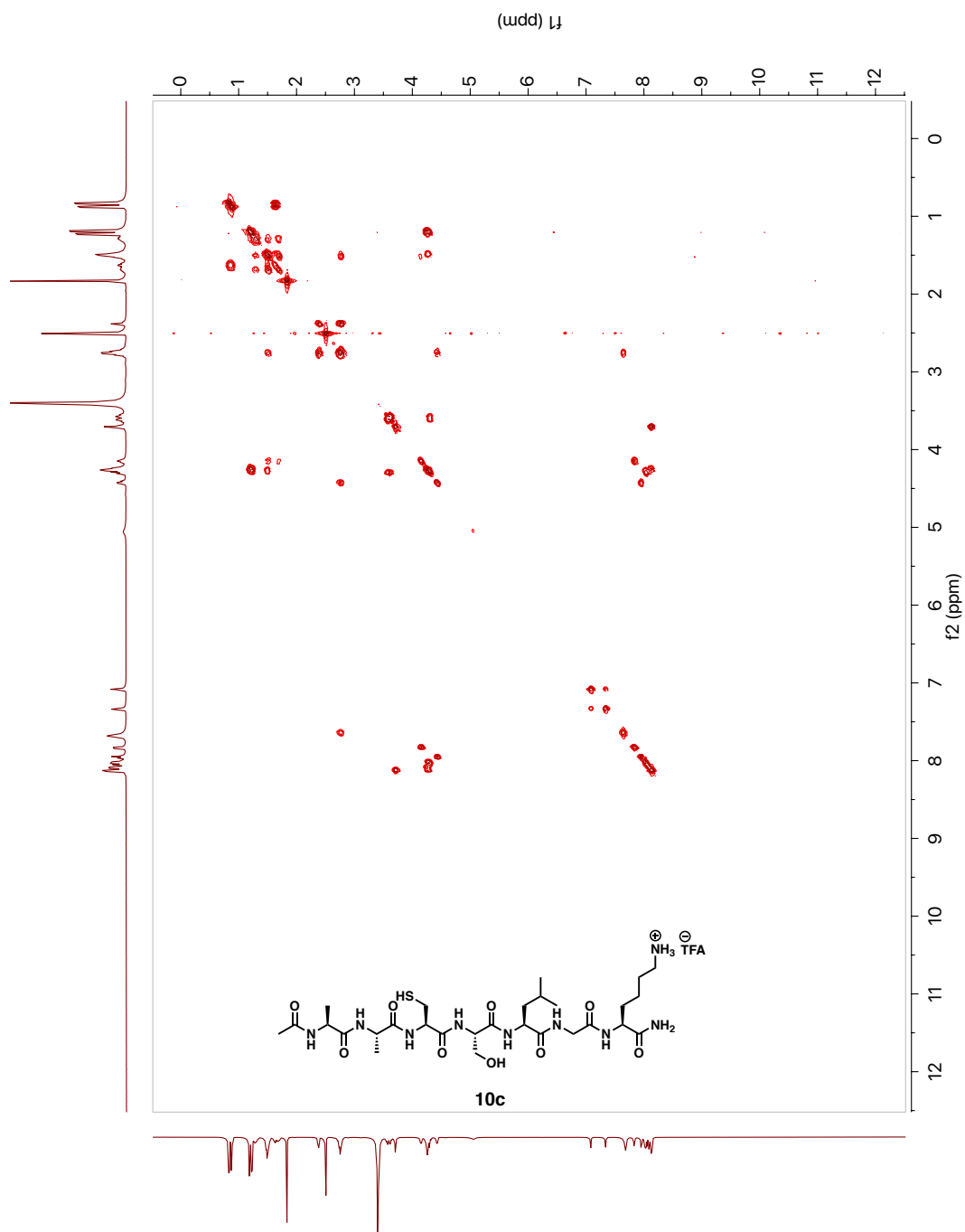




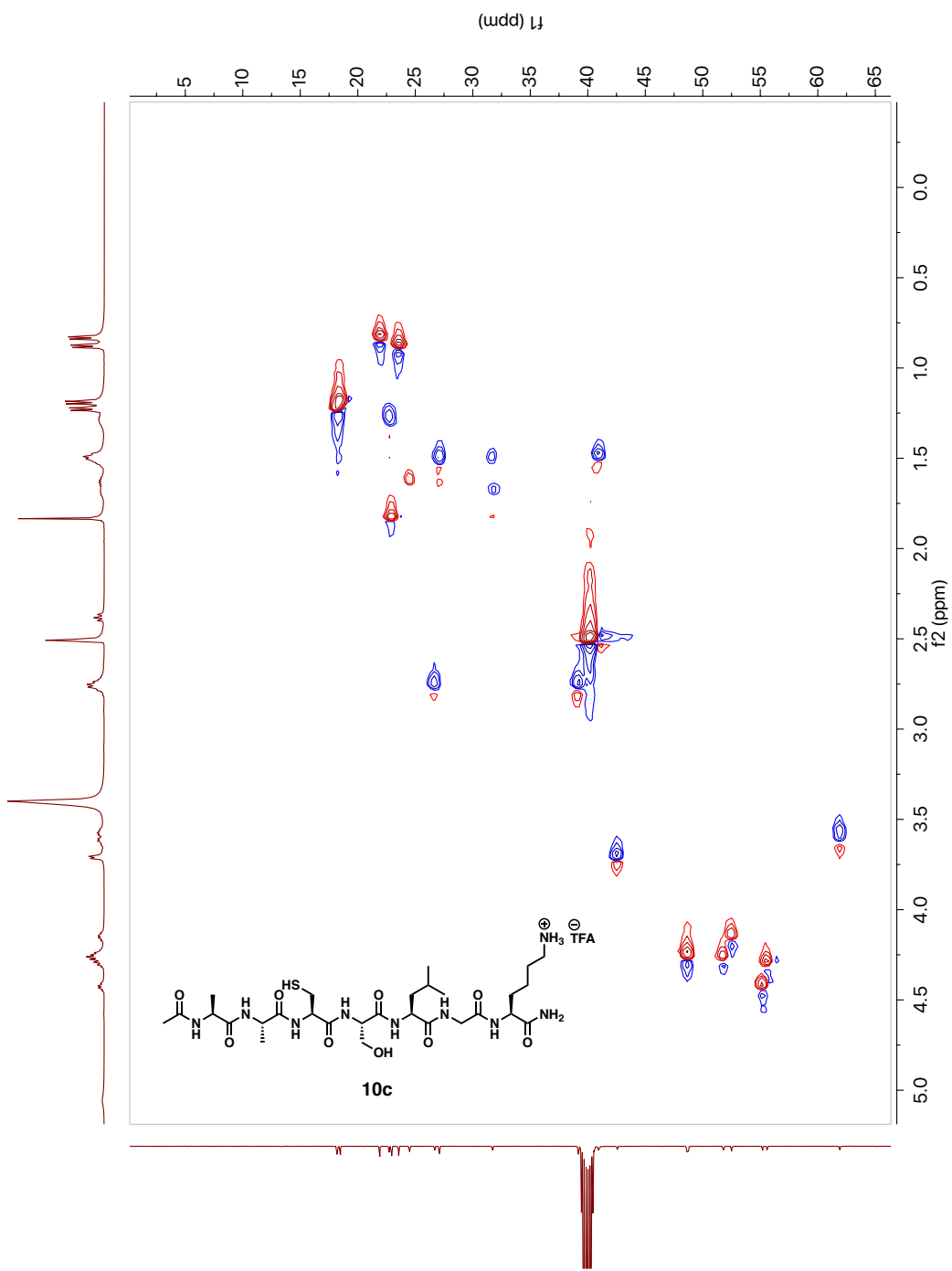
**Figure A.14.** 126 MHz <sup>13</sup>C-NMR Spectrum of Peptide 10c in *d*<sub>6</sub>-DMSO



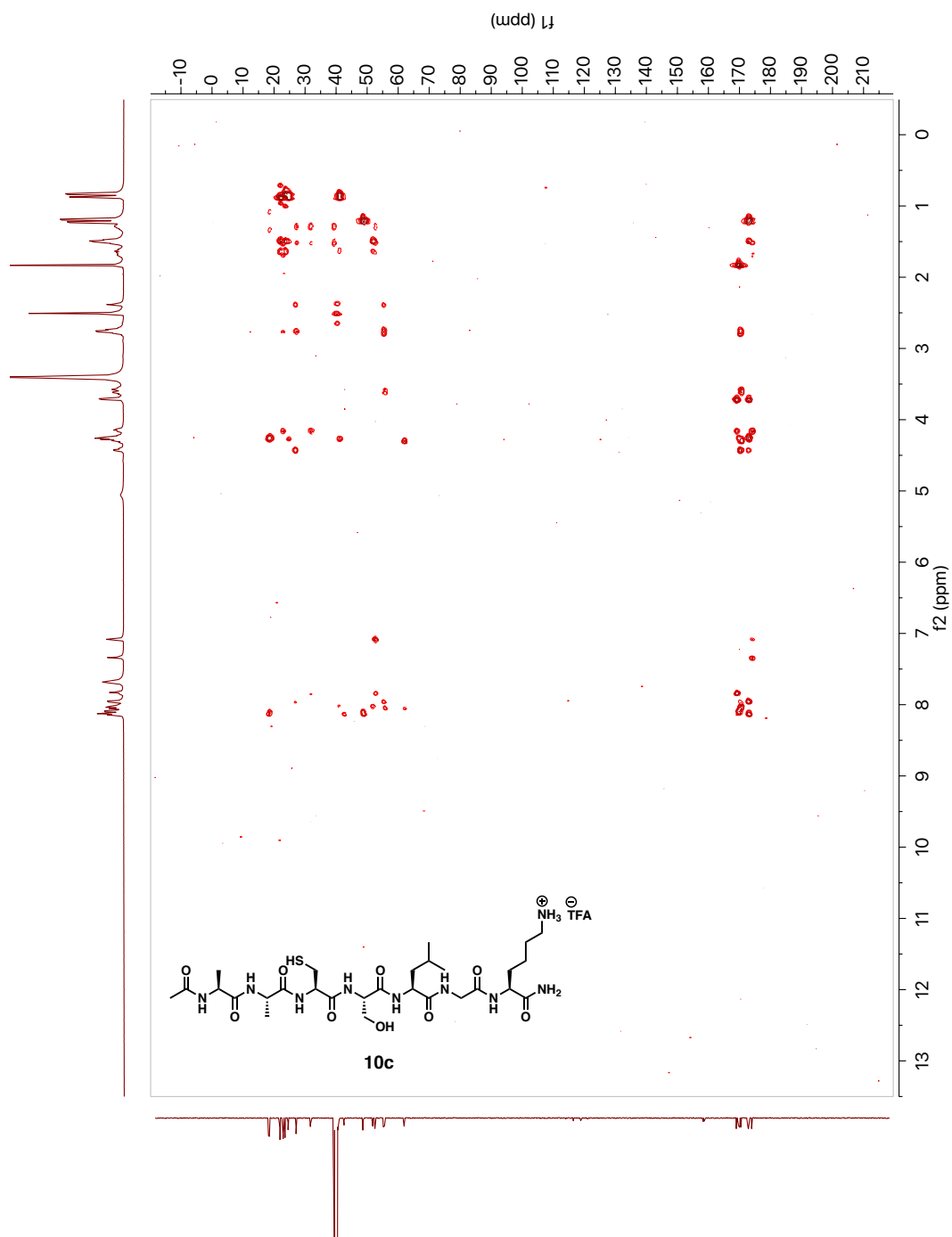
**Figure A.15.** 126 MHz DEPT-135 Spectrum of Peptide 10c in  $d_6$ -DMSO



**Figure A.16.** COSY Spectrum of Peptide 10c in  $d_6$ -DMSO



**Figure A.17.** HSQC Spectrum of Peptide 10c in  $d_6$ -DMSO



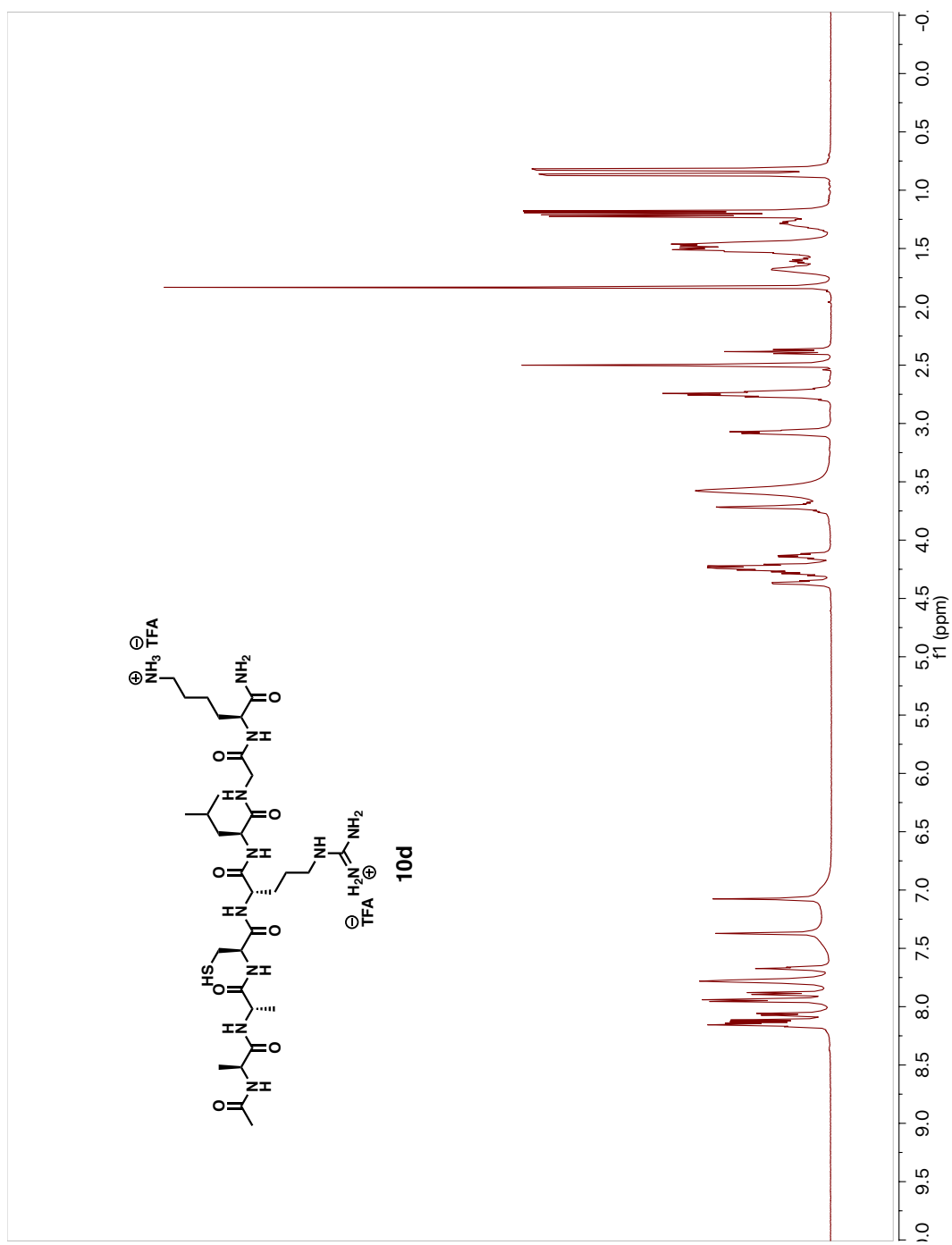


**Figure A.19.** 500 MHz <sup>1</sup>H-NMR Spectrum of Peptide 10d in *d*<sub>6</sub>-DMSO

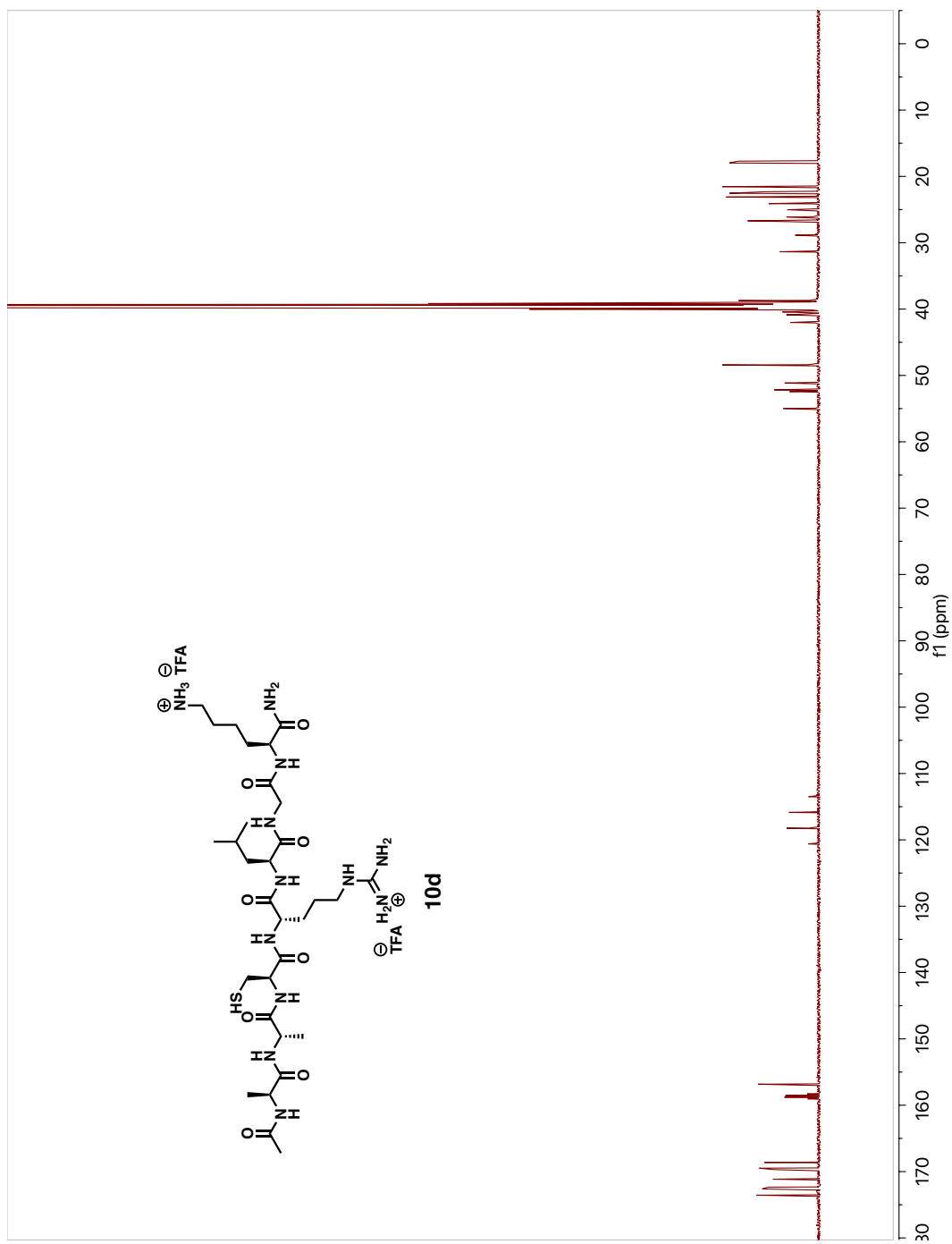


**Figure A.20.** 126 MHz  $^{13}\text{C}$ -NMR Spectrum of Peptide 10d in  $d_6$ -DMSO

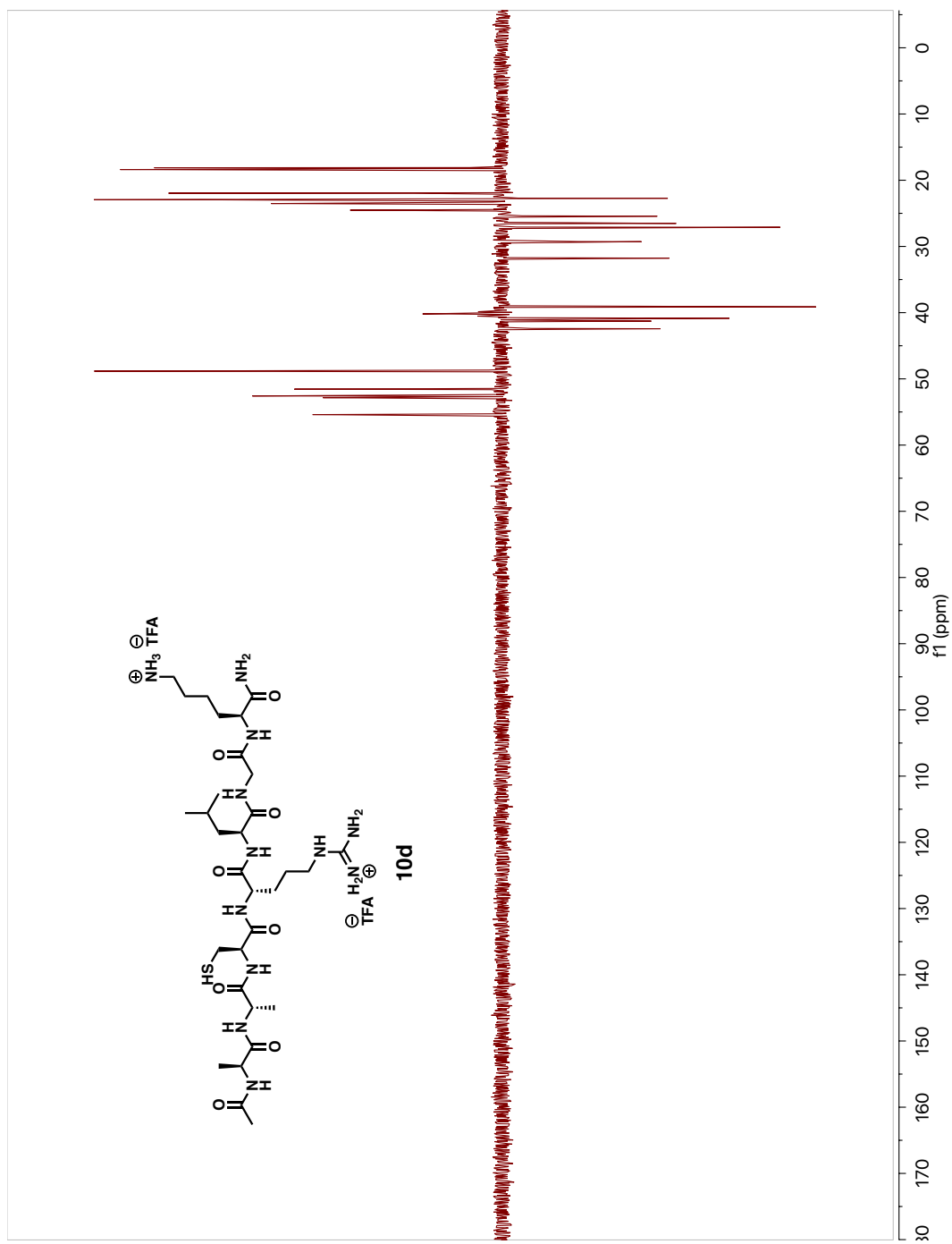


**Figure A.21.** 126 MHz DEPT-135 Spectrum of Peptide 10d in  $d_6$ -DMSO







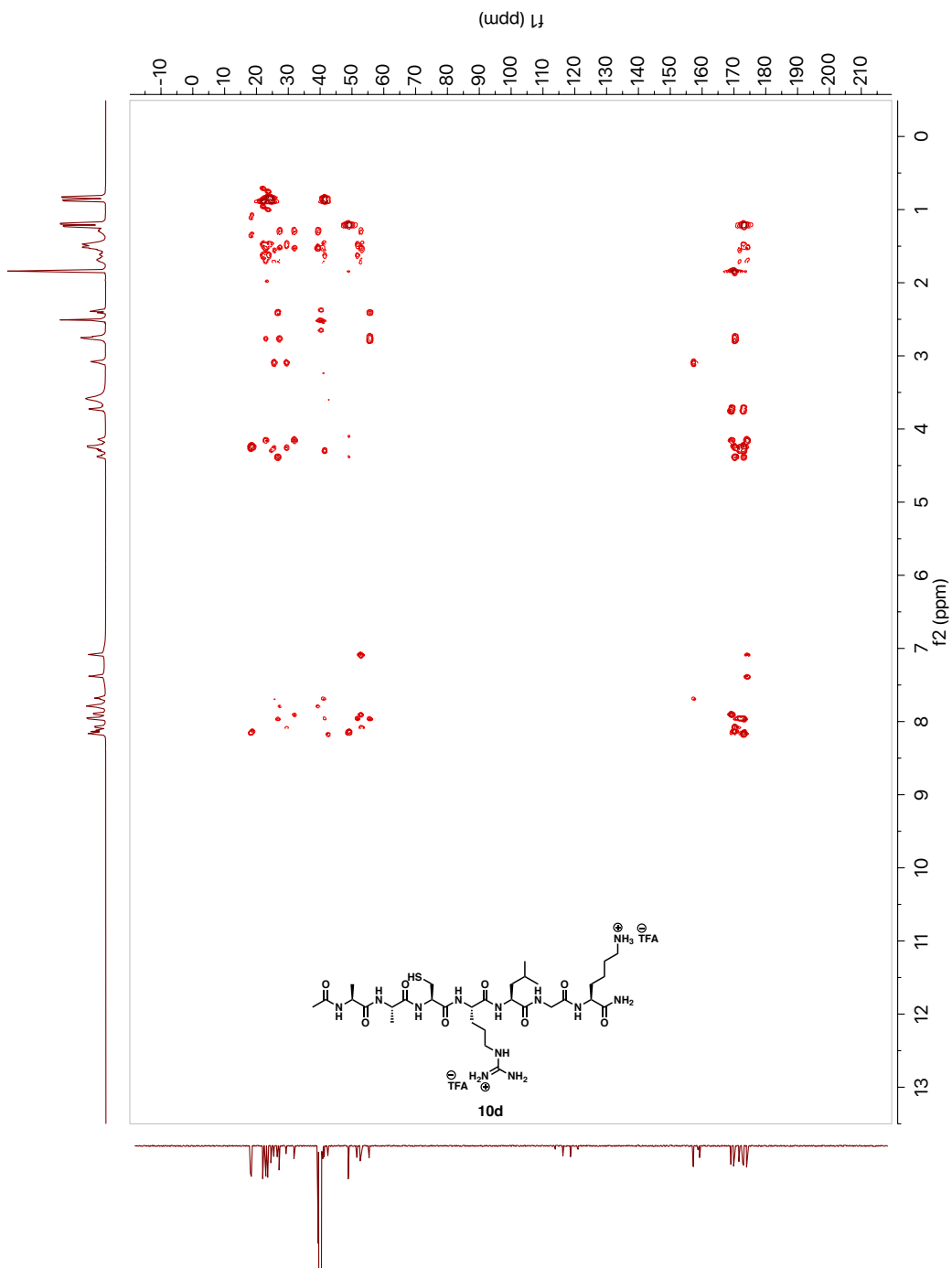


**Figure A.24.** HMBC Spectrum of Peptide 10d in  $d_6$ -DMSO

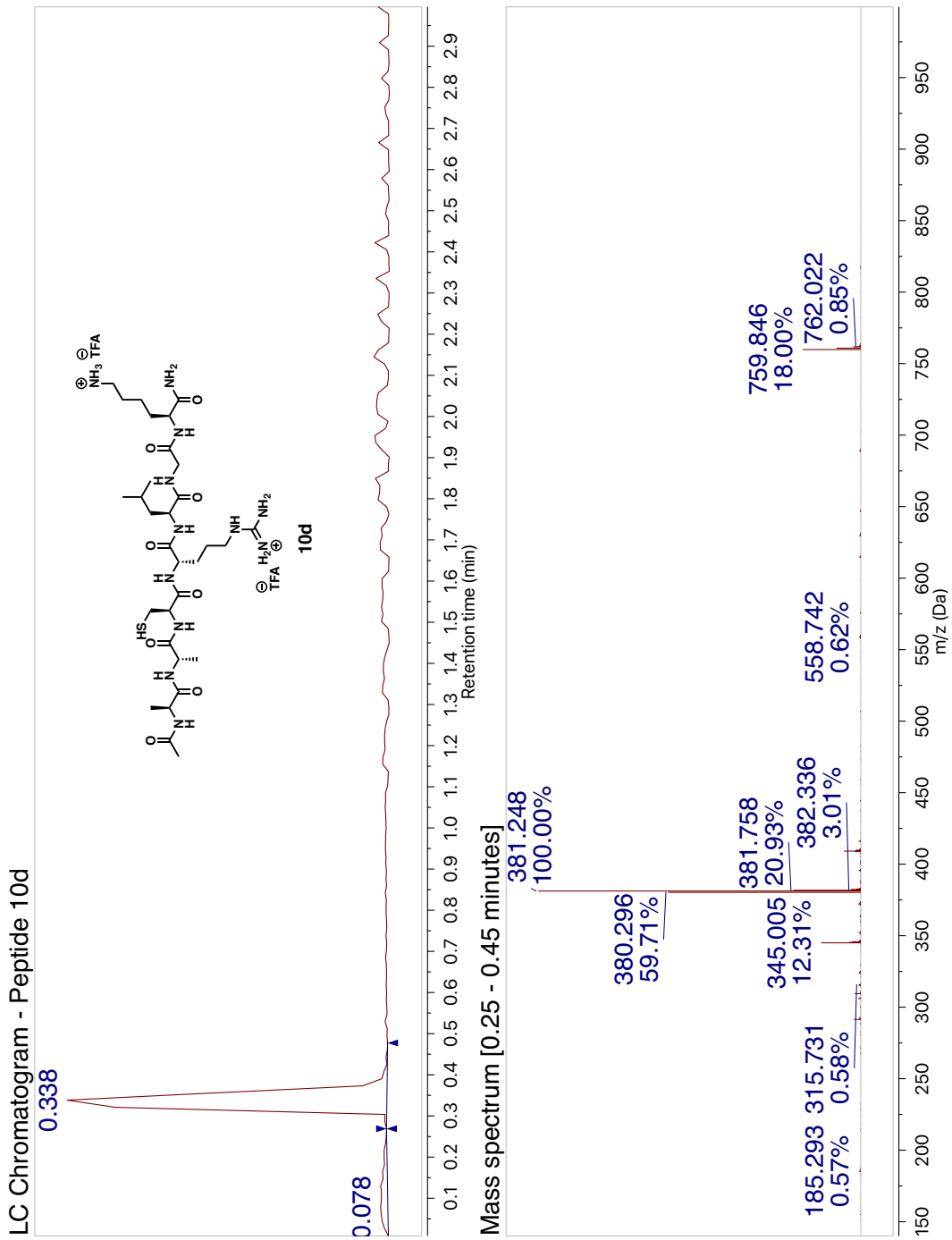
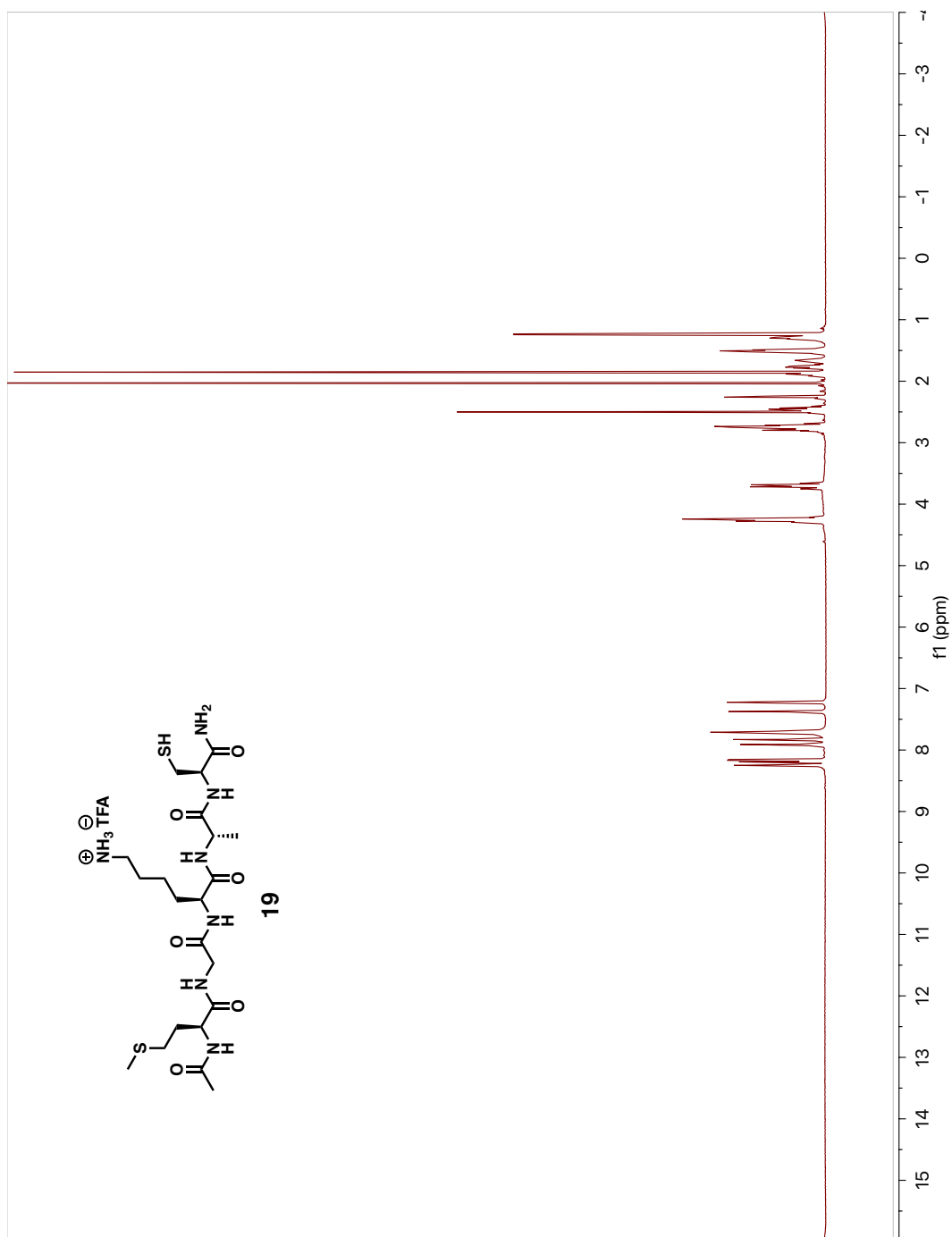
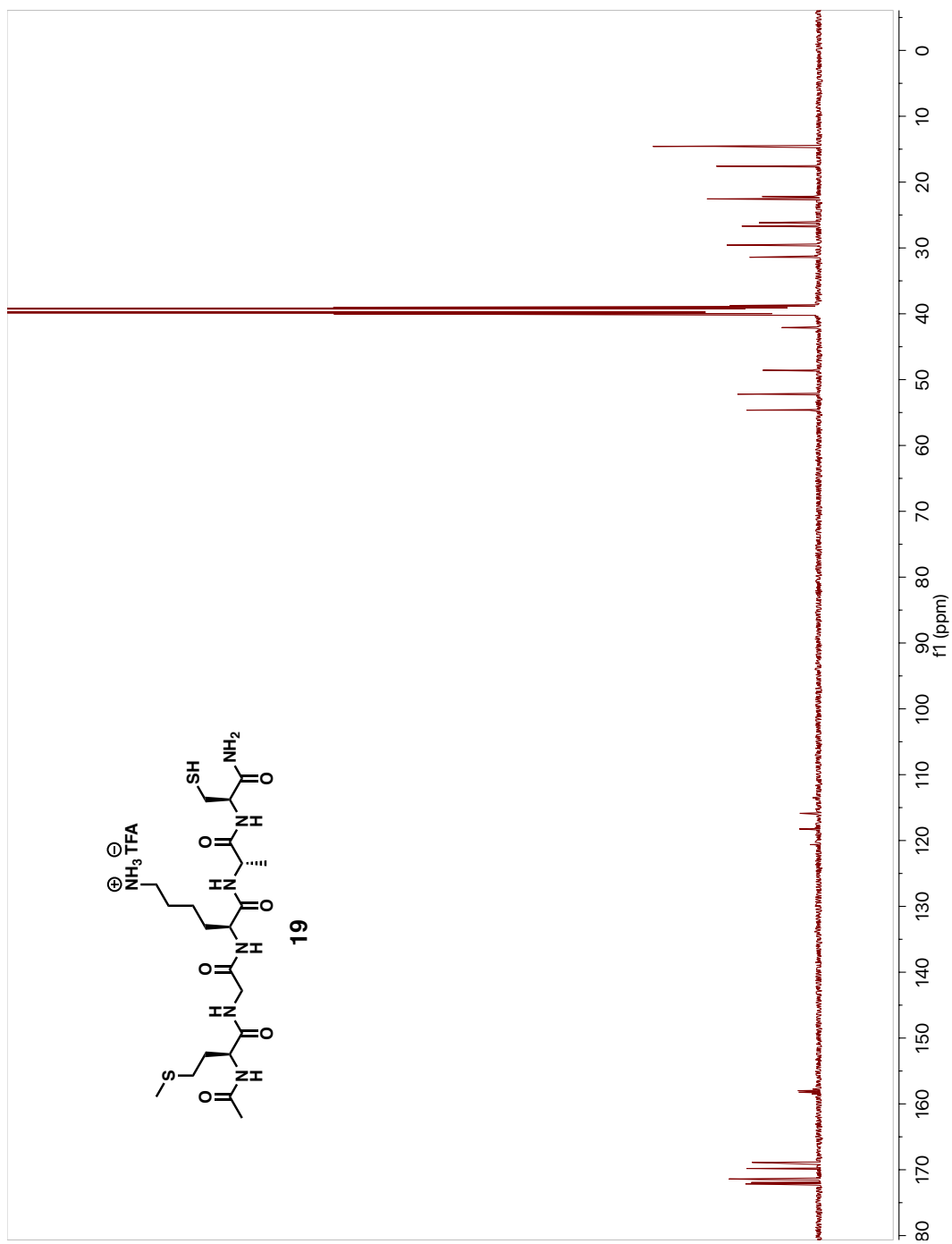


Figure A.25. LC/MS Chromatogram of Peptide 10d



**Figure A.26.** 500 MHz <sup>1</sup>H-NMR Spectrum of Peptide 19 in *d*<sub>6</sub>-DMSO



**Figure A.27.** 125 MHz  $^{13}\text{C}$ -NMR Spectrum of Peptide 19 in  $d_6$ -DMSO



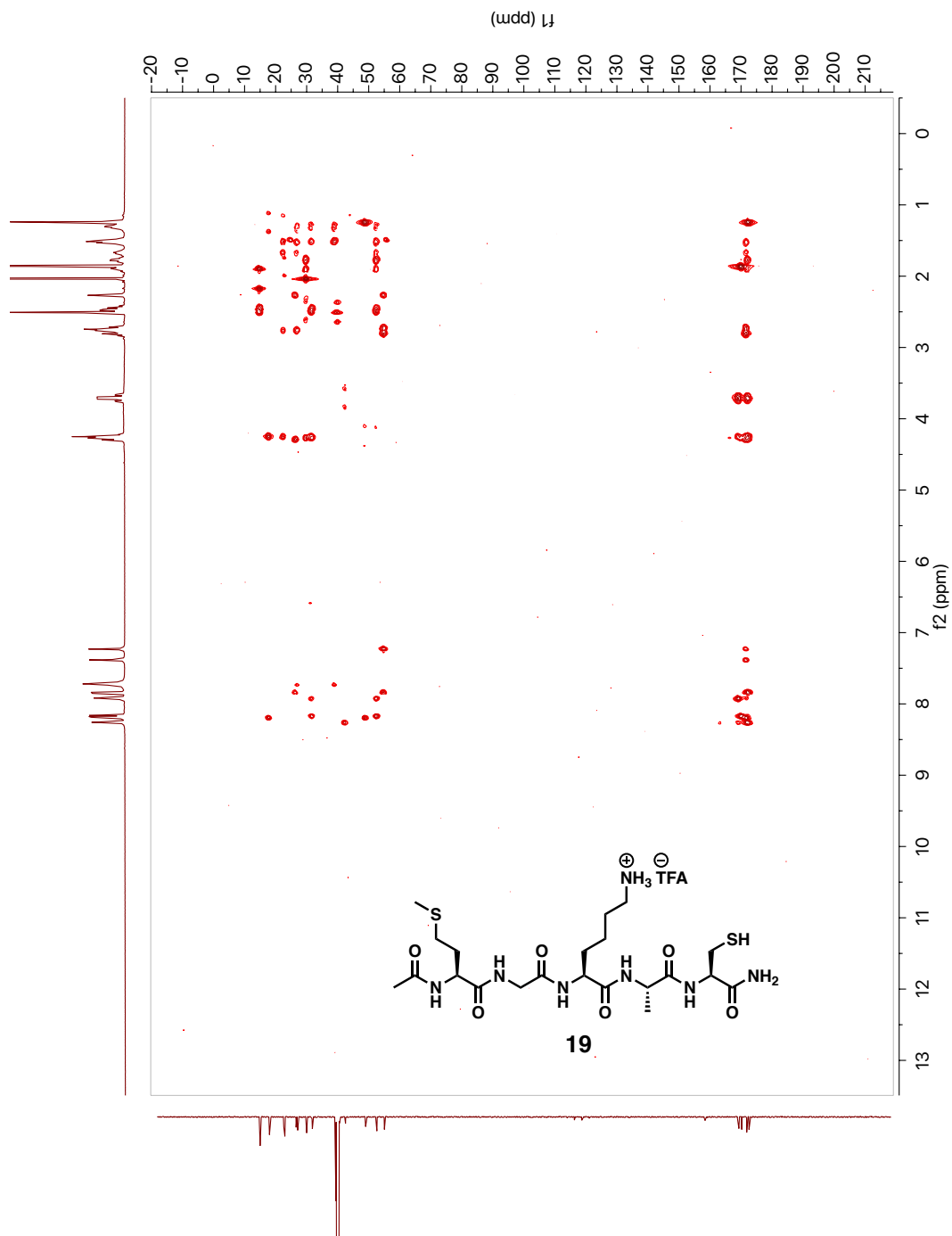


Figure A.29. HMBC Spectrum of Peptide 19 in  $d_6$ -DMSO



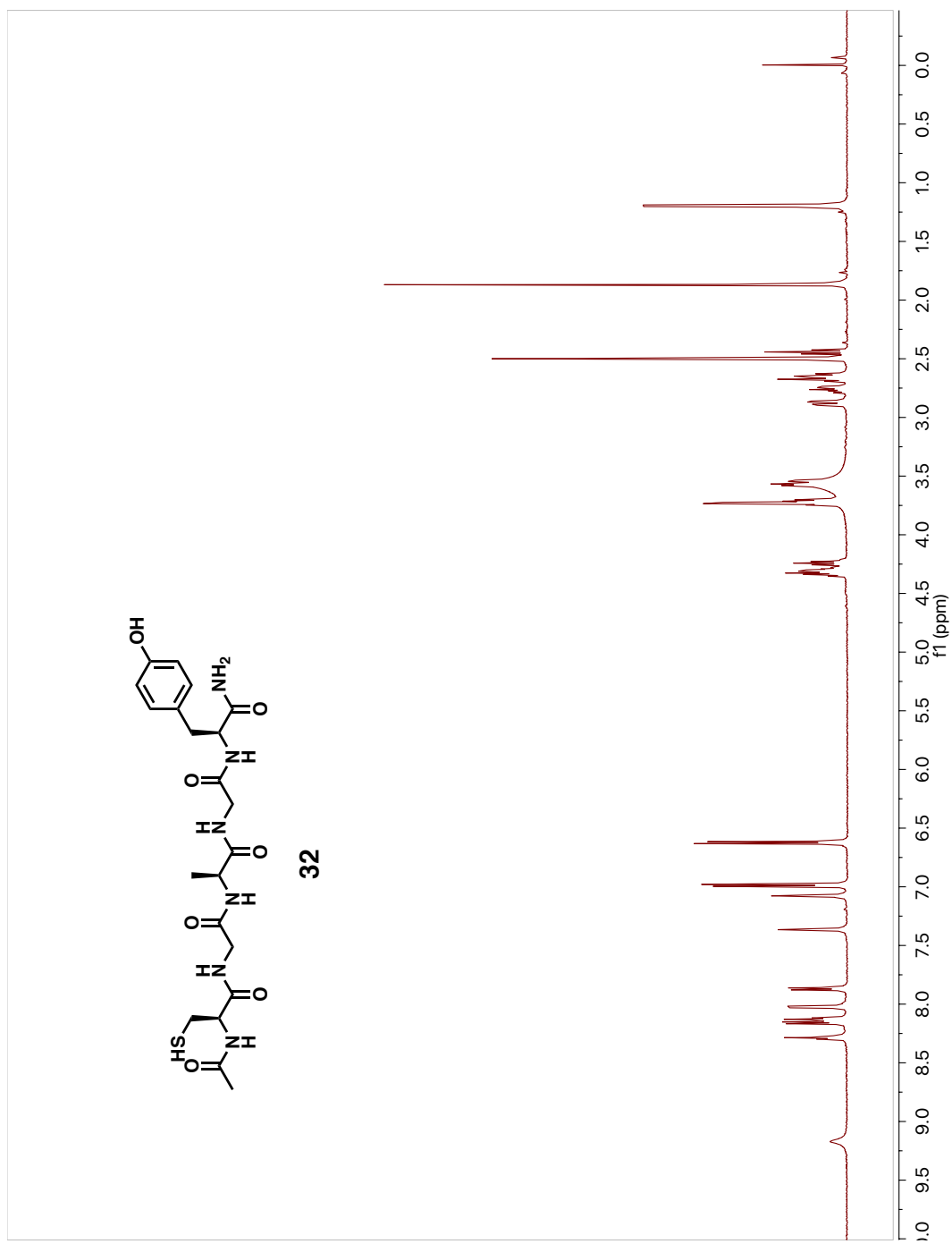
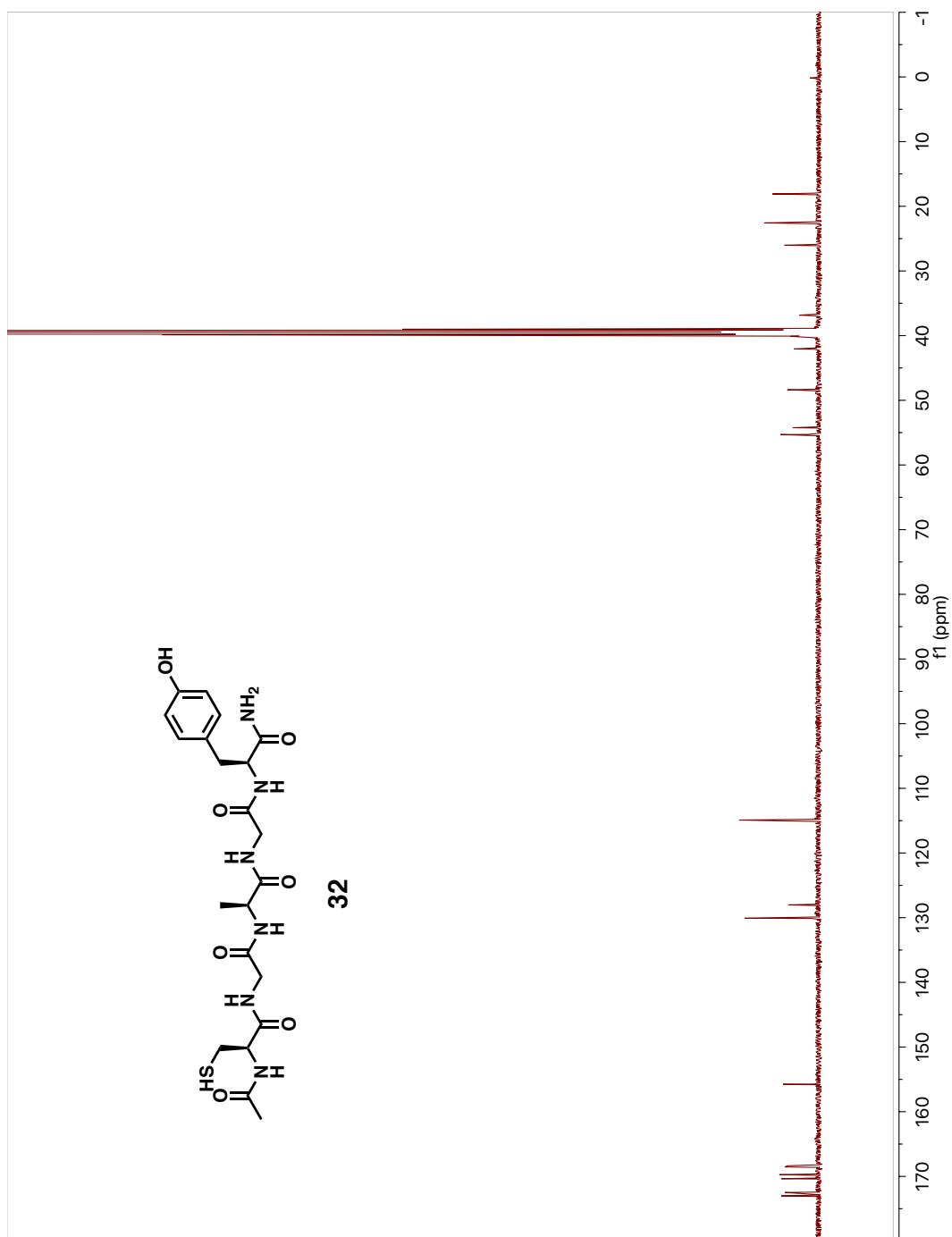
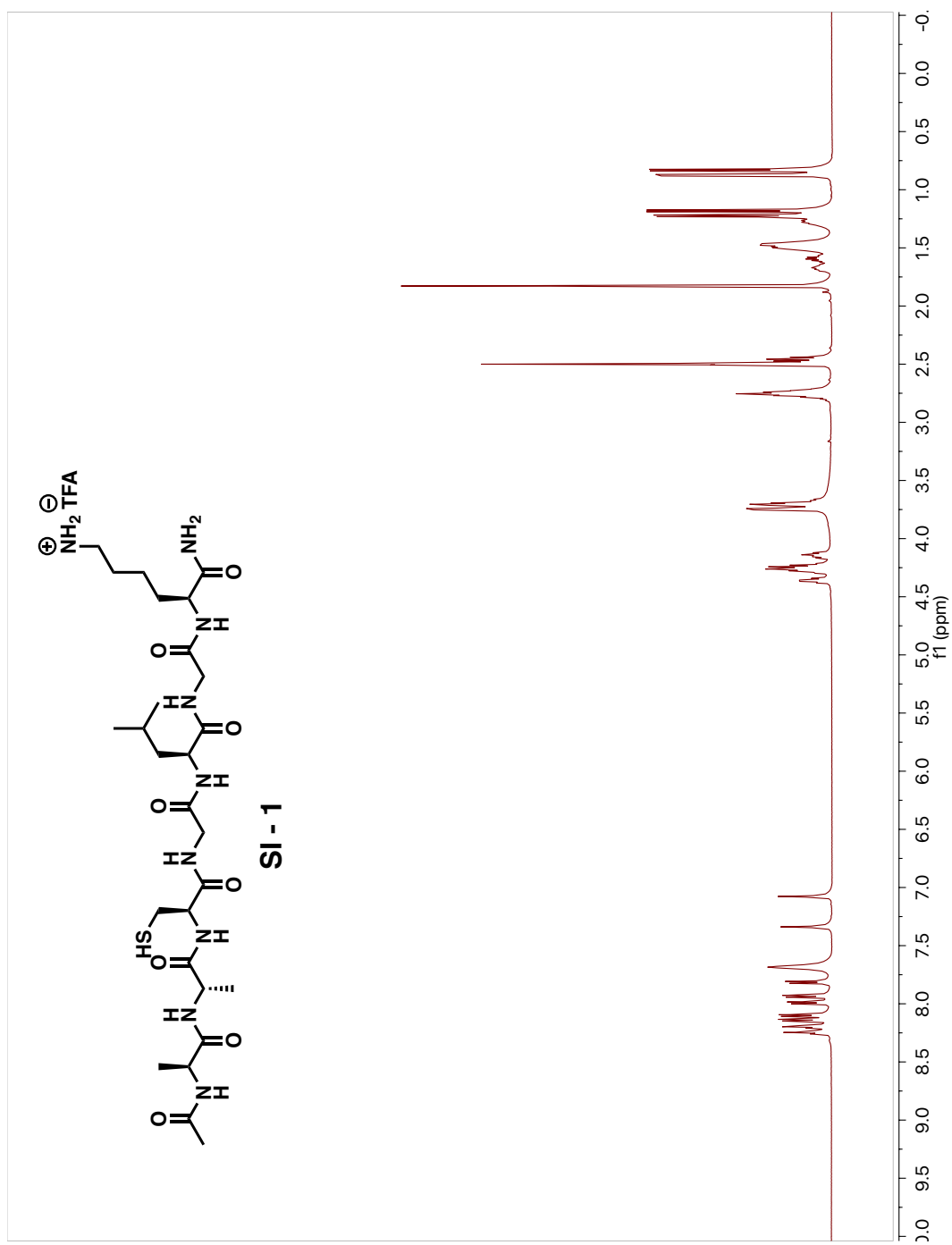
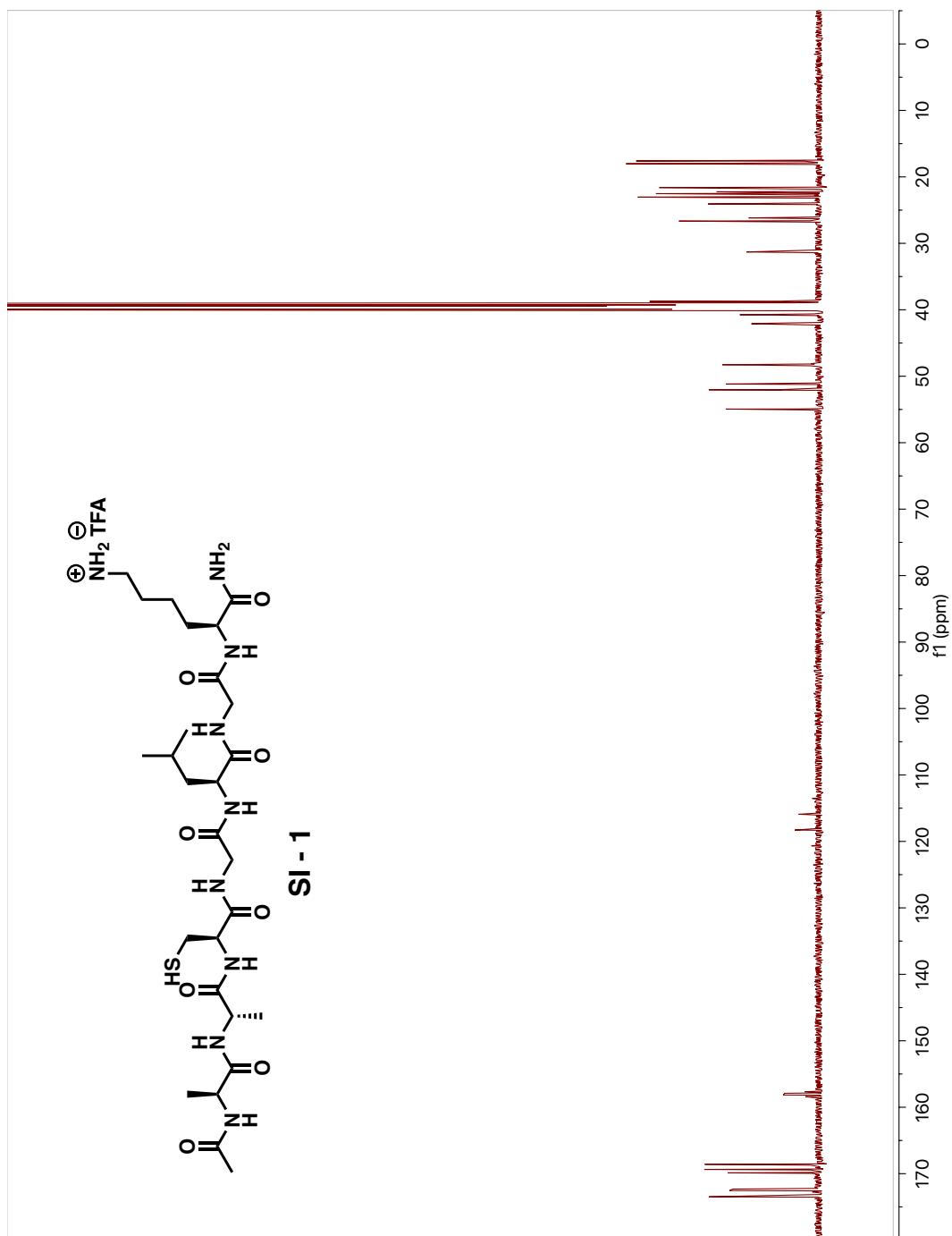


Figure A.30. 500 MHz <sup>1</sup>H-NMR Spectrum of Peptide 32 in *d*<sub>6</sub>-DMSO

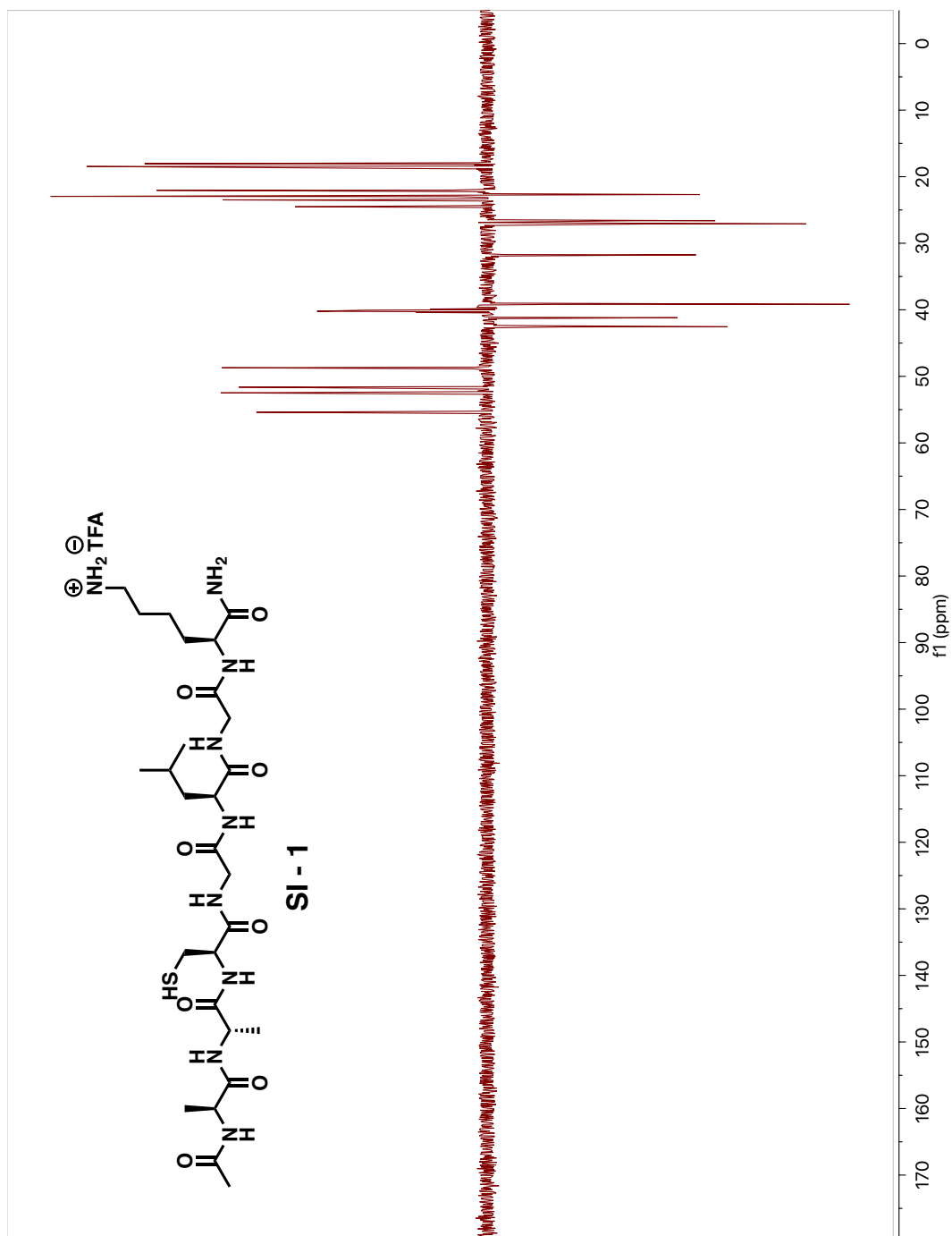


**Figure A.31.** 126 MHz  $^{13}\text{C}$ -NMR Spectrum of Peptide 32 in  $d_6$ -DMSO



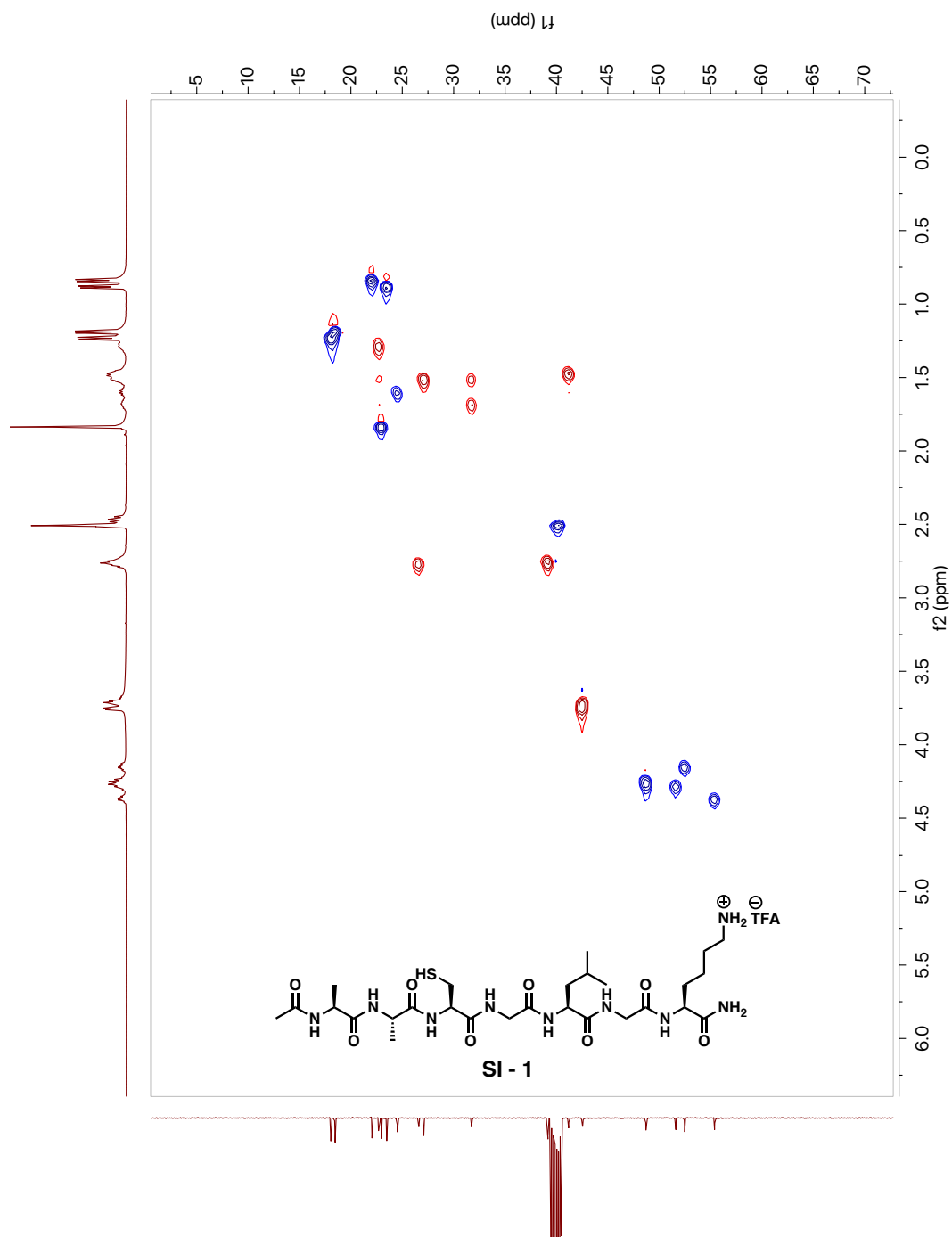


**Figure A.33.** 126 MHz  $^{13}\text{C}$ -NMR Spectrum of Peptide SI-1 in  $d_6$ -DMSO

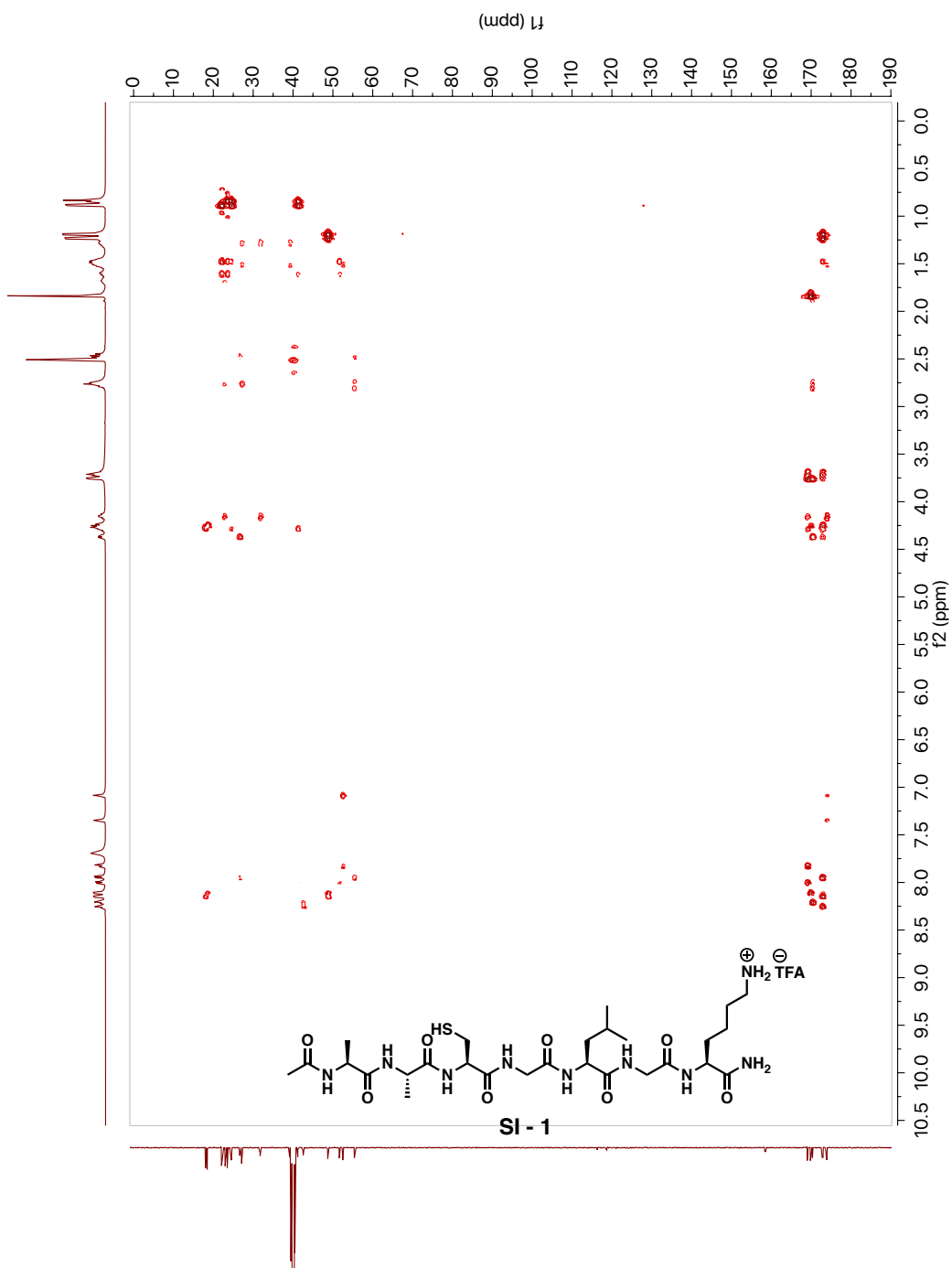


**Figure A.34.** 126 MHz DEPT-135 Spectrum of Peptide SI-1 in *d*<sub>6</sub>-DMSO





**Figure A.36.** HSQC Spectrum of Peptide SI-1 in  $d_6$ -DMSO





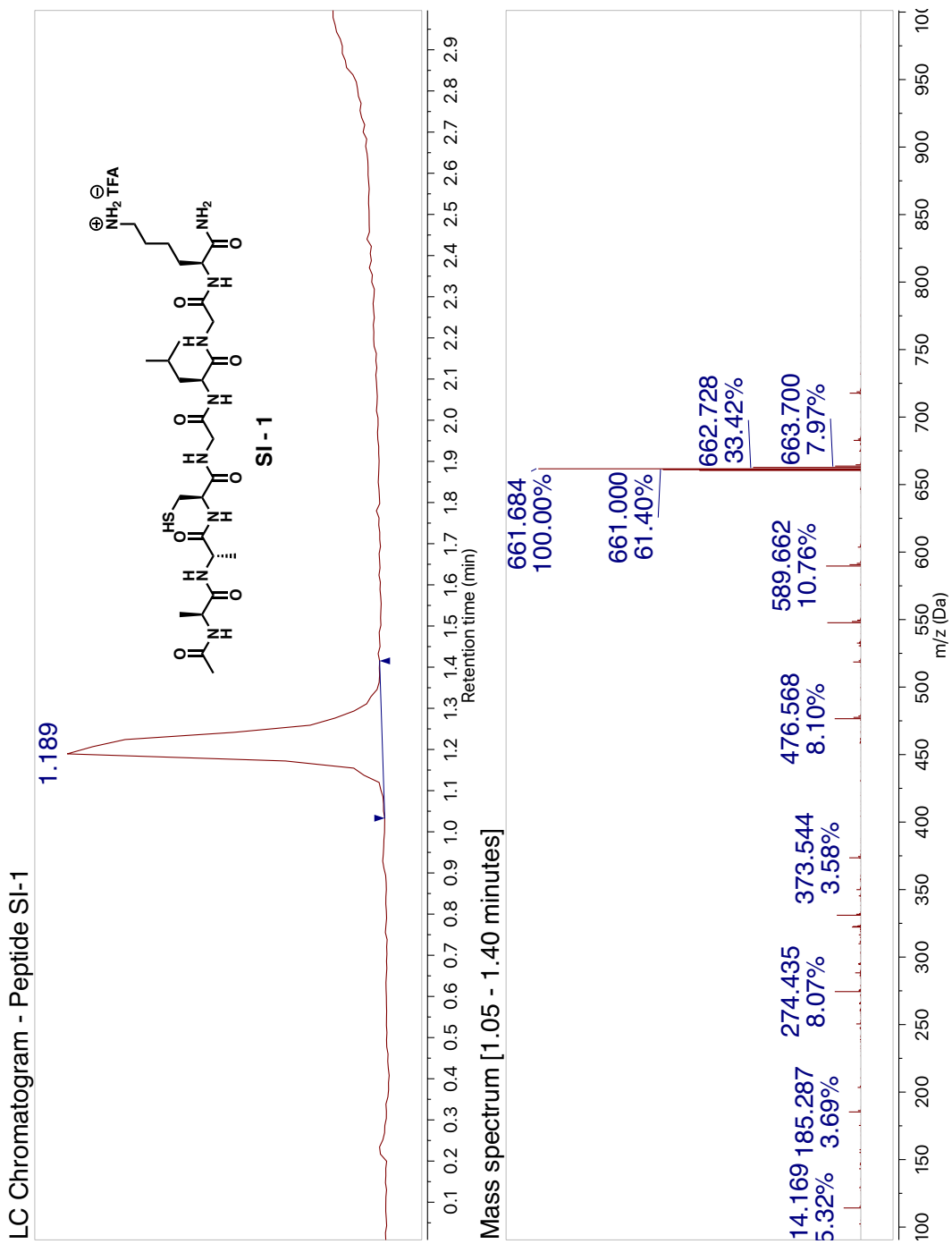
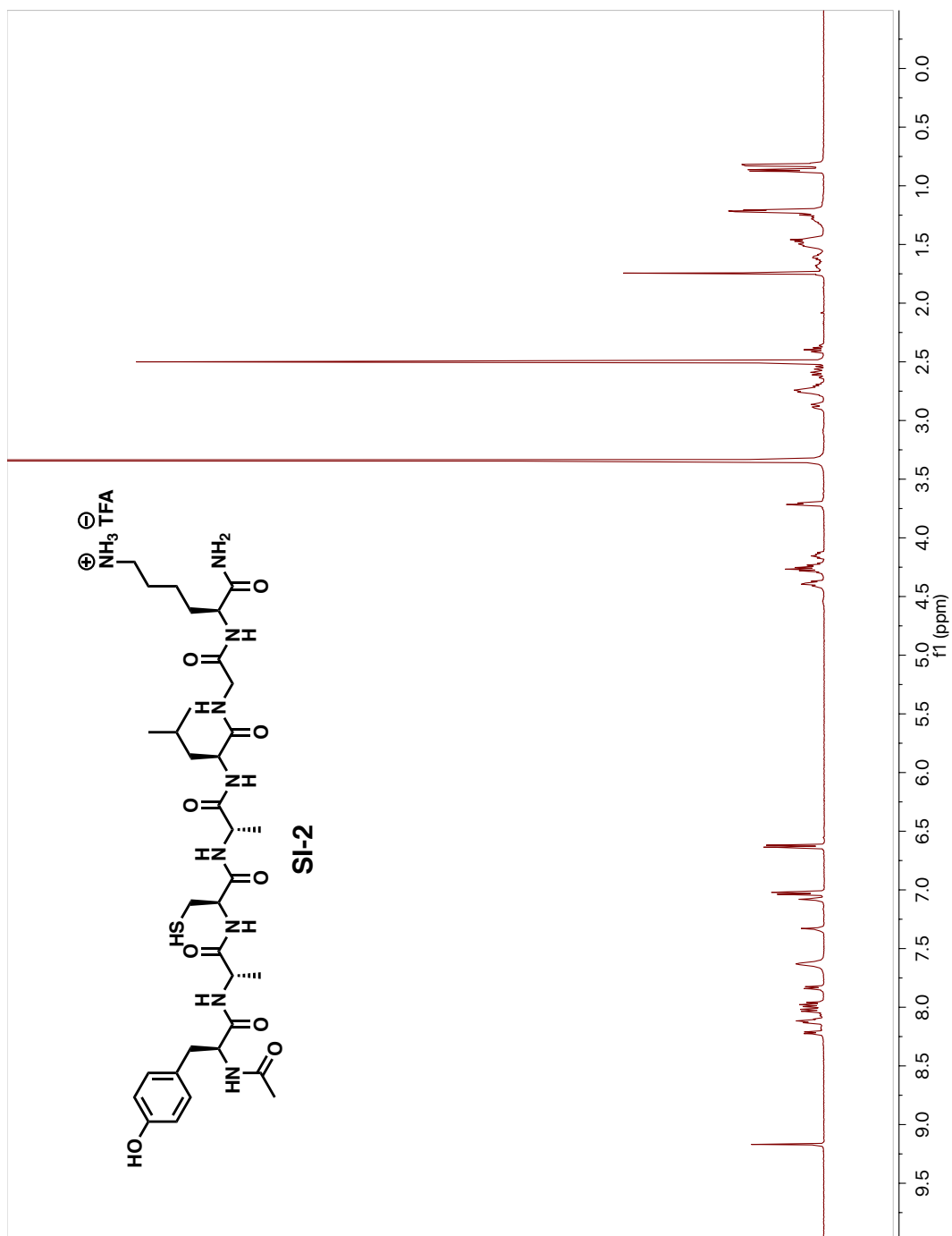
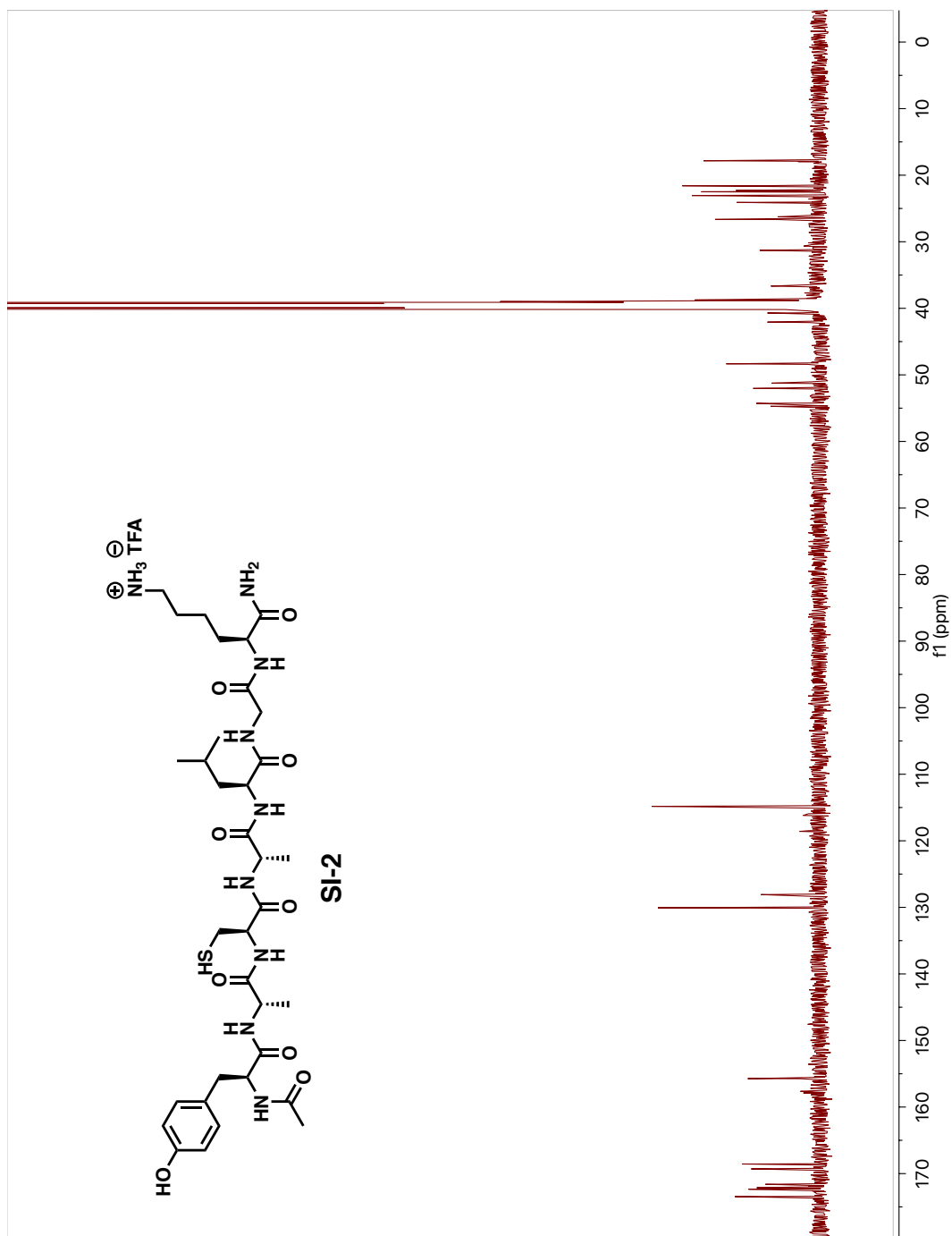


Figure A.38. LC/MS Chromatogram of Peptide SI-1



**Figure A.39.** 500 MHz <sup>1</sup>H-NMR Spectrum of Peptide SI-2 in *d*<sub>6</sub>-DMSO



**Figure A.40.** 126 MHz  $^{13}\text{C}$ -NMR Spectrum of Peptide SI-2 in  $d_6$ -DMSO

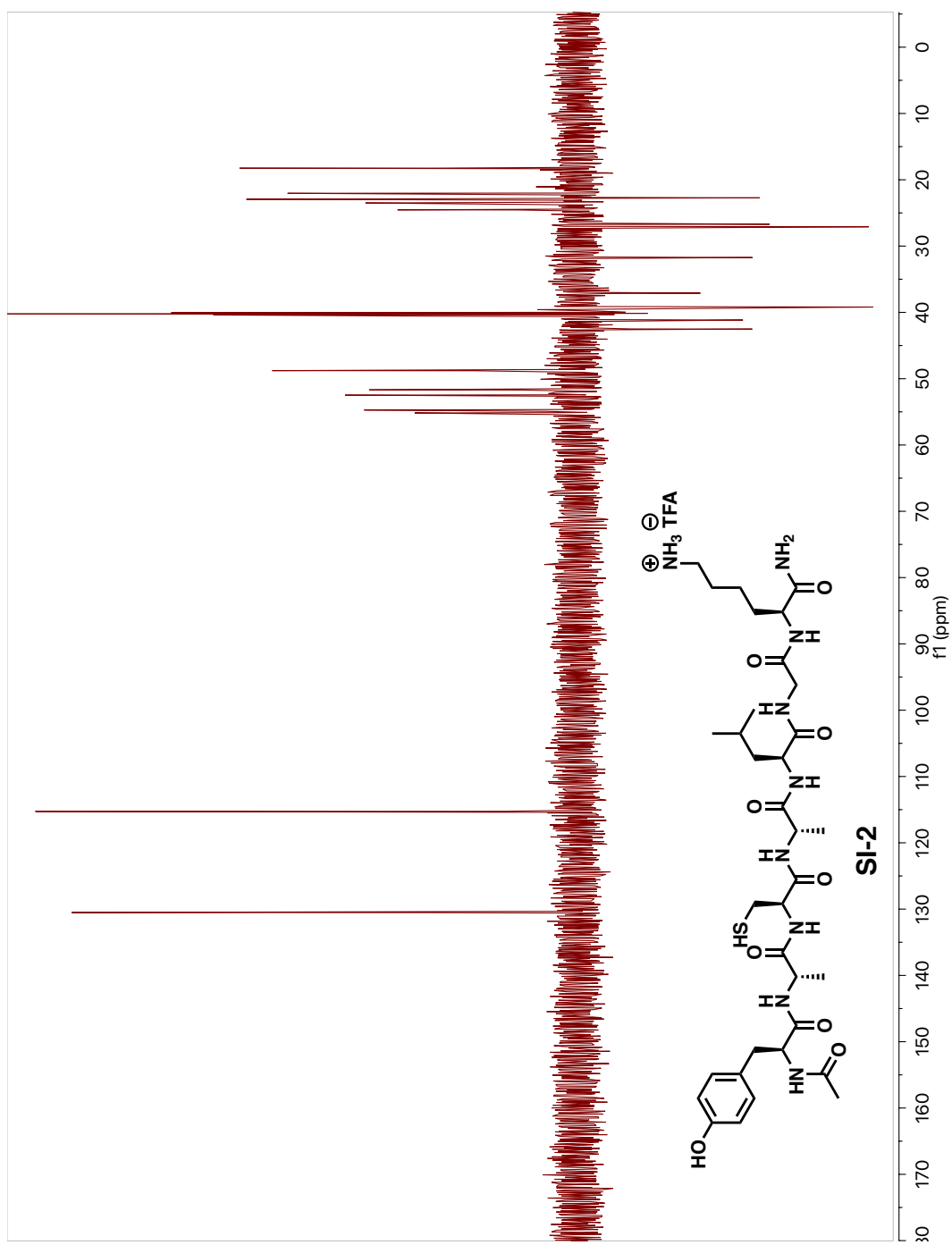
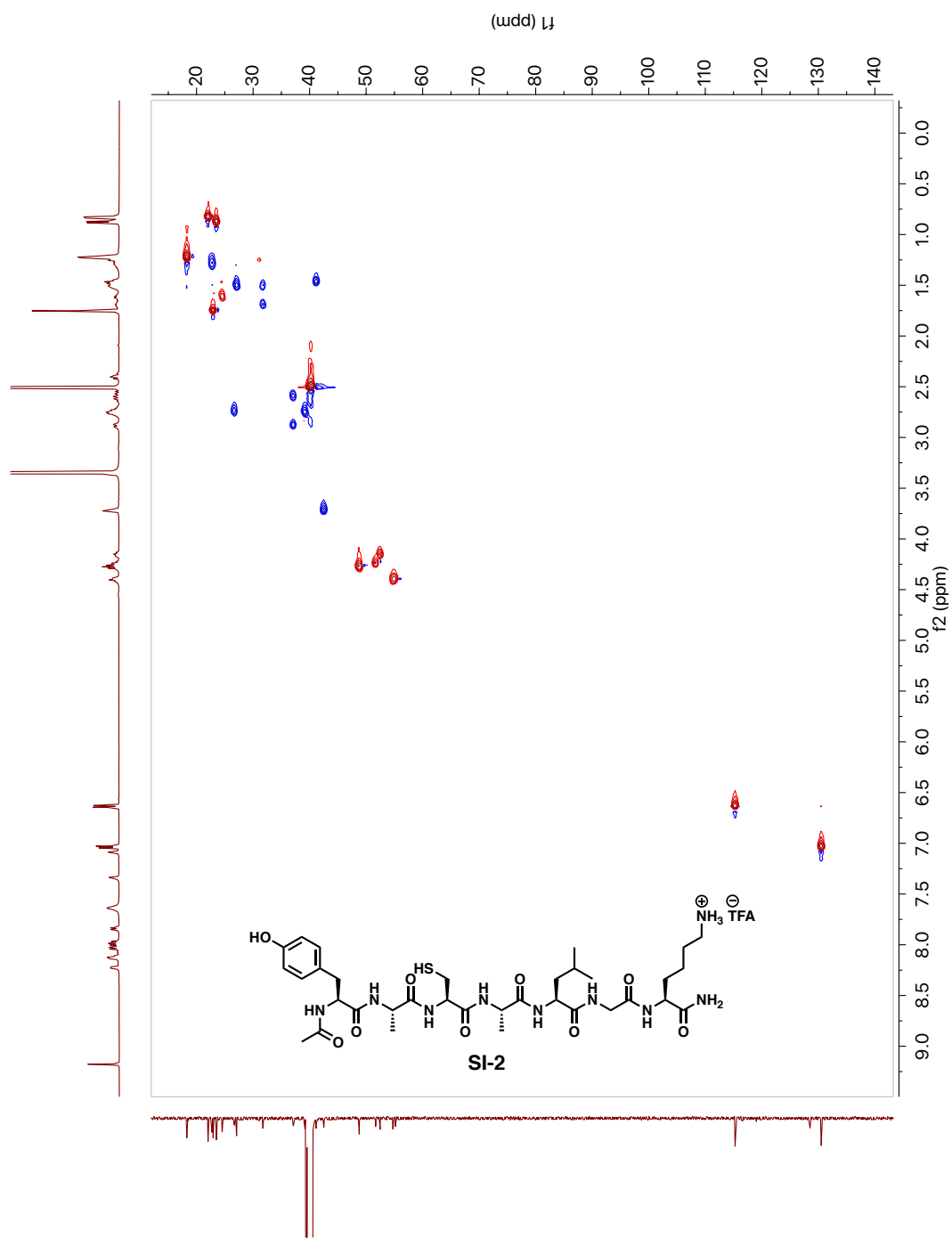
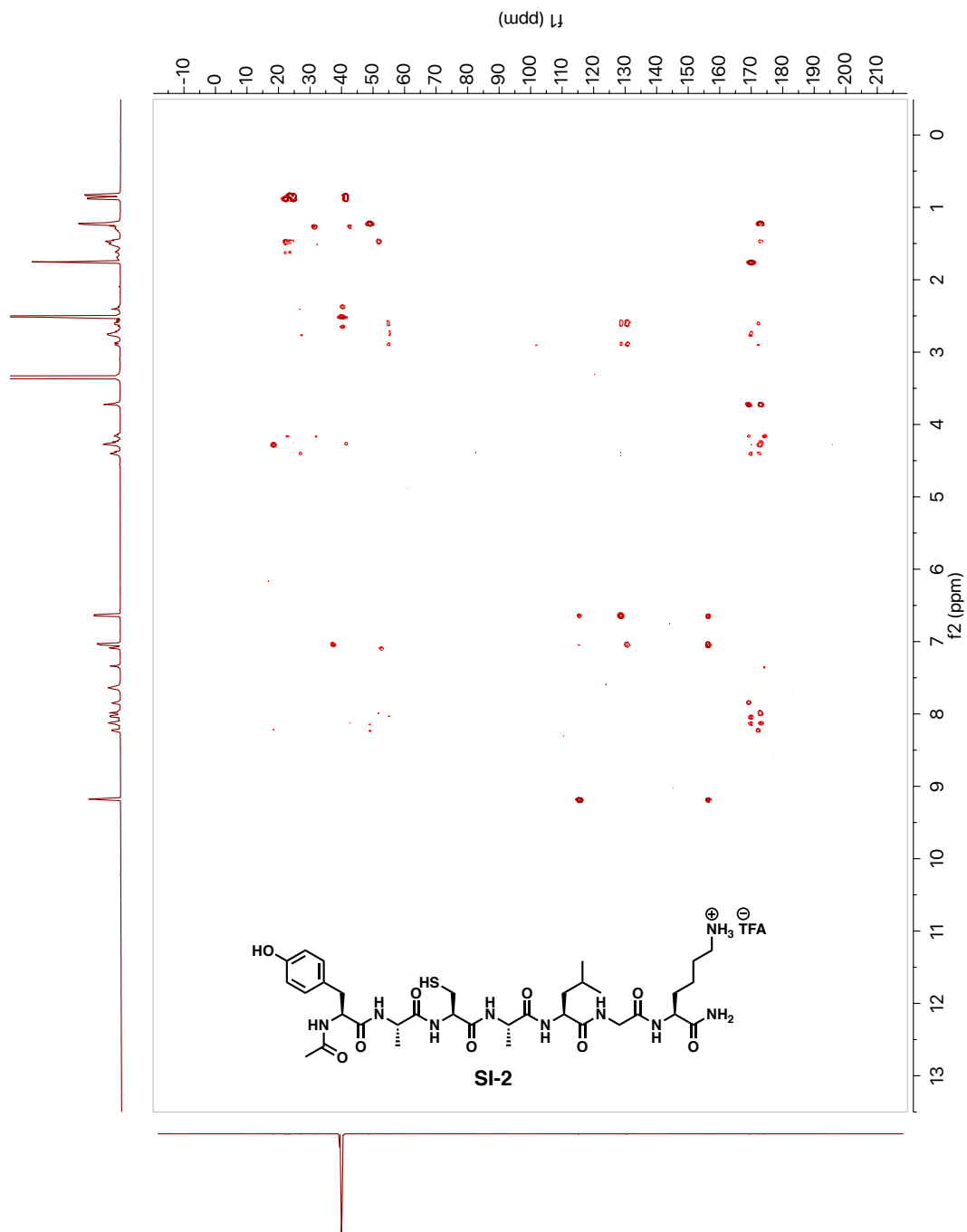


Figure A.41. 126 MHz DEPT-135 Spectrum of Peptide SI-2 in  $d_6$ -DMSO





**Figure A.43.** HSQC Spectrum of Peptide SI-2 in  $d_6$ -DMSO



**Figure A.44.** HMBC Spectrum of Peptide SI-2 in  $d_6$ -DMSO

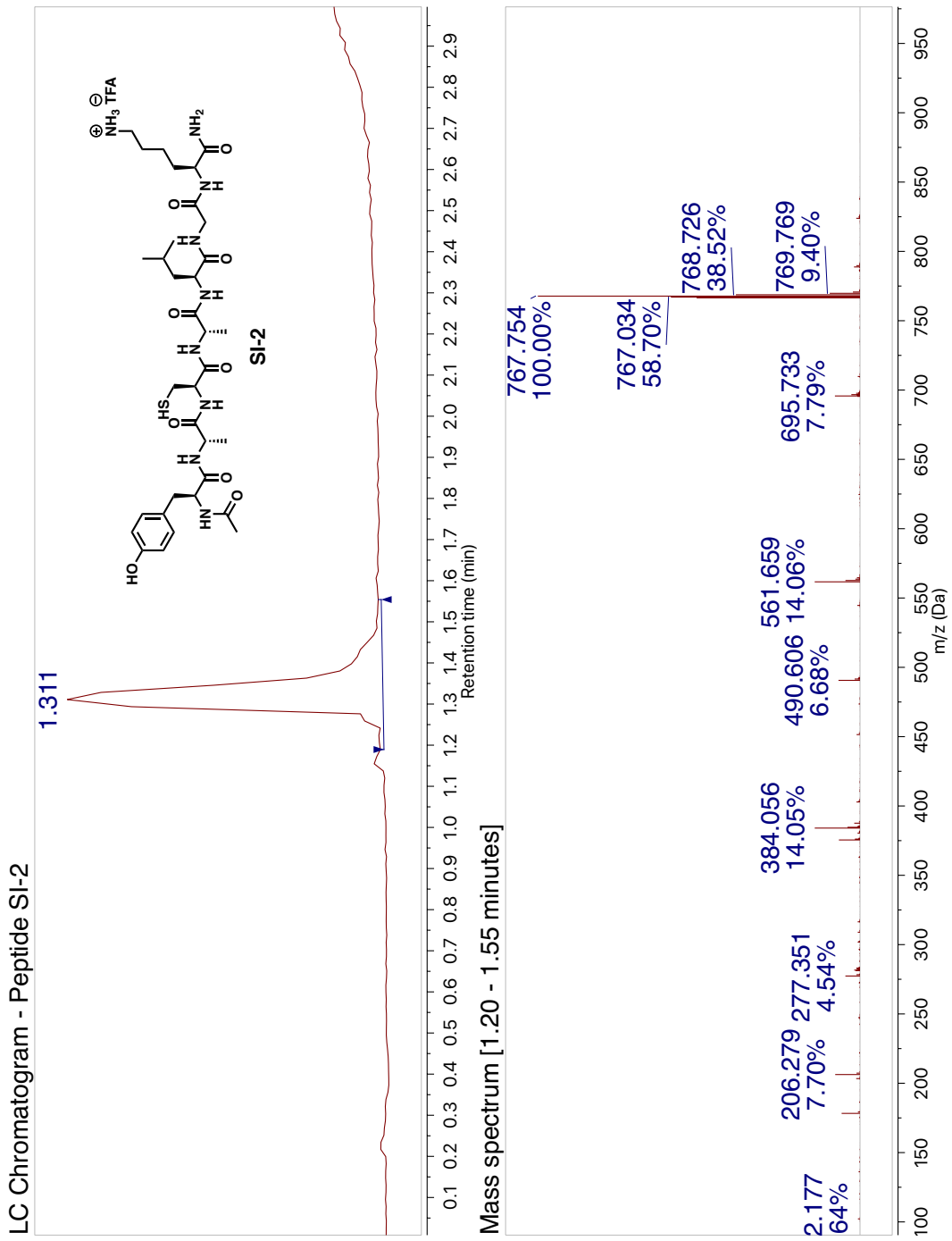
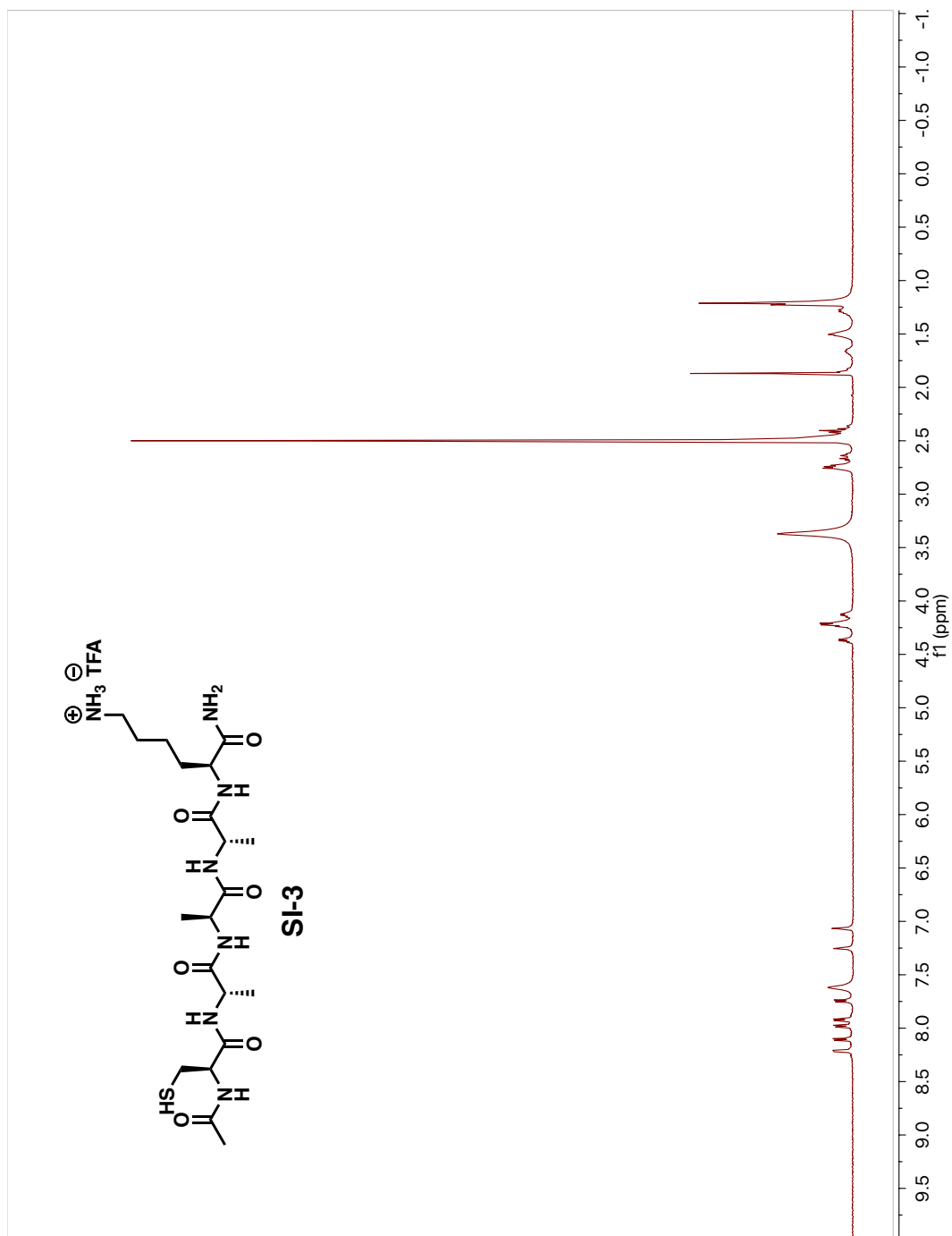
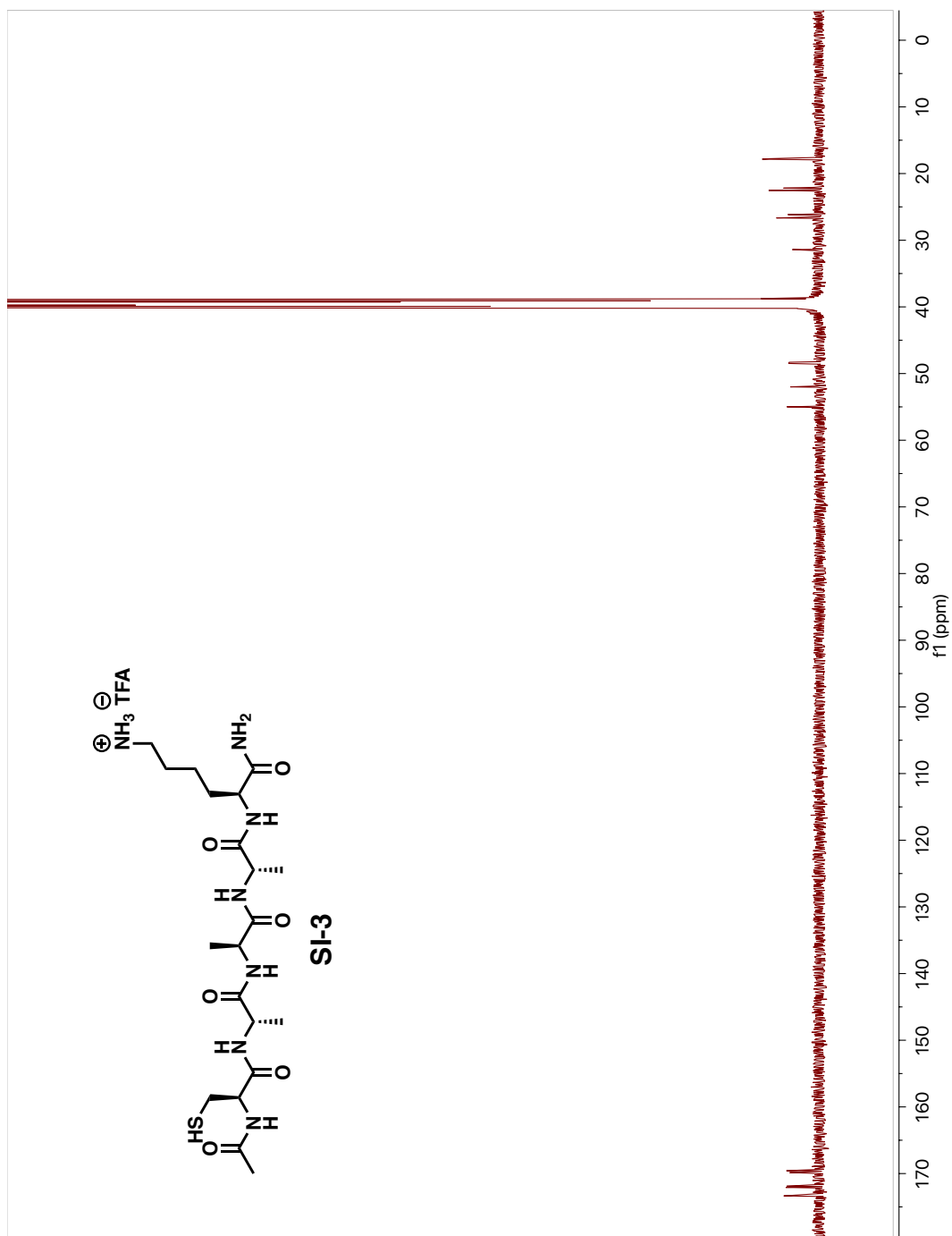


Figure A.45. LC/MS Chromatogram of Peptide SI-2





**Figure A.46.** 500 MHz <sup>1</sup>H-NMR Spectrum of Peptide SI-3 in *d*<sub>6</sub>-DMSO



**Figure A.47.** 126 MHz  $^{13}\text{C}$ -NMR Spectrum of Peptide SI-3 in  $d_6$ -DMSO

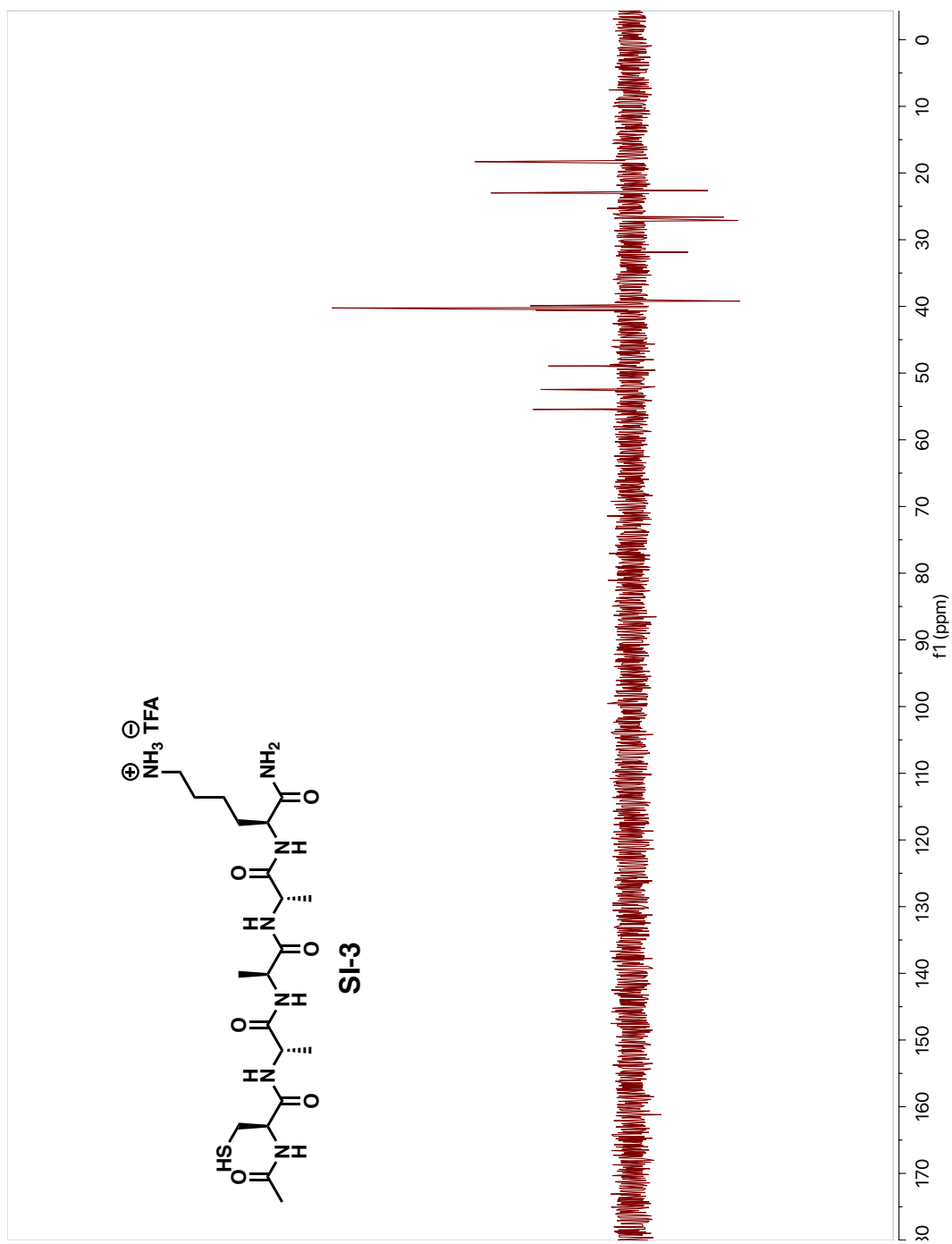


Figure A.48. 126 MHz DEPT-135 Spectrum of Peptide SI-3 in  $d_6$ -DMSO

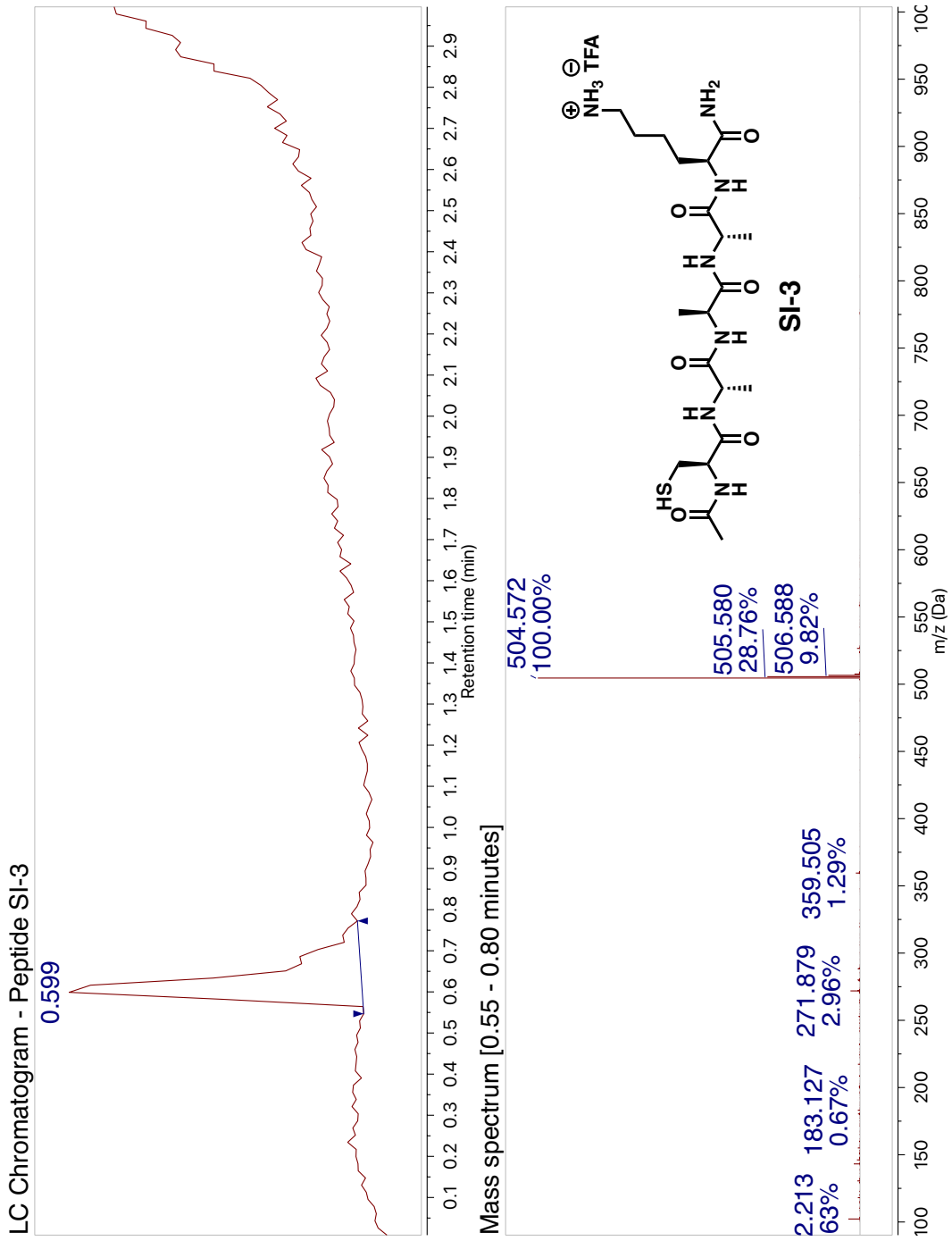
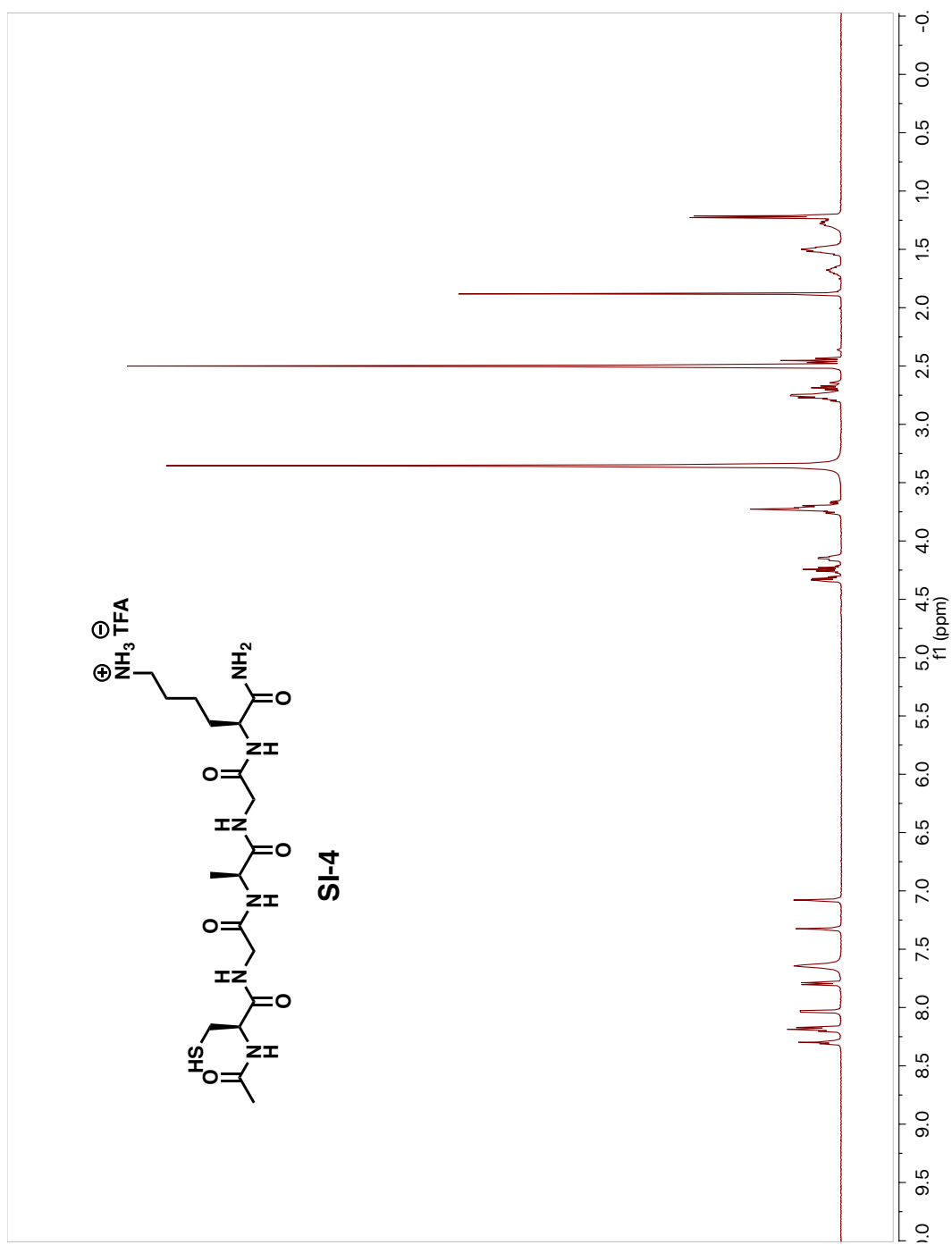
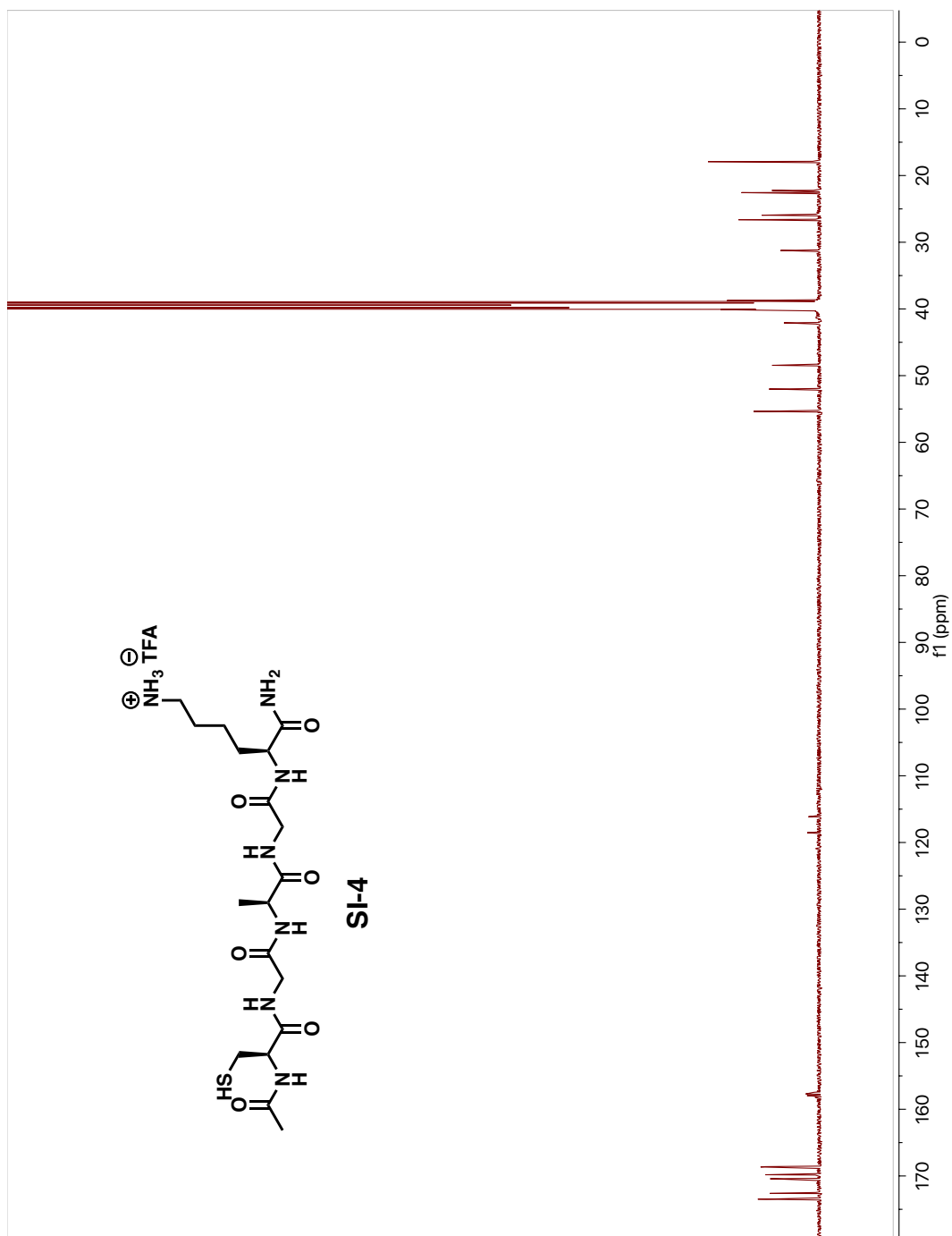


Figure A.49. LC/MS Chromatogram of Peptide SI-3



**Figure A.50.** 500 MHz <sup>1</sup>H-NMR Spectrum of Peptide SI-4 in *d*<sub>6</sub>-DMSO



**Figure A.51.** 126 MHz <sup>13</sup>C-NMR Spectrum of Peptide SI-4 in *d*<sub>6</sub>-DMSO

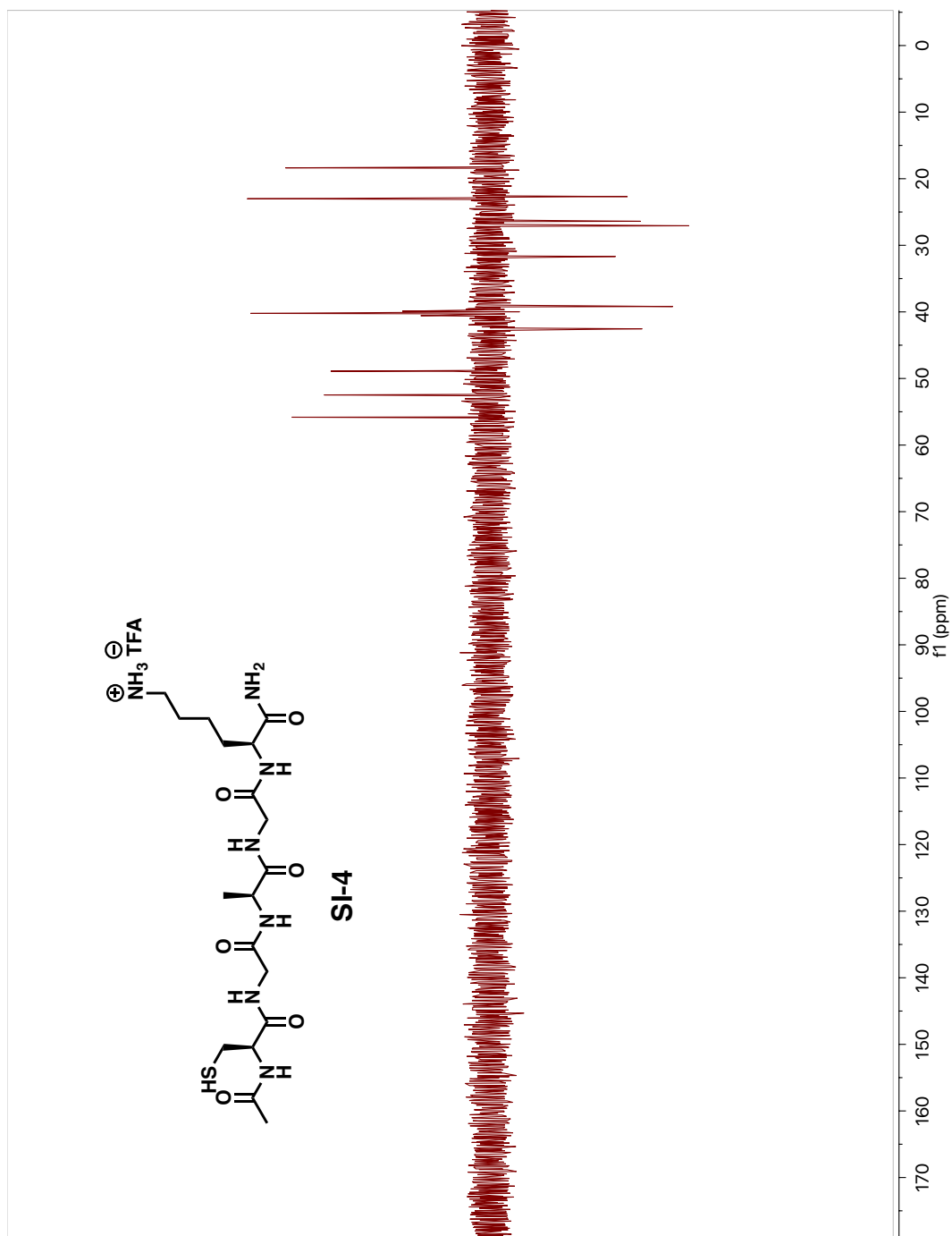


**Figure A.52.** 126 MHz DEPT-135 Spectrum of Peptide SI-4 in  $d_6$ -DMSO

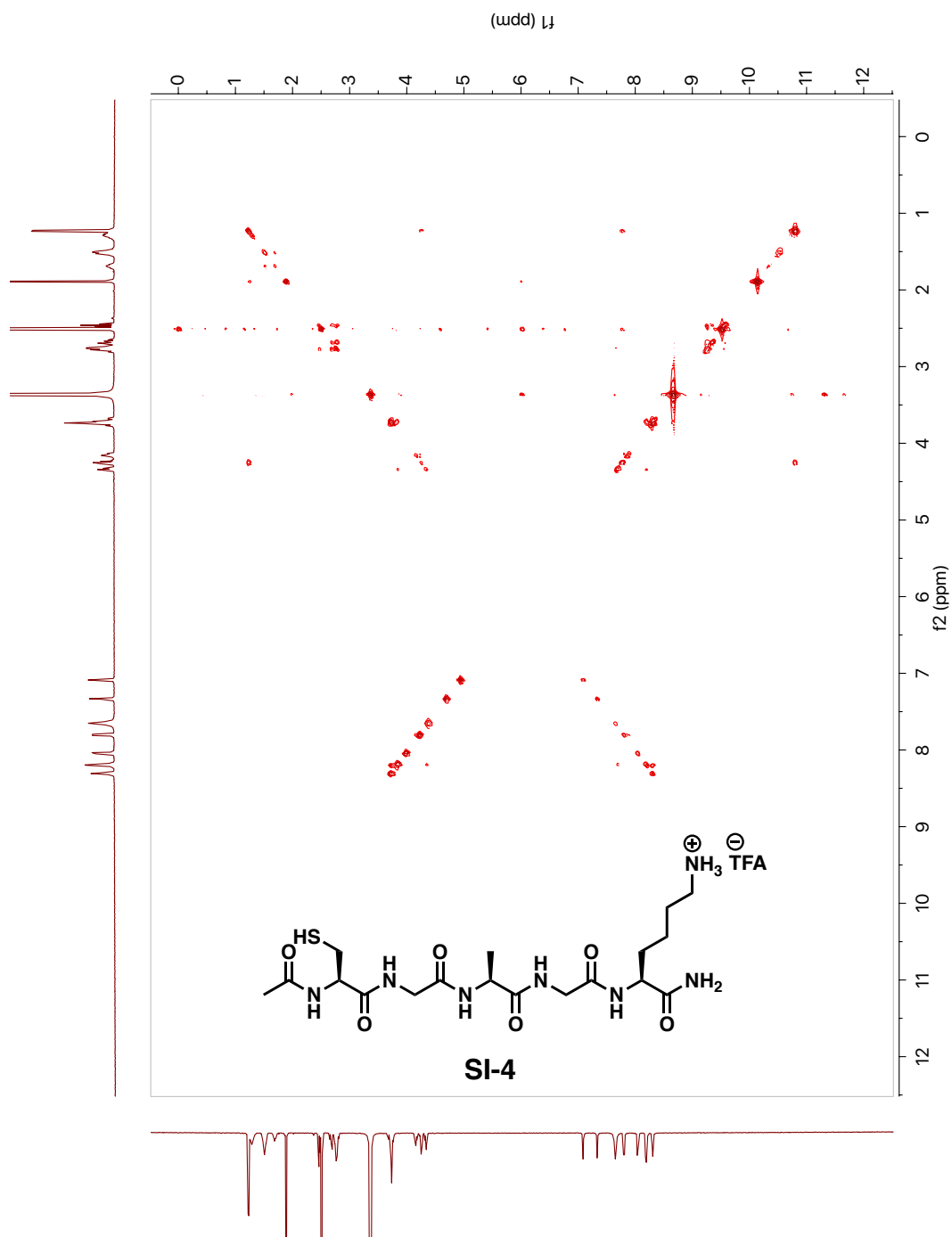
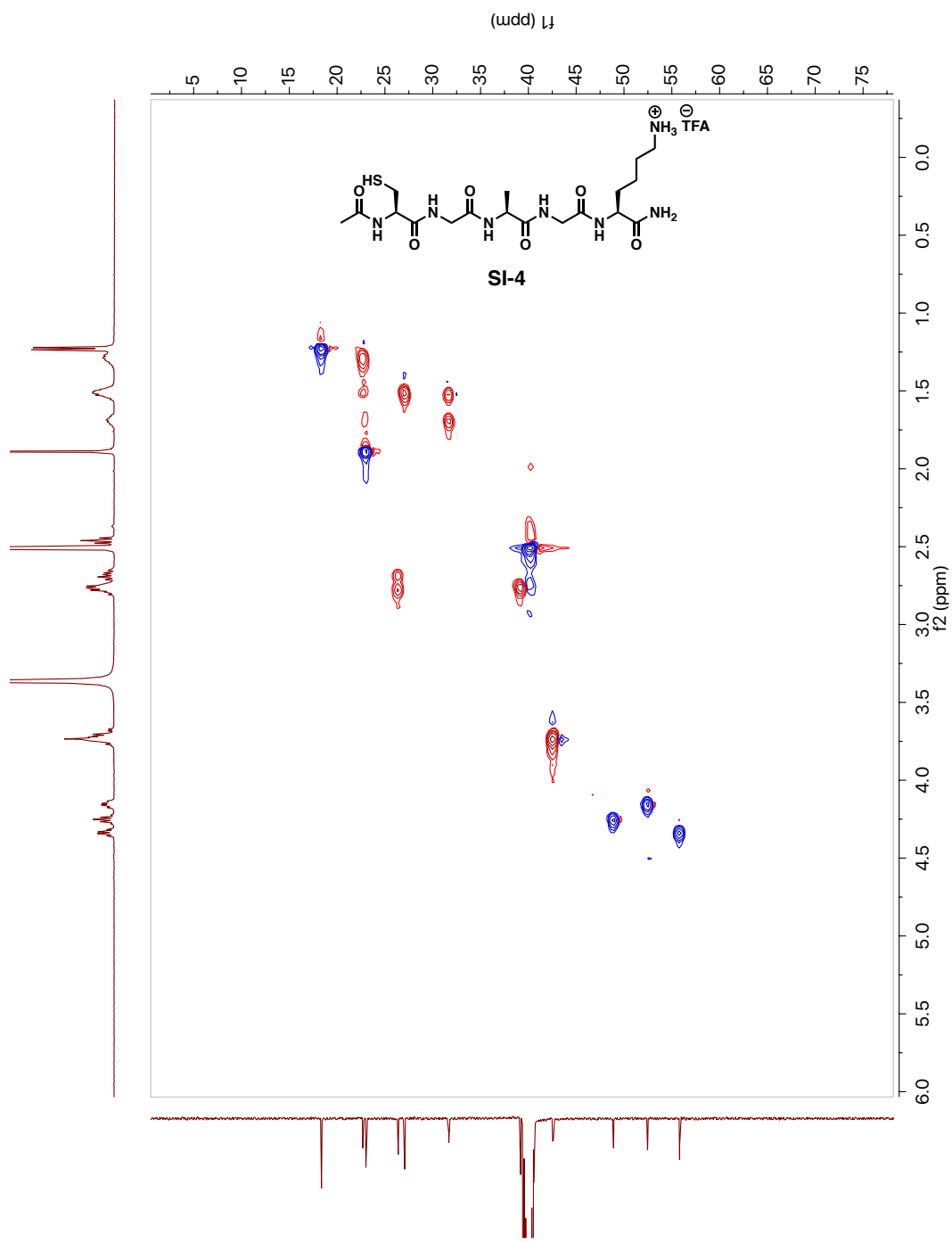


Figure A.53. COSY Spectrum of Peptide SI-4 in  $d_6$ -DMSO





**Figure A.54.** HSQC Spectrum of Peptide SI-4 in  $d_6$ -DMSO

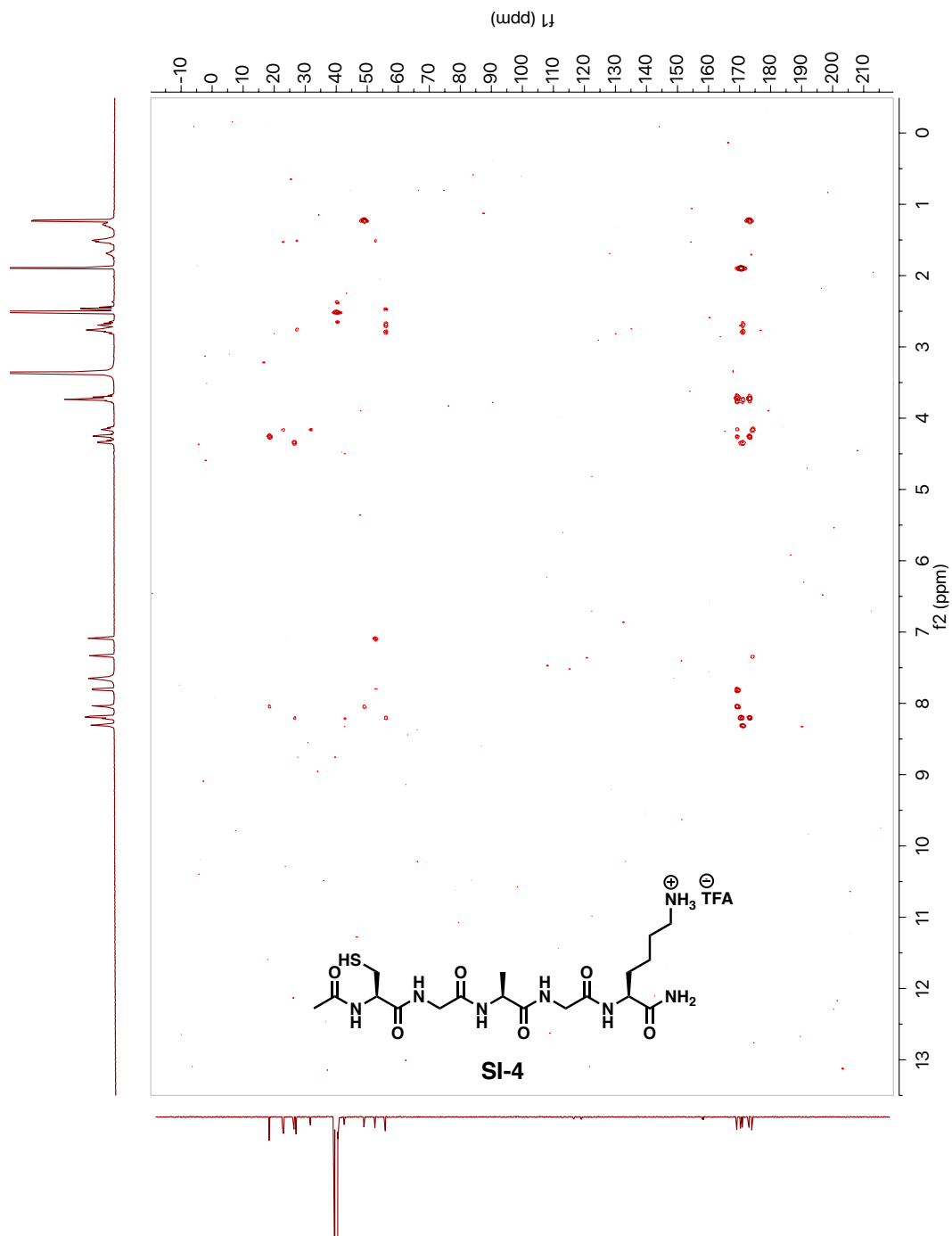


Figure A.55. HMBC Spectrum of Peptide SI-4 in  $d_6$ -DMSO



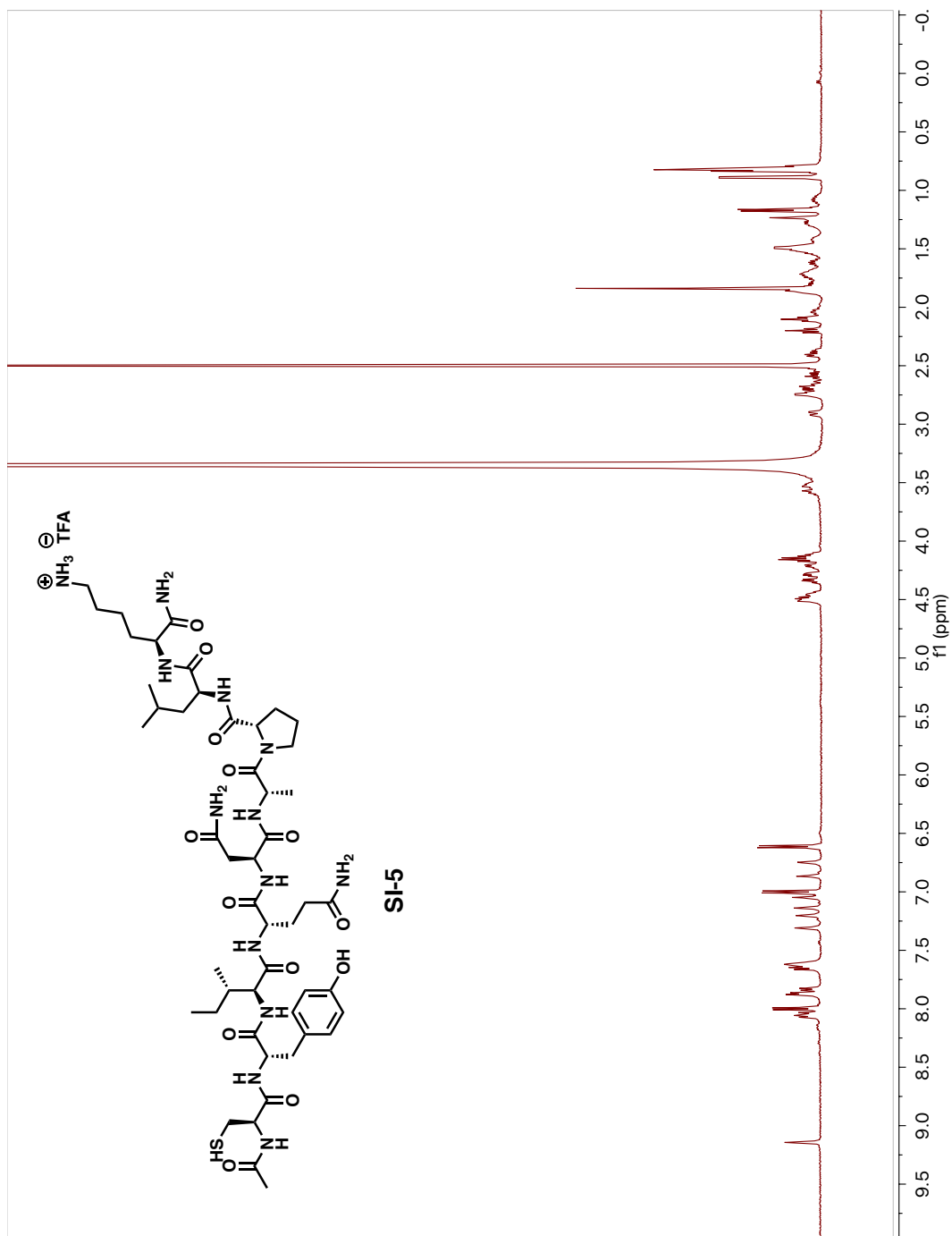
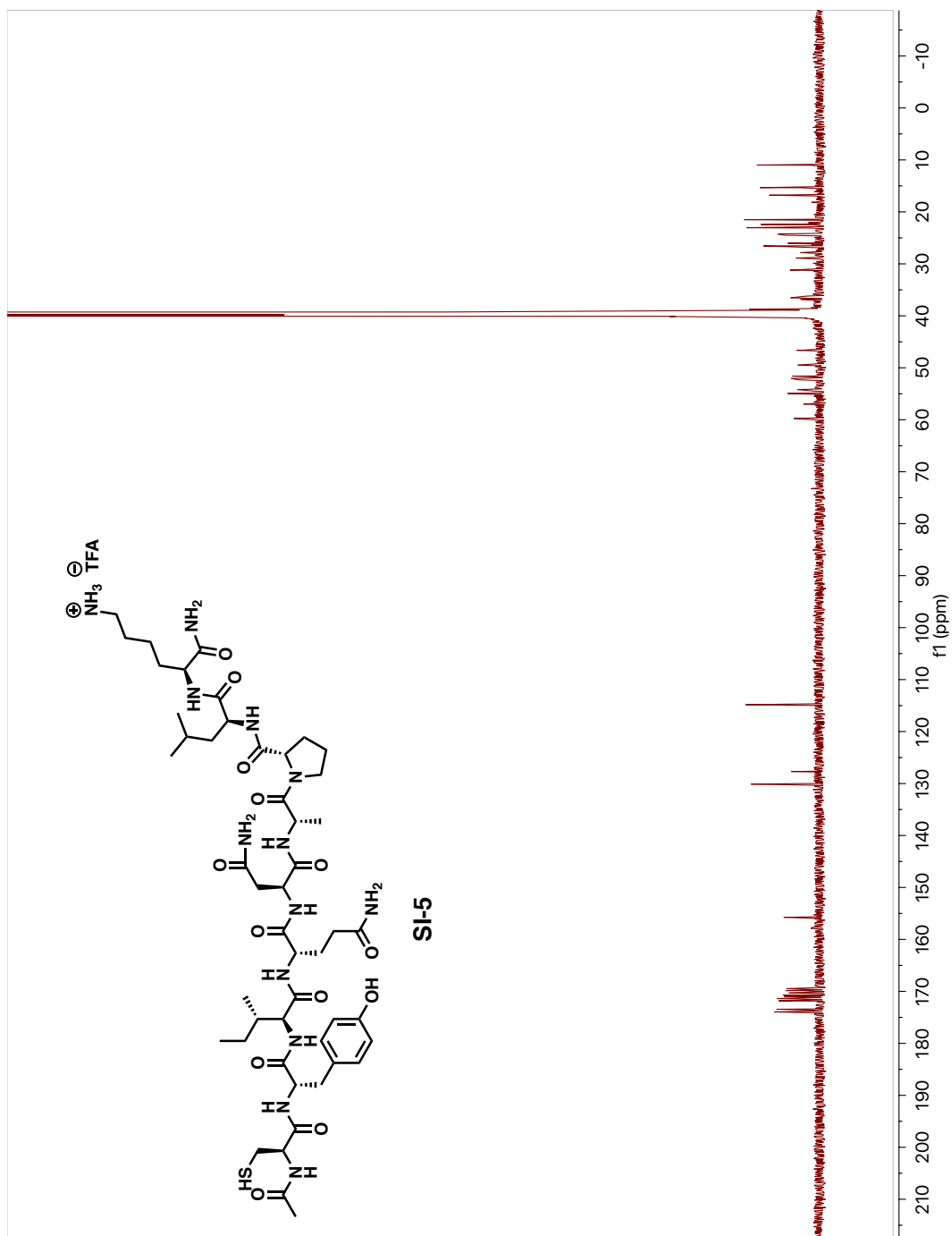
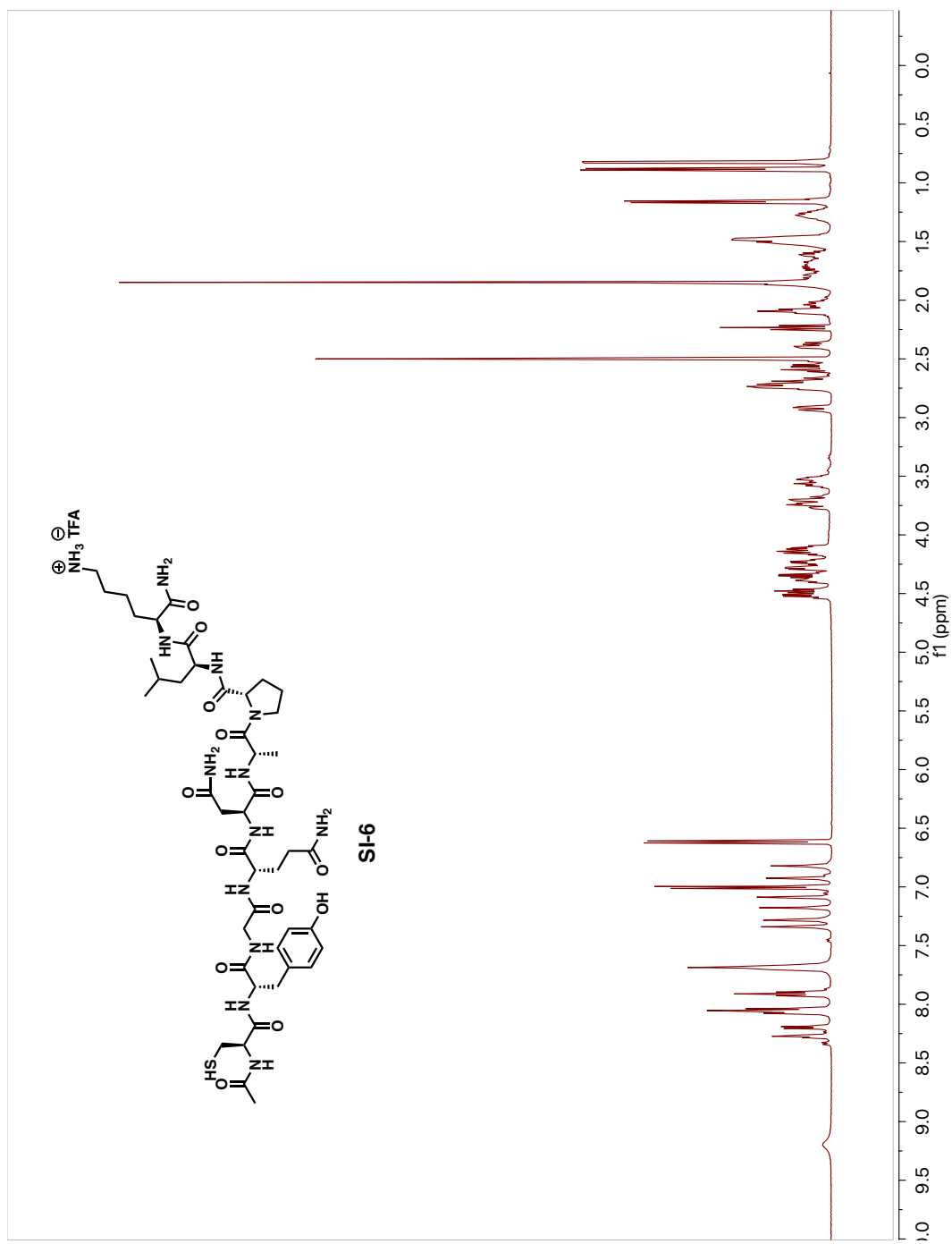


Figure A.57. 500 MHz <sup>1</sup>H-NMR Spectrum of Peptide SI-5 in *d*<sub>6</sub>-DMSO

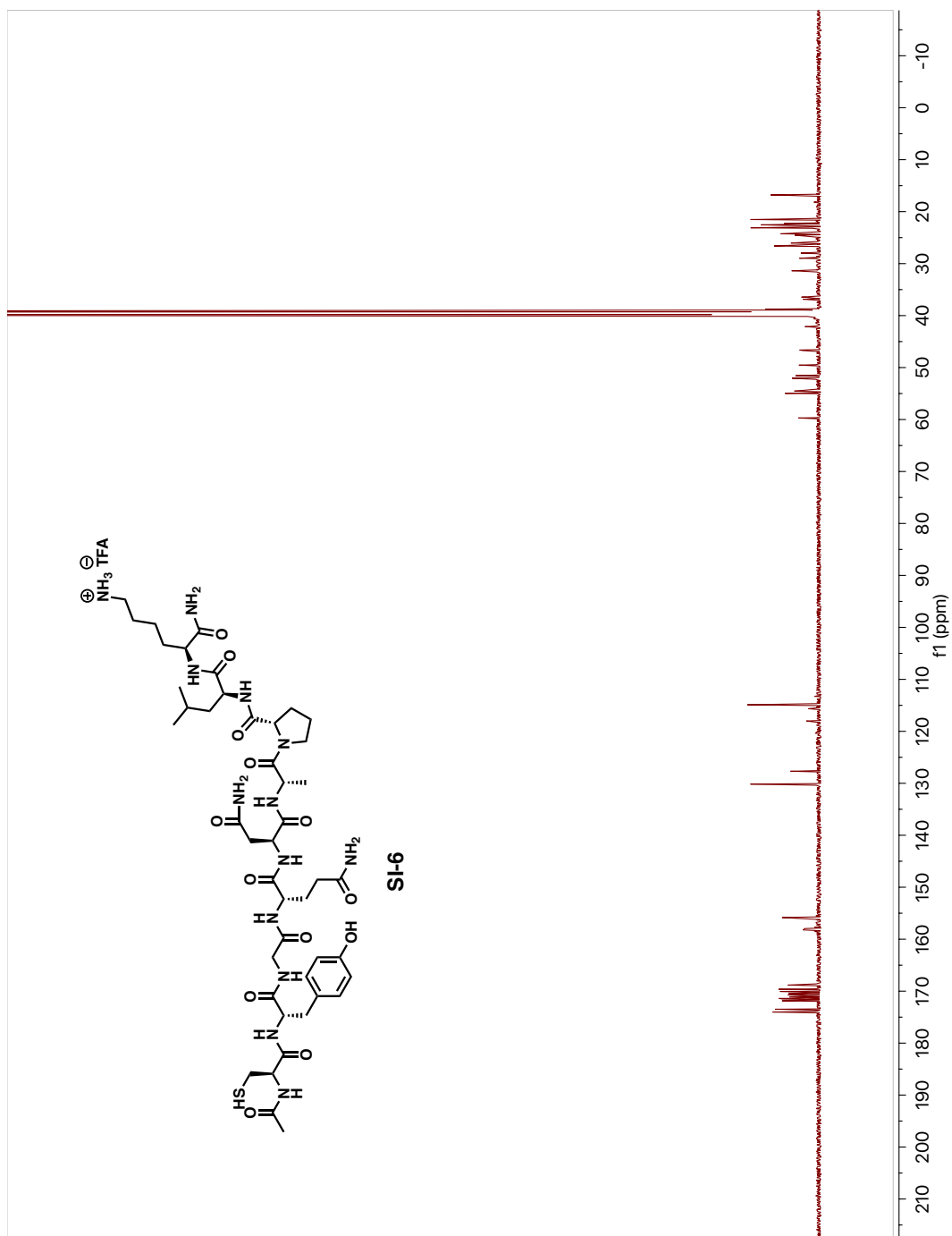


**Figure A.58.** 126 MHz  $^{13}\text{C}$ -NMR Spectrum of Peptide SI-5 in  $d_6$ -DMSO





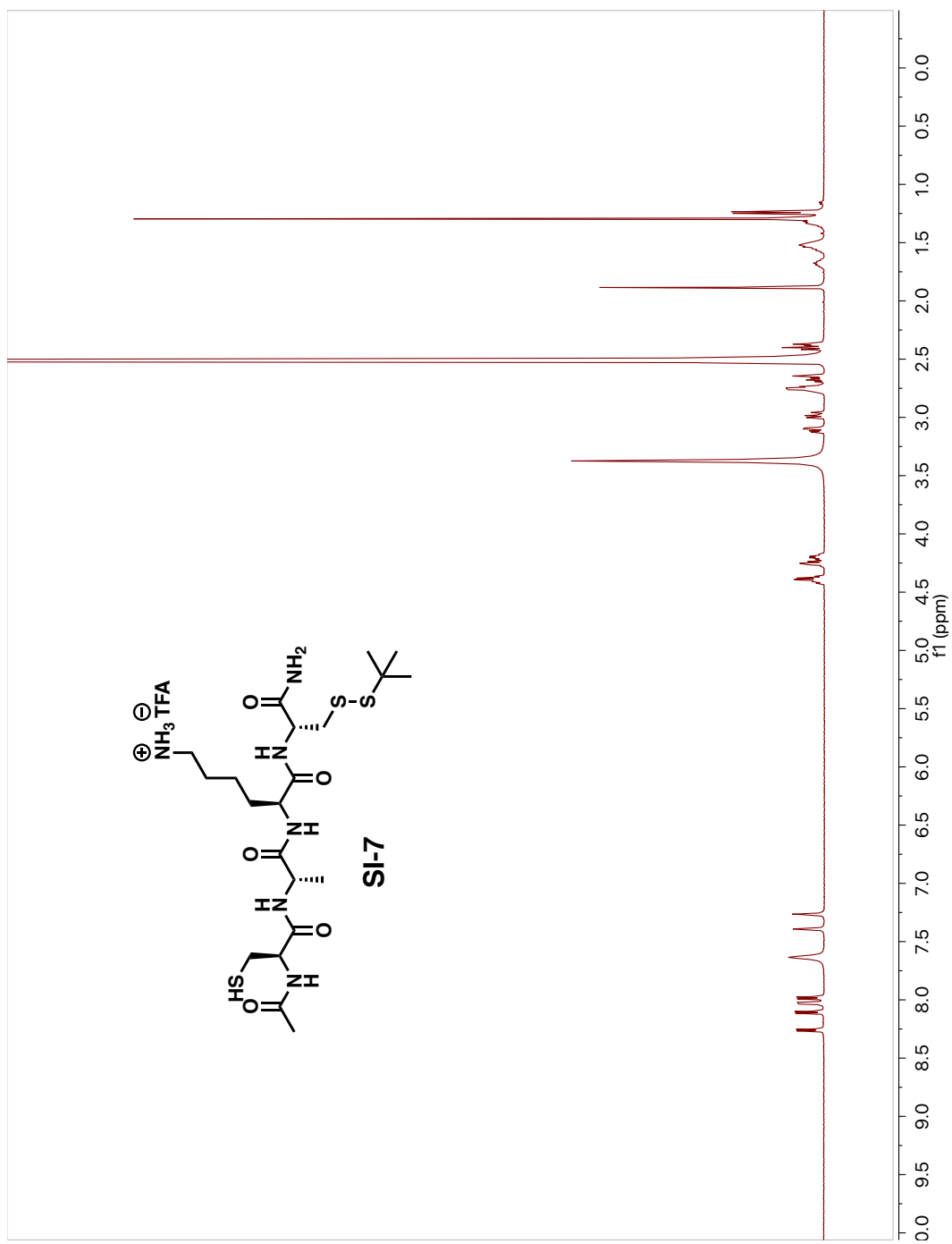
**Figure A.60.** 500 MHz <sup>1</sup>H-NMR Spectrum of Peptide SI-6 in *d*<sub>6</sub>-DMSO



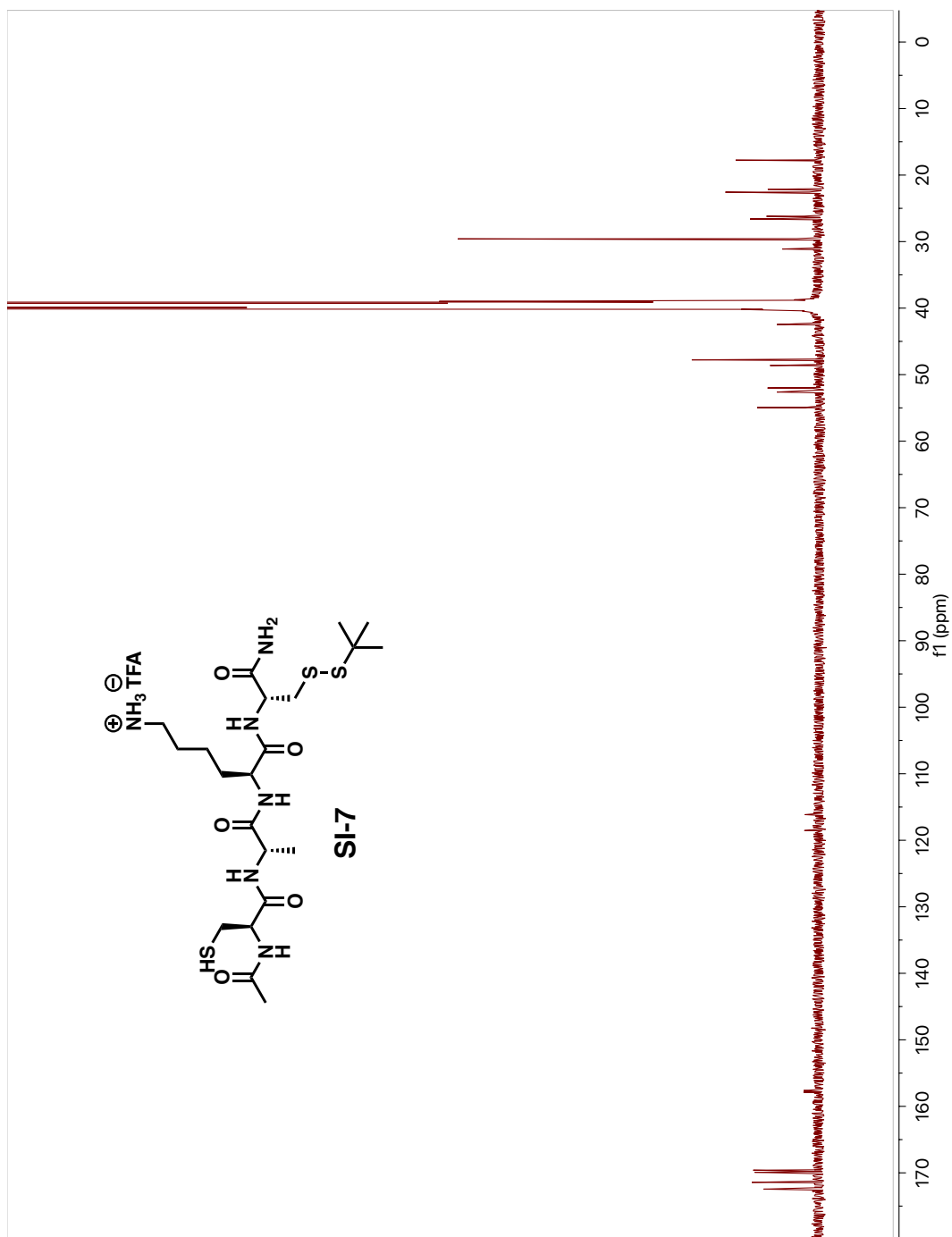
**Figure A.61.** 126 MHz <sup>13</sup>C-NMR Spectrum of Peptide SI-6 in *d*<sub>6</sub>-DMSO



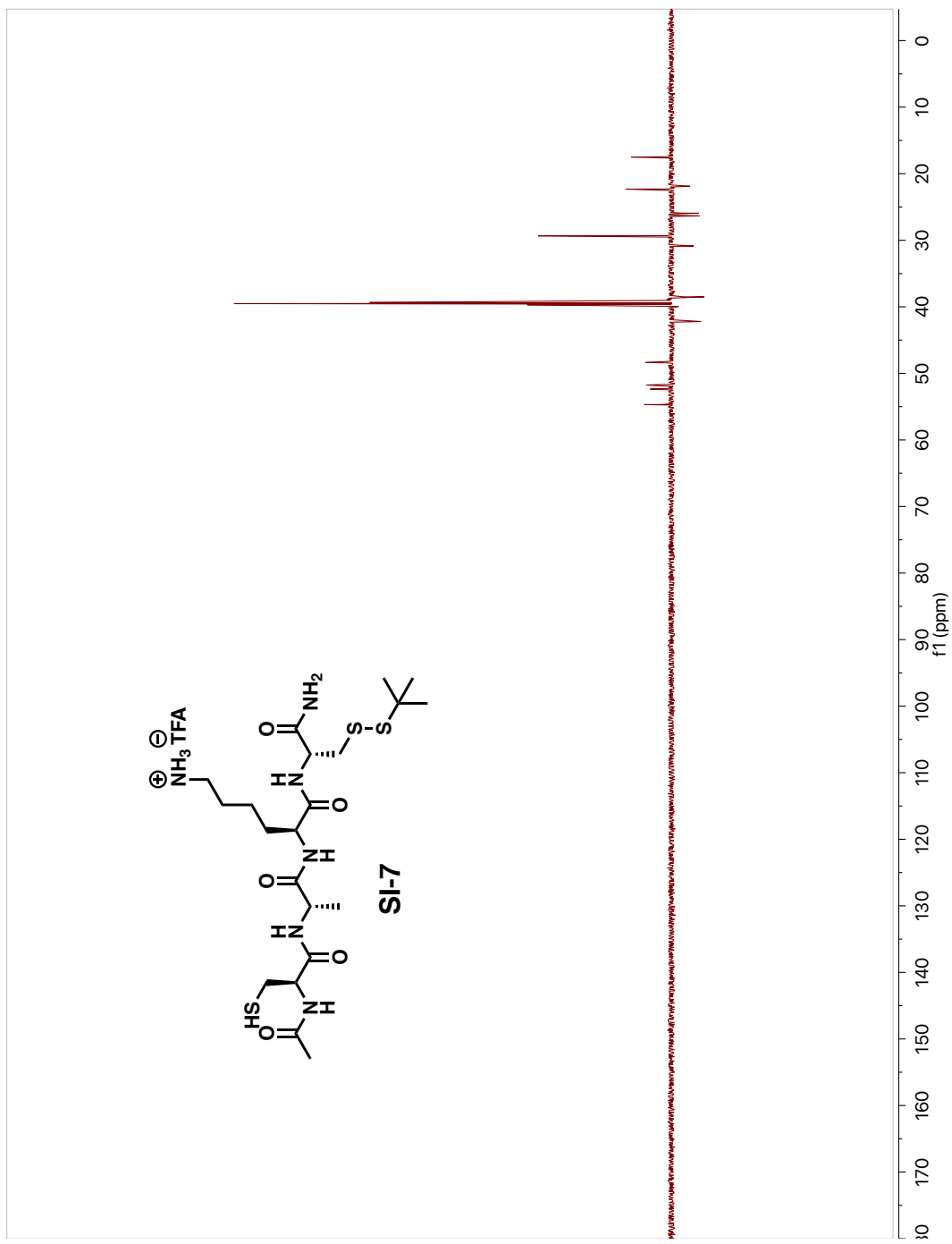




**Figure A.63.** 500 MHz <sup>1</sup>H-NMR Spectrum of Peptide SI-7 in d<sub>6</sub>-DMSO



**Figure A.64.** 126 MHz  $^{13}\text{C}$ -NMR Spectrum of Peptide SI-7 in  $d_6$ -DMSO



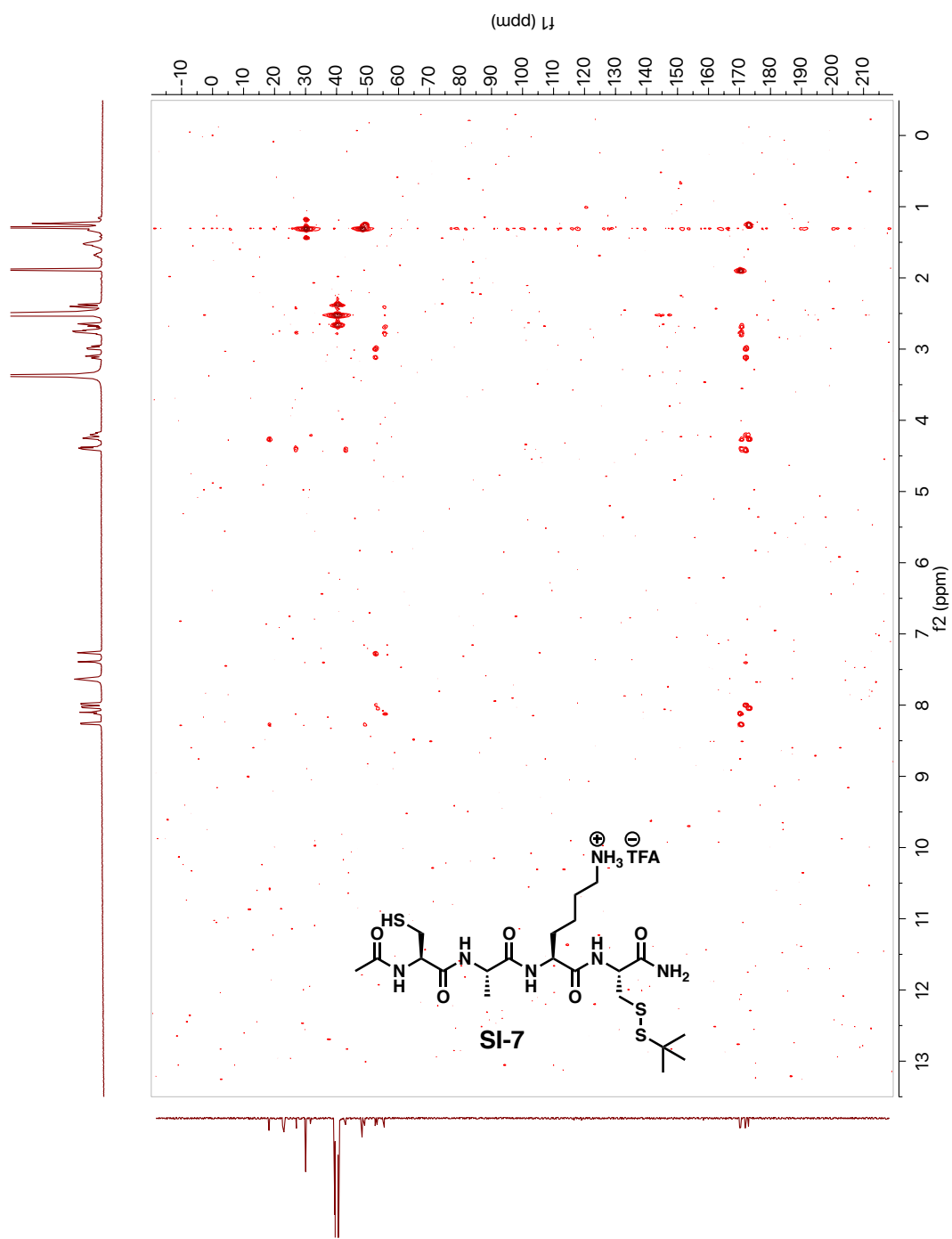


Figure A.66. HMBC Spectrum of Peptide SI-7 in  $d_6$ -DMSO

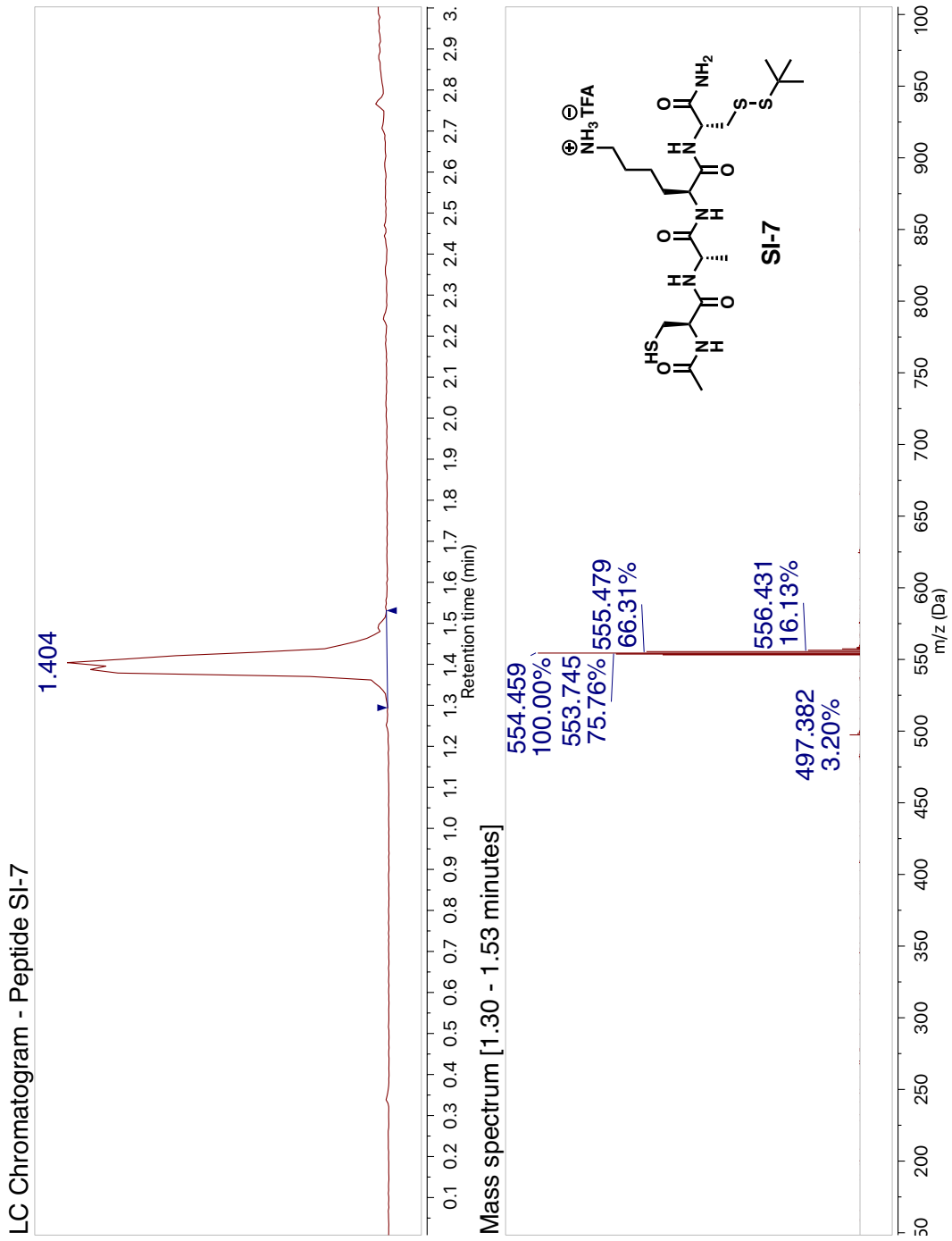


Figure A.67. LC/MS Chromatogram of Peptide SI-7



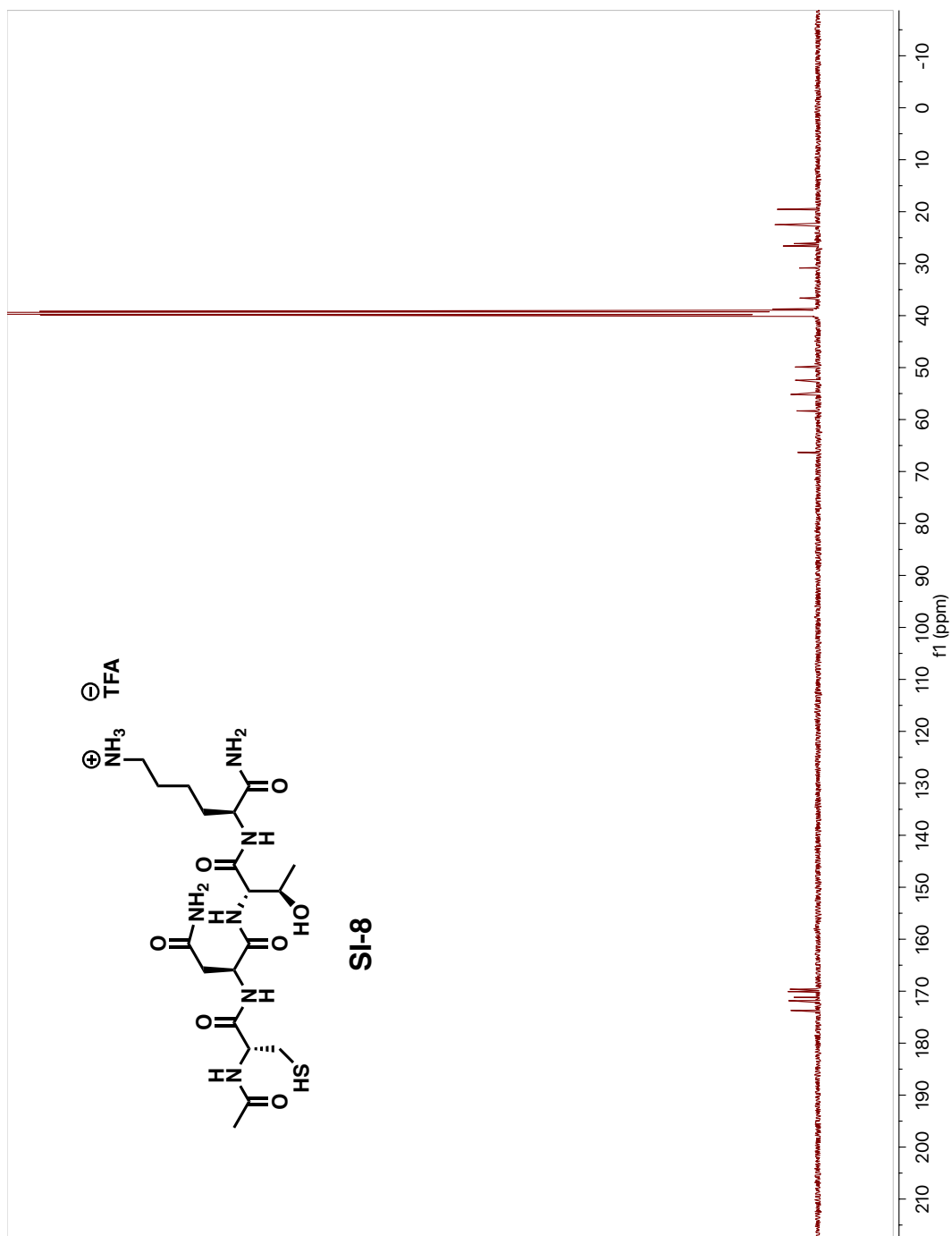
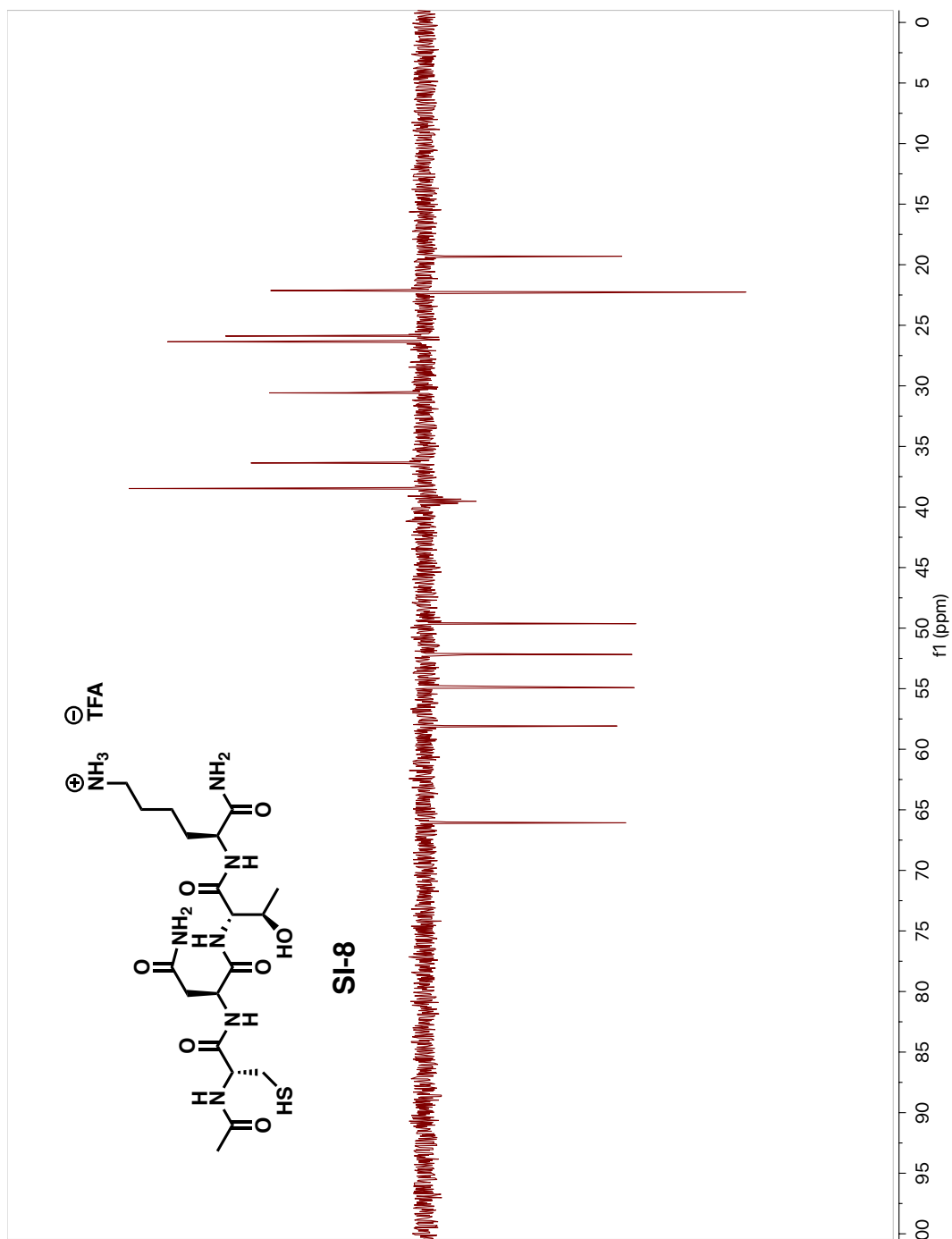


Figure A.69. 126 MHz  $^{13}\text{C}$  NMR Spectrum of Peptide SI-8 in  $d_6$ -DMSO





**Figure A.70.** 126 MHz DEPT-135 Spectrum of Peptide SI-8 in  $d_6$ -DMSO

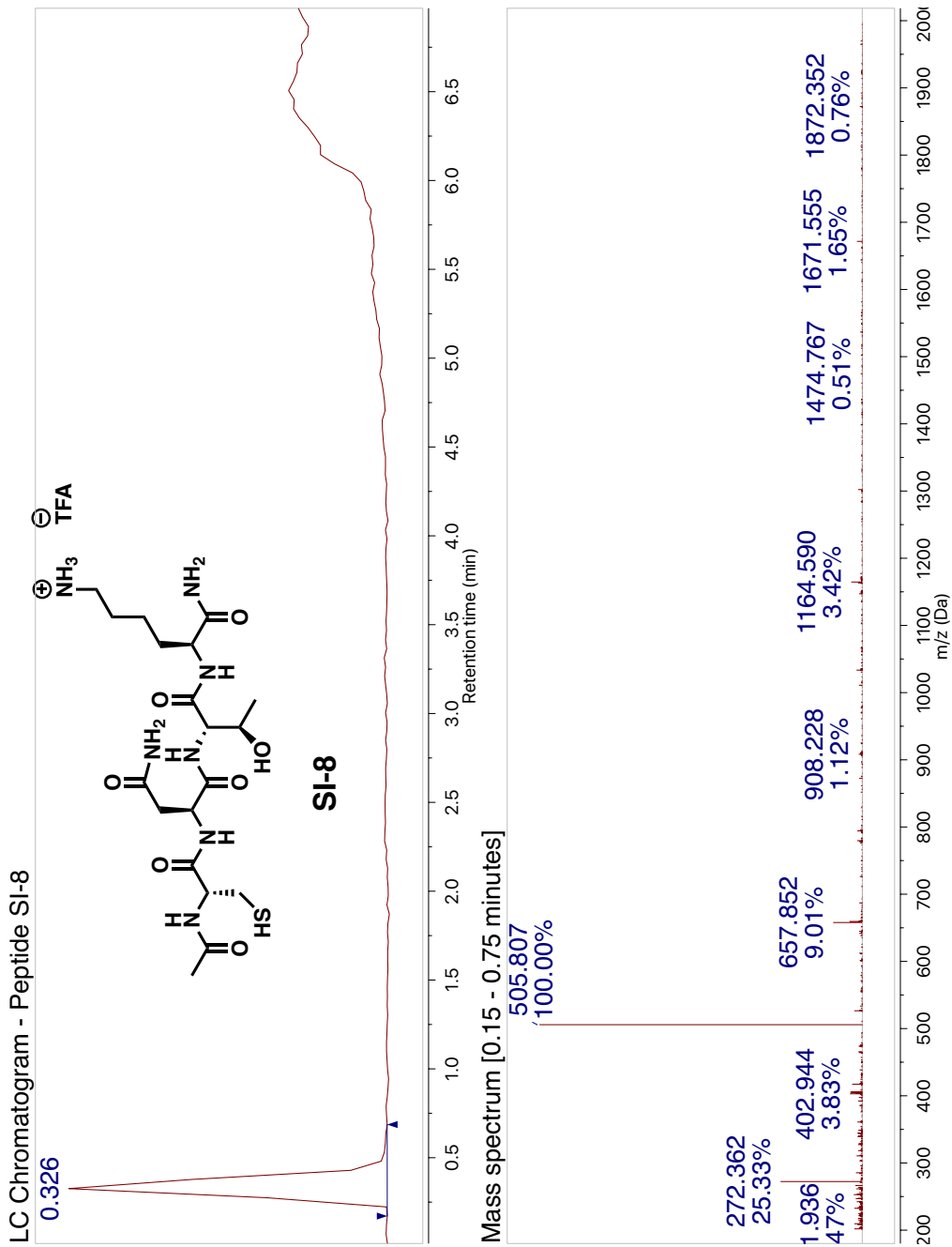
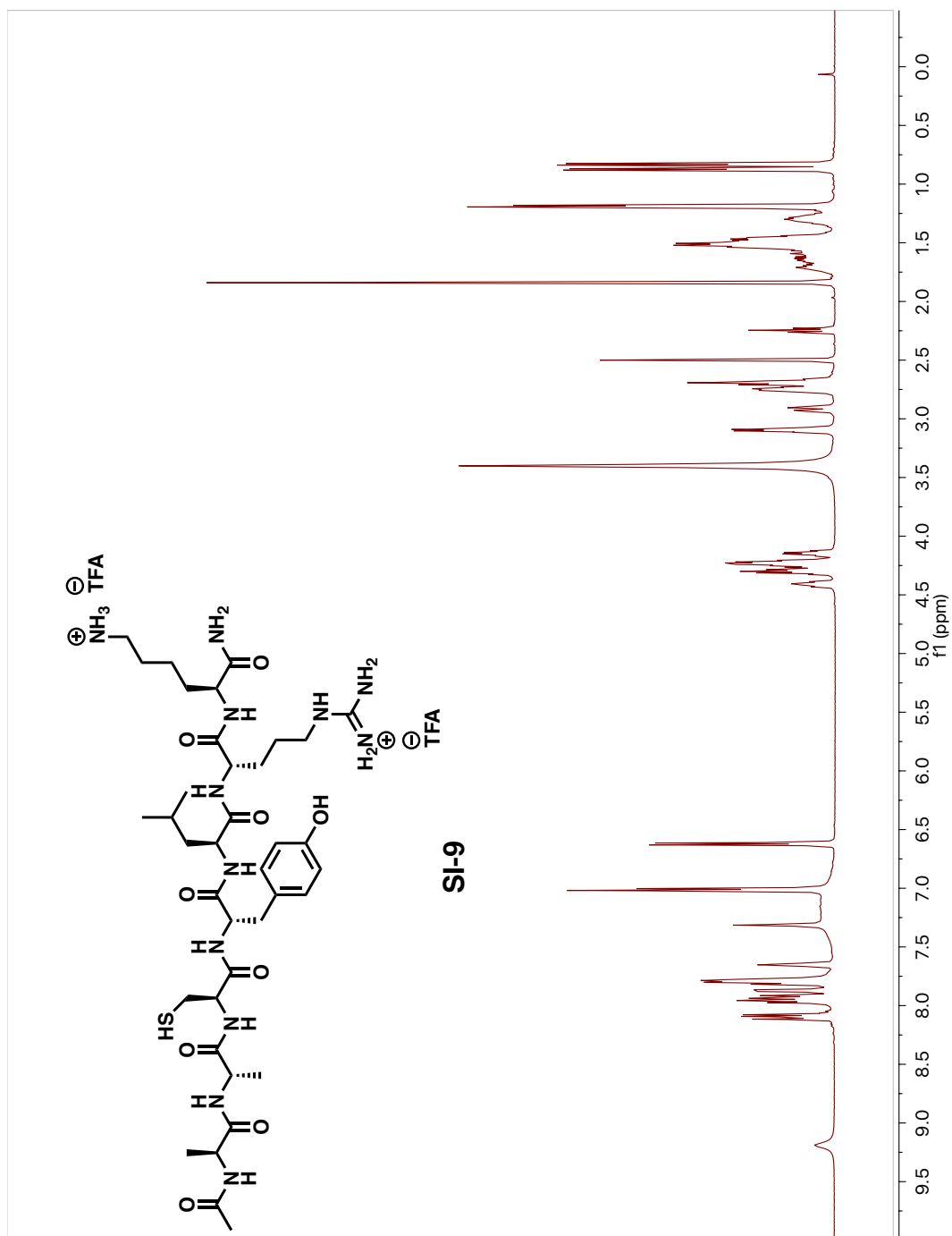


Figure A.71. LC/MS Chromatogram of Peptide SI-8



**Figure A.72.** 500 MHz <sup>1</sup>H-NMR Spectrum of Peptide SI-9 in *d*<sub>6</sub>-DMSO

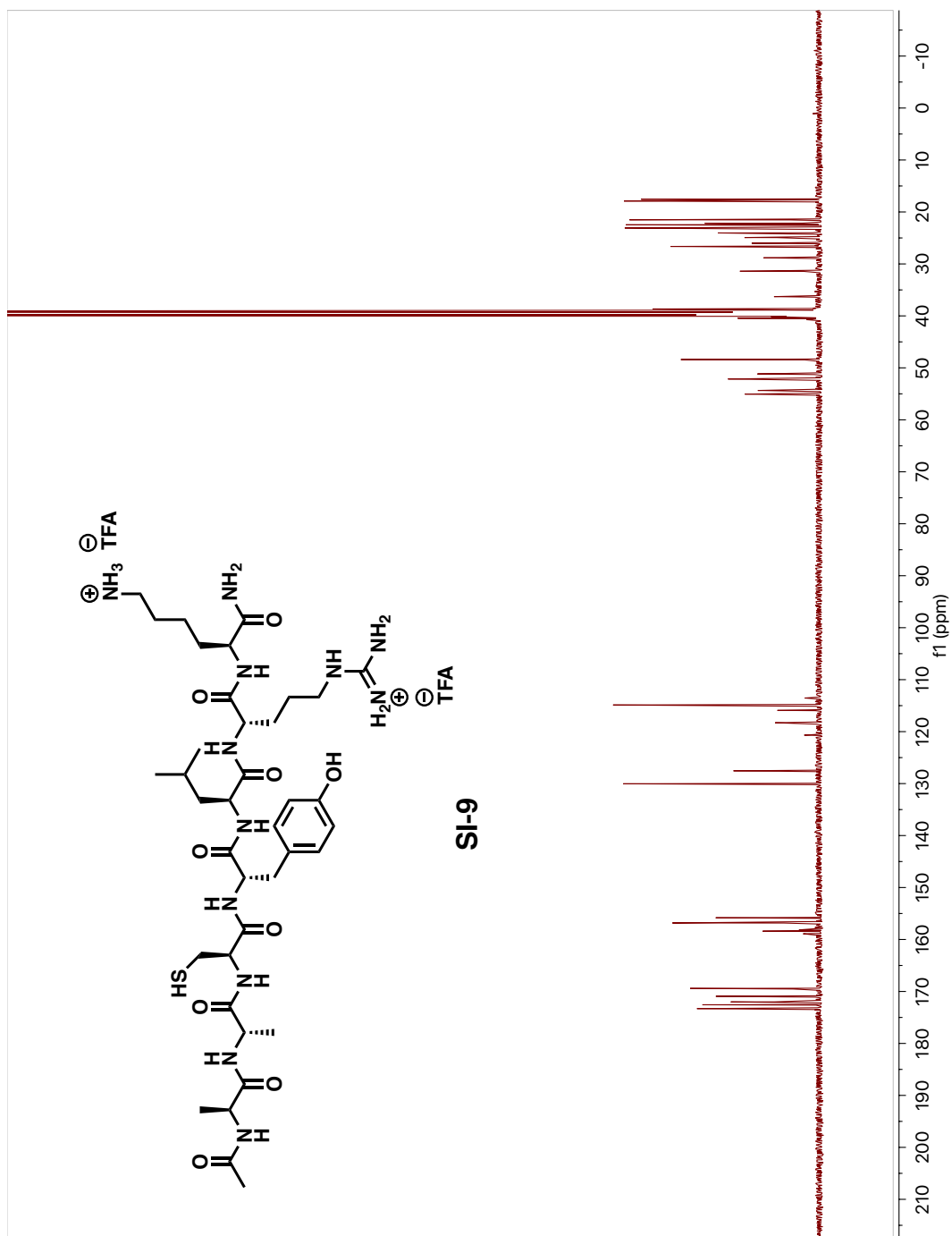


Figure A.73. 126 MHz  $^{13}\text{C}$  NMR Spectrum of Peptide SI-9 in  $d_6$ -DMSO

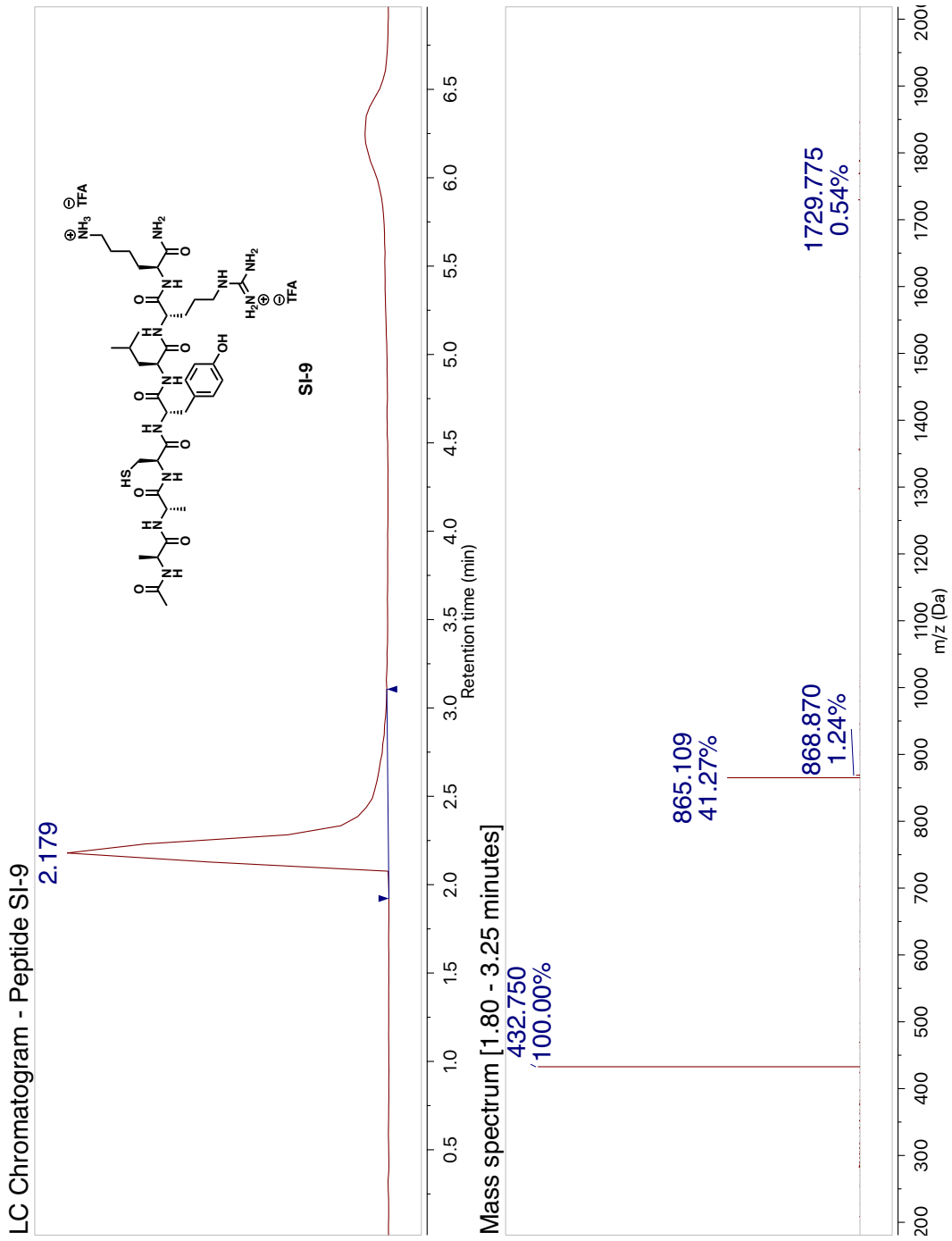
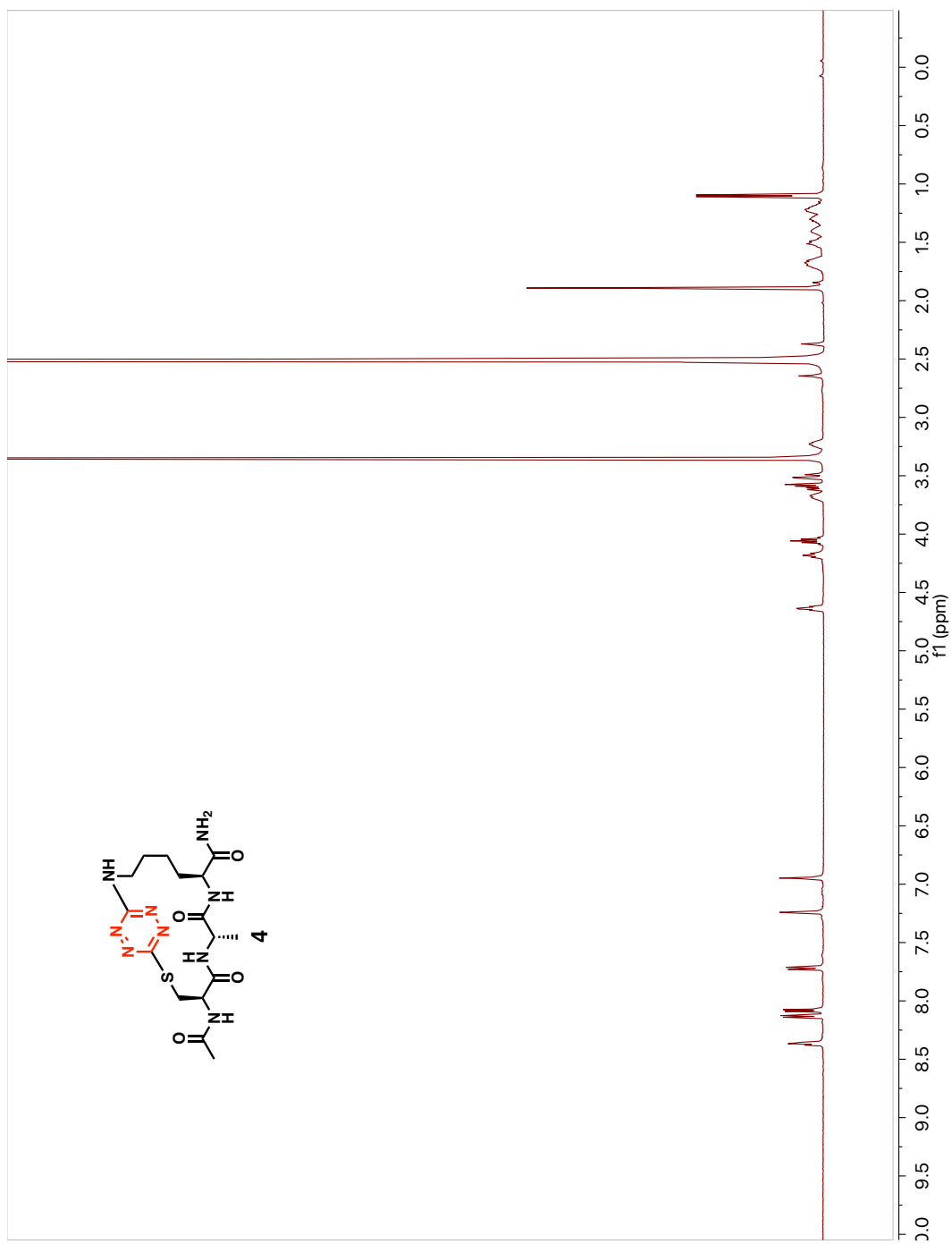
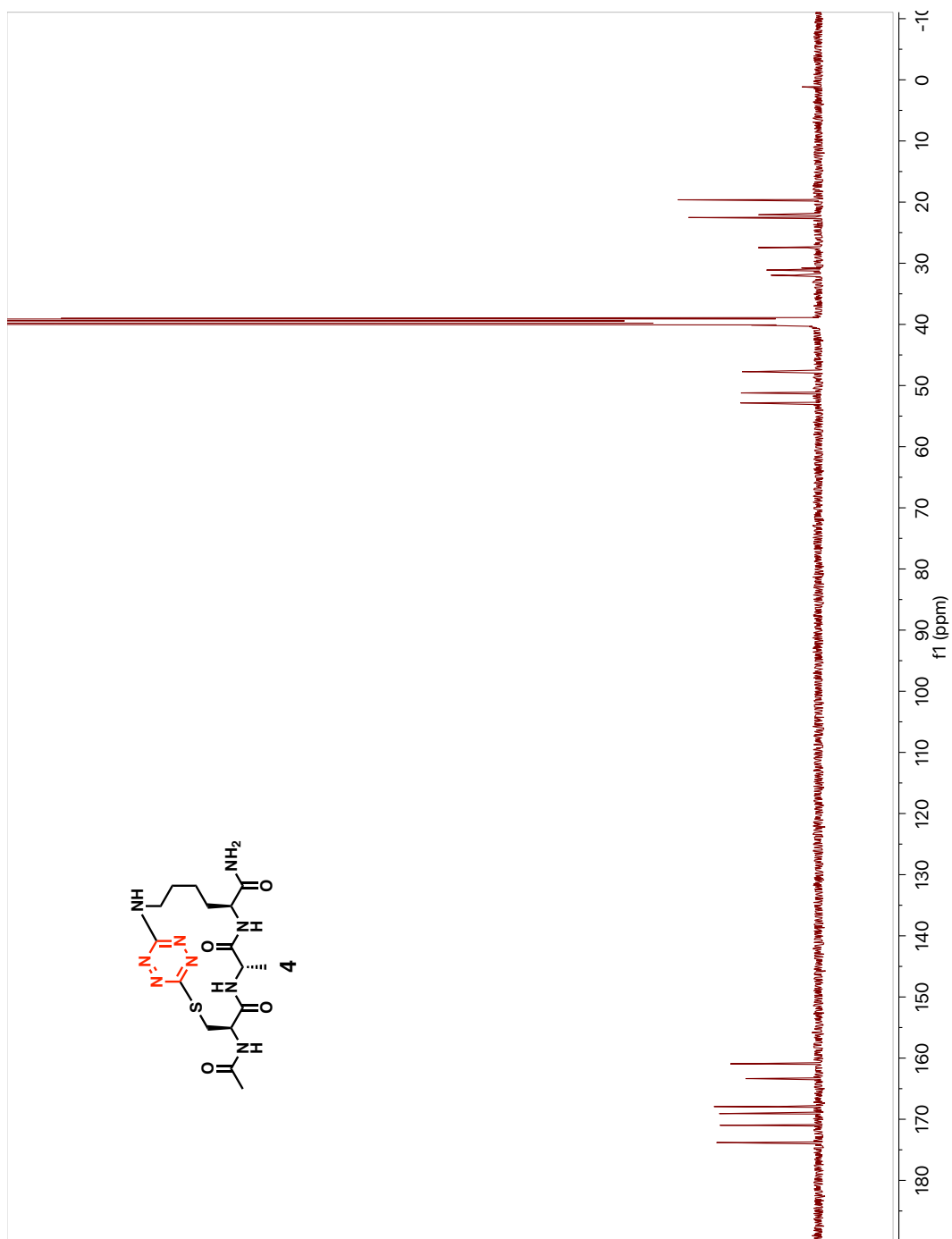


Figure A.74. LC/MS Chromatogram of Peptide SI-9



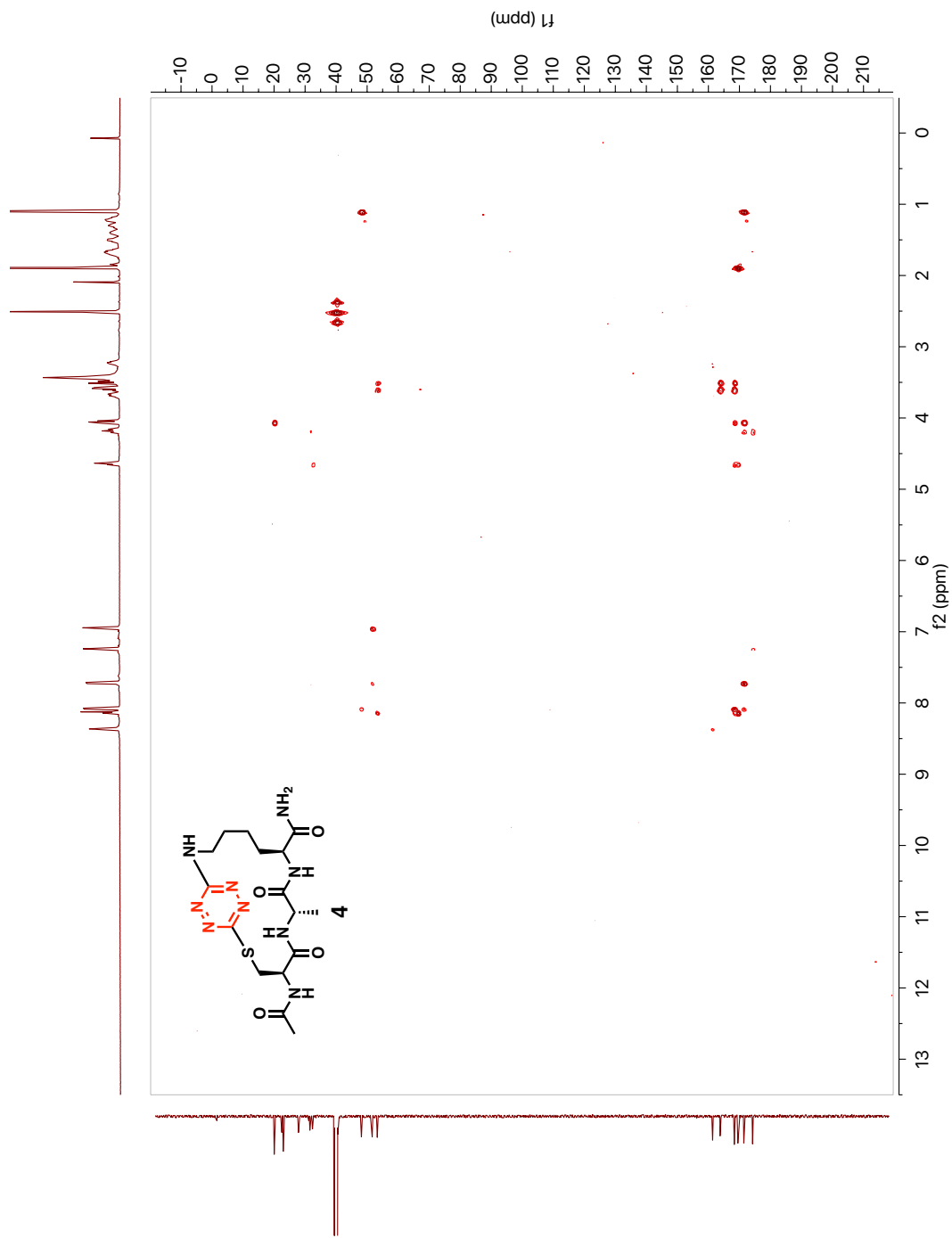
**Figure A.75.** 500 MHz <sup>1</sup>H-NMR Spectrum of Macrocycle 4 in d<sub>6</sub>-DMSO (1% v/v TMS)



**Figure A.76.** 126 MHz <sup>13</sup>C Spectrum of Macrocycle 4 in *d*<sub>6</sub>-DMSO (1% v/v TMS)







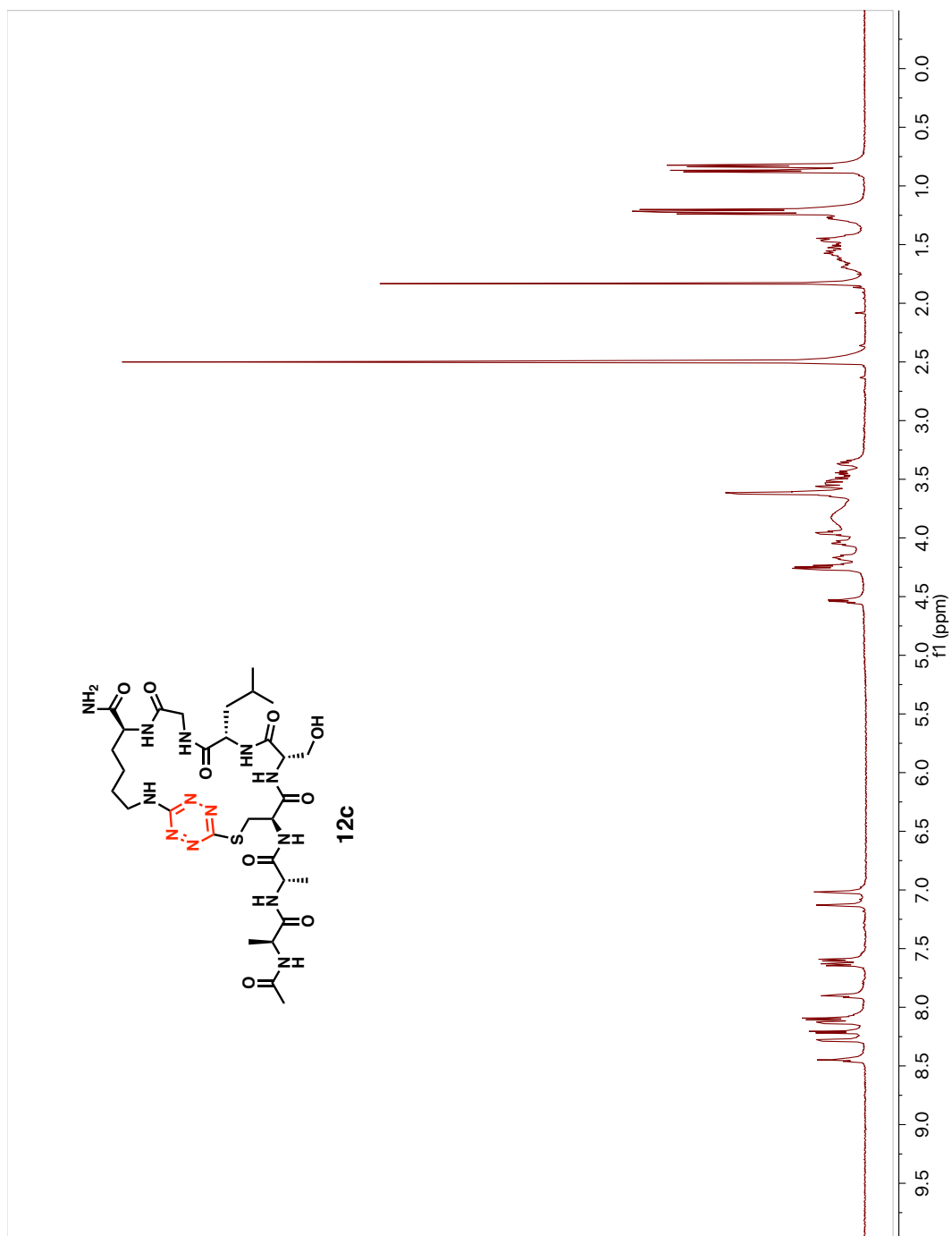


**Figure A.79.** 500 MHz <sup>1</sup>H-NMR Spectrum of Macrocycle 12c in *d*<sub>6</sub>-DMSO

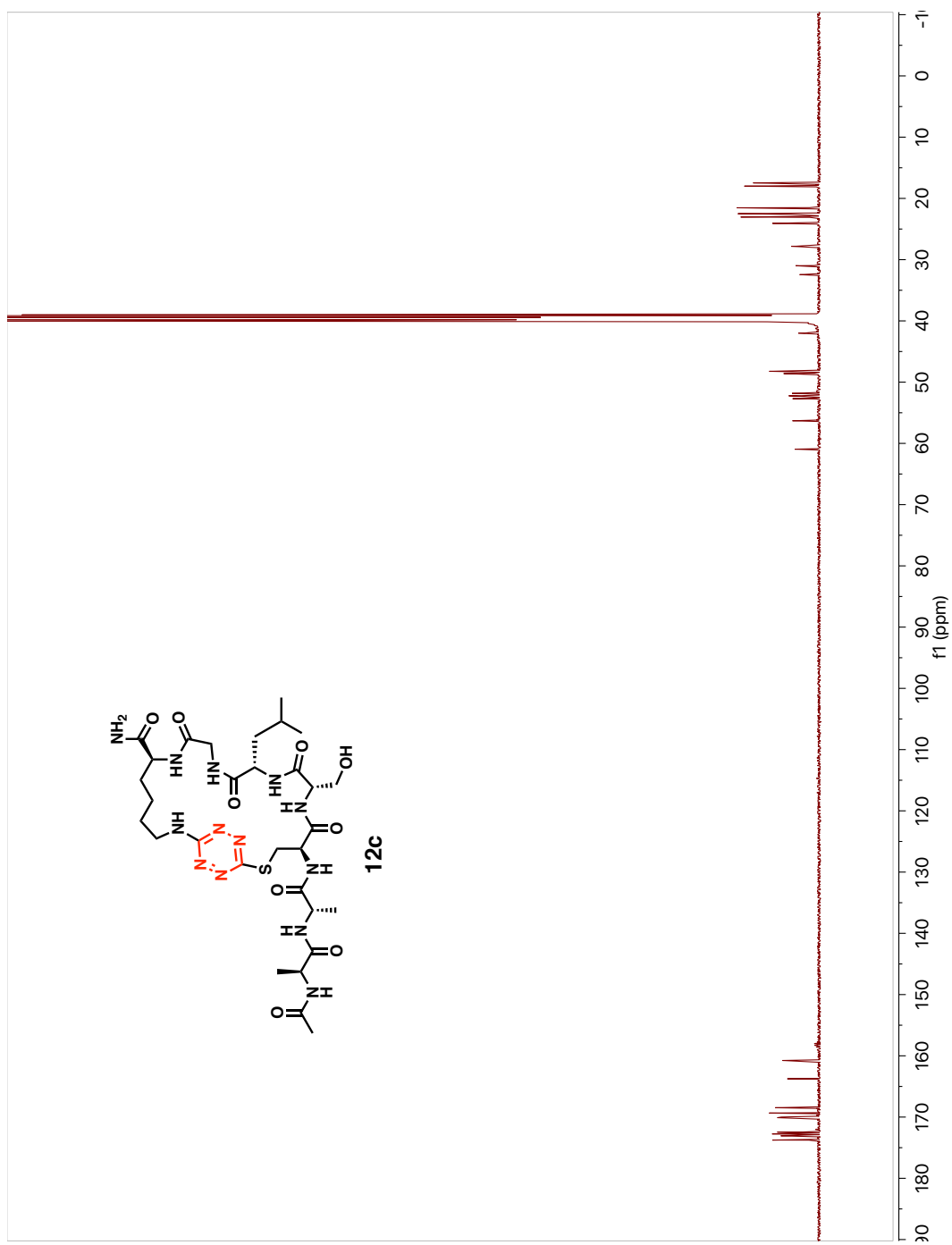


**Figure A.80.** 126 MHz  $^{13}\text{C}$ -NMR Spectrum of Macrocycle **12c** in  $d_6$ -DMSO

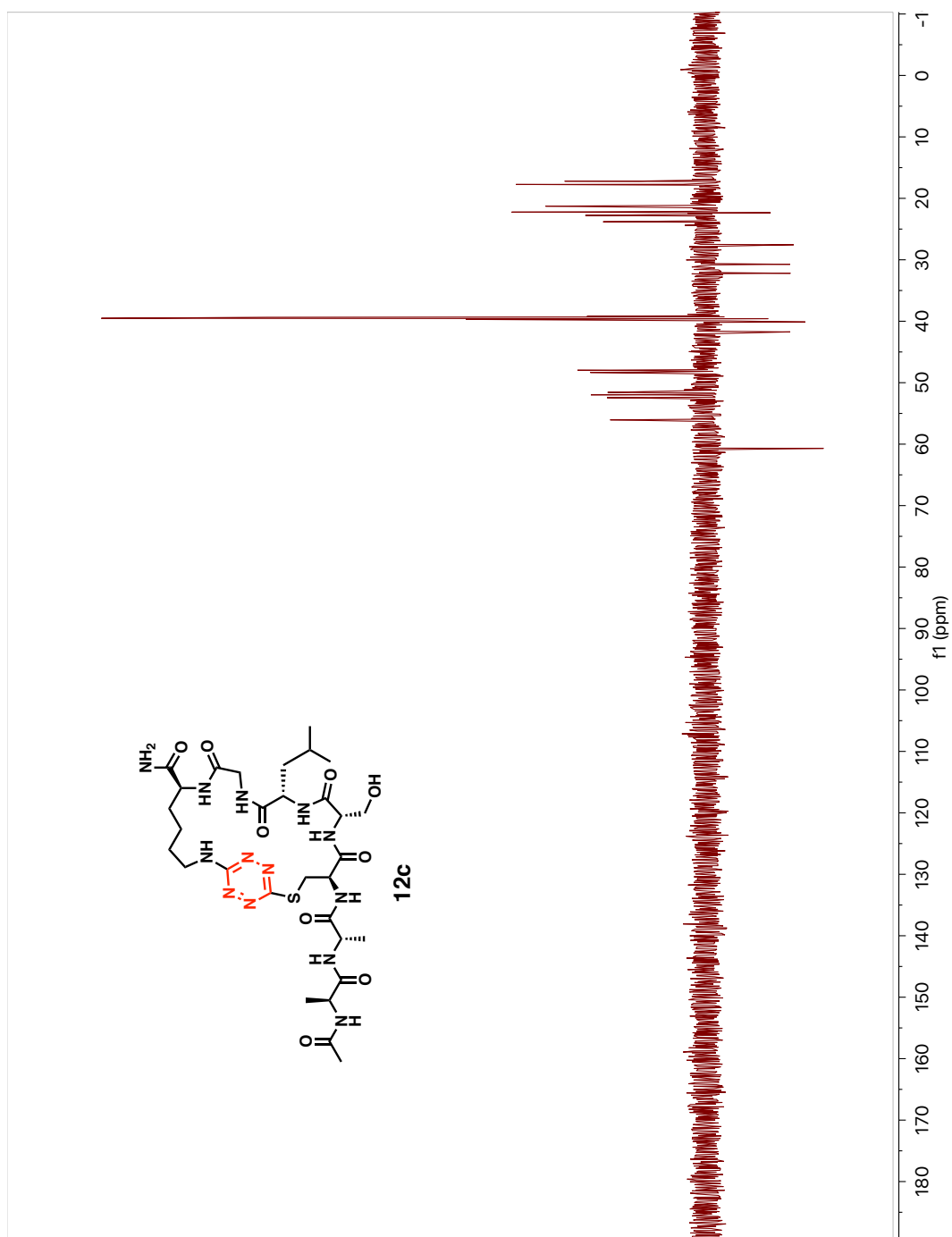


**Figure A.81.** 126 MHz DEPT-135 Spectrum of Macrocycle **12c** in *d*<sub>6</sub>-DMSO

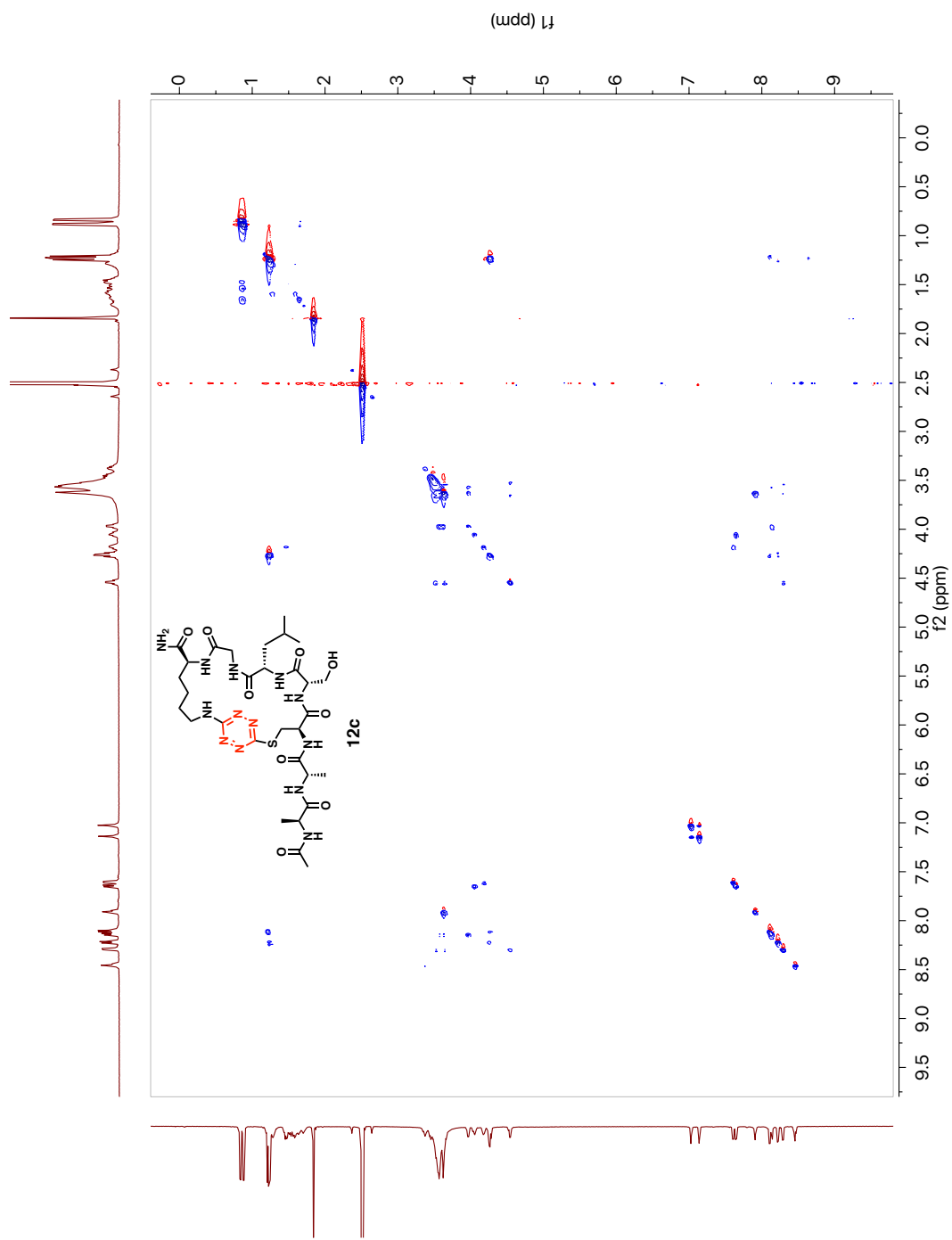


**Figure A.82.** TOCSY Spectrum of Macrocycle **12c** in  $d_6$ -DMSO

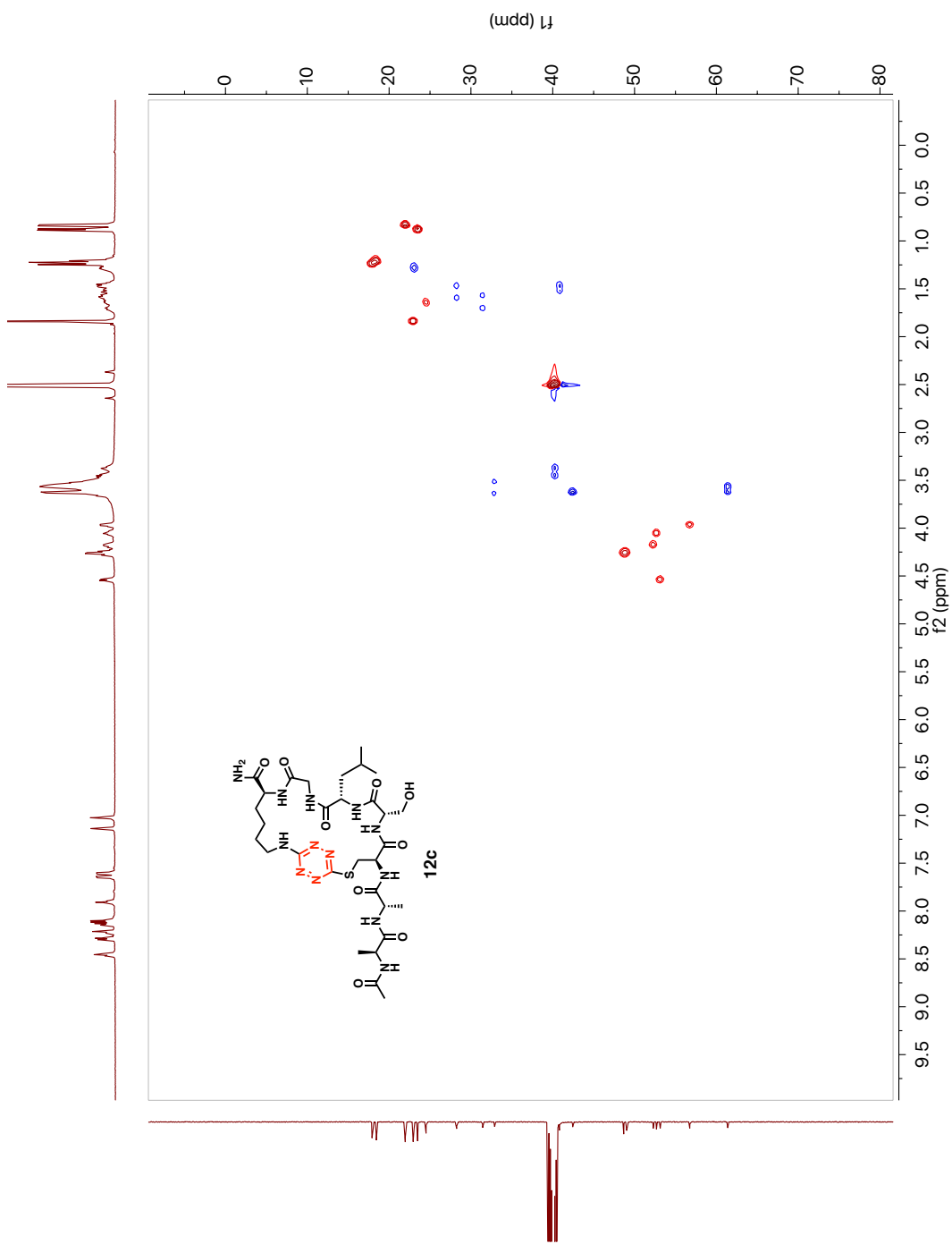


**Figure A.83.** HSQC Spectrum of Macrocycle 12c in  $d_6$ -DMSO

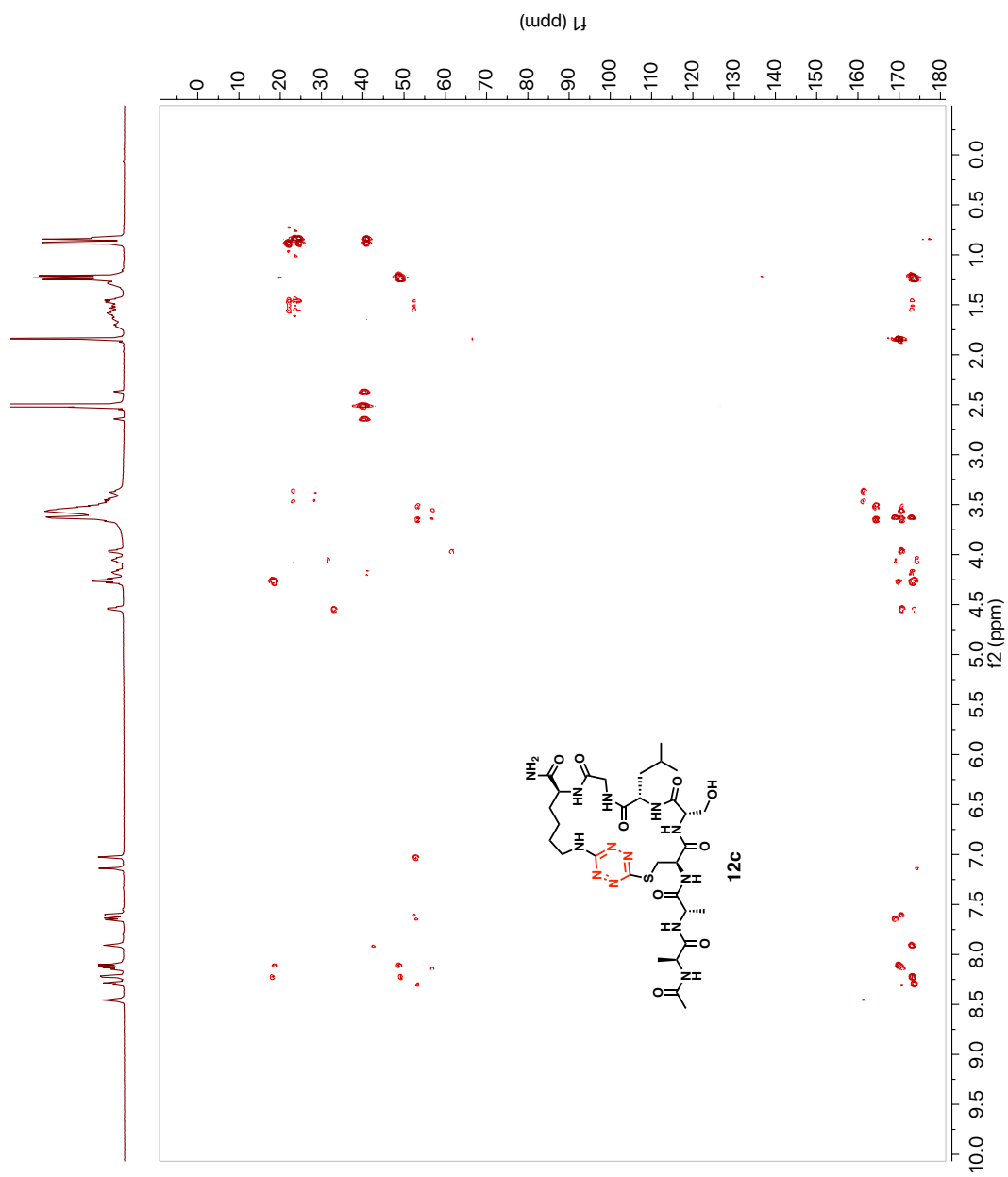


**Figure A.84.** HMBC Spectrum of Macrocycle 12c in  $d_6$ -DMSO

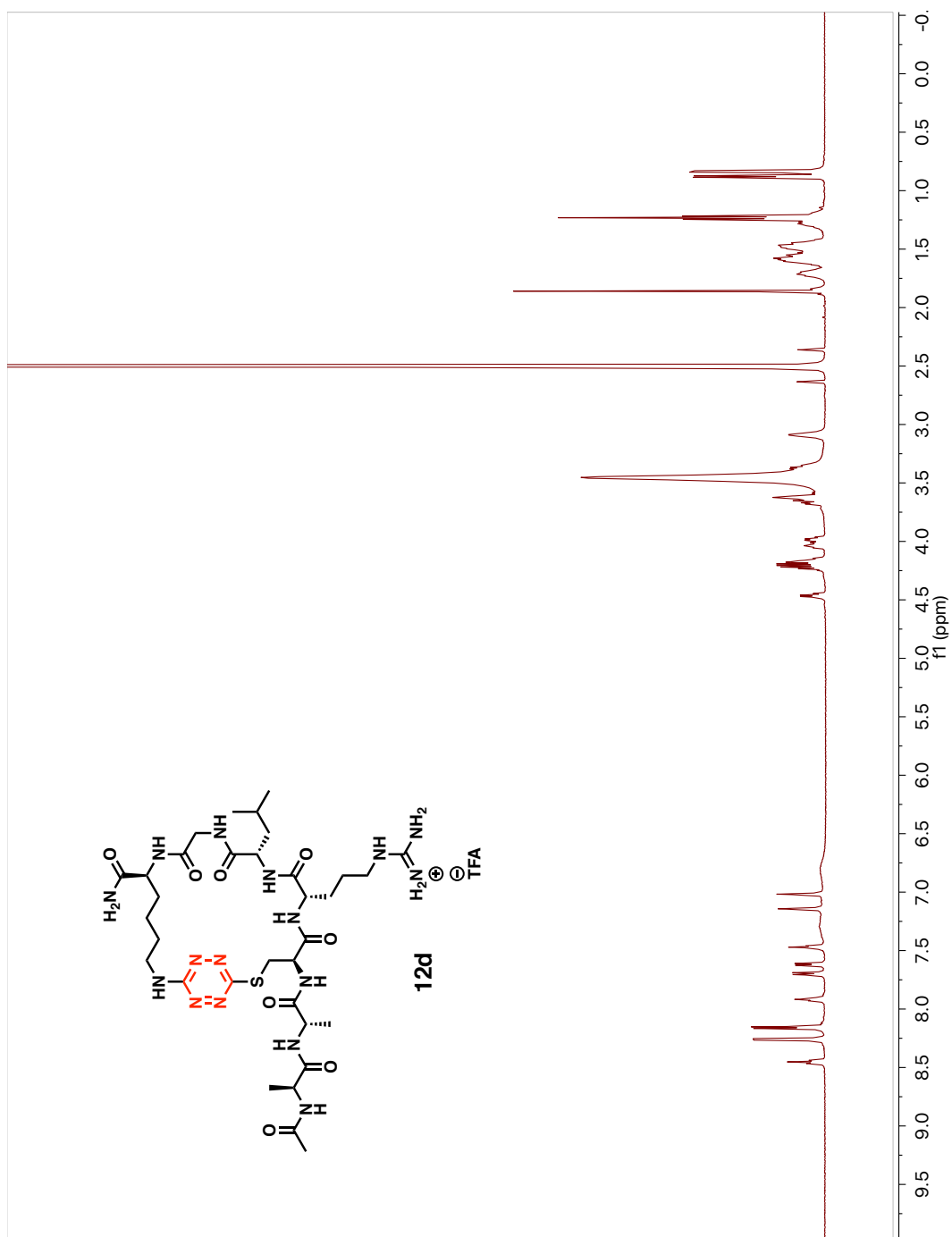


**Figure A.85.** 500 MHz <sup>1</sup>H-NMR Spectrum of Macrocycle 12d in *d*<sub>6</sub>-DMSO



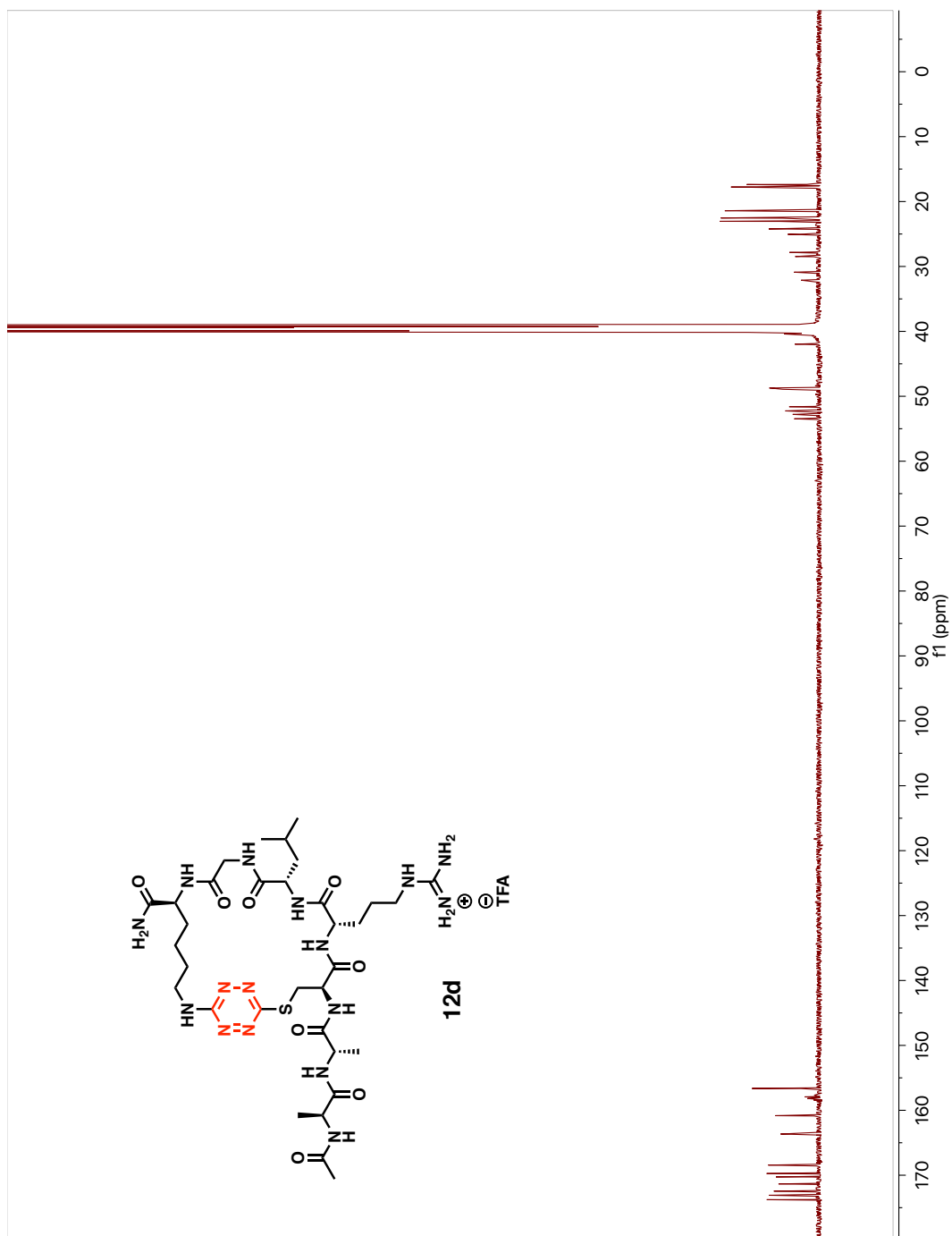


**Figure A.86.** 126 MHz  $^{13}\text{C}$ -NMR Spectrum of Macrocycle **12d** in  $d_6$ -DMSO

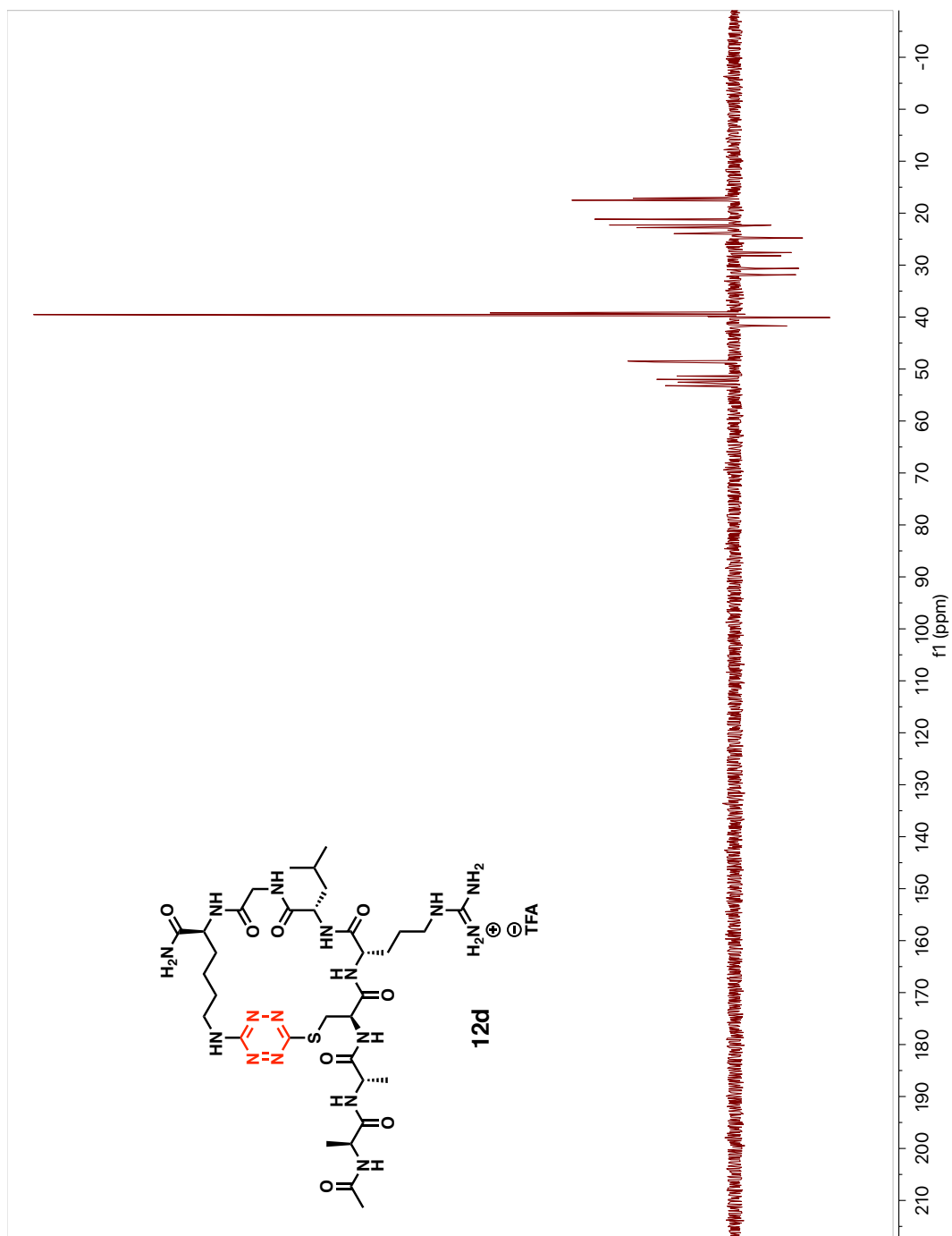


**Figure A.87.** 126 MHz DEPT-135 Spectrum of Macrocycle **12d** in  $d_6$ -DMSO

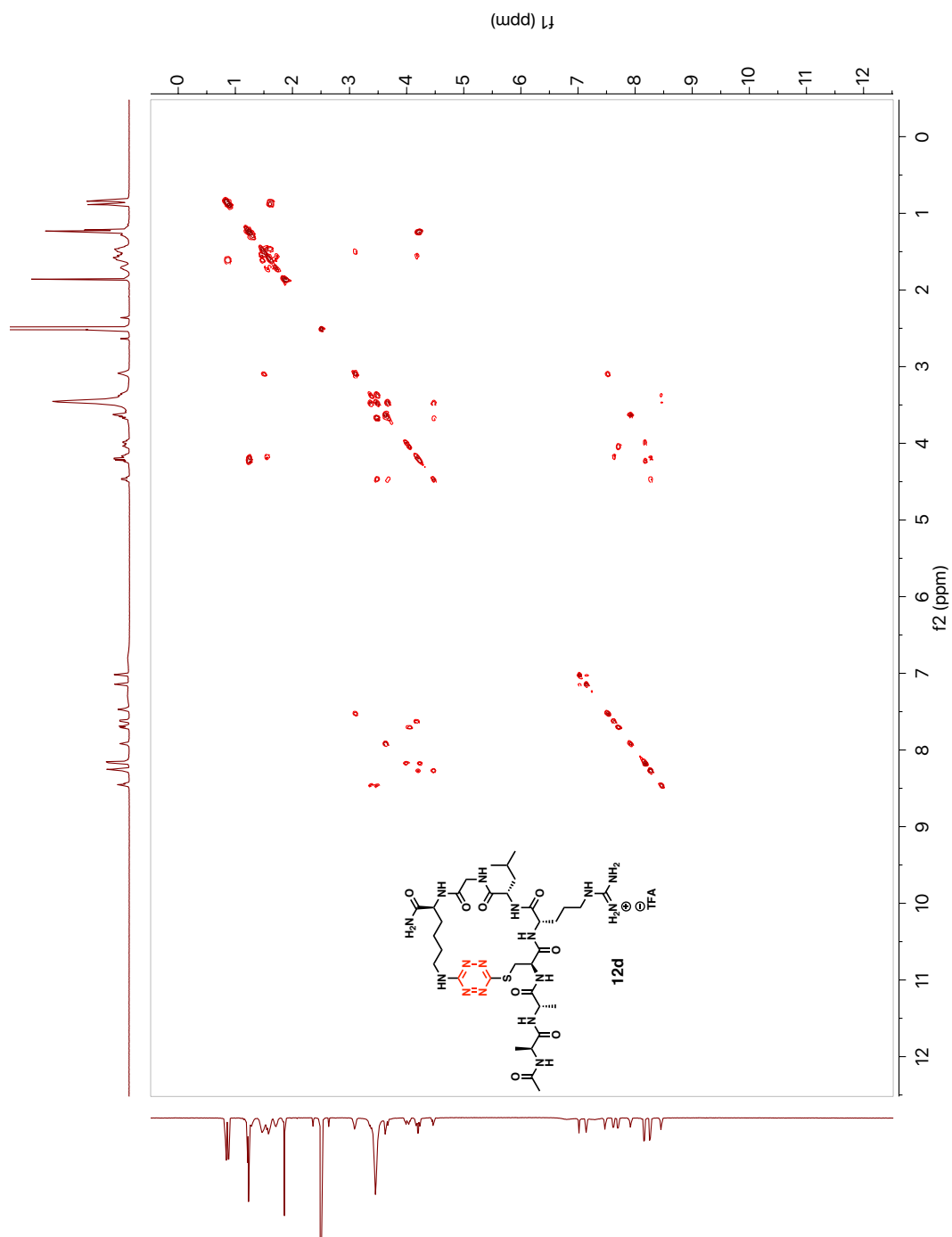


**Figure A.88.** COSY Spectrum of Macrocycle 12d in  $d_6$ -DMSO

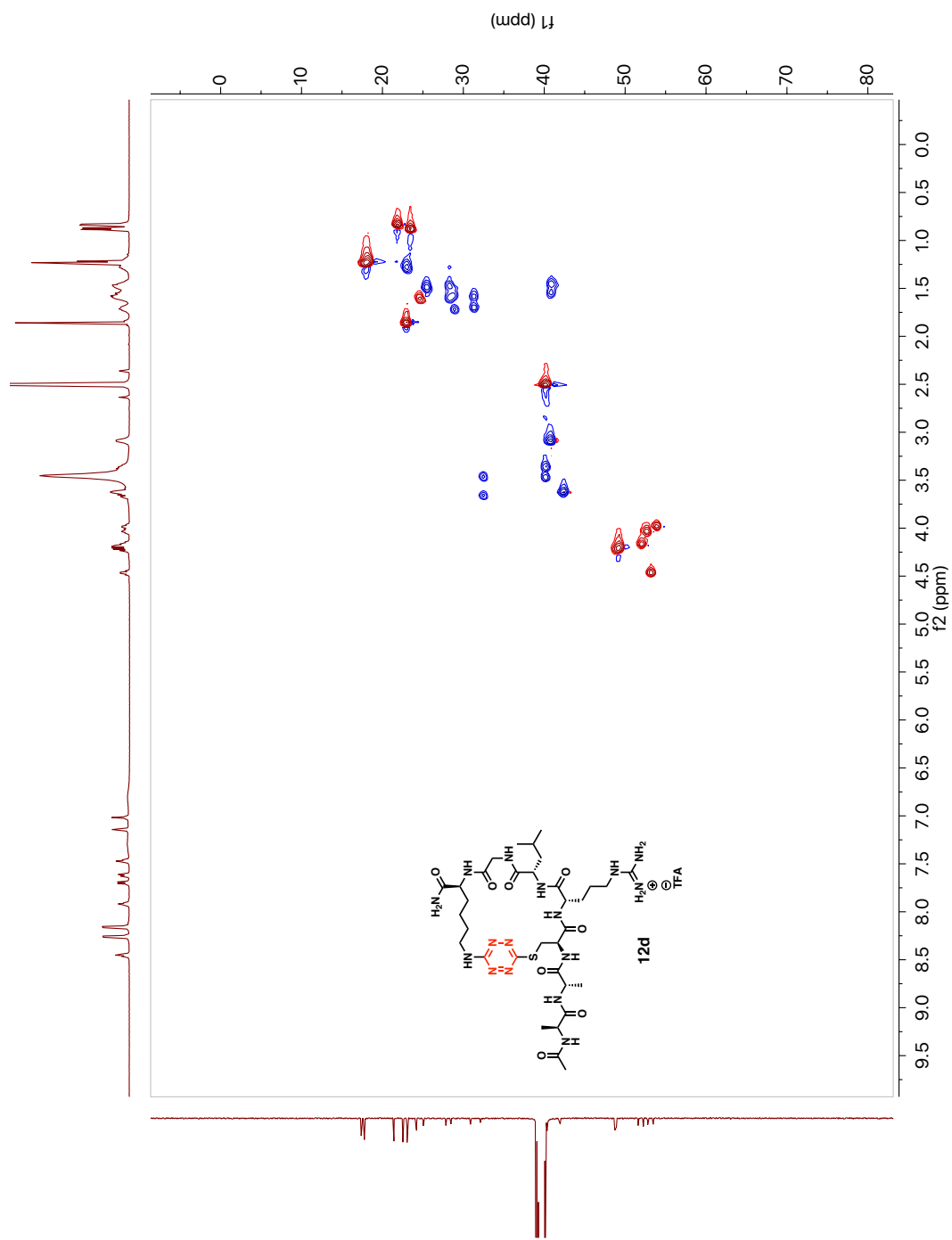


**Figure A.89.** HSQC Spectrum of Macrocycle 12d in  $d_6$ -DMSO

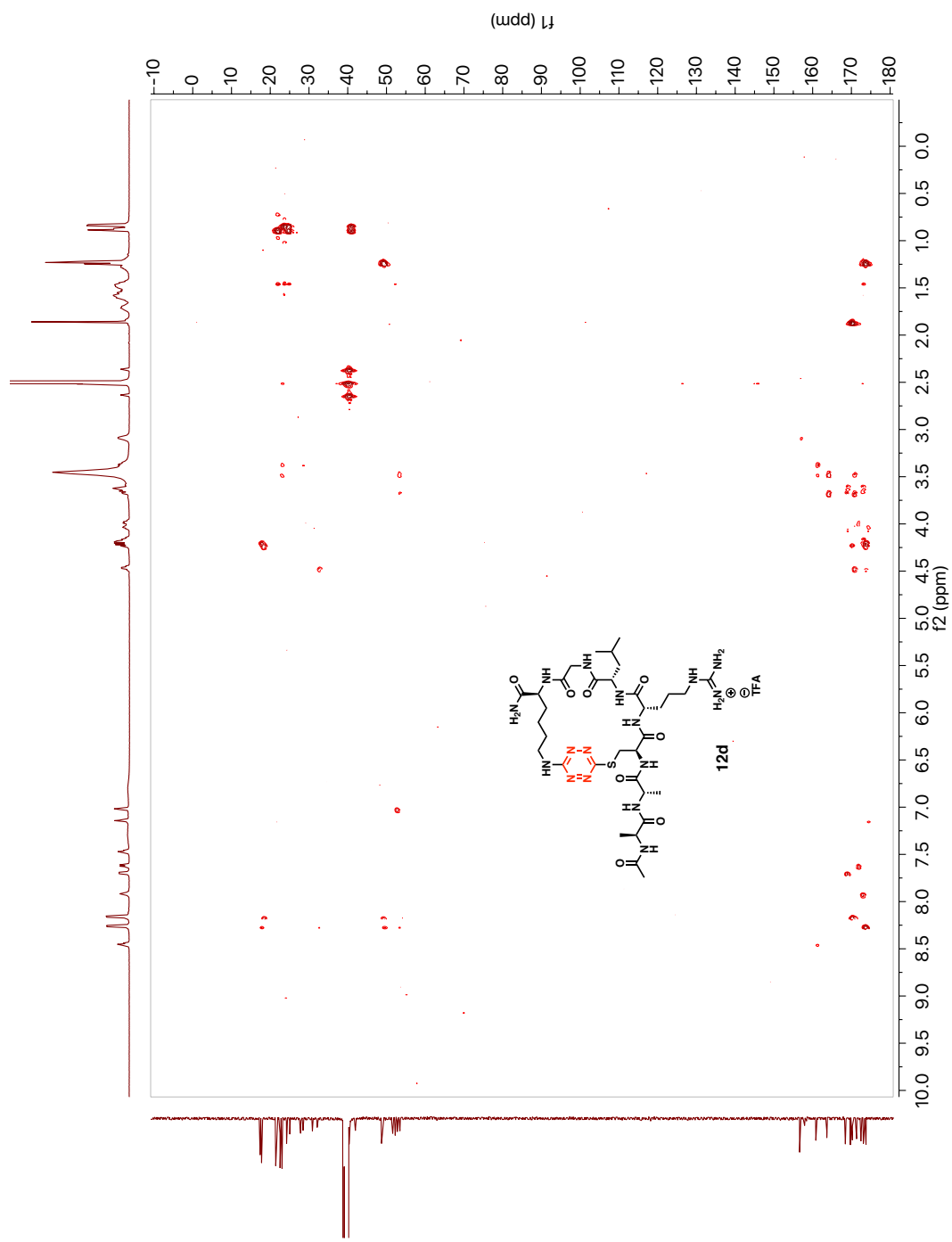


**Figure A.90.** HMBC Spectrum of Macrocycle 12d in  $d_6$ -DMSO

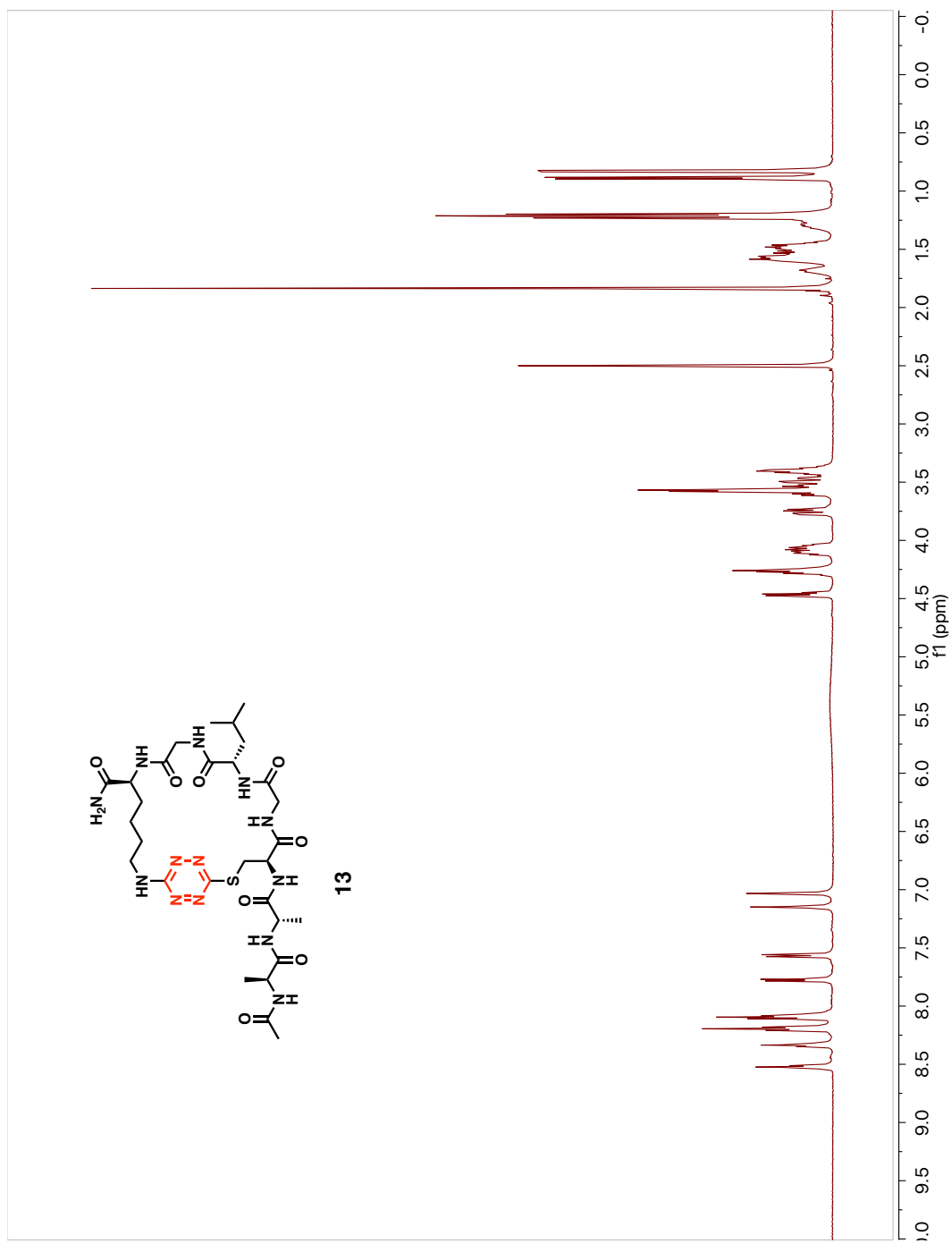


**Figure A.91.** 500 MHz <sup>1</sup>H-NMR Spectrum of Macrocycle 13 in d<sub>6</sub>-DMSO

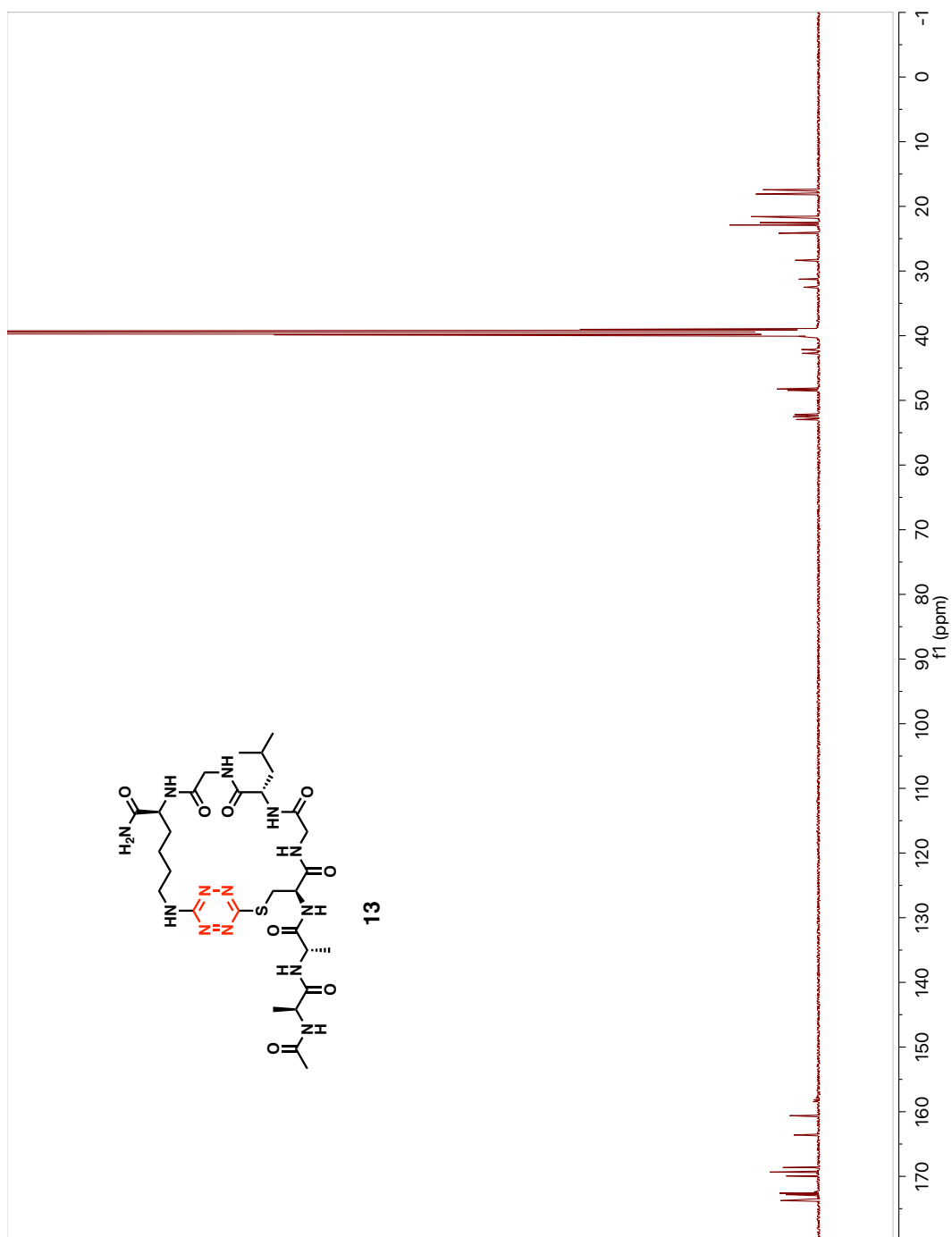


**Figure A.92.** 126 MHz <sup>13</sup>C-NMR Spectrum of Macrocycle 13 in *d*<sub>6</sub>-DMSO

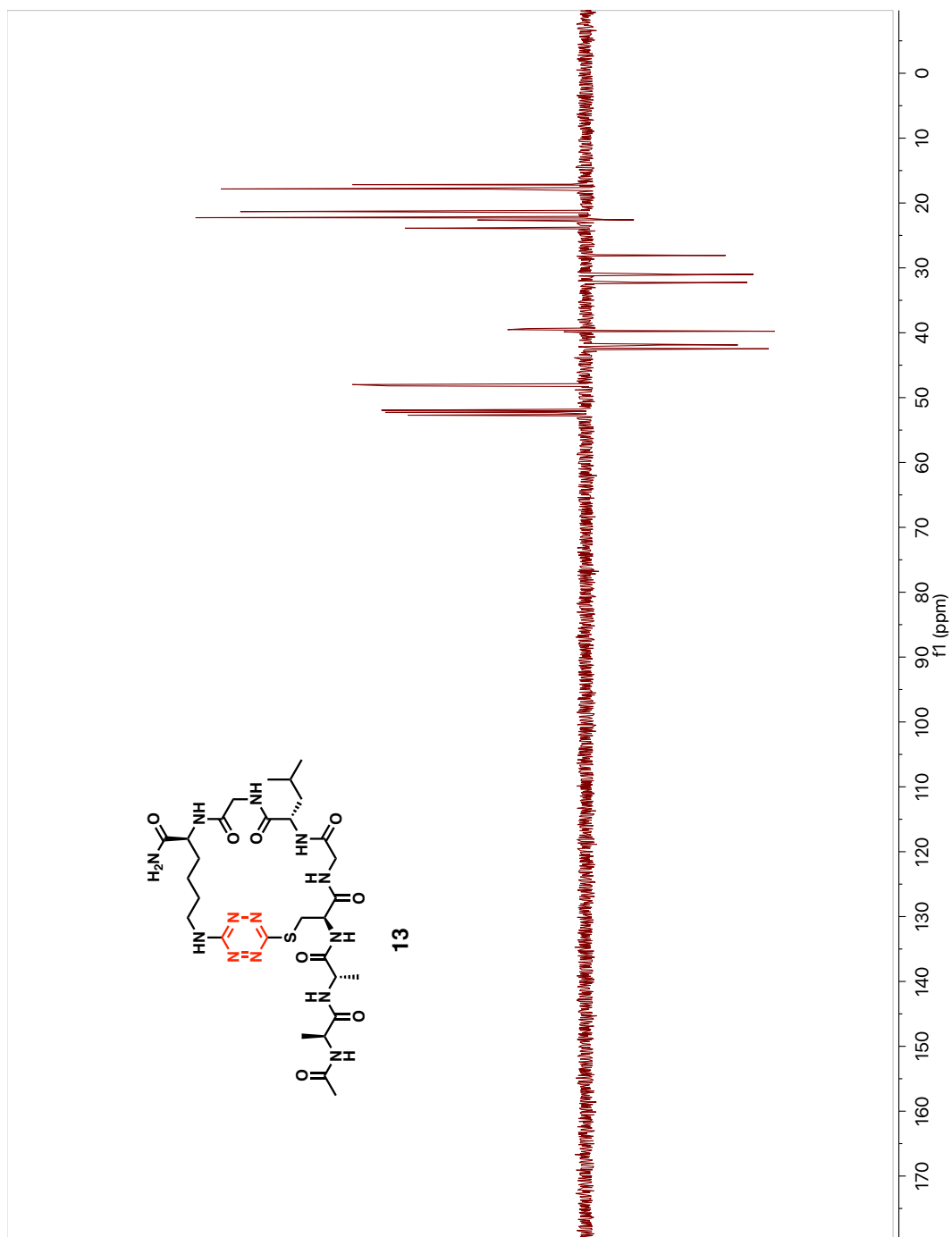


**Figure A.93.** 126 MHz DEPT-135 Spectrum of Macrocycle 13 in  $d_6$ -DMSO



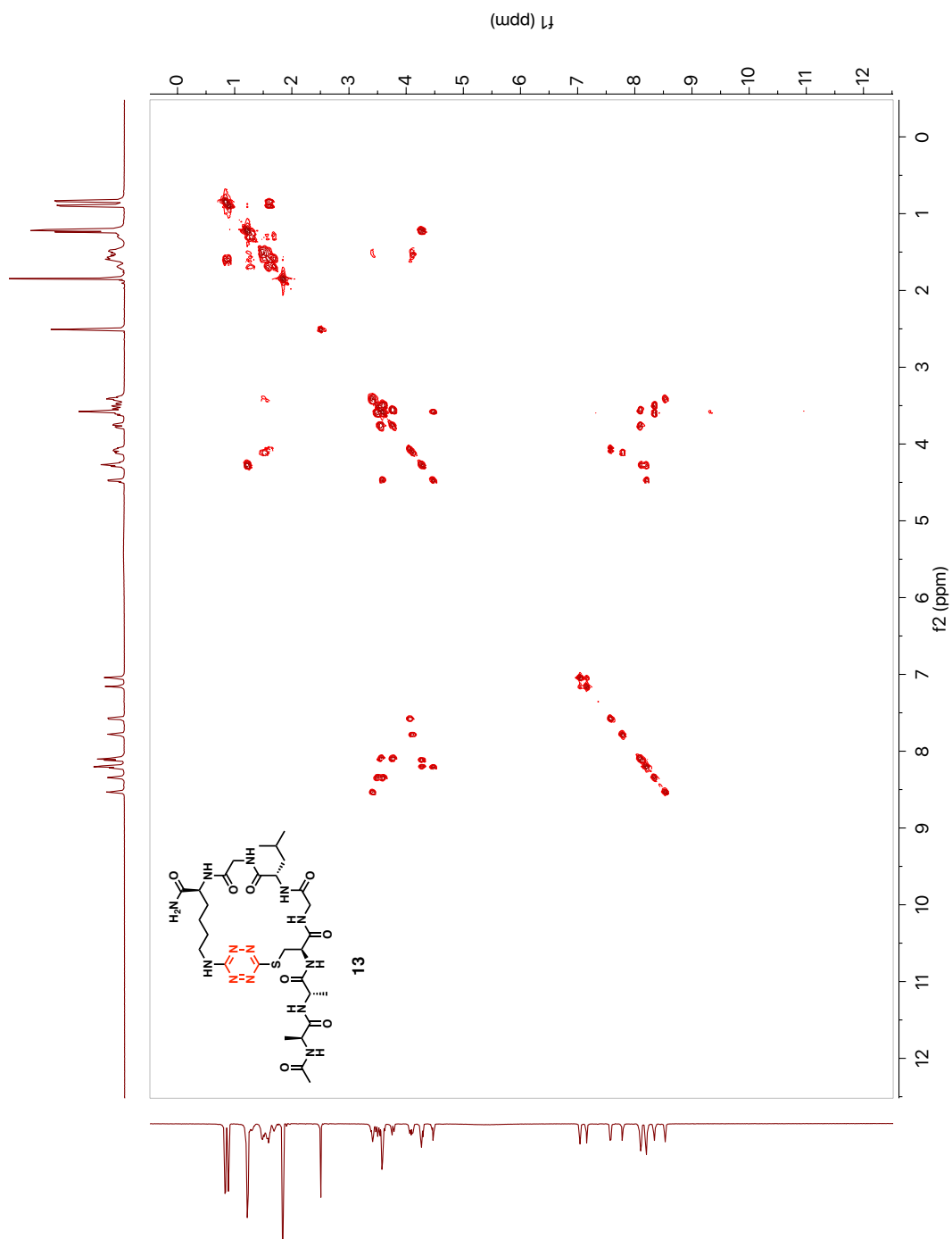


**Figure A.94.** COSY Spectrum of Macrocycle **13** in  $d_6$ -DMSO



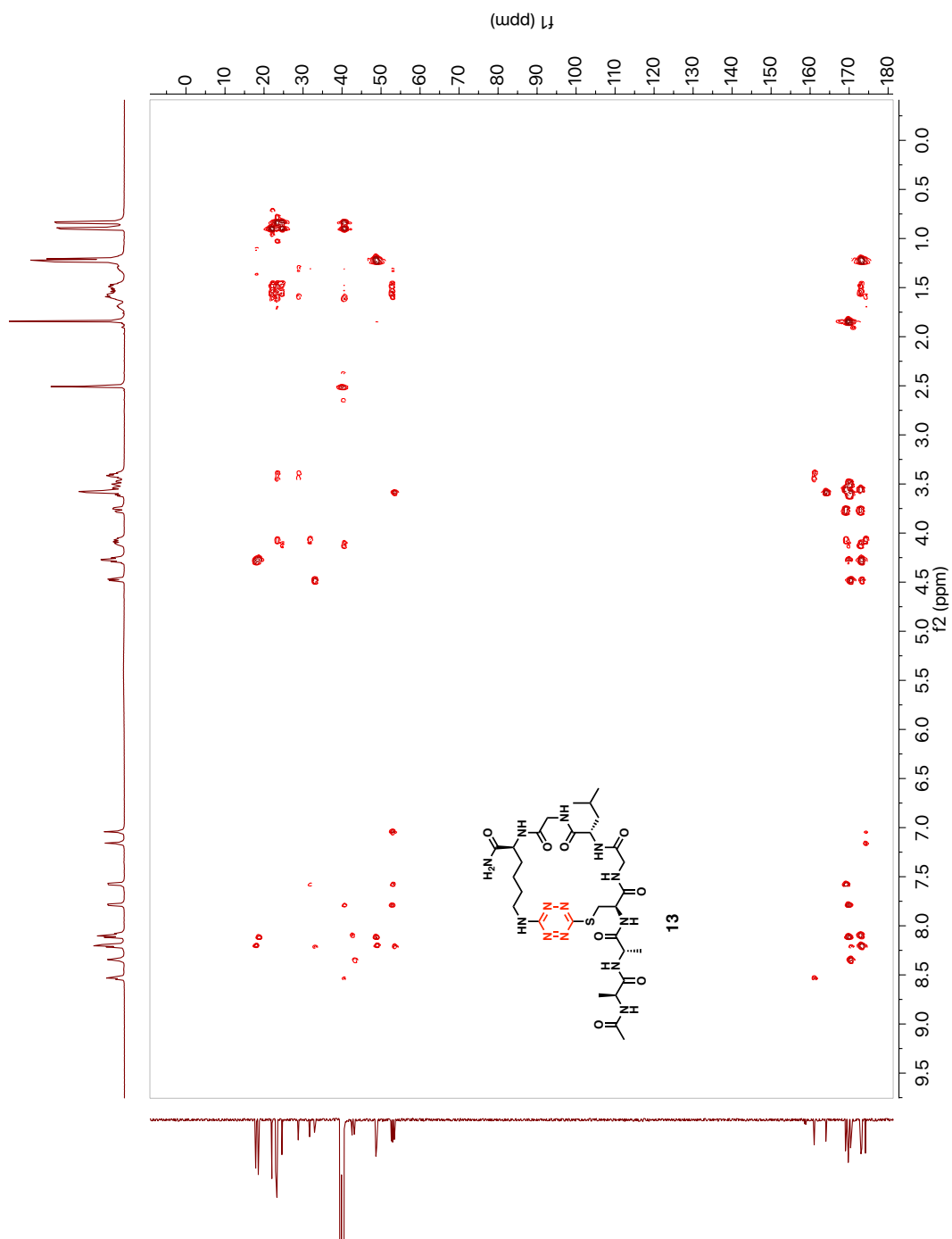


**Figure A.96.** HMBC Spectrum of Macrocycle **13** in  $d_6$ -DMSO



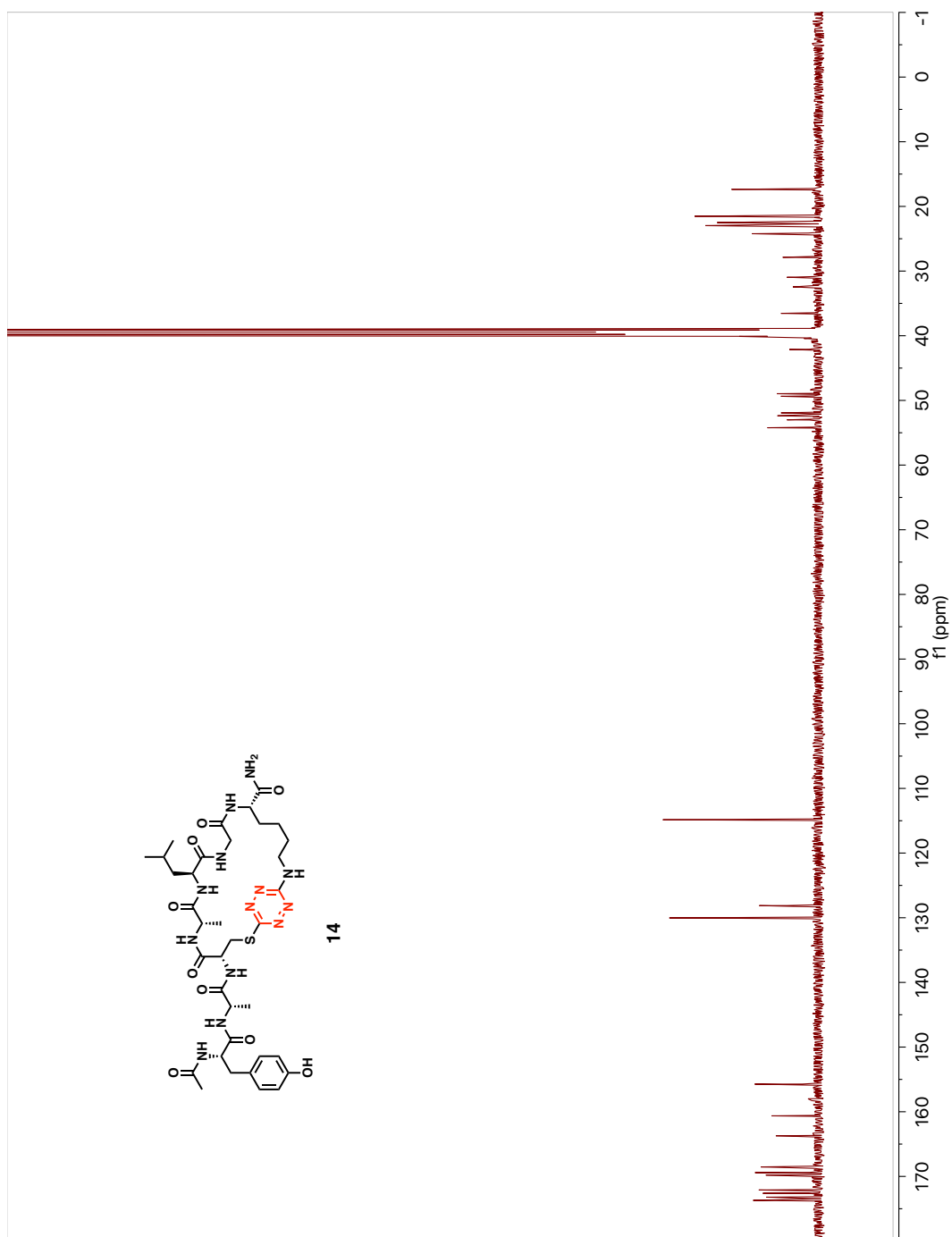


**Figure A.98.** 126 MHz  $^{13}\text{C}$  Spectrum of Macrocycle 14 in  $d_6$ -DMSO

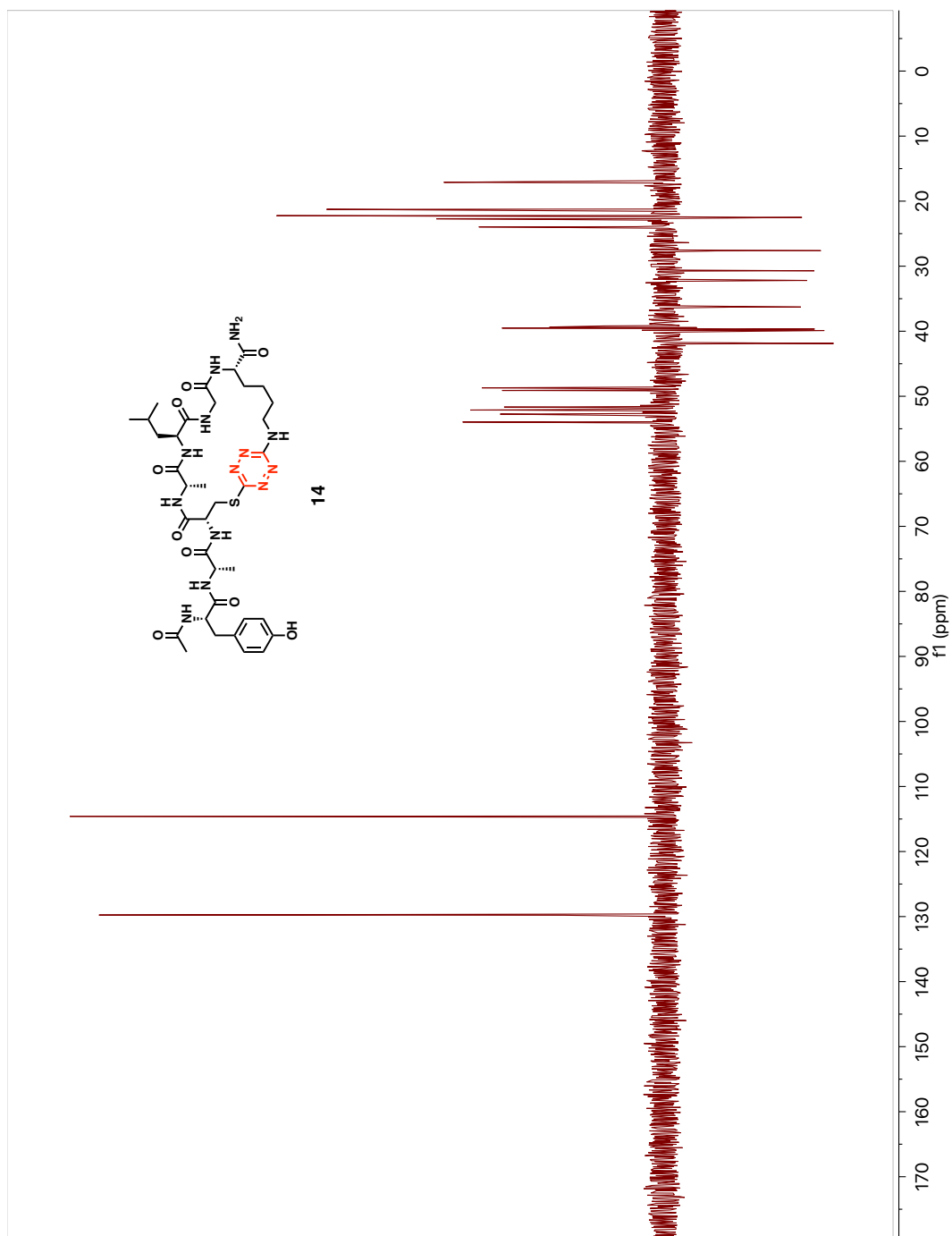


**Figure A.99.** 126 MHz DEPT-135 Spectrum of Macrocycle 14 in  $d_6$ -DMSO

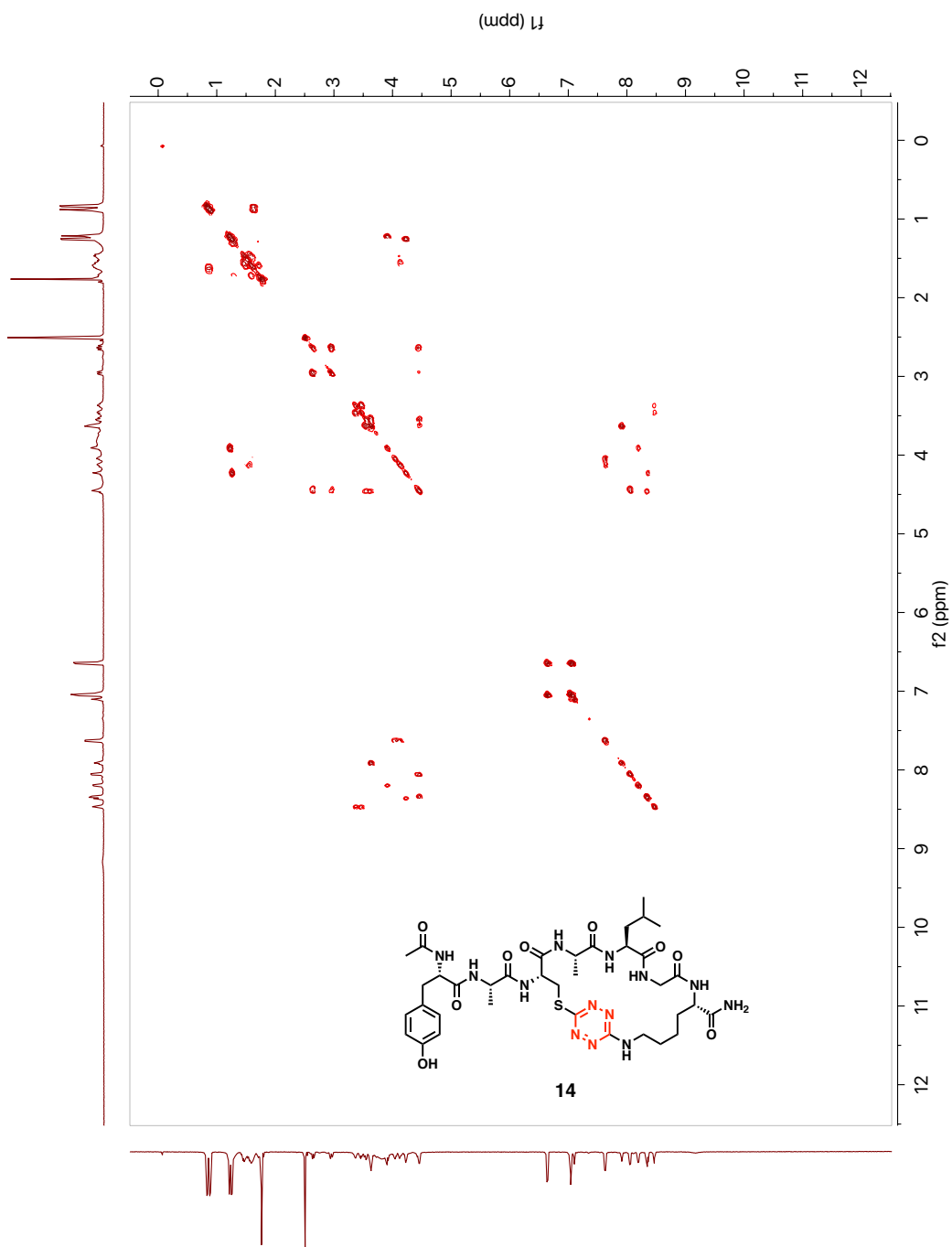


**Figure A.100.** COSY Spectrum of Macrocycle **14** in *d*<sub>6</sub>-DMSO

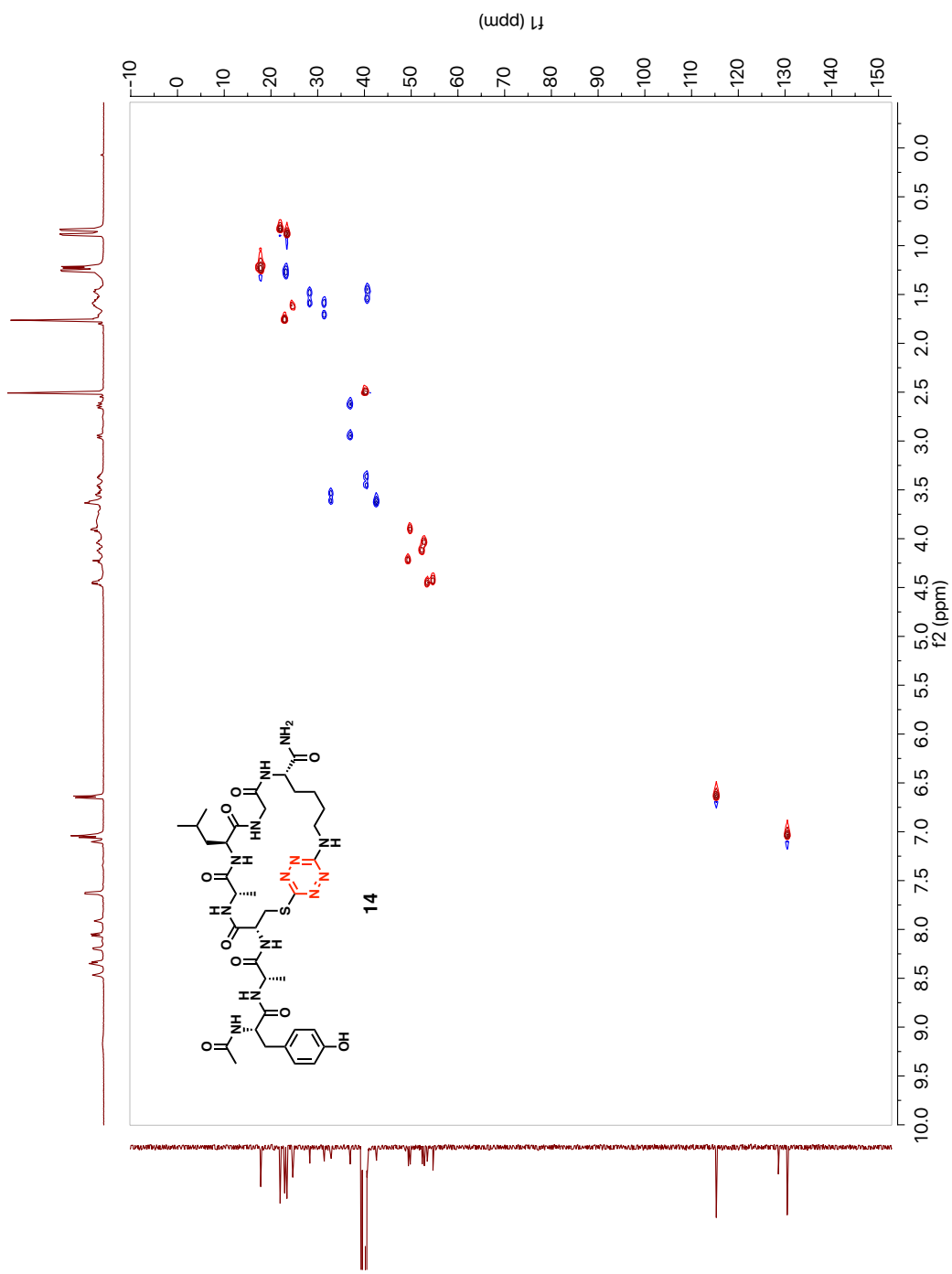


**Figure A.101.** HSQC Spectrum of Macrocycle 14 in  $d_6$ -DMSO



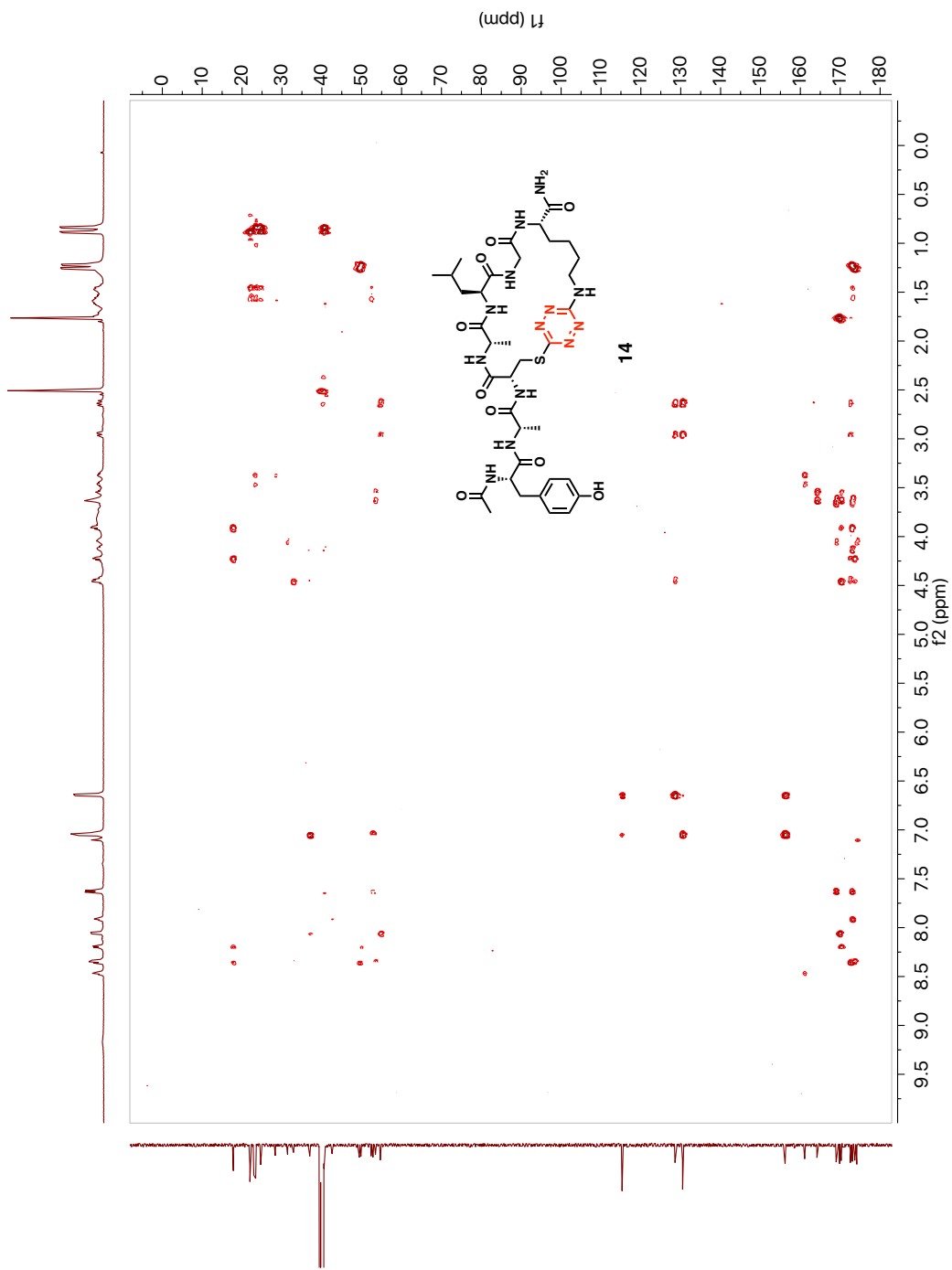


**Figure A.102.** HMBC Spectrum of Macrocycle 14 in  $d_6$ -DMSO

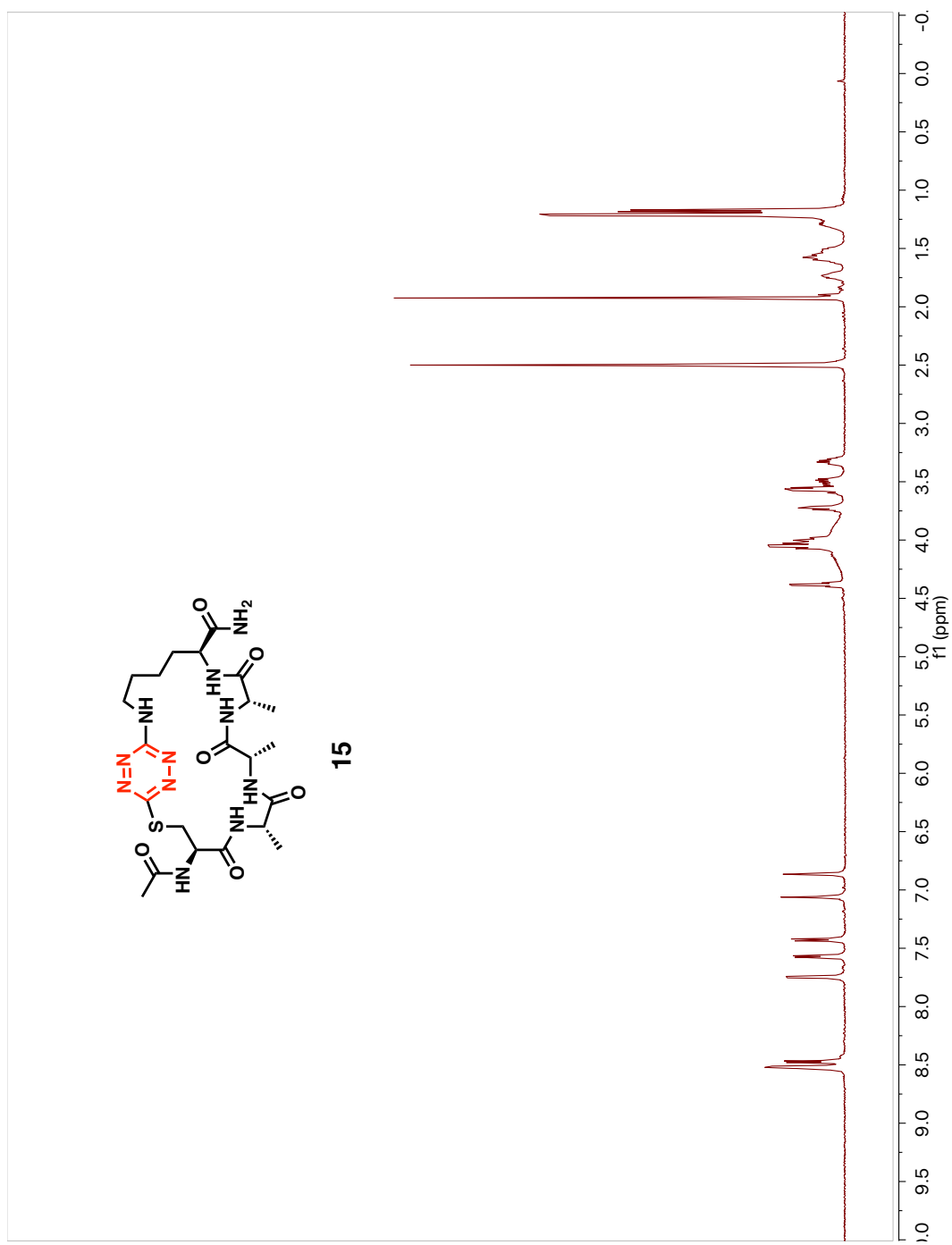


**Figure A.103.** 500 MHz <sup>1</sup>H-NMR Spectrum of Macrocycle **15** in *d*<sub>6</sub>-DMSO

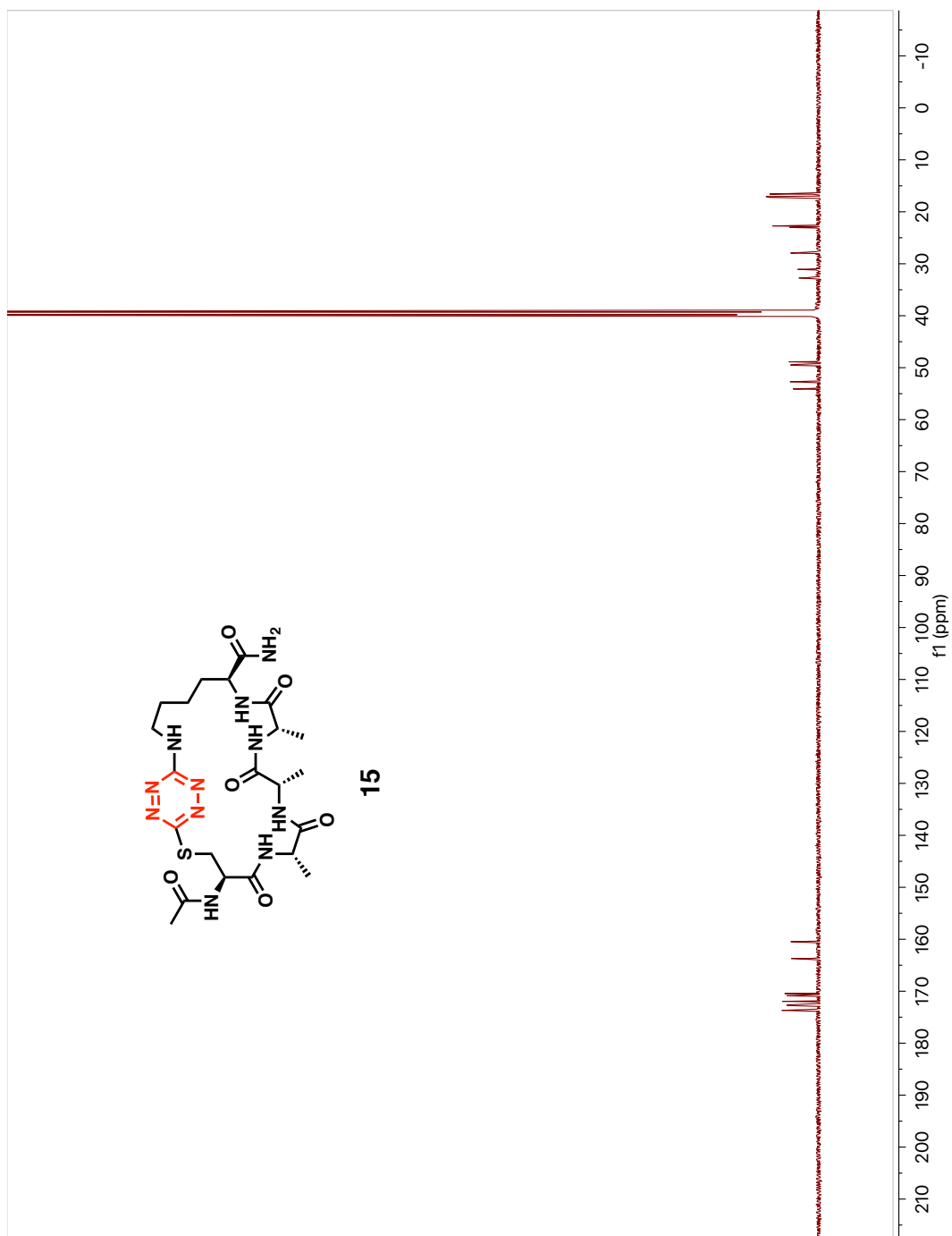


**Figure A.104.** 126 MHz  $^{13}\text{C}$  Spectrum of Macrocycle **15** in  $d_6$ -DMSO



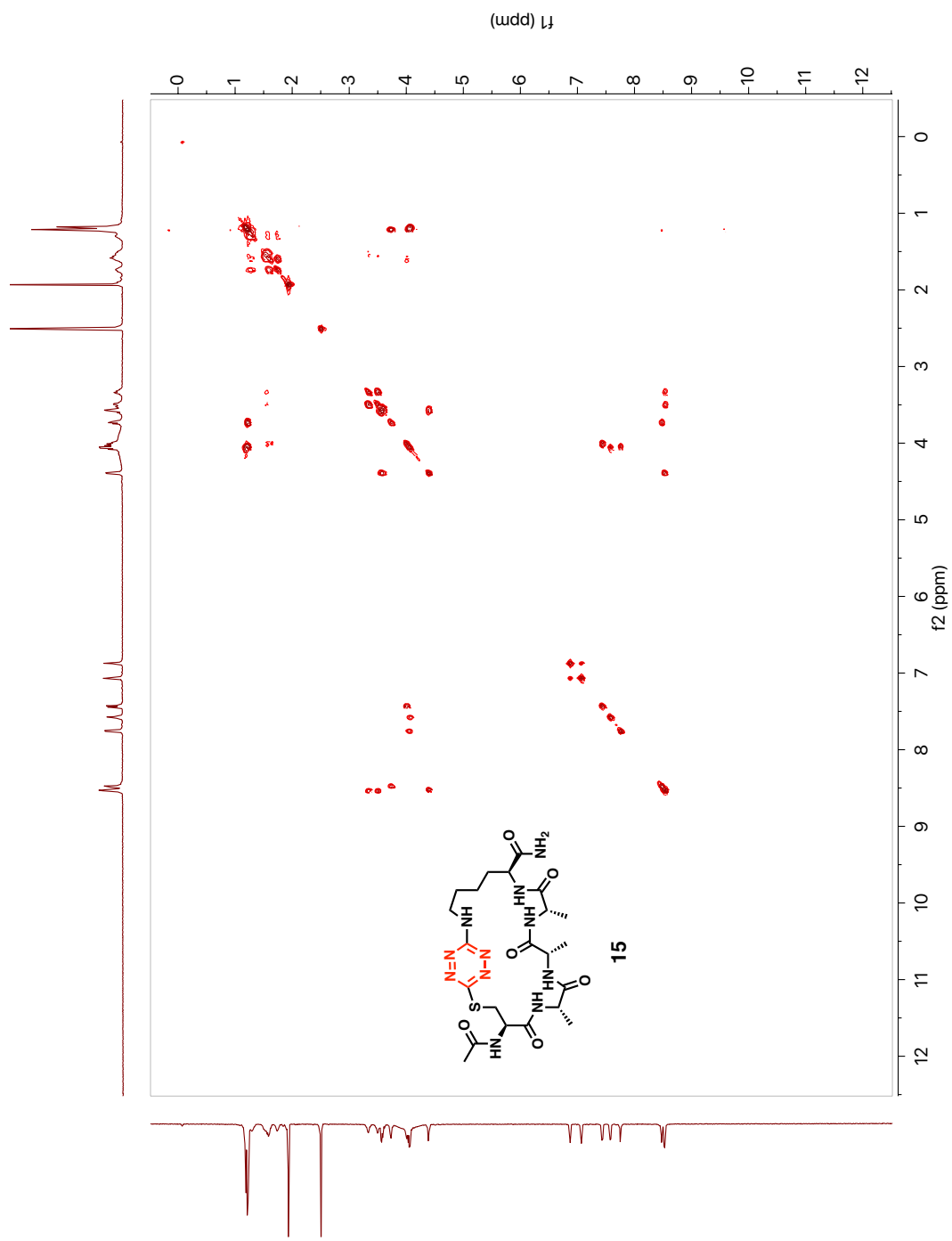


**Figure A.106.** COSY Spectrum of Macrocycle **15** in  $d_6$ -DMSO

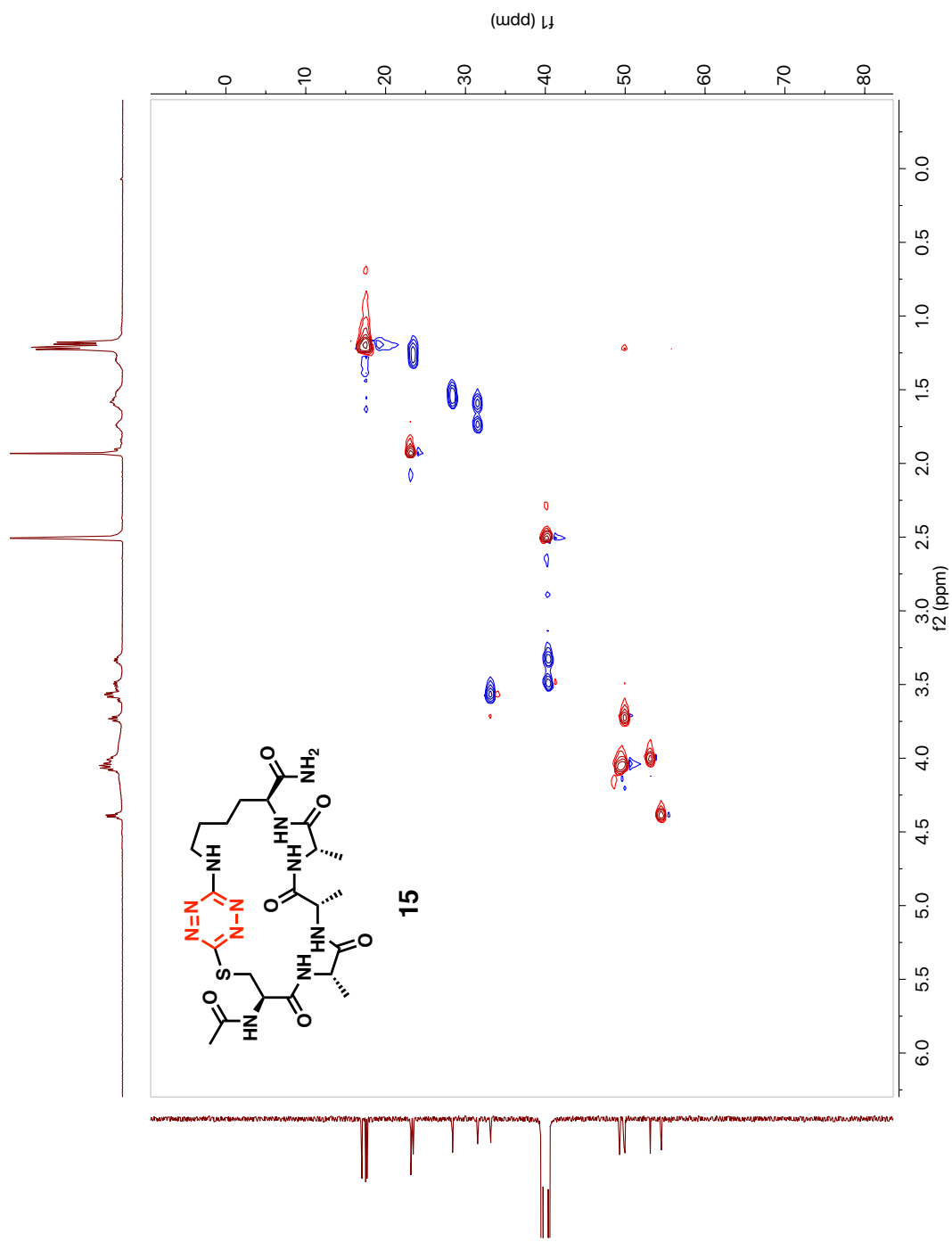


**Figure A.107.** HSQC Spectrum of Macrocycle **15** in  $d_6$ -DMSO

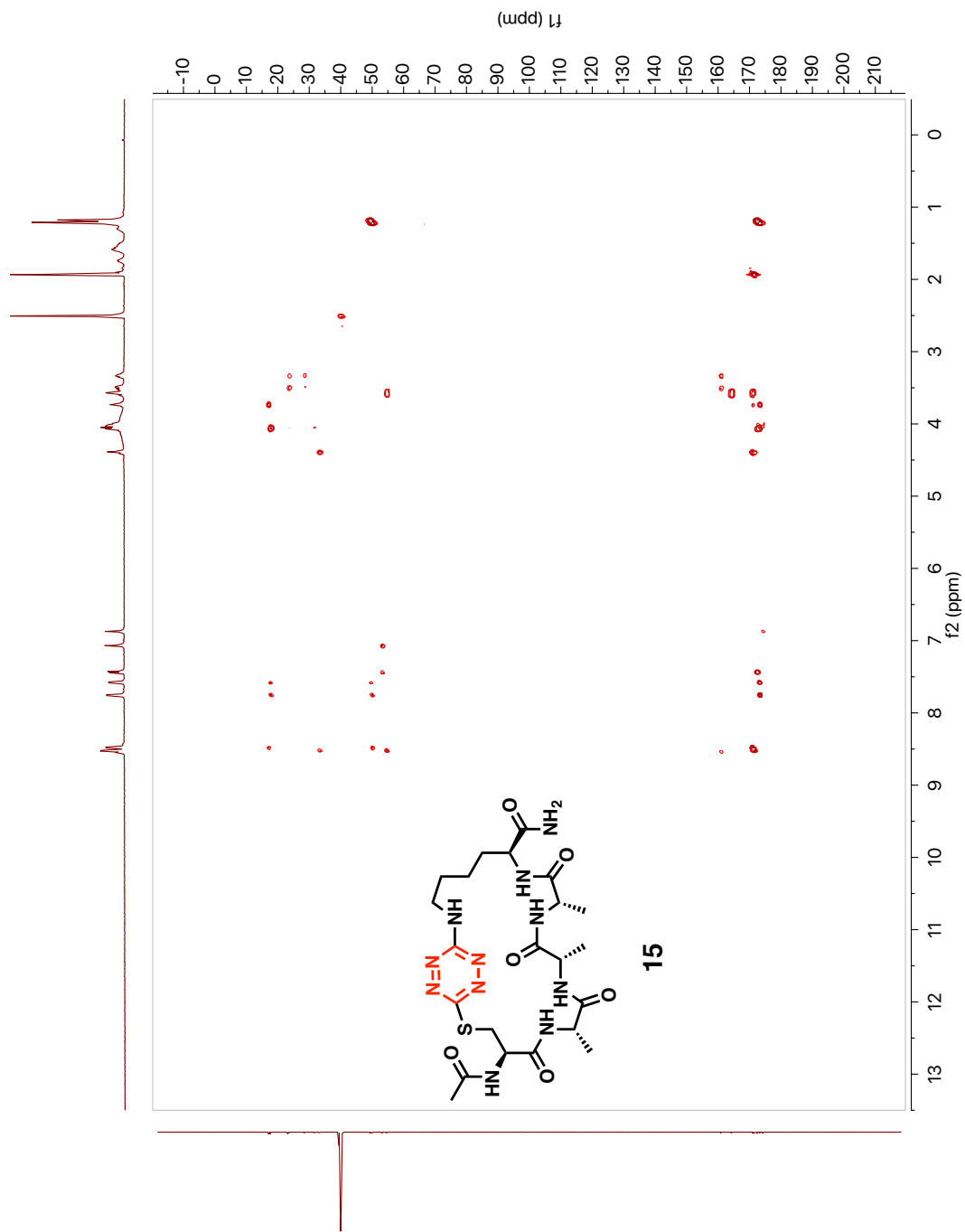


**Figure A.108.** HMBC Spectrum of Macrocycle **15** in  $d_6$ -DMSO

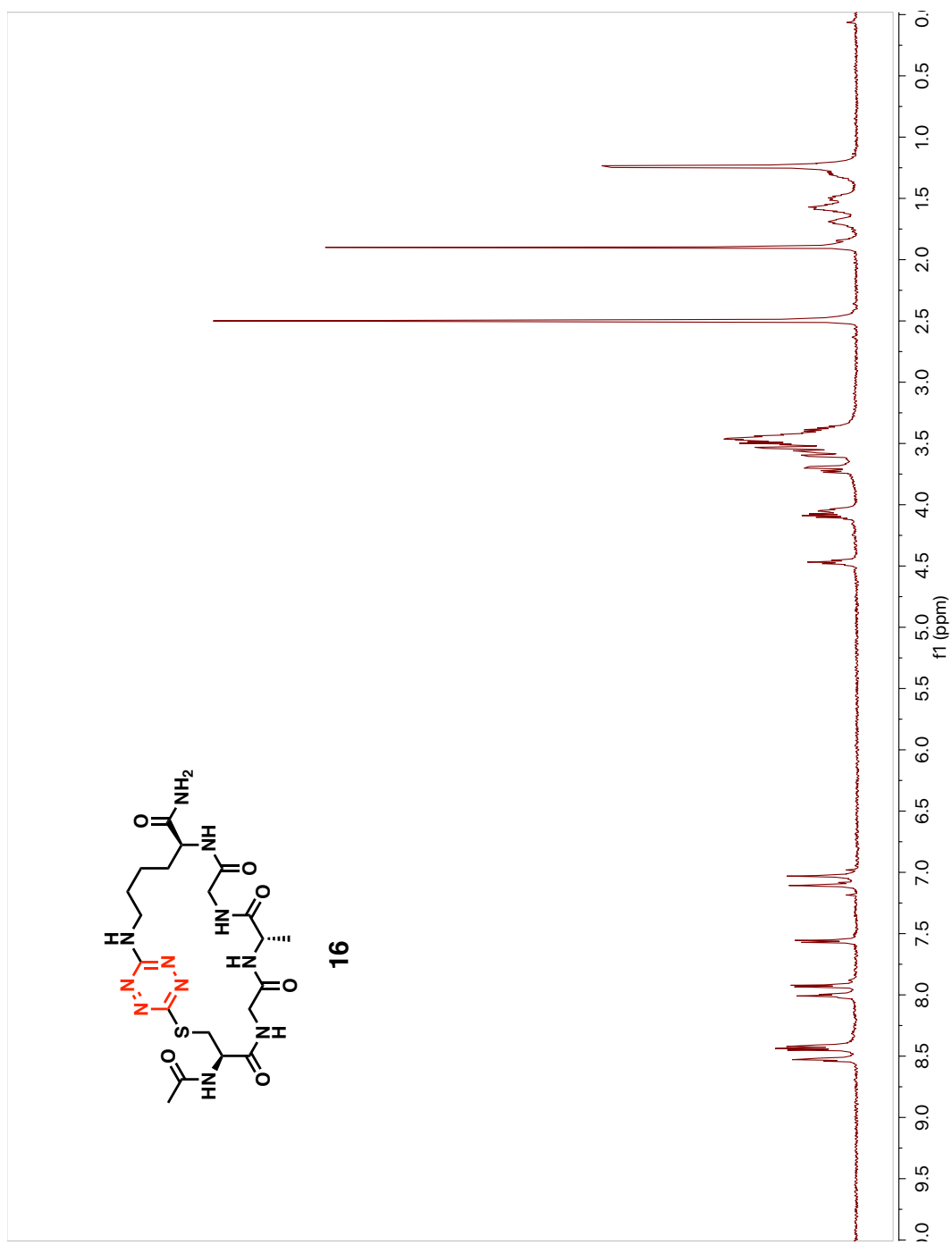


**Figure A.109.** 500 MHz <sup>1</sup>H-NMR Spectrum of Macrocycle 16 in *d*<sub>6</sub>-DMSO



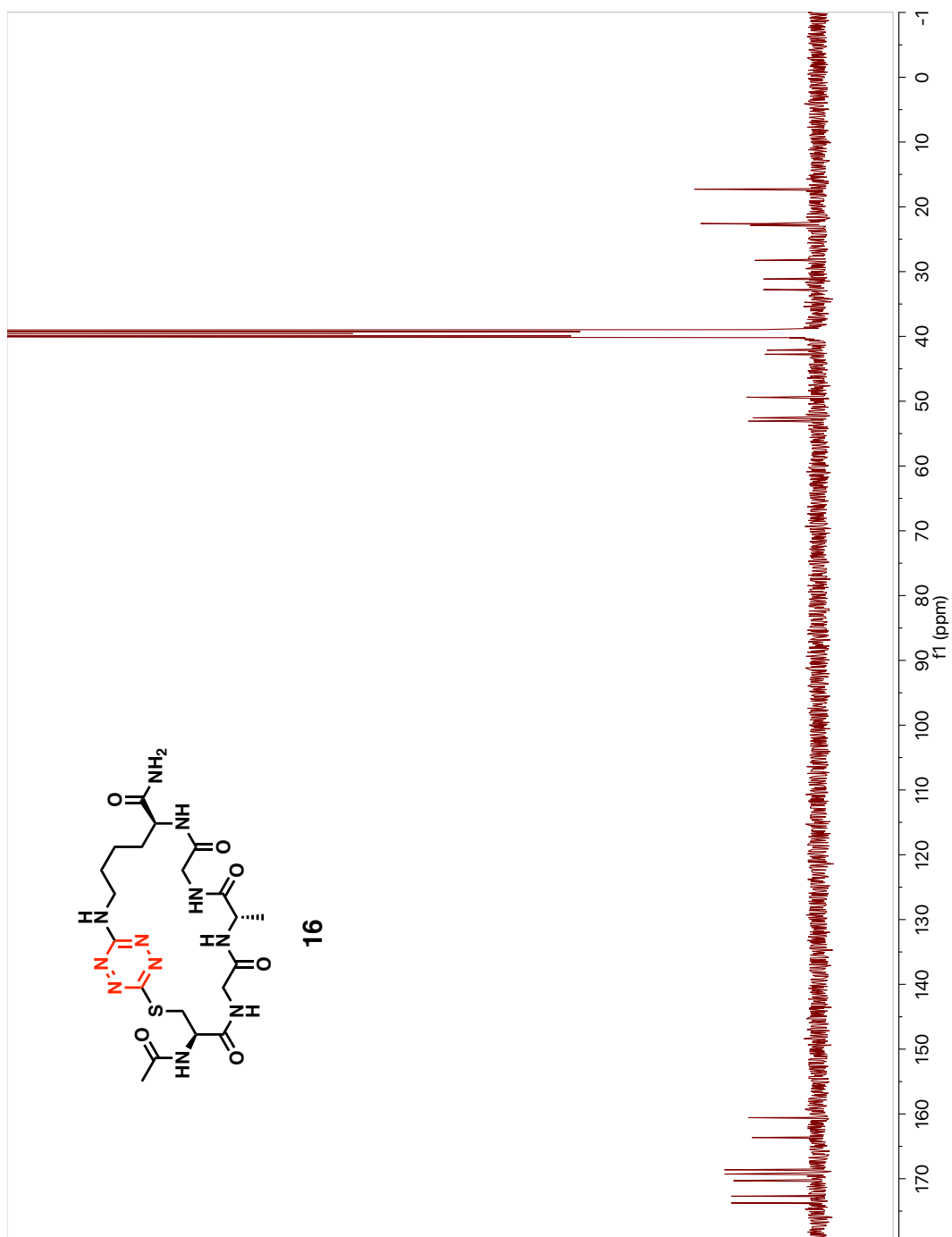
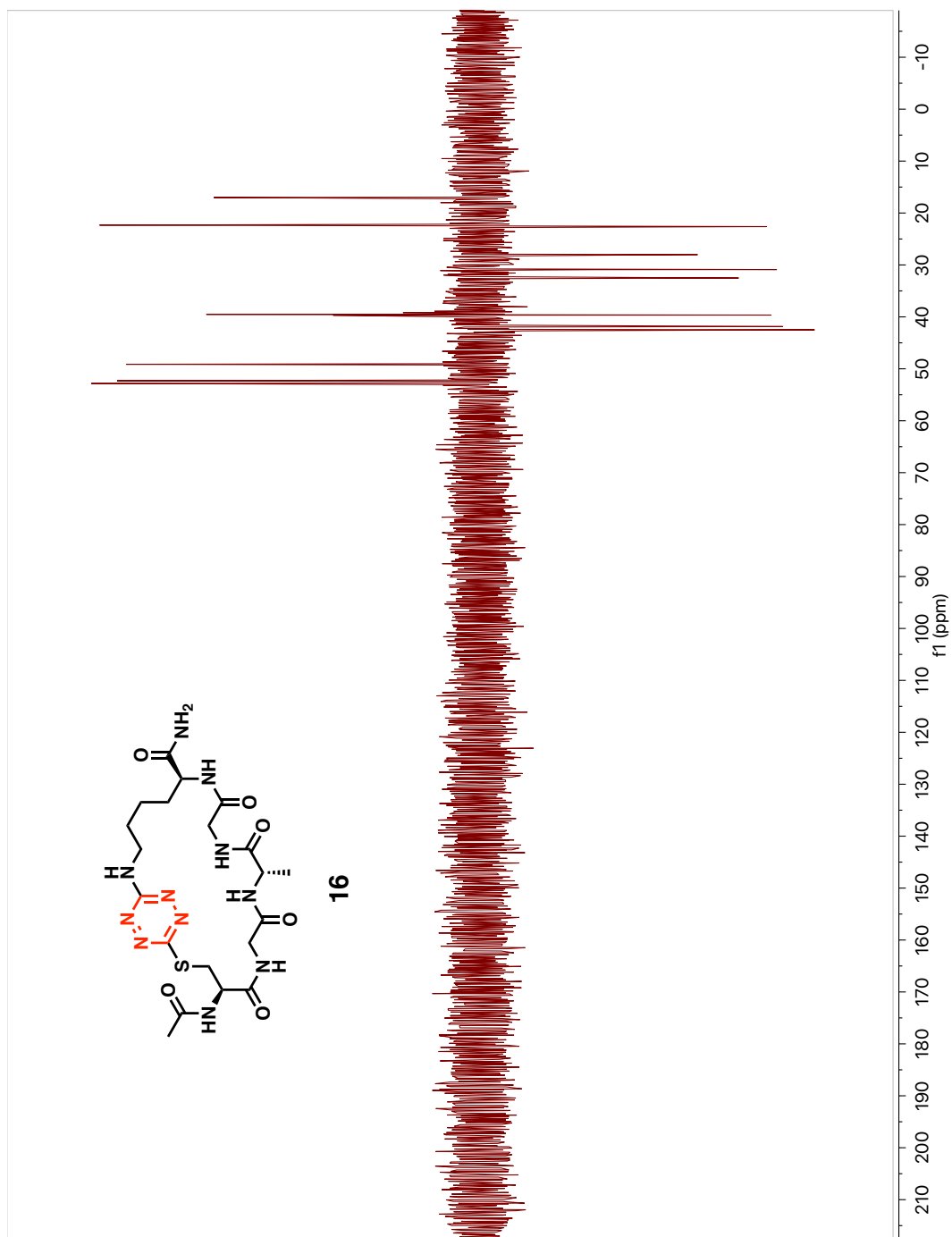
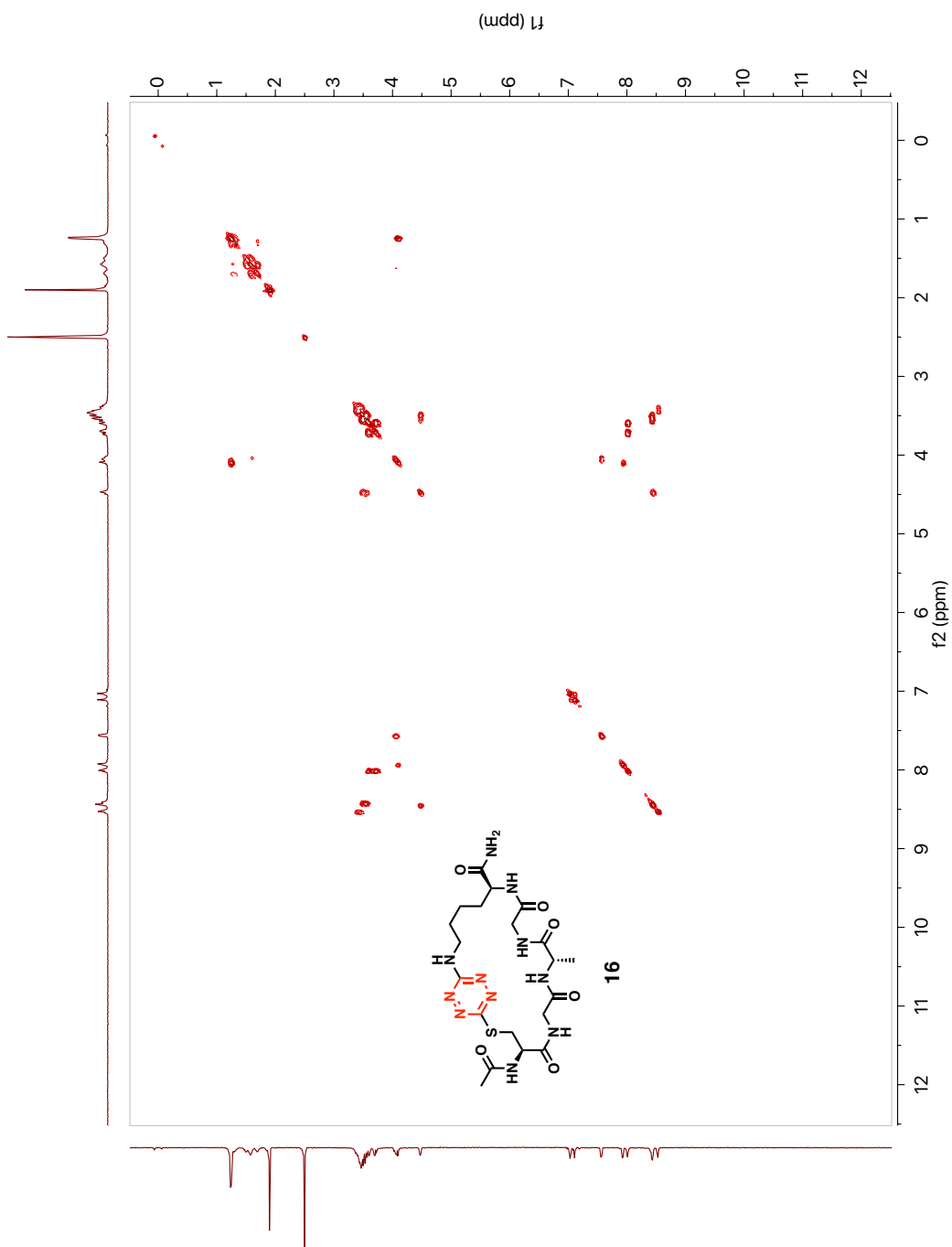


Figure A.110. 126 MHz  $^{13}\text{C}$  Spectrum of Macrocycle 16 in  $d_6$ -DMSO



**Figure A.111.** 126 MHz DEPT-135 Spectrum of Macrocycle **16** in *d*<sub>6</sub>-DMSO



**Figure A.112.** COSY Spectrum of Macrocycle **16** in *d*<sub>6</sub>-DMSO



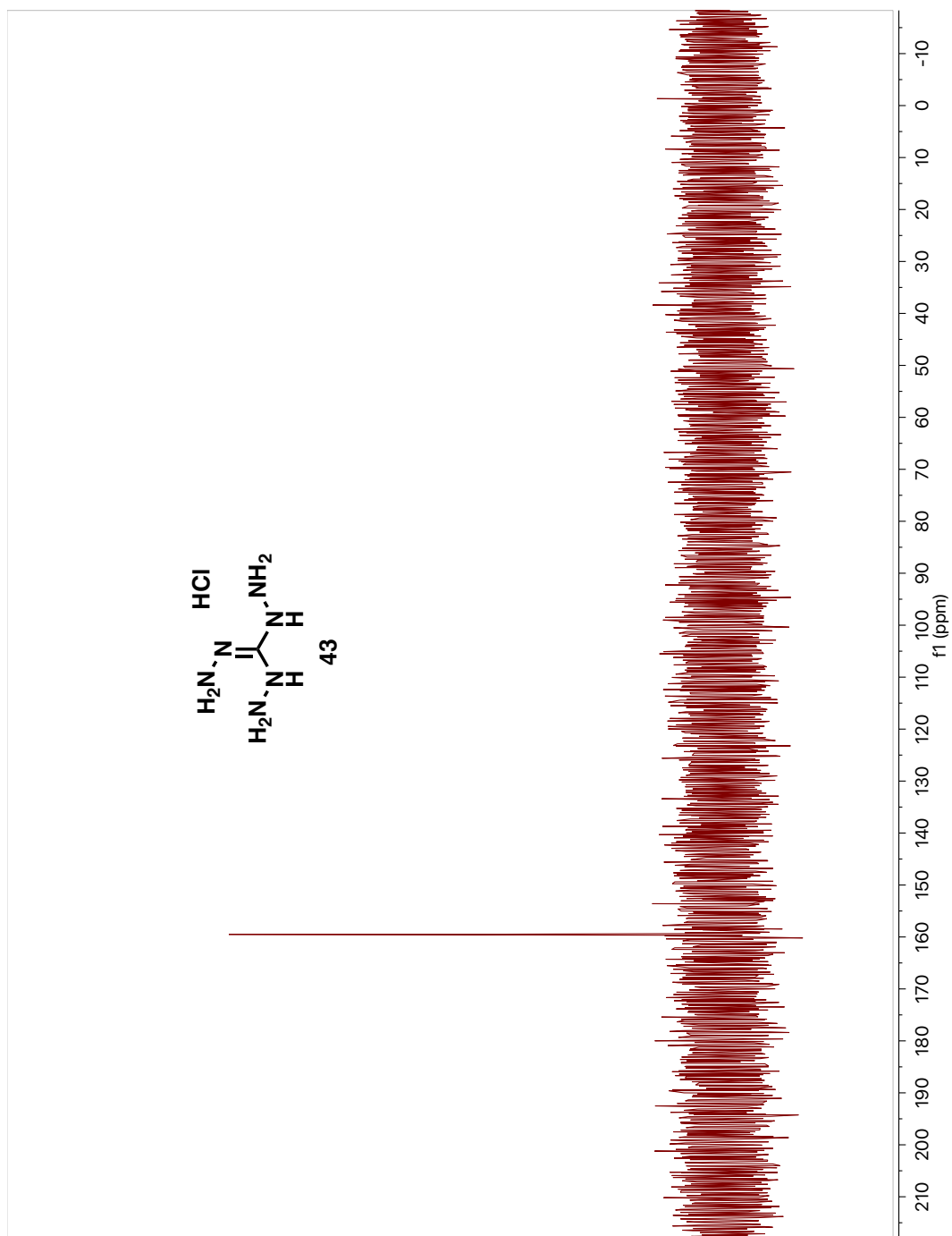


**Figure A.114.** 126 MHz  $^{13}\text{C}$  Spectrum of **Compound 43** in  $\text{D}_2\text{O}$

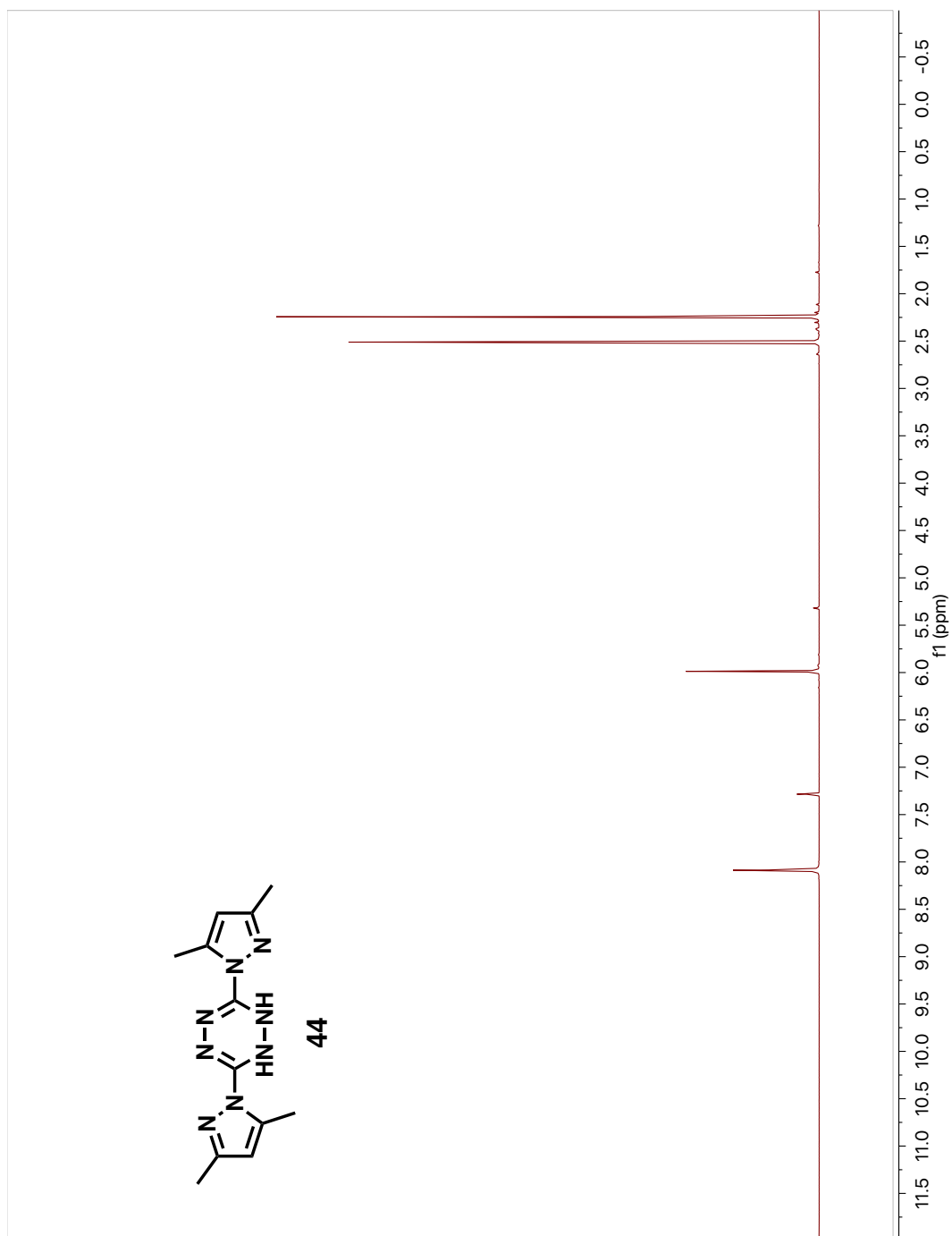


**Figure A.115.** 500 MHz <sup>1</sup>H-NMR Spectrum of Compound 44 in CDCl<sub>3</sub>

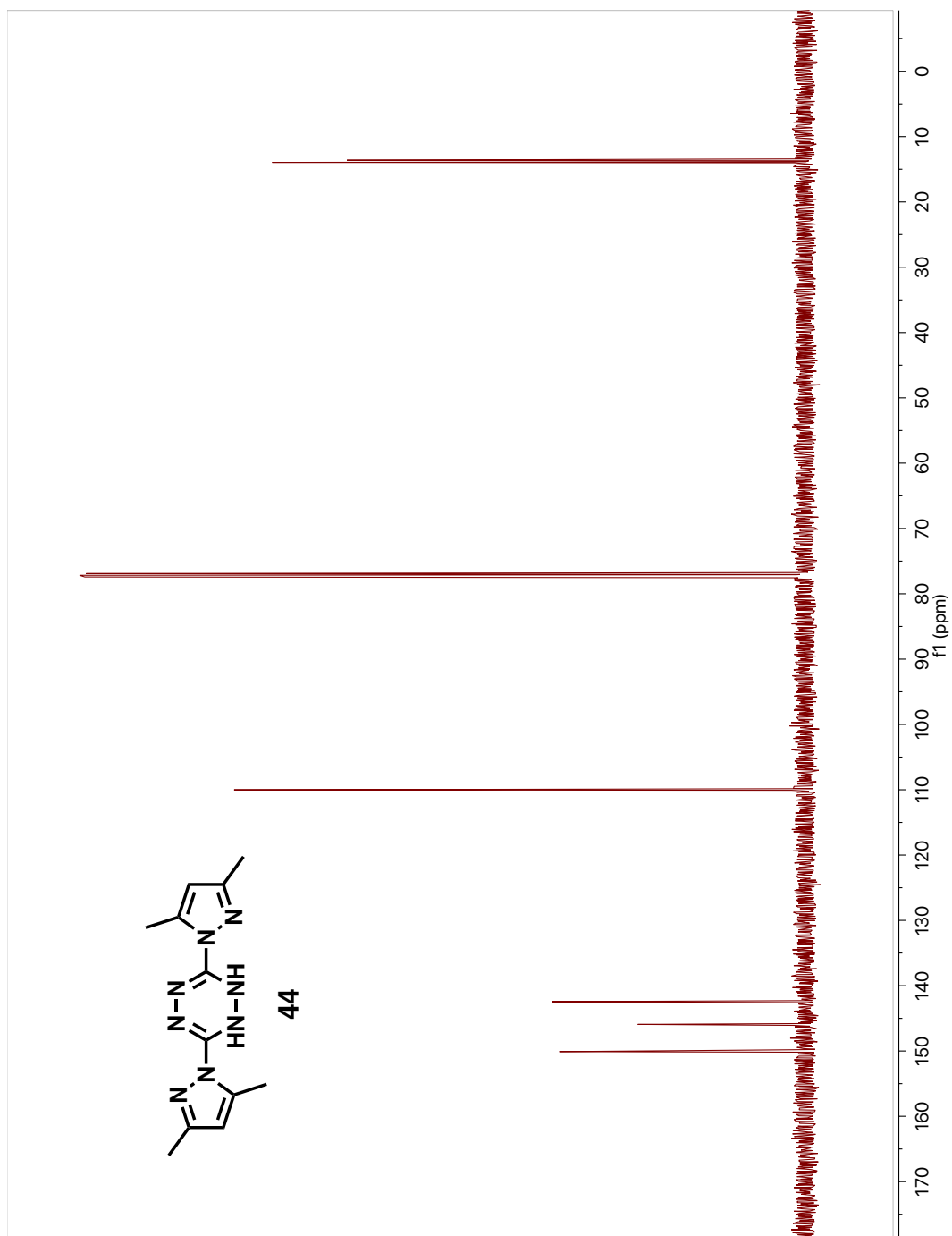
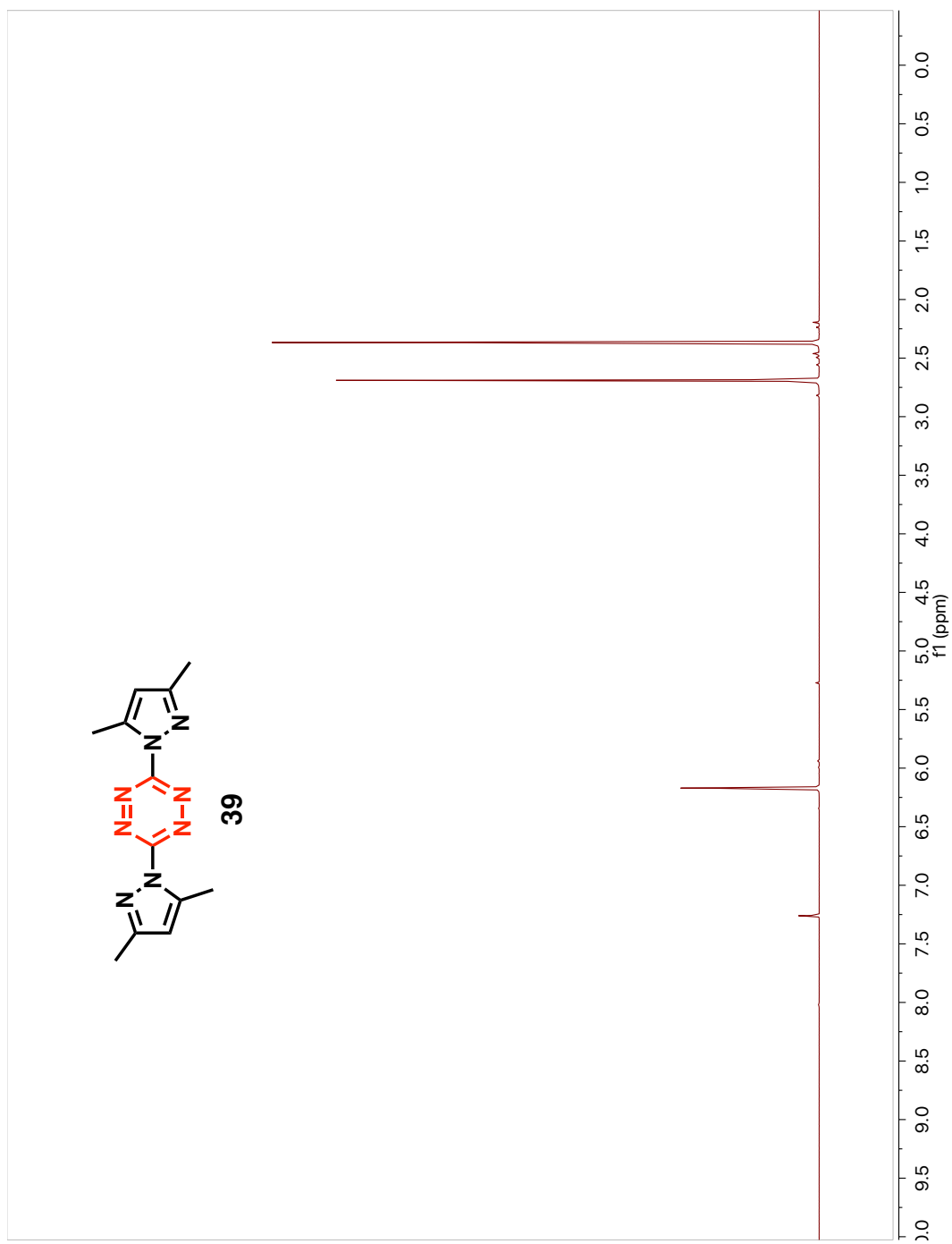
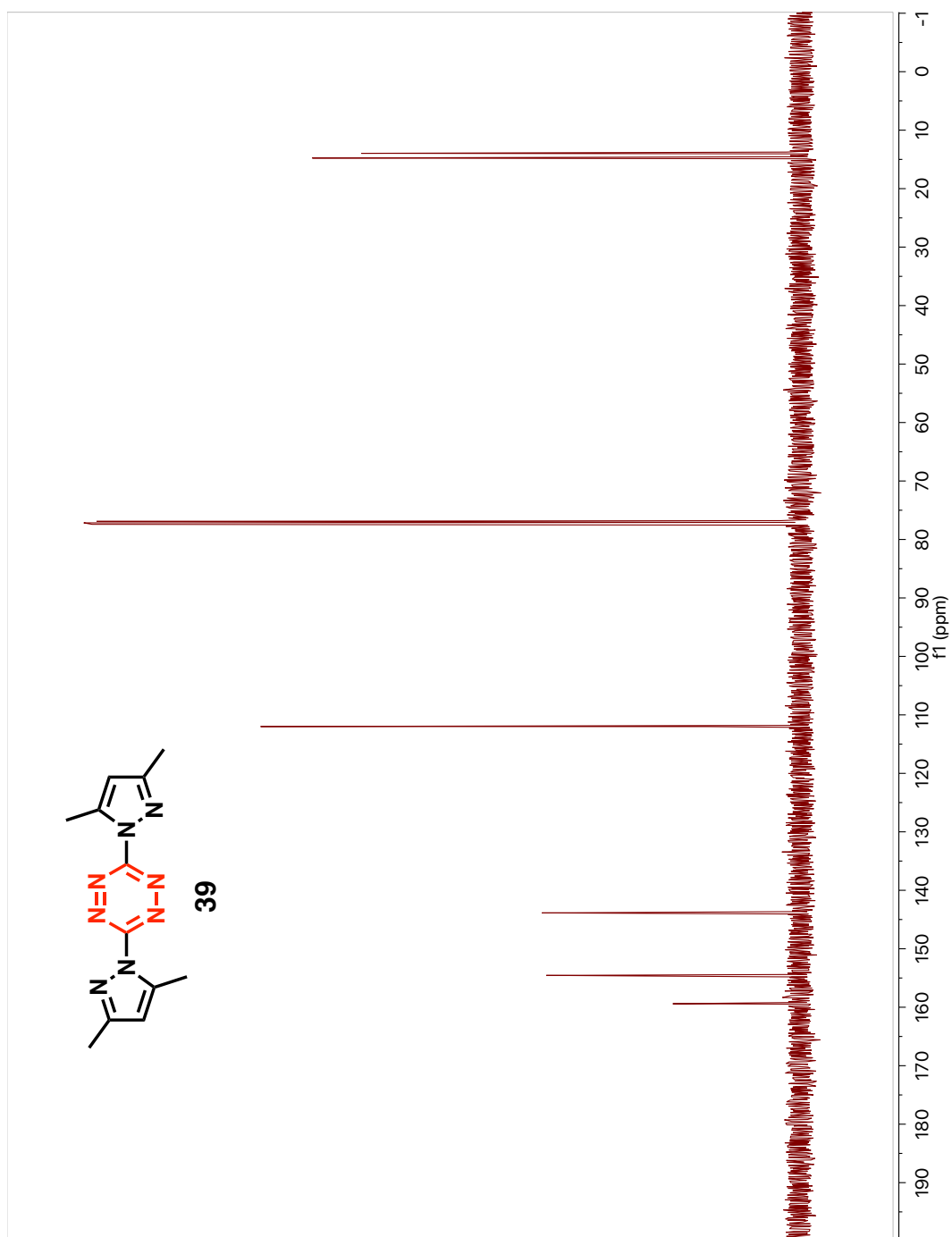


Figure A.116. 126 MHz  $^{13}\text{C}$  Spectrum of Compound 44 in  $\text{CDCl}_3$



**Figure A.117.** 500 MHz <sup>1</sup>H-NMR Spectrum of Compound **39** in CDCl<sub>3</sub>





**Figure A.118.** 126 MHz  $^{13}\text{C}$  Spectrum of **Compound 39** in  $\text{CDCl}_3$

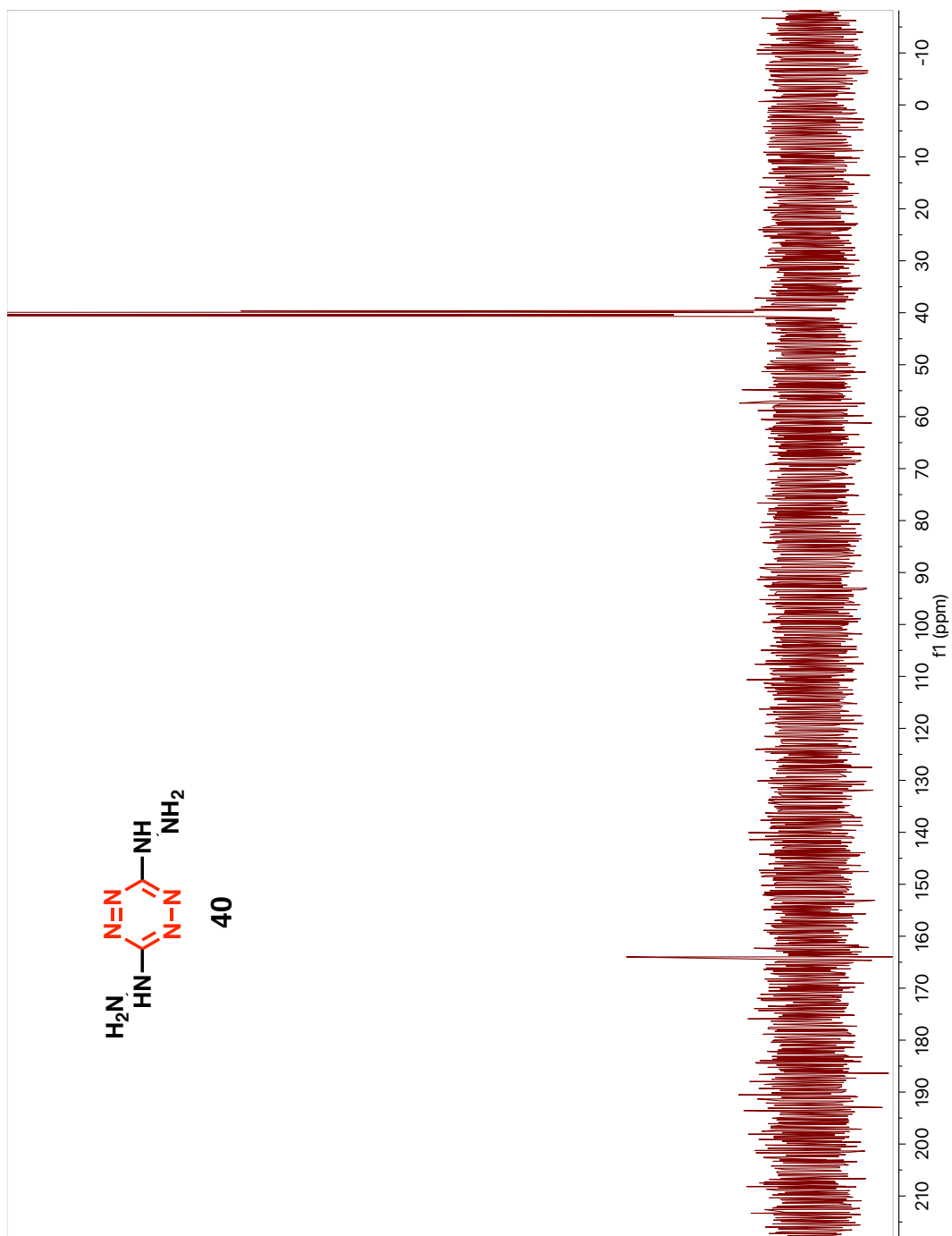


**Figure A.119.** 126 MHz  $^{13}\text{C}$  Spectrum of Compound 39 in DMSO

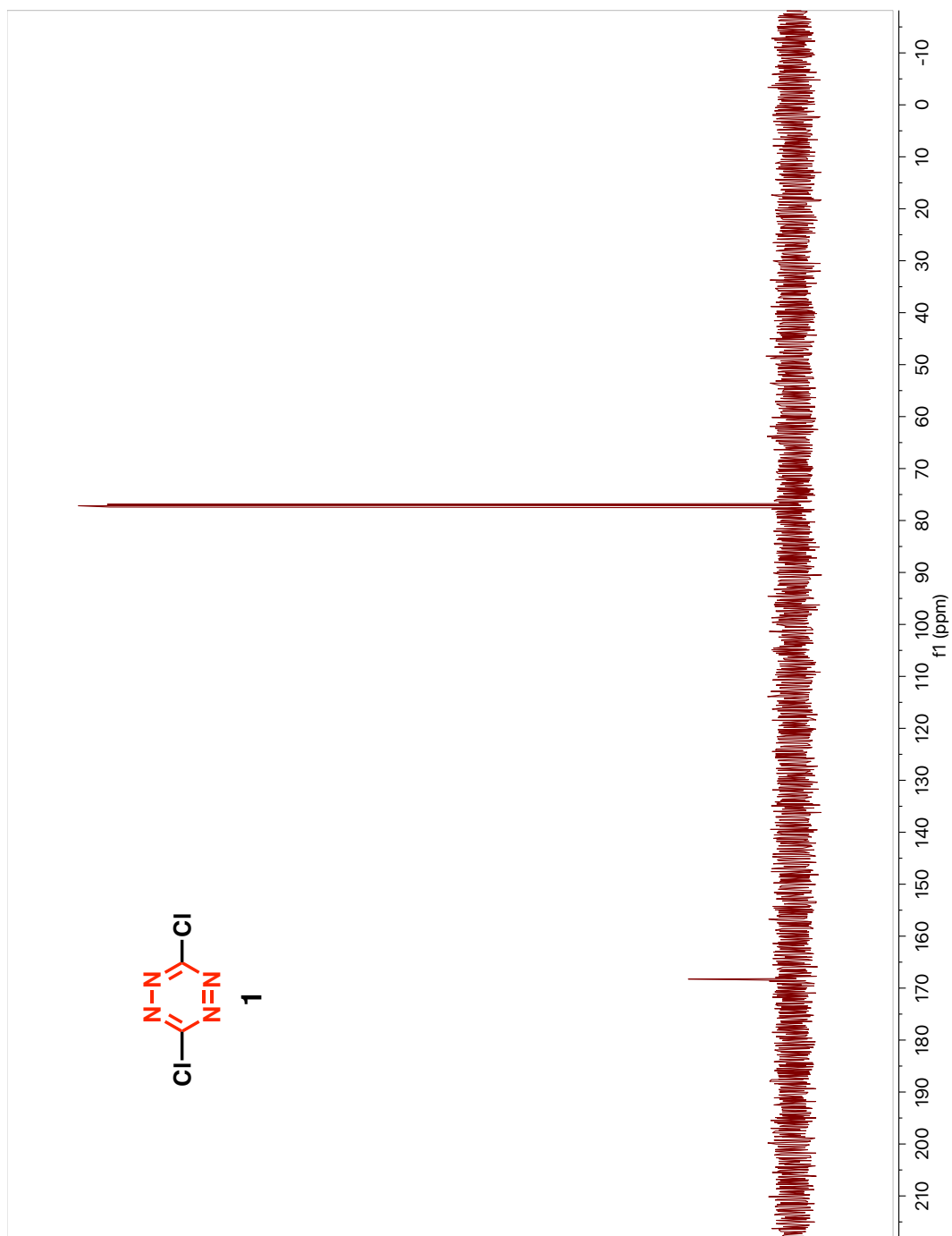


**Figure A.120.** 126 MHz  $^{13}\text{C}$  Spectrum of **Compound 1** in  $\text{CDCl}_3$